Modelling the interactions between geomorphological processes and Natural Flood Management

Eleanor Grace Pearson

Submitted in accordance with the requirements for the degree of Doctor of Philosophy

The University of Leeds

School of Geography

November 2020

The candidate confirms that the work submitted is her own and that appropriate credit has been given where reference has been made to the work of others.

Acknowledgements

Firstly, I would like to thank Dr Jonathan Carrivick, your continual support through the last four years has to no end aided this process. Thank you for your constant open door, time driving around the Aire and writing feedback. Thank you for guiding me to make decisions which have improved this project endlessly.

Particular thanks go to Dr Barry Hankin, you have gone above and beyond to help me through this process, regardless of how busy you have been and your seamless integration into the team behind this project has been invaluable. Your interest has been inspirational and for that I am truly grateful. Thank you for all your guidance, modelling help, lunchtime chats, lockdown catch ups and fieldwork assistance – I am so glad we went to Lothersdale when we did!

I am indebted to the support from JBA Trust. My thanks go to Professor Rob Lamb, Alex Scott and Steve Rose. From the start of this process you have given me support and opportunities to step away from the computer and showcase my work. Rob, thank you additionally for the support you have given me in achieving the tangible outputs to this project.

To Dr Andrew Sleigh and Professor Nigel Wright, thank you for your contributions to discussions throughout this project, they have guided and provided insight into the modelling process.

I am very grateful for the support of the wider School of Geography community, particularly Dr Tom Willis and Zora Van Leeuwen, you have both given me great advice and provided me with a space to discuss my project more holistically. To everyone else who I have met at university in the last four years, thank you for the corridor chats, tea breaks, lunchtimes, Friday cakes and evening socials, they have given me the balance every PhD needs.

I would like to thank my family. You have always encouraged me to achieve regardless of whether you have understood what I have been doing. Your support throughout has helped me finish this process and I am particularly grateful for what you have done in the last year, who knew moving back home would have been so enjoyable. To Mark, thank you endlessly for your love and patience, I am looking forward to enjoying a more typical work life with you by my side.

Abstract

Natural Flood Management (NFM) measures are being implemented across the UK and Europe in an effort to reduce flood impacts in a cost-effective and sustainable manner. Presently, NFM measures are often constructed without consideration of their geomorphological impact. There is also little evidence for NFM measures such as Runoff Attenuation Features (RAFs), which include leaky barriers, having an impact at larger (> 10 km^2) catchment scales and for extreme events (> 100 year return period). This thesis examines both the hydrological and geomorphological effects of RAFs through; (i) morphodynamic modelling of RAFs of differing shapes, sizes and quantities at catchment scale (~41 km^2) for an extreme event (120 year return period), (ii) comparison between a morphodynamic model and geomorphological processes estimated from outputs of a hydraulic model, which enables (iii) hydraulic modelling of differences in leaky barrier design.

The results indicate that a RAF can be designed to increase water storage and floodplain connectivity. However, hydrologically beneficial designs can produce erosion and deposition and scour to the feature itself. These effects are all localised and at catchment scale no notable peak discharge reduction was observed. Thus relying solely on RAFs will only likely reduce localised, low magnitude flooding and future research should look to strengthening this argument alongside increasing understanding of structure failure within networks of RAFs.

Qualitatively, the geomorphological outputs derived from CAESAR-Lisflood (a morphodynamic model) and HEC-RAS 2D (a hydraulic model) agreed with each other. However, methodological refinement is needed before hydraulic model outputs can be repurposed into geomorphological process estimations on a wider, national scale with little detailed validation. Overall, the HEC-RAS 2D methodology should be used to consider local problems requiring a high spatial resolution including changes in infrastructure design. CAESAR-Lisflood should be used to consider catchment dynamics and where NFM measures induce bed morphology changes.

Table of Contents

List of Figures

List of Tables

Abbreviations

AEP	*Annual Exceedance Probability*
CEH-GEAR	*Centre for Ecology and Hydrology Gridded Estimates of Areal Rainfall*
DEFRA	*Department for Environment, Food and Rural Affairs*
DEM	*Digital Elevation Model*
DTM	*Digital Terrain Model*
EFRA	*Environment, Food and Rural Affairs Committee*
FCERM	*Flood and Coastal Erosion Risk Management*
FEH DDF	*Flood Estimation Handbook Depth-Duration-Frequency*
FWAG	*Farming and Wildlife Advisory Group*
GIS	*Geographic Information System*
GSD	*Grain Size Distribution*
IOD	*In-Out Difference*
IQR	*Interquartile Range*
LEM	*Landscape Evolution Model*
LiDAR	*Light Detection and Ranging*
MAE	*Mean Absolute Error*
MRE	*Mean Relative Error*
NBS	*Nature Based Solutions*
NFM	*Natural Flood Management*
NSE	*Nash-Sutcliffe Efficiency*
OST	*Office of Science and Technology*
RAF	*Runoff Attenuation Feature*
ReFH	*Revitalised Flood Hydrograph*
RMSE	*Root Mean Squared Error*

RP	*Return Period*
SEPA	*Scottish Environment Protection Agency*
SRC	*Sediment Response Catchment*
TBR	*Tipping Bucket Rain Gauge*
WFD	*Water Framework Directive*
WwNP	*Working with Natural Processes*
YDNPA	*Yorkshire Dales National Park Authority*
YDRT	*Yorkshire Dales Rivers Trust*
YPP	*Yorkshire Peat Partnership*

Chapter 1
Introduction

1.1 Flooding in the UK

Within Europe and the UK, flooding is the most common natural hazard (Wilby et al., 2007). In the UK, approximately every one in six properties are at risk from flooding (Thorne, 2014), with great economic consequences. Penning-Rowsell (2014) estimating the annual economic risk of flooding to be between £ 0.192 bn and £ 0.268 bn, however government quoted figures are much higher (> £ 1 bn) (Environment Agency, 2009). Historical precipitation has shown trends for wetter winters and drier summers (Jones and Conway, 1997), however, under climate change, predictions suggest an increase in summer flash flooding (Kendon et al., 2014) alongside increases in winter precipitation (Fowler and Ekström, 2009; Kendon et al., 2014). To be resilient to these climatic changes, the long term annual average investment in UK infrastructure needs to be £1bn per year (Environment Agency, 2019a).

1.1.1 Notable recent events

Although not historically unprecedented in terms of frequency or magnitude (Foulds and Macklin, 2016), a number of major flood events have occurred in the UK since the turn of the century, namely in 2000-2001, 2007, 2012, 2013-2014 and 2015-2016.

In 2000, the wettest autumn in 270 years resulted in flooding of approximately 10,000 properties costing an estimated £1 billion, with records of repeated floods (up to five times in the year) and flooding where no previous floods had been recorded (Environment Agency, 2001). Approximately 280,000 homes were however, protected by defences. The Environment Agency recommended a number of actions in response to the 2000 floods, including a reassessment of the attribution of responsibility for watercourse management to reduced confusion, the expansion of Floodline, improvements to society preparedness and flood warning systems, the need for flood emergency planning to have a sound statutory and financial footing and a full review into the state of flood defences (Environment Agency, 2001).

In the summer of 2007, extreme levels of rainfall over short periods of time resulted in the wettest summer since records began (Pitt, 2008). A total of 55,000 properties were flooded and 13 people died. The floods were estimated to have cost in the region of £4 billion (Chatterton et al., 2010). The floods were so severe they were classified as a national disaster and an independent review was undertaken by Sir Michael Pitt, concluding with 92 recommendations spanning topics from prediction to recovery and included a delivery guide with timescales for implementation of recommendations (Pitt, 2008).

2012 was a year of climatic extremes, with the driest January to March since 1953 followed by the wettest nine month period in the England and Wales Precipitation series (Parry et al., 2013). Widespread and sustained flooding occurred in several months of the year, with an estimated cost of £ 1.3 billion to rural Britain due to the drought and subsequent extreme rainfall causing waterlogging. Despite record levels of runoff, only 8,000 properties were flooded, mainly due to overwhelmed drainage systems as opposed to fluvial flooding and aided by the flood defence network and importantly timed dry spells (Parry et al., 2013). However, 2012 highlighted the need to adapt to extreme variability in the UK climate.

The winter of 2013-2014 was the wettest in the observational records of the UK and stormiest in 20 years (Kendon and McCarthy, 2015). Persistent storms resulted in over 8,000 flooded homes and 3,000 flooded commercial properties, with estimated damages totalling £1.3 billion (Chatterton et al., 2016). The Somerset Levels were particularly badly affected, however, nationally, it was estimated that flood defences protected approximately 1.4 million properties and 25,000 ha of agricultural land (Chatterton et al., 2016). In the government inquiry following the floods, the main conclusion was that protection should take priority over cost-cutting (Environment, Food and Rural Affairs Committee (EFRA), 2014).

December 2015 was the wettest month and the winter as a whole was the second wettest winter since 1910 (Barker et al., 2016). Successive storms and extreme rainfall resulted in approximately 16,000 flooded properties in England in December alone, with more flooded properties in January. Despite defences protecting over 20,000 properties in the December 2015 floods, some however, were overtopped, although they did provide the time for residents to relocate their

belongings (Marsh et al., 2016). The estimated costs of the 2015-2016 floods was £1.6 billion, however, unlike previous flood events, the damage to business property was significantly greater than to residential property (Environment Agency, 2018a). As a result of the 2015-2016 floods, the National Flood Resilience Review was published in September 2016 which focussed on the vulnerability to the country's key infrastructure to extreme flood events and highlighted the need for improved resilience, incident response, innovative flood defence, long-term modelling, flood risk communication and surface water flooding (Cabinet Office, 2016).

Although a full appraisal is yet to be published, in the 2019-2020 winter season, a number of catchments recorded new daily flow maxima from November to February, with some matching that of 2015 (Muchan et al., 2019 and Sefton et al., 2020). Flooding of around 1,000 properties occurred in November 2019 and over 3,000 in February 2020 (Muchan et al., 2019 and Sefton et al., 2020) with estimated economic losses set to be approximately £ 333 million (Environment Agency, 2020).

1.1.2 Climate change

Climate change is also likely to increase the frequency and magnitude of flood events, albeit with substantial uncertainty (Arnell and Gosling, 2016, Kay et al., 2009). The effects of climate change are already being attributed to UK flood events, including those of the winter 2013-2014 floods in the UK, where climate change was thought to have had a small but significant role in increasing severity of rainfall and consequential flooding (Schaller et al., 2016). Flood risk management therefore needs to be resilient in the future to the potential increase in risk relating to climate change. Resilience may be increased through, for example, accounting for additional flood volumes in defences, considering the entire catchment through the use of natural flood management to increase potential storage across the widest possible area, or greater consideration to flood risk in new building developments, such as appropriate locations and green infrastructure.

Initial climate change resilience within UK flood risk guidance was a sensitivity assessment whereby flood alleviation schemes needed to account for an increase of 20 % to peak river flows over 50 years, thought now to be relatively

precautionary with the chance of over- or under-adaptation due to the nation-wide approach (Reynard et al., 2017). Since, England has been divided into eleven river basin districts, allowing regional differences in climate change resilience. Each river basin district has a set of peak river flow allowances, based on percentiles (50^{th}, 70^{th} and 90^{th}) of potential peak flow scenarios under a number of climate change scenarios. Allowances range from 10 % to 25 % for the three percentiles for anticipated change up to 2039, increasing up to 105 % for change from 2070 to 2115 (South east 90^{th} percentile) (Environment Agency, 2016). Most recently, the 2020 Flood and Coastal Erosion Risk Management (FCERM) Strategy for England (Environment Agency, 2020) highlights the need to be resilient to flooding to the year 2100 through three long-term ambitions:

- “Climate resilient places…
- Today’s growth and infrastructure resilient in tomorrow’s climate…
- A nation ready to response and adapt to flooding and coastal change”

(Environment Agency, 2020, pg.12).

The strategy emphasises the need for the embrace of a wide range of resilience actions alongside more traditional flood defence work including greater preparation and response to flooding, avoiding inappropriate floodplain developments, quicker community and economic recovery alongside the inclusion of nature based solutions to slow and store flows and flood water (Environment Agency, 2020).

1.2 The rise of integrated flood risk management and nature based solutions

The floods that have occurred within the last 20 years have highlighted the need for more to be done to better equip the UK for future flooding, particularly under the threat of climate change. Hard engineering is not only harmful to the environment (Downs and Gregory, 2004), but is widely accepted not to be able to eliminate flood risk completely, with a need for environmental sustainability if it is to be effective (Harman et al., 2002). Sustainability in this thesis refers to the need to consider a holistic approach, using the entire catchment to increase storage through both creating storage areas and improving land use to increase soil water capacity, as in the 2004 Foresight project, to increase resilience of flood

risk management to climate change (Office of Science and Technology (OST), 2004). A whole catchment approach has increased in popularity as a cost-effective way to improve flood risk alongside more traditional approaches.

Following the Foresight project (OST, 2004), the UK government begun a new strategy for flood risk in the UK, called making space for water, aiming to bring a more holistic and sustainable approach to flood risk in the UK, including through the use of rural land management (Department for Environment, Food and Rural Affairs (DEFRA), 2005). The Pitt Review following the 2007 floods also highlighted the need to work with natural processes (Recommendation 27, Pitt, 2008). Since, a number of research projects led by the Environment Agency have looked to identify the research needs and disseminate evidence on “working with natural processes” or WwNP, defined as “taking action to manage flood and coastal erosion risk by protecting, restoring and emulating the natural regulating function of catchments, rivers, floodplains and coasts” (Environment Agency, 2012a, pg. 10). A number of funding opportunities have aided the uptake and improved the understanding of WwNP techniques, such as £1 million for three demonstration projects in Pickering (Slowing the Flow), the upper Derwent Valley (Moors For The Future) and Holnicote (Source to Sea) (Environment Agency, 2012a) and £15 million for projects across the country (DEFRA, 2017).

The largest WwNP research project was published by the Environment Agency in 2017 and brought together the current knowledge on all WwNP management techniques in one place (Environment Agency, 2017). This was advantageous for those wanting to learn more given the numerous commonly used and interchangeable terms for working with nature to aid flood management such as Natural Flood Management (NFM) and Nature Based Solutions (NBS) (Lane, 2017). The project included an evidence directory, alongside case studies and opportunity maps for woodland creation, runoff attenuation features and floodplain reconnection (Environment Agency, 2017).

1.2.1 What is being implemented?

Techniques implemented span the entirety of the catchment and range in scale, from leaky barriers and headwater drainage management in the upper catchment, to woodland creation, land management, water storage and river and floodplain restoration to coastal management (Figure 1.1). A key feature of many

WwNP measures is the ability to store and attenuate floodwater to reduce flood risk. Several measures aim to do this including certain headwater drainage management, leaky barriers, run-off attenuation features, offline and online storage features (Figure 1.1). Differences between these features typically relate to the size, structure and location within the catchment however they need to be designed to control inflow and outflow to ensure sufficient flood storage capacity when it is most needed (Ngai et al., 2017, Lane, 2017).

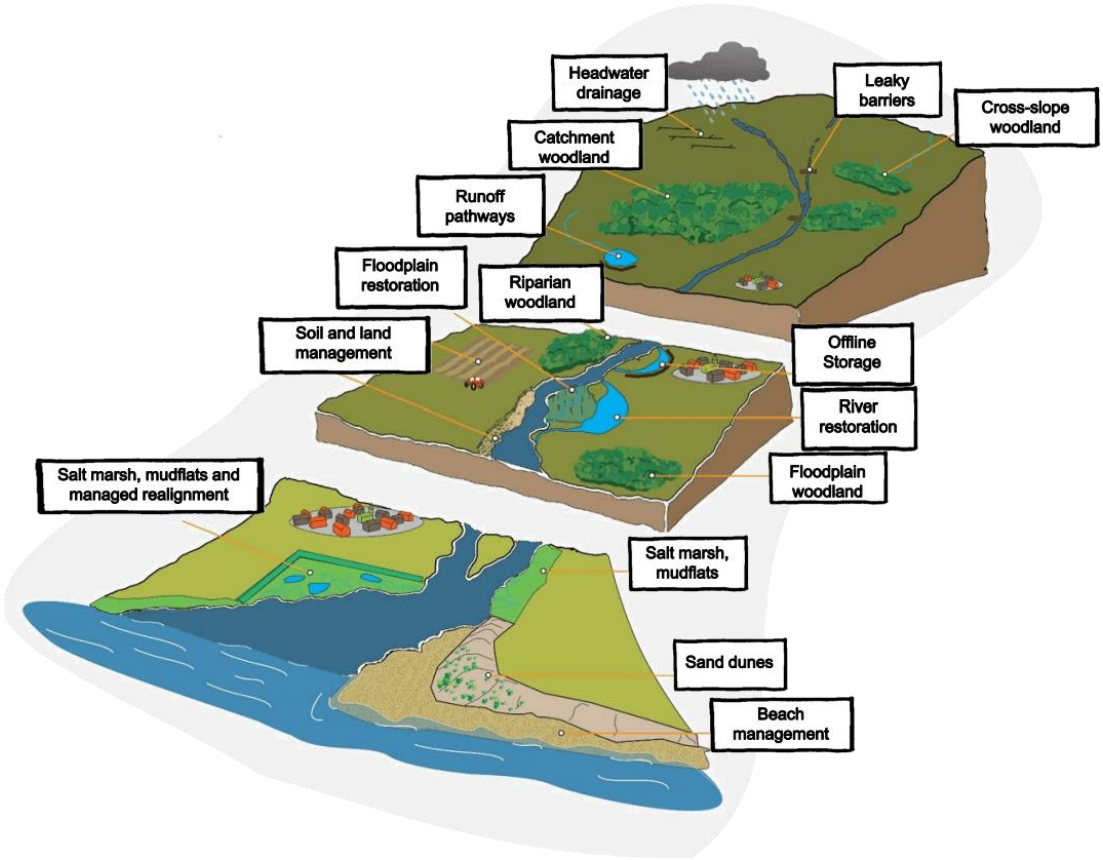

Figure 1.1: Diagram of working with natural processes measures from Burgess-Gamble et al. (2017, p. 3)

1.2.1.1 Headwater drainage management

Grip blocking involved the use of peat dams, heather bales and stone dams up to approximately 2 m in width to restore the natural drainage pattern of headwater heath and blanket bog (Yorkshire Peat Partnership (YPP), 2017). This allows for the regrowth of vegetation and a reduction in erosion (Holden, Gascoign and Bosanko, 2007). They can also act as small-scale additional flood storage, increasing travel times and reducing peak flows, although evidence for their flood

risk benefit is inconsistent (Shepherd et al., 2013). Grip blocking is perhaps the smallest (in terms of size) natural flood risk reduction measure.

Slightly larger than grips, naturally occurring gullies are slope-aligned, erosional features within peat. In a similar manner, to grip blocking, gullies can also be blocked (< 4 m) through the use of timber or stone dams to encourage the regrowth of vegetation and restabilisation of the gully (Trotter et al., 2005). In doing this, there is also the opportunity to increase travel time through the reduction of flow velocities and creation of temporary flood storage (Parry et al., 2014).

1.2.1.2 Runoff pathway management features

Runoff is the movement of water over the land surface towards a body of water. Known collectively as runoff attenuation features (RAFs), ponds, sediment traps and swales are implemented to disconnect runoff pathways, slow and store runoff water, increasing the travel time and attenuating the flood water (Nicholson et al., 2012). Although single features are unlikely to provide any flood risk benefit, a number of features distributed throughout the catchment network, provides the potential to temporarily store flood water (Quinn et al., 2013). Characteristically, RAFs are created by excavating an area or utilising a naturally occurring concavity with a permeable barrier at the outlet to allow for the controlled movement of some water whilst maintaining flood storage (Environment Agency, 2012b). RAFs can be dry until sufficient runoff causes them to be utilised, or permanently wet. RAFs additionally allow for the deposition of fine sediment, which provides water quality benefits, however this may also require management if the outlet pipe becomes blocked, particularly if sedimentation occurs through smaller events (Barber and Quinn, 2012).

1.2.1.3 Leaky barriers

Leaky barriers are mainly composed of pieces of wood in river channels which retain and slow the movement of water, attenuating flood waves and reducing average flow velocity (Gippel, 1995). They are both naturally occurring or can be engineered within flood risk management projects and vary in shape, size and for engineered ones, vary in terms of their “naturalness” (Dodd et al., 2016). Many different terms are used for leaky barriers, with leaky dams, large woody debris dams and jams and engineered log jams all commonly used within the literature.

Barriers can either partially or fully block the width of a channel, however they do not fully impede flow, with baseflow allowed to freely move below barriers and floodwater allowed to leak between tree trunks and branches that make up the barrier (Wallerstein and Thorne, 1997; Dodd et al., 2016). Leaky barriers can slow the flow of water and divert flows and increase floodplain connection (Sear et al., 2010). They can also retain sediment and induce localised bed and bank scour and provide new habitat and food sources for local biota (Nagayama and Nakamura, 2010). The increase in popularity of engineered leaky barriers for flood risk and river restoration purposes over the last couple of decades has led to a number of uncertainties in their use (Grabowski et al., 2019), from the size and design of individual barriers, location within the catchment, local upstream and downstream risk, maintenance and public perception.

1.3 Understanding the geomorphological impact of RAFs

The preceding sections highlight the running theme of the selected measures discussed, they block or partition a runoff pathway or channel to a greater or lesser extent depending on the measure with the aim of attenuating flow. Although located across the catchment and varying in size, albeit small scale compared to traditional flood defence works, collectively they can be described as runoff attenuation features, or RAFs (Quinn et al., 2013). Their impact on geomorphology is understood with less certainty, particularly when looking at features constructed from a flood risk perspective. Comparisons can however, be drawn from features which are similar, such as traditional river infrastructure, natural wood in rivers, erosion control measures and sediment traps.

Geomorphological impacts of traditional river infrastructure, which have similar hydraulic behaviours to RAFs such as weirs and culverts, can be used to gain additional understanding of analogous NFM features. Culverts force water to be constricted through a narrow opening, similar to the gap beneath a leaky barrier, or the outlet pipe infrastructure of offline storage bunds. The geomorphological impacts of bottomless culverts, in which the natural bed is intact, are erosional, in which Crookston and Tullis (2012) observed scour at the culvert inlet, the downstream half of the culvert and at the culvert outlet. Once flow exits any culvert, a scour hole can be created, depending on bed material (Rajaratnam and

Berry, 1977; Liriano et al., 2002). In traditional culverts, made of unerodbile materials, it is unlikely that erosion will occur within the culvert itself.

Weirs cause small increases in the difference in upstream and downstream water depths, similar to an overtopping leaky barrier or earthen bund, however water is not typically stored for long periods upstream and weirs are submerged in flood events (Csiki and Rhoads, 2010). At low flows, weirs cause a backwater effect, with lower velocities and a greater chance for sediment deposition upstream of the weir (Wildman and MacBroom, 2005). As stage increases, the backwater effect decreases and sediment deposited at low flows may be re-mobilised (Csiki and Rhoads, 2010). Once a weir is fully submerged, suspended sediment transport is unimpeded, the likelihood of larger sediment being transported over the weir would be dependent on the flow conditions and power required to entrain and transport the material over the blockage to flow (Csiki and Rhoads, 2010). Longitudinal impacts of weirs on geomorphology will depend on the hydraulic conditions on the channel and flow event. If a weir is not trapping sediment, there is likely to be little downstream geomorphological influence. If a weir is trapping sediment, erosion may occur downstream of the structure (Csiki and Rhoads, 2010).

Leaky barriers, as a type of within channel RAF, are also analogous in design to natural accumulations of wood in rivers. The geomorphological impact of woody debris in rivers is well understood and researched. Naturally occurring wood, be that pieces or logjams, affects geomorphology at a variety of scale, from channel roughness and grain size to the formation of landforms. Woody debris can block the channel and therefore trap and store sediment, creating bar formations (Montgomery et al., 2003). Blockages by woody debris can also cause scour whereby logs which are located above the bed force flow downwards causing bed scour (Beschta, 1983; Hogan, 1986; Robison and Beschta, 1989; Wood-Smith and Buffington, 1996). If a gap has been left at the bed to allow flow to be unimpeded, scour may also occur to the bed immediately below the structure (Wallerstein and Thorne, 2004; Schalko et al., 2019). Woody debris can also locally direct the flow towards banks and cause localised bank scour of material that is often finer and more susceptible to erosion (Hogan, 1986; Nakamura and Swanson, 1993; Davis and Gregory, 1994; Abbe and Montgomery, 2003). If the in channel woody feature is designed to allow for inundation of the floodplain,

localised bank erosion where the flow pathway is forced onto floodplain is likely to occur (Wohl, 2013). Once on the floodplain, water forming a dendritic network of micro channels allows for settling of fine sediment and flow concentration has the potential to scour secondary channels (Jefferies et al., 2003; Sear et al., 2010).

An offline runoff attenuation feature which is located on a hillslope, is likely to have water enter slowly and remain for some time, which allows fine sediment to fall out of the water column (Nakamura and Swanson, 1993; Holden, Gascoign and Bosanko, 2007; Barber and Quinn, 2012). This can be a positive or negative, allowing sediment to settle can improve downstream water quality as nutrients and metals can sorb to sediment particles (Fiener et al., 2005; Wallage et al., 2006; Law et al., 2016). If the water is particularly sediment laden, allowing it to settle out has the potential to decrease the capacity of the feature to store and attenuate water (Metcalfe et al., 2017). However, UK headwaters are susceptible to erosion as historical management practices have reduced vegetation cover (Holden, Shotbolt et al., 2007). Features located within fields have the aid of the grass to protect the basin of features against erosion (Pan and Shangguan, 2006) and the roughness of the grass will assist in fine sediment deposition (Daniels and Gilliam, 1996).

The geomorphological impact of a feature will be dependent on its size in relation to the size of the flood event. If features are overtopped, not only do they provide little further attenuation benefit (Wilkinson, Quinn and Welton, 2010), the force of the water over the top of the feature may cause erosion if the feature is made from soil (Nicholson, 2013). Furthermore, the force exerted on a structure in large events can lead to failure (Nichols and Ketcheson, 2013), although stability of wood placements for river restoration varies greatly (Roni et al., 2015).

These geomorphological impacts of RAFs are important. Their influence on erosion and deposition can increase habitat heterogeneity (Abbe and Montgomery, 1996), improve water quality (Barber and Quinn, 2012), reduce erosion and restabilise moorland (Trotter et al., 2005). However, if their structural integrity is undermined, not only would they have no attenuation benefits, sediment previously held within features will be mobilised (Linstead and Gurnell,1999) which may choke downstream sediments making up healthy fish habitats (Marks and Rutt, 1997). Therefore it is important that they are maintained

correctly and checked regularly (Verstraeten and Poesen, 1999; Grabowski et al., 2019). Design specifications may require more engineered aspects including reinforcement of susceptible parts including spillways (Wilkinson, Quinn, Benson and Welton, 2010). If the system is particularly sediment laden, blocking flow pathways leading to subsequent sedimentation and reduction in capacity will increase the need for long term management of the removal of sediment (Quinn et al., 2013).

1.4 Assessing the geomorphological impact and hydrological effectiveness of RAFs

A number of key projects have been set up in the UK to showcase the effectiveness of RAFs from a flood risk perspective. They span from demonstration catchments which are fully monitored, to projects where both monitoring and modelling have been used to assess the effectiveness of RAFs, to modelling only projects that have provided scenario based assessment to quantify RAF requirements to match certain levels of flood risk protection.

Monitoring prior to the installation of any measures allows for the geomorphological and hydrological character of the catchment to be assessed to avoid unforeseen reactions to the implementation of features. It also allows for vital local knowledge to be included to aid location and design of features (Skinner and Bruce-Burgess, 2005). Monitoring is required in post-project appraisals if compliance is needed under the Water Framework Directive, however the extent and frequency of monitoring varies greatly depending on the risk and uncertainty relating to construction and is often basic. A lack of monitoring is impeded by the lack of budget and timeframes for which it needs to be spent compared to the timescales over which geomorphological changes may occur (Skinner and Bruce-Burgess, 2005). England et al. (2008) highlight the need to monitor a few projects well as opposed to monitoring all schemes poorly taking into account the scale and novelty of the technique when deciphering the level of detail required.

Modelling allows for high resolution analyses to be made across a wide range of spatial and temporal scales which are unachievable to the same extent in monitoring networks (Hankin et al., 2017). Modelling allows for a number of scenarios to be run for feasibility testing of designs, locations and networks of features in response to a variety of flood events to refine project proposals and

engage landowners prior to construction (Hankin et al., 2017). It also provides the opportunity to assess the impact of features over multiple events and long timescales to assess management needs and gradual geomorphological changes. Modelling is therefore computationally expensive in terms of expertise, data needs and time required to set up and run models (Lane, 2017).

However, modelling, particularly for geomorphological questions, is often beneficial given the variability of geomorphological processes, the dearth of baseline sediment monitoring data available in the UK (Skinner and Bruce-Burgess, 2005) and the difficulty and expense in accurately measuring erosion, transport and deposition of sediment over spatial and temporal scales necessary for meaningful conclusions (Graf, 2008). Given the scarcity of geomorphological data within the UK, exploratory modelling, in that models are set up and parameterised based on real-world catchments but not necessarily validated against monitoring data from them, provides an opportunity to efficiently investigate general effects of runoff attenuation features in a number of situations as described above. Such modelling is important to increase our understanding of, particularly, the potential hydro-geomorphological impacts of RAFs whilst monitoring data is collected over a wide range of RAF types, designs and catchment types and designs.

Exploratory model data may also provide insight for monitored projects in the meantime to, for example, refine effective designs and locations. Monitoring data can be then fed into the model to allow for more accurate predictions of the measures which allows for the model to assess the impact of measures over a range of spatial scales for flood magnitudes which rarely occur naturally (Hankin et al., 2017). A hybrid approach such as this provides an important feedback loop between modelling and monitoring efforts to increase our understanding and reduce model uncertainty (Stewardson and Rutherfurd, 2008). It is however, a highly expensive approach given the need for both complex modelling and monitoring, and thus many studies focus on one over the other to provide evidence and data for future applications.

1.4.1 Main case studies

1.4.1.1 Pickering

Perhaps most nationally recognisable, the NFM work undertaken in Pickering Beck (69 km^2) received much media coverage when the measures were attributed to reducing the Boxing Day 2015 flood peak by between 15 and 20 % (Slowing the Flow Partnership, 2016). Aided by a £ 3.2 m large engineered bund with a storage capacity of 120,000 m^3 located the furthest downstream of all the features, the additional 129 large woody debris dams and 187 heather bale check dams provided an additional 8,000-9,000 m^3 of storage (Nisbet et al., 2015). Tree planting, moorland reseeding and farm improvements were also undertaken. The relative contribution to the Boxing Day flood peak reduction between the large bund and other features was estimated to be roughly half and half (Slowing the Flow Partnership, 2016).

Although a monitoring network was implemented, insufficient time to acquire baseline data, a lack of out of bank flows for discharge rating and differences between rainfall events inhibits comparison and evaluation of the features effectiveness (Nisbet et al., 2015). Modelling did however provided the project with estimated levels of flood risk reduction for individual measures. The large bund provided a flood risk reduction in any given year from 25% to 4% (Nisbet et al., 2015). HEC-RAS was utilised to assess storage of the smaller features, with the large woody debris dams resulting in estimated storage between 0.1 m^3 and 108.9 m^3 individually and a combined estimated storage for all 129 dams of 1,300 m^3 (Nisbet et al., 2015). Although their geomorphological impact has not been noted, a failed dam in 2012 and two other dams, one which had shifted, were causing localised bank scour as flow was deflected around them and towards the bank. Given their location alongside the North Yorkshire Moors Railway, they were subsequently removed in 2014 to avoid the possibility of undercutting and were replaced by 5 dams in a different location (Nisbet et al., 2015).

1.4.1.2 Belford

The size of the 6 km^2 Belford catchment and a lack of space meant traditional flood defence works were unfeasible. However, 25 properties within the village were still at risk from 1 in 2 year flood events and 54 properties and a caravan park were at risk from a 1 in 100 year flood event (Nicholson et al., 2017).

Approximately 40 runoff attenuation features were implemented in a number of phases including large woody debris dams, overland flow interceptors, small storage features and soil bunds (Nicholson et al., 2020). Storage capacities ranged from between 50 m^3 – 150 m^3 for online ditch features and large woody debris dams to 200 m^3 – 3000 m^3 for offline ponds and 1000 m^3 – 3000 m^3 for opportunistic RAFs (Quinn et al., 2013).

Five years of intensive rainfall, stage and flow monitoring have been completed, with almost a year of baseline data prior to construction of first features. Level monitoring within the RAFs themselves was also included (Nicholson et al., 2017). Monitoring of levels in one of the pilot features, a timber barrier with a storage capacity of approximately 800 m^3 resulted in an average 15 min delay to flood peak travel time over 1 km compared to before it was constructed, although no significant change was observed further downstream (Wilkinson, Quinn and Welton, 2010). Observed data has also allowed for refinement of designs of RAFs implemented (Quinn et al., 2013). Although a lack of data inhibited the estimation of a catchment response (Nicholson, 2013), pond forensic analysis allowed for the effects of individual features to be analysed and showed offline features have minor effects on downstream discharge for high magnitude, long duration events as they fill too early (Nicholson, 2013). The observed data has however allowed for the validation of “the pond model” which through the use of simple hydraulic equations to represent the inflow and outflow of a feature, could be used to explore changes to design (Nicholson et al., 2020). Nicholson et al. (2020) used the pond model in a network to assess the impact of multiple identical offline features in sequence. By incrementally increasing the number of features within the network, discharge was significantly reduced, with 35 features creating storage of 20,000 m^3 having the potential to reduce a 1 in 12.5 year event (classified by the 24 hour rainfall total) by approximately 30 % (Nicholson et al., 2020).

With regards to their geomorphological impact and management needs, sedimentation was qualitatively noted in some of the RAFs (Wilkinson, Quinn and Welton, 2010). Quantitatively, one of the overland flow interceptors built, consisting of a soil bund with a storage capacity of ~ 500 m^3 (Barber, 2013), caused 0.99 tonnes of sediment to be deposited in one flood event in 2011. Suspended sediment exiting the outflow pipe was also noted (Palmer, 2012). The

possible requirement for periodic removal of sediment to maintain overall capacity of pond was therefore highlighted (Barber and Quinn 2012, Wilkinson et al., 2014, Nicholson, 2013). Despite the sedimentation behind the bund, a significant proportion of polluted runoff was not retained due to the underlying tile drainage (Barber, 2013). A different RAF in the catchment with a capacity of 200 m^3 was seen to quickly collect sediment at the inlet however nutrient loads were insignificantly different at the inlet compared to the outlet (Barber, 2013). It was theorised that sediment was delivered to the pond via chronic runoff during smaller events, aiding relief here, but remained ineffective in larger storms, with the addition of sediment being unsettled adding to their failure (Barber, 2013). Considerations were also made in relation to possible scour. Large woody debris dams were placed in close succession to reduce stream power and the possibility of bank erosion (Wilkinson, Quinn, Benson and Welton, 2010), timber bunds were erected as opposed to soil bunds in some circumstances to avoid possible erosion from cattle grazing (Wilkinson, Quinn and Welton, 2010) and outlet pipes were located in bunds to reduce the likelihood of overtopping and the possibility of scour (Barber and Quinn, 2012).

1.4.1.3 Holnicote

Holnicote was one of the original three DEFRA multi-objective food management demonstration projects (National Trust, 2015). Spanning two adjacent catchments (Aller and Horner Water), a wide range of techniques were implemented. In the 18 km^2 Aller catchment, old ponds were cleared alongside the creation of floodplain bunds adjacent and perpendicular to the channel to increase flood water storage (Glendell, 2013). A small floodplain woodland and some woodland buffers were planted in addition to arable reversion of four fields (Glendell, 2013). In Horner Water (22 km^2), upland ditch blocking was undertaken, alongside the addition of large woody debris dams, and grass reversion works (National Trust, 2015).

An extensive rainfall, stage and flow monitoring network was instated alongside a water quality sampling regime in the Horner Water catchment to assess the impact of the features across the two catchments. Results from hydrograph analysis were generally inconclusive and a range of factors were highlighted to be affecting this, including climate variability, short monitoring timescales and the failure of key monitoring equipment (National Trust, 2015). However, small

improvements have been noted with regards to hydrograph delay from the combination of large woody debris dams and the drain blocking in the Horner Water catchment (National Trust, 2015). Monitoring evidence also suggested the floodplain storage measures in the Aller catchment were having an effect, but only for extreme flood events when out of bank flow occurred (National Trust, 2015). The monitoring network also provided data for modelling efforts, used to aid the siting of features and to assess their hydrological impact. A linked ISIS and TUFLOW 1D-2D hydrodynamic floodplain and channel model was created to refine the design of the floodplain bunds, the results of which aided the consent process (National Trust, 2015). The Aller's 5 offline storage ponds with a holding capacity total of ~25,000 m^3, were shown to reduce the flood peak by 10 % for a 1 in 75 year event from 2013 in addition to reducing the flood extent downstream (National Trust, 2015). Further reductions in peak flow were calculated with a possible 25 % reduction for a 1 in 5 year event.

The Holnicote project focuses less on the geomorphological impact of the features implemented, perhaps due to a lack of financial incentive given the good status of the Aller and Horner Water under the Water Framework Directive (Rodgers et al., 2015). The Horner Water water quality sampling showed ditch blocking had no significant impact in the catchment (Glendell, 2013). It was however, noted that due to high visitor numbers and soft bedrock, erosion had occurred to some of the ditch blocking features requiring improvements to be made to increase their resilience (Hester et al., 2017).

1.4.2 Evidence gaps

Regardless of the approach taken to increase the understanding of the impact of runoff attenuation features, there is a notable imbalance between the focus on hydrological evidence compared to geomorphological evidence. This is most likely due to the difficulties in monitoring and modelling geomorphological change as highlighted previously, particularly when projects have tight timeframes and budgets.

1.4.2.1 Design

There is limited evidence available on the specific design of NFM measures (Burgess-Gamble et al., 2017), one of the barriers to wider uptake highlighted by several authors (Blanc et al., 2012; Waylen et al., 2018; Wells, 2019). Design

principles and criteria alongside maintenance guidance is coming (Ciria, 2018) with publication aimed for end of 2021 (Mott Macdonald, 2020). Some indicative designs of certain measures (e.g. leaky barriers) are openly available to qualify for certain funding streams such as Higher Tier Countryside Stewardship. For payments of £461.39 for a small and £764.42 for a large leaky barrier, they firstly need to be built in sequences of three, extend 3 to 6 m onto the floodplain and contain between 3 to 4 logs depending on size (Rural Payments Agency, 2020). However most projects rely on recommendations (e.g. Farming and Wildlife Advisory Group (FWAG) South West, 2018) with examples including the spacing between leaky barriers being seven times the channel width with a height above baseflow of 300 mm (Yorkshire Dales Rivers Trust (YDRT), 2018a). Many features, of a wide variety of designs, have been implemented without robust supporting empirical evidence for wide ranging catchment and reach types. For larger measures such as large bunds and storage features, more specialised designs are required for consent purposes, with land drainage specialists or consultancies often being involved (Yorkshire Dales National Park Authority (YDNPA), 2017 and e.g. YDRT, 2018b).

Although the implementation of measures should be focused on the individual catchment's needs and a one size fits all design is unlikely to be effective (Lane, 2017), quantifying the impacts of different designs will reduce the uncertainty in the overall uptake of NFM. Reducing the uncertainty may lead to improvements in legislation and funding opportunities (Wells et al., 2020). It will also aid those with smaller budgets who may not have the capacity for a specialist design process.

1.4.2.2 Scale

Even when evidence on NFM design is published, features will behave differently at different scales. Such interactions are also understudied (Dadson et al., 2017). There is still a lack of evidence into the effectiveness of features seeking to naturally attenuate flow and store water, such as leaky barriers, on and offline storage and run-off attenuation features at catchment scale for larger flood events (Burgess-Gamble et al., 2017). It is however, assumed that the effect will decrease with increasing flood magnitude and spatial scale (Dadson et al., 2017). In addition to this, their effectiveness as small-scale measures alone, how they perform through a storm event and cumulative effects as features distributed

throughout a catchment are also not well understood (Burgess-Gamble et al., 2017). Although it is understood that a lot of these features will trap sediment, the flood risk benefits of trapping sediment is not known, such as whether this improves downstream conveyance of channels (Burgess-Gamble et al., 2017). The absence of confidence in the effectiveness, governance and funding of NFM measures has inhibited their national uptake (Wells et al., 2020).

1.5 Research questions

This thesis aims to provide an understanding of both the hydrological and geomorphological impact of runoff attenuation features to alleviate the evidence gaps relating to the design of features and their impact at a variety of scales. With consideration of the evidence gaps and an understanding of the complexity of investigating catchment scale effects through the use of monitoring, this thesis takes an exploratory modelling approach to seek an answer to the following three overarching research questions:

1. What are the hydrological and geomorphological impacts of runoff attenuation features implemented within a morphodynamic model at catchment scale?
2. Can geomorphological processes be estimated without recourse to morphodynamic models?
3. How does leaky barrier design affect the hydrological and geomorphological impact at increasing event magnitudes at reach scale?

1.6 Thesis structure

To answer the aforementioned research questions so they can, not only be read together but also stand alone as separate pieces of research, each of the research chapters contains a focussed introduction to the literature, methodology, results, discussion and conclusion.

Considering the modelling nature of this thesis, following this introduction chapter, Chapter 2 provides a site description and an overview of the morphodynamic model (CAESAR-Lisflood) set up and how the understanding gained from the process is used within the first two research chapters. The full model set up sensitivity analysis is available at the end of the thesis in Appendix A.

Chapter 3 answers the first of the research questions and involves the use of CAESAR-Lisflood to assess the hydrological and geomorphological impacts of runoff attenuation features of differing designs for a ~41 km^2 Yorkshire catchment.

Chapter 4 seeks to answer the second research question through a comparison between CAESAR-Lisflood and HEC-RAS 2D to assess whether HEC-RAS 2D can alone be used to approximate geomorphological processes. Evidence gathered from visits to the ~13 km^2 sub-catchment following a recent flood event alongside repeat aerial imagery was used to aid the comparison process.

Chapter 5 takes lessons learnt from the previous research chapters and applies the highest modelling resolution and smallest spatial extent of the three chapters in HEC-RAS 2D to assess a hydraulic structure implementation of a single leaky barrier. The effect of leaky barrier design on hydrological and geomorphological metrics is assessed for increasing event magnitudes.

Chapter 6 discusses the major outcomes of the three research chapters and how they fit together to decrease the uncertainty in the understanding of the hydrological and geomorphological impacts of runoff attenuation feature design and differences occurring at different spatial scales and from different event magnitudes.

Chapter 7 includes the concluding remarks from this thesis' research and findings.

Chapter 2
CAESAR-Lisflood model set up

This chapter provides a catchment description and an explanation of the set up of the CAESAR-Lisflood models used to answer the project's research questions as seen in Figure 2.11 and as detailed in Chapters 3 and 4. In order to keep this chapter clear, details of model set up have been provided, the sensitivity of each change on water and sediment discharge, water volume and net elevation change are given in Appendix A, alongside additional information on individual parameters where deemed necessary.

2.1 Site choice and description

The Eastburn Beck catchment, West Yorkshire, was chosen for this study as there are known flooding and sediment issues in the catchment and natural flood management has been proposed as a recommendation to reduce future flood risk by North Yorkshire County Council (NYCC, [no date]). Zonal statistical analysis using SCIMAP (Reaney et al., 2011) data across the wider Aire catchment in which Eastburn Beck sits, showed that Eastburn Beck had the highest mean channel sediment accumulated risk of any of the Aire sub-catchments (Figure 3.1b). The catchment also has a gravel trap near the catchment outlet which fills regularly and it is underachieving in the Water Framework Directive (WFD) for sediment issues. Villages around Eastburn Beck, including Sutton-in-Craven, Glusburn and Cross Hills have flooded regularly in recent years. In 2004, 70 properties were affected in Sutton-in-Craven (Yorkshire Flood Resilience, [no date]). In 2015, the largest flow was recorded at the river gauge at the outlet of the catchment. Within the villages near the catchment outlet, 19 properties were flooded in Cross Hills, 8 properties were flooded in Glusburn and 10 properties flooded in Sutton-in-Craven (NYCC, [no date]).

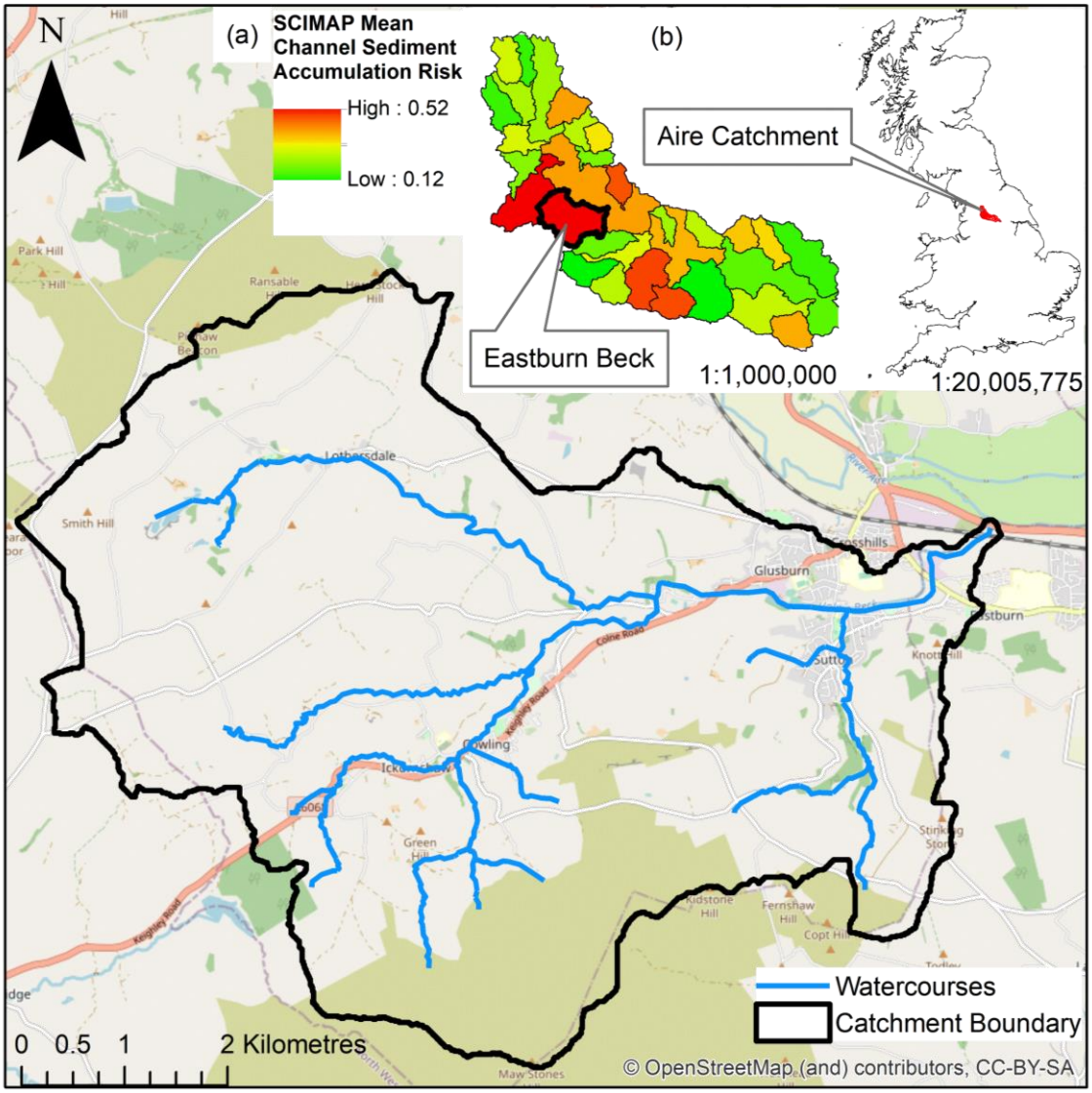

Figure 2.1: Eastburn Beck catchment location with insets of (a) location of Eastburn Beck in the wider Aire catchment annotated with mean SCIMAP channel sediment accumulation risk, calculated for each sub-catchment and (b) the location of the Aire catchment in the UK.

Eastburn Beck is the final name of the watercourses in the 40.8 km^2 catchment with river channels 20.3 km in length. The catchment is a typical steep upland catchment in the UK and drains primarily sheep grazed fields and moorland, before flowing through the low-lying settlements of Glusburn and Sutton-in-Craven to its confluence with the River Aire approximately 1 km downstream of Kildwick (Figure 3.1a). The catchment is situated within the wider River Aire catchment, to the north west of Leeds (Figure 3.1b).

The elevation rises from a minimum of 87.9 mAOD in the east to a maximum of 442.1 mAOD in the south. The geology of the area is low permeability Millstone Grit, however the majority of the catchment is covered by Till superficial depositions of mixed permeability (Figure 2.2) (NRFA, [no date]). The soil is

thought to be highly permeable, with a shallow water table (NYCC, [no date]). The BFIHOST is a base flow index, in which a higher value suggests a strong baseflow influence and lower values have a weaker baseflow influence. In Eastburn Beck, the BFIHOST is 0.32, suggesting the catchment will respond quickly to heavy periods of rainfall. In addition to the BFIHOST, PROPWET is a catchment wetness index and a measure of the proportion of the time in which the soils are wet. For Eastburn Beck, PROPWET is 0.62, suggesting the often saturated soils in the catchment are likely to contribute to larger flood events (NRFA, [no date]).

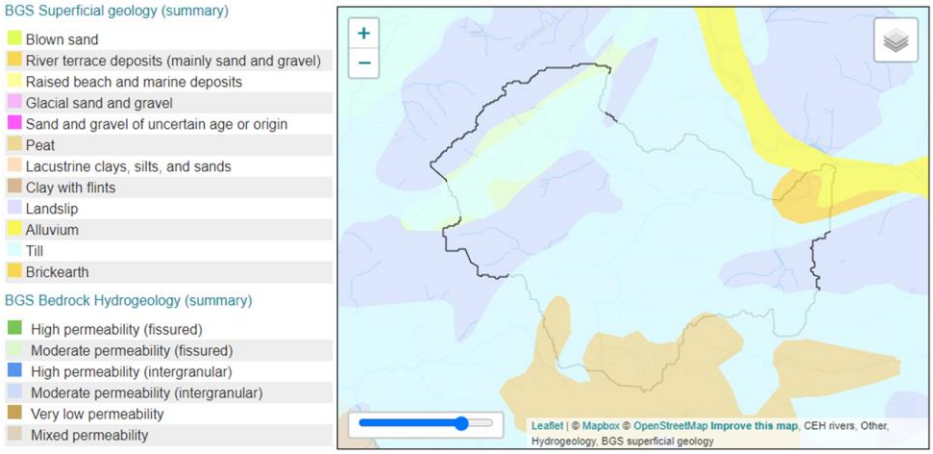

Figure 2.2: Geology of Eastburn Beck (NRFA, [no date])

The primary land cover in the catchment is grassland (Figure 2.3), which is predominantly grazed by sheep, with 76% coverage. Moorland is present in the south and north-west of the catchment (9%) and is the secondary land cover. Patches of arable woodland (6.39%) and arable farming (2.73%) are scattered across the catchment before the watercourse flows through the urban settlements in the low-lying land near the catchment outlet (4.38%).

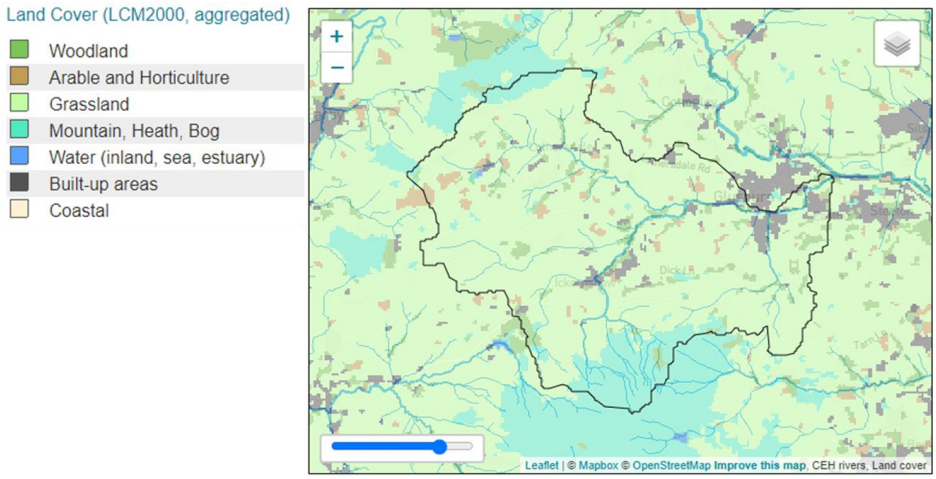

Figure 2.3: Land cover of Eastburn Beck (NRFA, [no date])

The villages near the catchment outlet are at risk from flooding from rivers and surface water (Figure 2.4). At particularly high risk are properties adjacent to the watercourse, which at this point is called Holme Beck. Once banks are overtopped, flood water flows through the fields between Glusburn and Eastburn before flowing towards the floodplain of the River Aire.

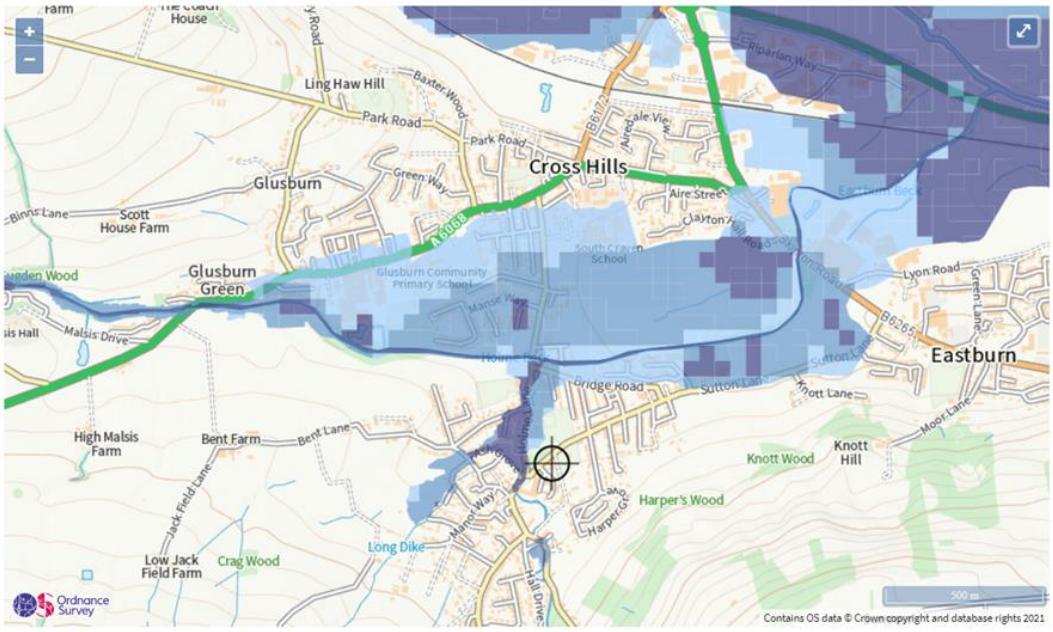

Extent of flooding from rivers or the sea

High Medium Low Very low Location you selected

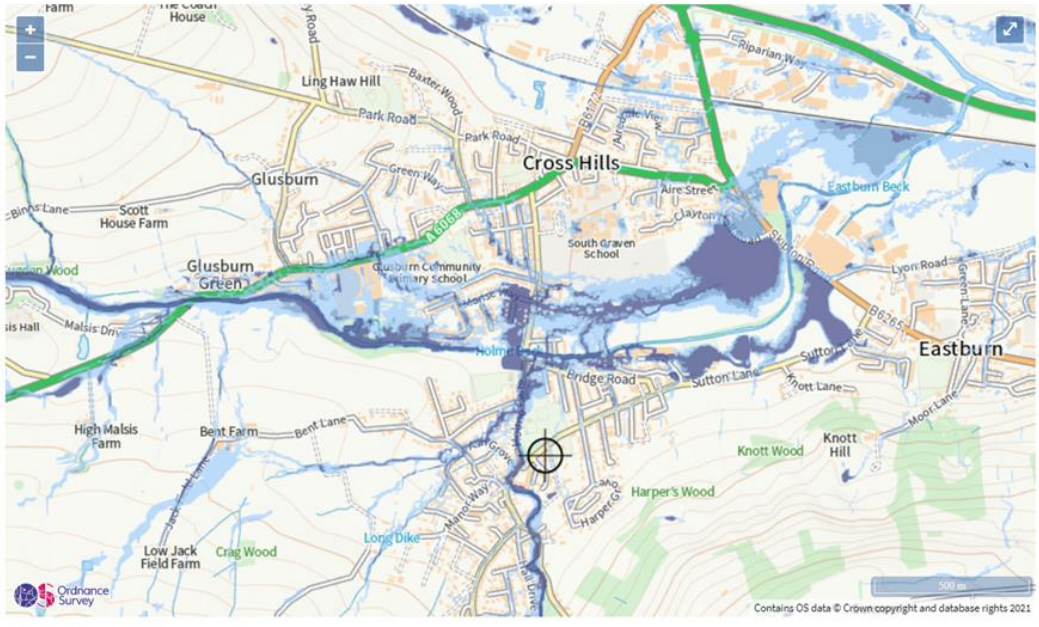

Extent of flooding from surface water

High Medium Low Very low Location you selected

Figure 2.4: Environment Agency's extent of flooding maps from rivers or the sea and from surface water for the settlements near the outlet of the Eastburn Beck catchment (Environment Agency, [no date])

2.2 Model set up

2.2.1 Model choice

CAESAR-Lisflood was chosen as the morphodynamic model for this project due to its ability to simulate erosion and deposition in a spatially distributed manner without inhibitively large data requirements and computational demands as seen in other physically-based spatially distributed models such as SHETRAN and WEPP (Meadows, 2014). CAESAR-Lisflood is a modified version of CAESAR, a Landscape Evolution Model (LEM) (Coulthard et al., 2013). It has advantages over other LEMs due to (Meadows, 2014):

- The implementation of a derivation of the LISFLOOD-FP flow model providing greater representation of water movement across the model.
- The ability to enter a 9-fraction grain size distribution allowing representation of the movement of suspended sediment, alongside lateral erosion to simulate meandering.
- The capacity to simulate at high temporal (hourly) resolutions allowing individual storms to be assessed.

2.2.2 Initial set up and sensitivity testing

2.2.2.1 Data Inputs

Ordnance Survey Terrain 5 m DTM was resampled using ArcGIS's resampling tool with bilinear resampling technique to 10 m resolution to allow for the entire catchment to be modelled (410,430 modelled cells). The DEM was then hydrologically corrected using the ArcGIS "Fill" tool. Given the need for a coarse resolution for model efficiency during sensitivity analysis, main channels were burnt into the DEM to allow for the issue of resampling reducing the height of banks and increasing the height of channel beds to be accounted for. The main channel network was derived from OS Open Rivers, which was checked against aerial imagery and expanded where necessary. Burning depths were based on the Strahler stream order with a single cell width line of DEM cells representing the channels being decreased by up to 2 m (Figure 2.5).

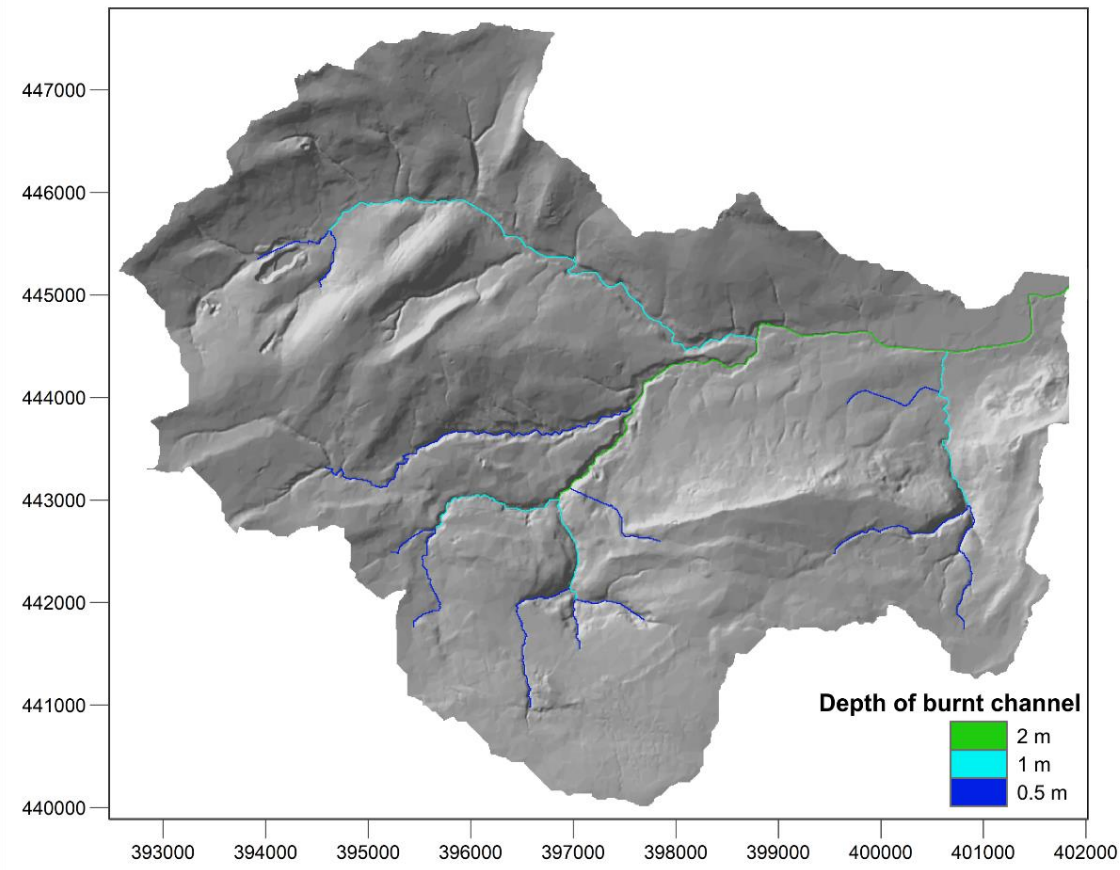

Figure 2.5: Depths of channels burnt into the Eastburn Beck catchment 10 m resolution DEM.

The CORINE 2012 data set was chosen to represent land cover (Figure 2.6) as it was freely accessible and was used in the Environment Agency's WwNP project (SC150005). It was converted into a 10 m resolution raster layer of land cover codes. Land cover codes were then converted into values of parameters that were proxies for land cover as discussed below such as Manning's n. The Manning's n roughness co-efficient is part of the Lisflood-FP flow model integrated into CAESAR-Lisflood and is included in the equation governing flow between cells (Bates et al., 2010). As a result of its use as a land cover parameter, many previous studies and handbooks have suggested appropriate values and a literature review was used to gather appropriate values from Chow (1959), McHugh et al., (2002), Kalyanapu et al., (2009), Grimaldi et al., (2010), Brunner (2016). The values found in the literature for each land cover were then averaged.

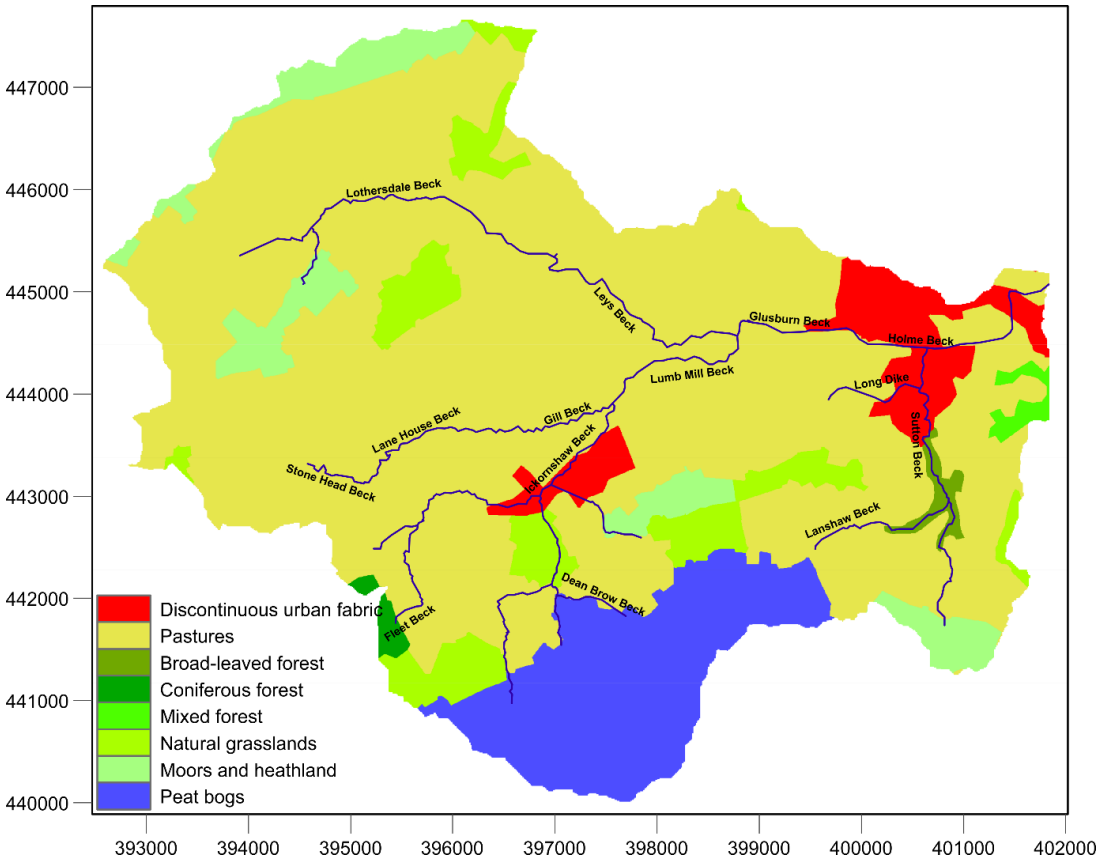

Figure 2.6: CORINE 2012 Land Cover for the Eastburn Beck catchment.

To model the December 2015 flood in CAESAR-Lisflood, daily rainfall data was used from the freely available and accessible Centre for Ecology and Hydrology Gridded Estimates of Areal Rainfall (CEH-GEAR) dataset. Two months (November and December 2015) of data from the grid cell at the centroid of the Eastburn Beck catchment was converted from daily totals into millimetres per hour and applied across the model domain.

2.2.2.2 Parameterisation and sensitivity analysis

Skinner et al.'s (2018) global sensitivity analysis on the River Swale was used as a basis for the selection of parameters to test in the application of CAESAR-Lisflood to the Eastburn Beck catchment. The most influential parameters for the River Swale were the sediment transport rule, Manning's n roughness co-efficient, in-out difference, grain size distribution and evaporation rate (Skinner et al., 2018). Previous studies have also shown sensitivity to the m parameter and rainfall input (Coulthard and Van De Wiel., 2017; Coulthard and Skinner, 2016).

CAESAR-Lisflood allows for the choice between two sediment transport rules, Wilcock and Crowe (2003) and Einstein (1950). Wilcock and Crowe (2003) was developed with coarser gravel field and laboratory data, whereas Einstein (1950)

was developed with sand based laboratory data. An initial, basic test on the two rules suggested that the Einstein rule dramatically over-estimated the amount of sediment exiting the catchment (max Qs = 2126 m^3hr^{-1}). Given the coarser nature of the sediment seen within the Eastburn Beck catchment and the overestimation of the Einstein rule, the Wilcock and Crowe rule was chosen for the remained of this research.

A sensitivity analysis of six CAESAR-Lisflood parameters and the rainfall input data was undertaken. These were Manning's n, m parameter, in-out-difference, grain size distribution, vegetation critical shear stress and evaporation rate, values tested can be found in A.1.1. Values for each parameter were based on those within the default CAESAR-Lisflood parameter set or values identified in the literature and from field visits. All model runs were compared for differences to water and sediment discharge, flood extent and net elevation change occurring from changes in parameter values. The full results of this sensitivity analysis can be found in A.2.1. To summarise, water discharge was sensitive to the intensity of rainfall and the *m* parameter (Section A.2.1.1). Parameters causing the most sensitivity to sediment related outputs were the grain size distribution and Manning's n (Section A.2.1.2).

An optimum parameter set was found by analysing the effect changing parameters values had on 21 model efficiency metrics including mean absolute error (MAE), mean relative error (MRE), Nash-Sutcliffe efficiency (NSE) and root mean squared error (RMSE) (Section A.2.1.3). When all optimum parameter values (Table A.6Table A.13) were run together, the optimum parameter set had the best fit for 12 metrics compared to the initial baseline parameter set. A large difference in the sediment output was observed between the baseline and optimum parameter sets, however the output for the baseline parameter values was thought to be unrealistically large (Section A.2.1.3).

2.2.3 Improvements to catchment representation within CAESAR-Lisflood

A sequence of improvements were made as shown in Figure 2.11 to the Eastburn Beck model, these involved changes that could be made within the existing model capabilities. Changes were appropriate to either improve the ability of the

CAESAR-Lisflood to model NFM measures or improve the computational efficiency and accuracy of scenarios.

Bedrock

CAESAR-Lisflood has the ability to add a bedrock layer to prevent unrealistic depths of erosion. Soil depth data was used from the UK Soil Observatory Parent Material Model of Great Britain (Lawley, 2012). This data set was descriptive, and thus was converted into depths up to 1.5 m for 1 km grid cells in the catchment, which was then subtracted from the DEM to result in a bedrock layer that was applied to the CAESAR-Lisflood for Eastburn Beck.

Spatially distributed m parameter

The spatially distributed m parameter is incorporated into CAESAR-Lisflood through spatially fixed pre-defined areas (Coulthard and Van de Wiel, 2017). Each area has a separate hydrological model, allowing for a different value of the m parameter and rainfall input and consequently differences in storage and runoff in each area. The spatial distribution of the m parameter was based on land cover (Figure 2.6) as not all land covers within the catchment respond to rainfall in the same way. A literature review was undertaken to find previous m parameter values used to represent different land uses (Table 2.1). As TOPMODEL was not designed for urban areas, it was assumed that a value for the 'discontinuous urban fabric' should be the lowest of the land covers due to a lack of infiltration in these areas, causing more rapid runoff, as would be seen on impervious surfaces (Shuster et al., 2005). There was also no differentiation between the forest types due to a lack of previous studies (Table 2.1). The values implemented were chosen so that the area averaged m value most closely matched the optimum lumped value of 0.001, this resulted in an area averaged m of 0.0036. This involved decreasing literature values by 40% to account for the wet antecedent conditions prior to the Boxing Day event.

Table 2.1: Land cover derived m parameter values implemented into the spatially distributed m parameter model.

Land Cover	m parameter value implemented
Discontinuous Urban Fabric	0.00066
Pastures	0.0042 (Gao et al., 2017)
Forests	0.0078 (Robson et al., 1992; Beven, 1997)
Natural Grasslands	0.003 (Coulthard and Van de Wiel, 2017)
Moors and Heathland	0.00066 (Metcalfe et al., 2015)
Peat Bogs	0.0018 (Gao et al., 2015)

Shortening of the model simulation and high resolution rainfall

To allow for the implementation of a different rainfall product, the model simulation needed to be shortened from November and December 2015 to just December 2015. This was required as the new rainfall product contained many data gaps for November 2015.

The CEH-GEAR dataset implemented in CAESAR-Lisflood thus far is derived from the network of rainfall gauges in the UK. Rain gauges often underestimate true rainfall rates during very intense events (Habib et al., 2001; Ebert, 2007) and even more so when the network is sparse within the catchment (Valters, 2017). However, ground-based precipitation radars in the UK return data every five minutes, extending to 250 km diameter around the individual radars (Harrison et al., 2012). This allows for temporally high resolution, spatially detailed rainfall data without the need for on-ground gauges in small catchments where the more traditional rainfall products are unavailable or sparsely available.

For the use in this study, the UK 1km composite product from the Met Office NIMROD system was used. The difference in the temporal resolution between the two datasets can be seen in Figure 2.7.

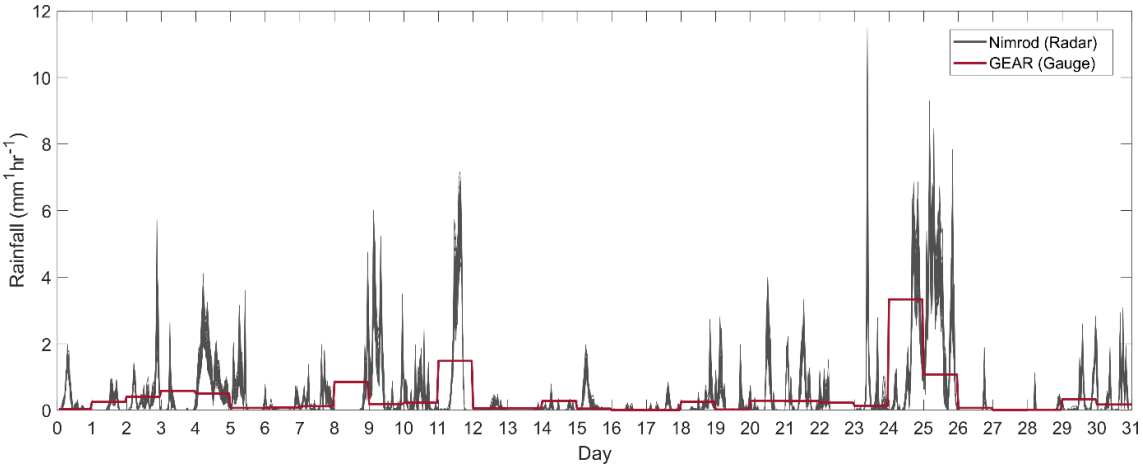

Figure 2.7: Temporal difference between the low resolution (GEAR) and high resolution (Nimrod) rainfall data sets. All 62 1 km^2 Nimrod grid cells were shown to highlight the spatial difference.

Shortening model simulation time for computational efficiency

For the purpose of decreasing the time CAESAR-Lisflood took to run with the foresight to increase the model resolution that is expected to increase model run

time, the model was started on the 11th December 2015 and the 21st December 2015. Long run times are inhibitive to allowing many iterations of different model implementations and therefore the further simulations started using rainfall from the 21st December 2015 onwards. All model runs were undertaken on an OEGStone CS-B x64-based PC, with an Intel® Core™ i7-4790 @ 3.60Ghz processor, with 16GB RAM and 250GB SSD Hard drive.

Enabling suspended sediment transport

Within CAESAR-Lisflood, the smallest grain size fraction can be treated as suspended sediment, given a corresponding fall velocity is entered. The deposition of suspended sediment is dealt with differently in CAESAR-Lisflood compared to bedload, whereby bedload is moved from cell to cell directly, whereas suspended sediment is dependent on the sediment concentration in suspension and the fall velocity (Coulthard et al., 2013). Entrainment of suspended sediment occurs as per the law used also for bedload. For this study, a grain size of 0.075 mm with a fall velocity of 0.0044 m s^{-1} was tested. This was the size of fine sand (Wentworth, 1922), known to be in the Eastburn catchment due to sedimentation at the catchment outlet (Figure 2.8b). To this point of model set up, version 1.9b of CAESAR-Lisflood was used, however, an issue with the formulation of the suspended sediment transport in CAESAR-Lisflood 1.9b whereby sediment discharge was overestimated was identified in December 2018 (Coulthard, 2018). Therefore the latest version of the model (1.9h), where the issue had been fixed, was also tested before suspended sediment was enabled.

Figure 2.8: Photographs suggesting grain size distribution in the Eastburn Beck catchment. Photo A taken in Lothersdale Wood, in the headwaters of the catchment. Photo B provided by the Environment Agency of a sediment build up less than 500 m downstream of the modelled catchment outlet.

The improvements that resulted in the largest changes to the water and sediment outputs were the inclusion of a bedrock layer to limit the depth to which erosion can occur (Section A.2.2.1), the initial shortening of model simulation time (Section A.2.2.2) and the inclusion of a high resolution rainfall product (Section A.2.2.3).

2.2.4 Accounting for a lack of validation data

The sensitivity analysis highlighted the model's sensitivity to Manning's n and grain size distribution. However, having a dearth of sediment related validation data for the catchment, it was important to acknowledge the uncertainty resulting from changes in values of these two parameters. To do this, twenty-one Manning's n land cover based distributions were established through step wise changes of 5% to the minimum values found in the literature up to ±50% (Table A.1). Grain size distributions used as part of the initial sensitivity analysis (Figure A.1) were taken and the smallest of the two (GSD -75% and GSD -50%) were removed after a more thorough investigation into the sediment sizes occurring within the catchment, leaving five possible grain size distributions.

Each Manning's n set and grain size distribution were combined and run to total 105 combinations. Once the sediment yield had been calculated for all combinations, the parameter sets associated with the minimum, median and maximum sediment yields were used in scenarios henceforth (Figure 2.9). These three parameter sets were thought to represent the worst to best case scenarios in terms of potential sediment outputs and were called "sediment response catchments" or SRCs (Section A.2.3).

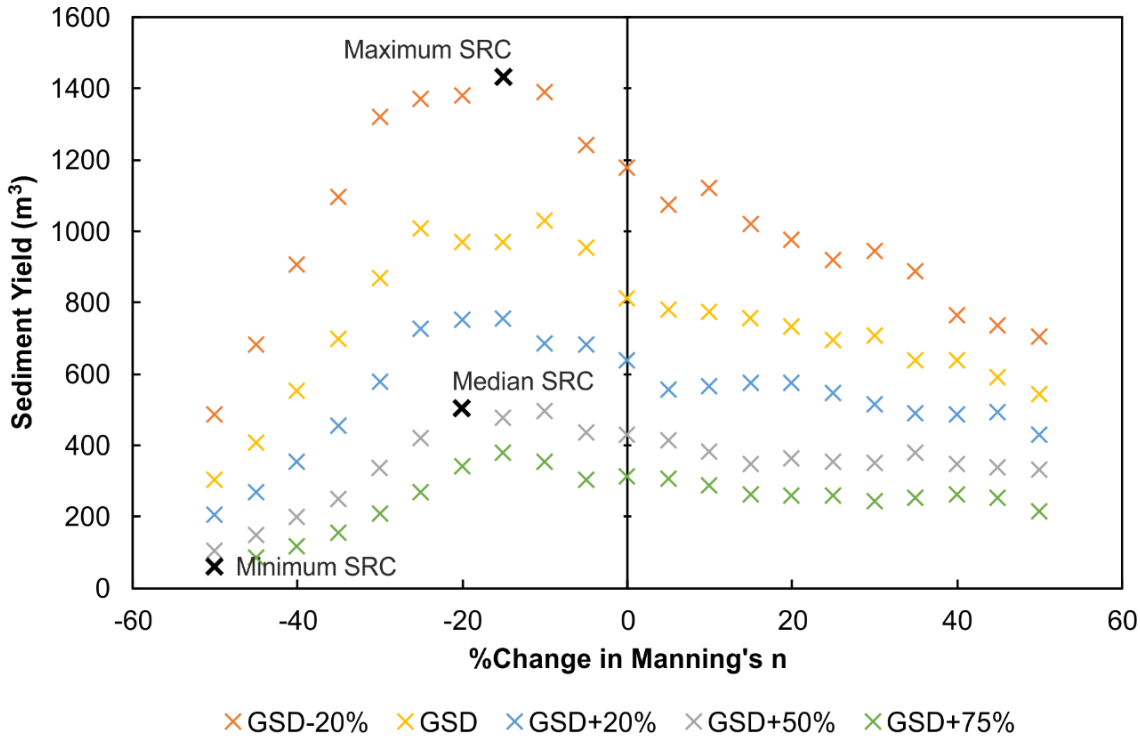

Figure 2.9: Catchment outlet sediment yield occurring from possible combinations of the GSD and Manning's n at 10 m model resolution. Highlighted points are the three statistically chosen parameter value combinations.

Once the SRCs were established a second set of models were created where there was a separate value of Manning's n for the channel, as defined in Figure 2.5, with the values for the channel varying according to each of the SRCs. The median SRC was given a channel Manning's n value of 0.035, the minimum SRC = 0.0175 and maximum SRC = 0.0357.

2.2.5 Increasing model resolution

To more accurately represent spatially distributed water-retention features within the CAESAR-Lisflood model, the model resolution needed to be increased from 10 m to 4 m. At a 10 m model resolution, small spatially distributed water retention features, which are popular in UK NFM schemes, would be hard to replicate, given features are often only a few metres wide. However, with an increase in model resolution comes a compromise with model run time. Originally a 2 m resolution was aimed for, however this was quickly increased to 4 m due to having unrealistically long run times (1.5 simulated days in 25 hours of real time). The compromise of 4 m allowed for an increase in output spatial quality, without excessively long run times.

The Environment Agency's 2 m composite LiDAR DTM data was chosen to allow for the best spatial coverage, with all channels, floodplains and riparian zones

being covered. To create a full catchment DEM, the OS 5 m Terrain DTM was resampled to 2 m using the bilinear sampling technique. These two products were mosaicked into a single raster, ensuring the 2 m LiDAR data was the priority when the two products overlapped. The DEM was then hydrologically corrected using the “Fill” tool in ArcGIS before being resampling the DEM to a 4m resolution using the bilinear sampling technique. Spatial analysis was undertaken between the DEM at 10 m and at 4 m using the 3D Analyst tools in ArcGIS to establish whether the 4 m DEM needed to have the channels burnt into it. Comparisons on cross sections throughout the catchment showed that the channel was much better represented in the 4 m DEM and thus channel burning was not undertaken, the difference in resolution can be seen in Figure 2.10. An associated bedrock layer was also created at a 4 m resolution using the same depths as implemented in the 10 m model improvements.

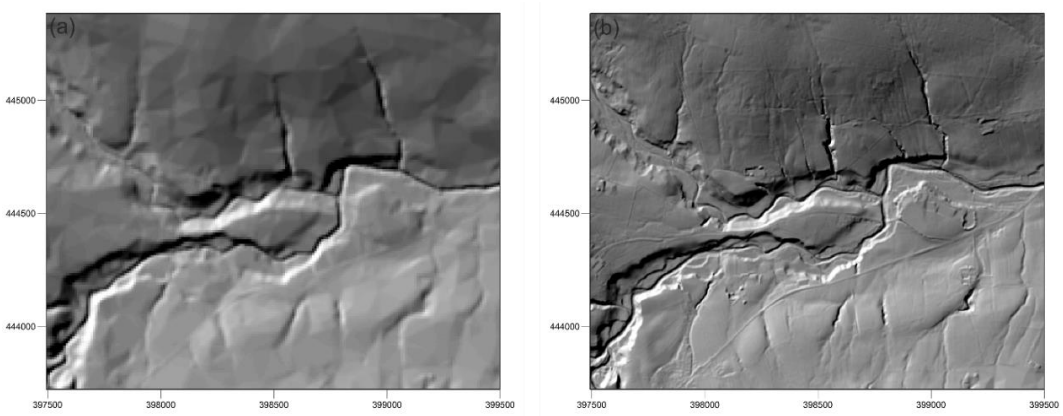

Figure 2.10: The difference in model resolution between (a) 10 m and (b) 4 m on the hillshaded DEM.

With the increase in model resolution came the opportunity to switch on lateral erosion as the channel would be represented by more than 1 cell in width. Lateral erosion rate is calculated based on the radius of curvature according to the edge counting method in Coulthard and Van de Wiel (2006). A value of 0.0001 is stated within the literature as a suitable value for a meandering river and a value of 0.00001 was also tested, with the latter resulting in a better representation of the channel in reference to aerial imagery.

The bedrock layer was also edited so that channel walls within the settlements near the catchment outlet were represented as unerodible as it was thought that channel walls would inhibit lateral channel movement.

Small increases to the water related model outputs were observed with the increase in model resolution. Sediment related outputs were more widely affected, with decreases in outlet sediment discharge but increases in the geomorphologically active area throughout the catchment (Section A.2.4). Adding lateral erosion into the model did increase the sediment discharge and the area affected by erosion and deposition within channels, however it allowed for the representation of meander geomorphological processes and the creation of gravel bars (Section A.2.4.1).

2.2.6 Model Spin-up

The addition of a spin-up period is required in landscape evolution modelling to allow for internal model adjustment, characterised by excessive sediment discharge, to create a heterogeneous grain size distribution throughout the catchment by preferentially transporting finer material (Hancock et al., 2010). A five-month rainfall time series was taken from a tipping bucket rain gauge within the catchment and was repeated four times, with the resulting Digital Elevation Model (DEM) and grain size distribution being used for baseline and NFM modelling scenarios.

Catchment outlet sediment discharge decreased following the implementation of a spin-up period alongside an increase in the variability in the catchment's median grain size (D_{50}) (Section A.2.4.2). This 4 m resolution model was used to answer the first research question (Chapter 3).

2.2.7 Sub-catchment model set up

The final modification to the CAESAR-Lisflood model was to take a sub-catchment and model it at 2 m resolution. Modelling the entire catchment at 2 m was found to be computationally challenging. To choose which sub-catchment to model, the Eastburn Beck catchment was divided into four sub-catchments. The choice between the four sub-catchments was made based on which had the greatest proportion of tree coverage free channel for easy comparison with aerial imagery.

The Environment Agency's 2 m composite LiDAR DTM was used and where this was unavailable within the catchment, the OS 5 m Terrain DTM was mosaicked together with the 2 m DTM for whole catchment representation following the same method as when creating the DTM for the 4m model. Other model inputs

remained the same, or were modified to be of 2 m resolution compared to 4 m resolution used previously. The values used for Manning's n and GSD, as identified as the most uncertain parameters, were for the median SRC, chosen as opposed to a range of values, given the extended run times for the more complex model.

Due to its smaller size, the in-out difference was expected to change to ensure all sediment movement would be accounted for. In-Out Difference (IOD) should be related to the low flow discharge, where below the set value, time steps for the flow and erosion/deposition models are detached, speeding up model processing. Therefore values of 1, 0.5, 0.1 and 0 m^3s^{-1} were tested to assess their impact on model run times and outputs. A large increase in model run time (additional > 2 days) was observed between a value of 0 and 0.1. Larger values saw large decreases in sediment discharge and yield, suggesting the model may not have been accounting for all sediment moving within the catchment. Therefore a value of $0.1m^3s^{-1}$ was chosen.

As with the larger models, spin up was required to allow for self-adjustment of the model. The same five month tipping bucket rainfall series was used, repeated four times for model spin up, which took 23 days to run, limiting the potential for a number of scenarios as with the lower resolution models. The post spin-up baseline model run had a decreased sediment discharge and an increased variability in the catchment wide median grain size (Section A.2.5.2). The resulting DEM and spatial grain size distribution was taken forward for model runs for the comparison with the hydraulic model (Chapter 4).

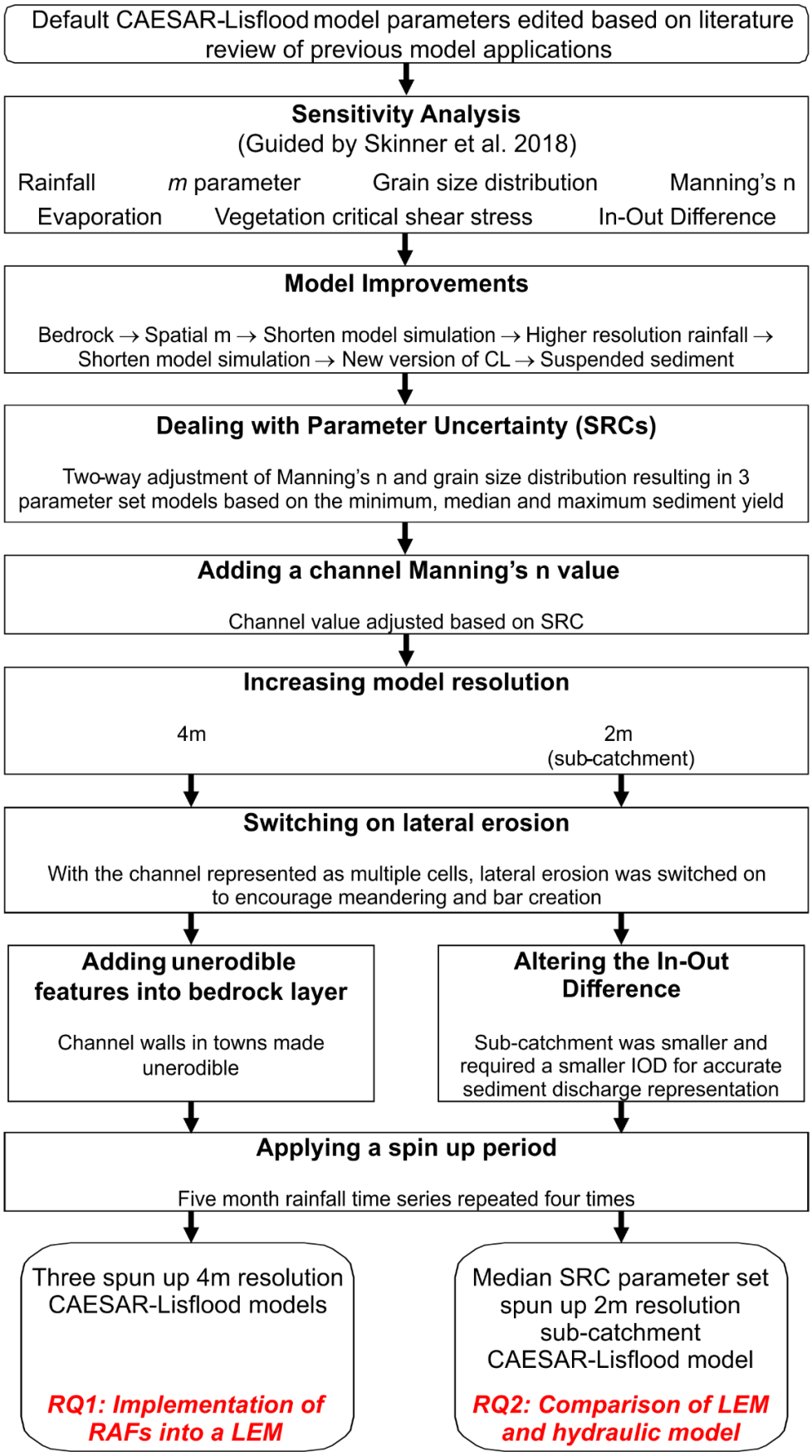

Figure 2.11: Summary of the CAESAR-Lisflood model set up and improvements flow diagram.

Chapter 3
Implementation of Runoff Attenuation Features into a Landscape Evolution Model

3.1 Introduction

Natural flood management (NFM) seeks to reduce flood risk by using techniques that work alongside natural processes and features (Scottish Environment Protection Agency (SEPA), 2016). Co-benefits of NFM include increasing biodiversity, improving water and soil quality, reducing soil erosion, increasing agricultural productivity and improving the health and well-being of the human population (Lane, 2017; Dadson et al., 2017). The umbrella term natural flood management covers a wide range of measures, from woodland planting, to large scale river and floodplain restoration, to soil and land management (SEPA, 2016).

The Environment Agency's Working with Natural Processes (WwNP) evidence base project (Burgess-Gamble et al., 2017) synthesised existing research on NFM into one location. This synthesis produced an evidence directory, potential area maps and study of the current research gaps that together have allowed for a wide community of interested parties to access up-to-date information on what measures are available and what their potential benefits may be. In recent years, an increase in community-led small-scale projects aiming to reduce flood risk has been seen, with the UK government allotting £1 million to a NFM competition specifically for smaller projects (DEFRA, 2017). This competition was announced alongside a further £14 million of funding for larger flood risk management projects. The popularity of NFM in the UK has also been aided by success stories highlighted in the media such as the scheme at Pickering, North Yorkshire (Slow the Flow, 2016).

Runoff attenuation features (RAFs) are an NFM technique that seek to intercept and slow the flow through increasing the connectivity between the channels and floodplains and creating temporary storage when runoff is high (Quinn et al., 2013). Another umbrella term, RAFs encompass a range of features, varying greatly in size and cost, from gully-blocking (e.g. Shuttleworth et al., 2019), to leaky barriers (e.g. Short et al., 2018) to large retention ponds and bunds (e.g. Nicholson et al., 2012). Whilst research into leaky barriers and offline storage areas has demonstrated their effectiveness at reducing local flow velocities,

temporarily storing water, reducing local flood risk and trapping fine sediment, the effectiveness of RAFs at larger catchment scales (> 20 km^2) in extreme events (>100 year return period (RP)) and the cumulative effect of many smaller measures distributed throughout the catchment remains understudied (Burgess-Gamble et al., 2017).

The lack of knowledge of RAF performance and of their 'system performance' together at a larger spatial scale is partly due to the high cost of imposing an effective monitoring system. Many NFM projects do not have enough scope in terms of capital, time and expert knowledge to implement quality monitoring networks (England et al., 2008). NFM projects also often implement a number of measures within the same area and therefore with minimal monitoring networks it is often difficult to disentangle contributions of individual features from the natural variation within larger catchments, even prior to the assessment of different designs (e.g. Slow the Flow, 2016). Changes to rivers are therefore being implemented without a thorough understanding of the benefits and potential disadvantages the implemented measures may bring under different circumstances such as scour or sedimentation.

One way to alleviate the challenges faced whilst monitoring RAFs would be to create a model that simulates the changes that are to be applied in each scheme. This model would also allow for a range of different scenarios to be tested including the scope of changes to be made and what effect this may have based on different rainfall events. Modelling would also allow changes occurring as a result of climate change to be evaluated.

Existing numerical modelling of RAFs include Metcalfe et al. (2018)'s use of a network solution of the 1D St Venant equations. 4,500 locations with 1 m high bunds within the River Eden headwaters (223 km^2) were simulated, accounting for over 8 million m^3 of potential storage. A likelihood-weighted median peak reduction of 5.8% for Storm Desmond (5-6th December 2015) was seen when RAF residence time was 10 hours (Metcalfe et al., 2018). Nicholson et al. (2019) created a simple pond network model, where up to 35 identical pond features, accounting for 19,250 m^3 of potential storage resulted in up to a 30% reduction in flood risk. Ghimire et al. (2014), used a combination of 1D and 2D numerical models to represent a 5,200 m^3 pond which resulted in a ~1% reduction of peak flow of a 1% annual exceedance probability (AEP) event. A 9,500 m^3 pond saw

a reduction of ~2.5 % (Ghimire et al., 2014). Hankin et al. (2020) sited 20 identical 1 m high leaky barriers in a ~450 m long 1D network model. They saw a 4 % decrease in peak discharge for the 1% AEP event simulated. However they noted redundancy in the barriers with not all 20 barriers being utilised fully. Eight barriers were also placed randomly across the network in a number of configurations, with the best resulting in a 3.4 % decrease in peak discharge, highlighting the benefits of careful leaky barrier placement (Hankin et al., 2020).

Despite the promise shown by these studies to disentangle the performance of RAFs in different settings, they have only focused on river hydraulics. There is a noticeable dearth of knowledge on the geomorphological effects of RAFs, particularly in modelling studies. Comparisons can be made to more traditional infrastructure such as weirs and culverts, as discussed in Section 1.3, where weirs can cause both sedimentation upstream and scour downstream of a feature, and culverts can cause scour at their outlet. Understanding the geomorphological impacts of RAFs is essential because sedimentation can be expected upstream of features and erosion could result in features failing. In both cases such geomorphological activity would seriously affect long term RAF efficiency and management (Quinn et al., 2013; Metcalfe et al., 2018). The support for these expectations comes from monitoring of RAFs that has shown sedimentation to be an issue. Barber and Quinn (2012) found significant amounts of silt accumulated at the inlet of a 200 m^3 pond, hypothesised to be from small events and Wilkinson et al., (2014) estimated that just under 1 tonne of fine sediment was captured behind a 500 m^3 retention bund, although a proportion was also lost via an outlet pipe. Of the few modelling studies to include a geomorphological appraisal, Adams et al., (2018) found small reductions in peak suspended sediment when using a linear storage-discharge relationship to model a 1.25 km^2 catchment and Hankin et al., (2019) found erosive shear stress above a large storage area, when estimating potential erosion and deposition through the classification of shear stress using a cascade coupling of Dynamic TOPMODEL and JFlow.

This study therefore has an overall aim to quantify the effects that runoff attenuation features (RAFs) can have on both the hydraulic and geomorphological response of an example river catchment during an extreme flood event using numerical modelling. Specifically, individual RAF design will be

investigated, with changes occurring from shape, size and quantity of features considered.

3.2 Methodology

3.2.1 Study site and flood event

The Eastburn Beck catchment is 40.8 km^2, with river channels 20.3 km in length. The catchment drains primarily sheep grazed fields, before flowing through the settlements of Glusburn and Sutton-in-Craven to its confluence with the River Aire approximately 1 km downstream of Kildwick (Figure 3.1a). The catchment is situated within the wider River Aire catchment, to the north west of Leeds (Figure 3.1b). Eastburn Beck was selected due to its known sediment issues. Zonal statistical analysis using SCIMAP (Reaney et al., 2011) data across the Aire catchment showed that Eastburn Beck had the highest mean channel sediment accumulated risk of any of the Aire sub-catchments (Figure 3.1b). The catchment also has a gravel trap near the catchment outlet which fills regularly and it is underachieving in the Water Framework Directive (WFD) for sediment issues. With regard to NFM, a number of opportunities are identifiable within the catchment in the Environment Agency's Working with Natural Processes evidence base project (SC150005) (Burgess-Gamble et al., 2017).

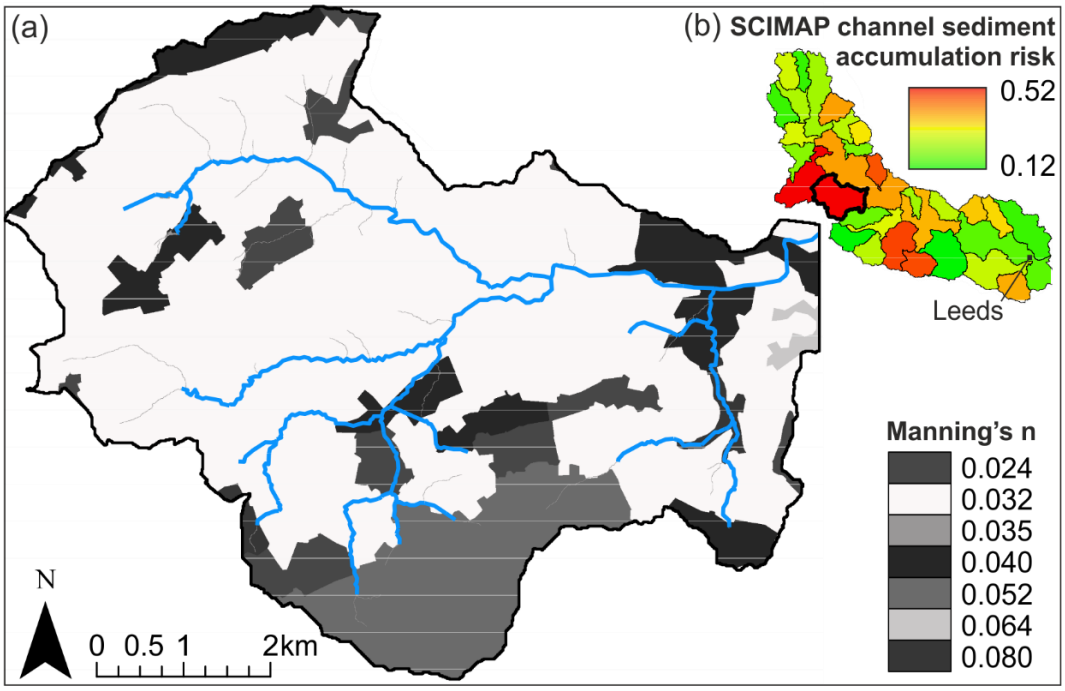

Figure 3.1: Eastburn Beck catchment location (a) locally with annotated watercourses and spatial distribution of Manning's n with values from the Median

SRC and (b) within the wider Aire catchment annotated with mean SCIMAP channel sediment accumulation risk, calculated for each sub-catchment.

In the Eastburn Beck catchment, the 2015-2016 winter recorded the highest flow levels since records began, with a peak discharge of 54.4 m^3s^{-1} being recorded on the 26th December 2015 at the catchment outlet (Figure 3.2). Only three other periods have seen peak discharges over 50 m^3s^{-1} and since 2010, peak discharge in a given year had not exceeded 40 m^3s^{-1} before the 2015-2016 season. This event was chosen as flood management schemes are designed for the larger events likely to occur within a catchment, however, the effect of RAFs under such extreme events is understudied and therefore poses an interesting research question.

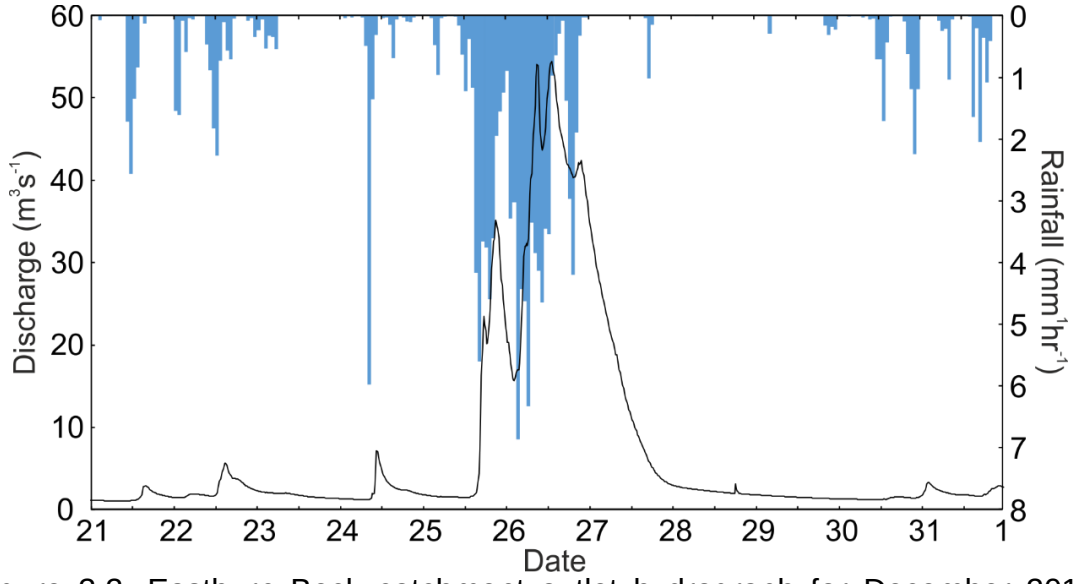

Figure 3.2: Eastburn Beck catchment outlet hydrograph for December 2015. Discharge data from Environment Agency 15 min flow data at Crosshills gauge (F1525) (Black). Hourly average rainfall rate from NIMROD radar data, averaged over Eastburn Beck catchment (Blue).

3.2.2 Numerical modelling

3.2.2.1 CAESAR-Lisflood model

A landscape evolution model (LEM) was chosen over more traditional soil erosion models (e.g. Revised Universal Soil Loss Equation (RUSLE) (Renard and Ferreira, 1993)) due to a LEM's ability to model erosion and deposition in a spatially distributed manner through the use of a Digital Elevation Model (DEM). CAESAR-Lisflood 1.9h was the chosen LEM for the implementation of RAFs. The advantage to using CAESAR-Lisflood over other LEMs, is that CAESAR-Lisflood has the ability to simulate erosion and deposition in river catchments down to fine

temporal resolutions (~ hour) allowing for the simulation of single flood events and process-understanding. CAESAR-Lisflood is also much more efficient than other models in terms of parameterisation and input requirements, such as the use of commonly used parameters, which have many parameter values cited in the literature (e.g. Manning's n and TOPMODEL's m) and moderate, yet sufficient, spatial input data requirements (DEM, bedrock depth, Manning's n and TOPMODEL's m). Furthermore it is a relatively efficient numerical model; it is capable of modelling such fine temporal resolutions without heavy computational requirements in part due to the reduced form shallow water equations within the model (Coulthard et al., 2013).

CAESAR-Lisflood is comprised of four modules. The hydrological model, an adaptation of TOPMODEL (Beven et al., 1979), calculates the runoff given the rainfall input, which is routed through the flow model, a conservation-based inertial formulation of the shallow water equations following the method in LISFLOOD-FP (Bates et al., 2010). The fluvial erosion and deposition model allows for a choice of sediment transport equations of either Einstein (1950) or Wilcock and Crowe (2003). Wilcock and Crowe (2003) was developed with coarser gravel field and laboratory data, whereas Einstein was developed with sand based laboratory data. Due to the coarse grain size of the upland Eastburn Beck catchment, the method of Wilcock and Crowe (2003) was chosen for this study. The fourth module considers slope processes, whereby sediment inputs from slopes are calculated based on a critical slope threshold.

3.2.2.2 Model Set Up

An exploratory CAESAR-Lisflood model based on the Eastburn Beck catchment was created. This model was not expected to be predictive, instead, Eastburn Beck was used as an example catchment to collect model data. The model was subsequently used for scenario testing of differences in RAF design as opposed to calculating exact rates and volumes which may be expected from implementing such features in the real world. The model was set up using a 2 m composite Light Detection and Ranging (LiDAR) Digital Terrain Model (DTM) resampled, using ArcGIS's resampling tool with bilinear resampling technique to a 4 m resolution. The model was too slow to run the entire catchment at 2 m resolution. It was thought that a resolution coarser than 4 m would not be detailed enough to realistically represent the RAFs. A second grid was created to simulate the

elevation of the bedrock, representing the point at which vertical erosion is no longer possible. Soil depths were estimated of up to 1.5 m from qualitative descriptions in the UK Soil Observatory Parent Material Model of Great Britain (Lawley, 2012) based on a 1 km grid. Channel walls present within the settlements near the catchment outlet were represented as unerodible features by setting values in the bedrock layer to the same as in the overlying DEM.

The rainfall storm event was represented in the model via radar rainfall data from the UK 1km composite product from the Met Office NIMROD system. Ground-based precipitation radars in the UK return data every five minutes, extending to 250 km diameter around the individual radars (Harrison et al., 2012). This allows for temporally high resolution, spatially detailed rainfall data without the need for on-ground gauges in small catchments where the more traditional rainfall products are unavailable or sparsely available, resulting in less accurate model input data. The rainfall time series spanned from the 21st December to the end of the 31st December 2015 in hourly time steps, calculated as the average of the 5 minute intervals within the radar data. For the full workflow of how NIMROD data was implemented into CAESAR-Lisflood, please see Appendix A.

Parameter values chosen within the model were based on field data, values previously stated in the literature and a wider sensitivity analysis (see Appendix A for full analysis). Grain size distribution (GSD) and Manning's n were found to be the most sensitive parameters in terms of sediment related outputs. These parameters were also found to be influential in a global sensitivity analysis of CAESAR-Lisflood undertaken by Skinner et al. (2018) based on the Swale catchment, which is a larger (181 km^2) catchment within Yorkshire and situated to the north-east of Eastburn Beck. Due to the lack of sediment validation data available for the Eastburn Beck catchment and the sensitivity to GSD and Manning's n, three parameter sets with varying values for both GSD and Manning's n were used to give a range of possible catchment outlet sediment yields. The relationship between all values of Manning's n and GSD tested can be found in Appendix A. The combinations taken forward were the parameter values associated with the minimum, median and maximum sediment yields (Table 3.1), named for ease in this study as possible 'sediment response catchments', or SRCs. Manning's n values varied within the catchment based on land cover in addition to a value specified for the channels. Nine separate grain

size fractions were implemented, the smallest of which was transported via suspension.

Table 3.1: Values of Manning's n and grain sizes implemented within the three sediment response catchments.

SRC	Manning's n	GSD (m)
Minimum	0.015 - 0.05	0.000875 - 0.224
Median	0.024 - 0.08	0.00075 - 0.192
Maximum	0.0255 - 0.085	0.0004 - 0.1024

It is important when using a LEM such as CAESAR-Lisflood to undertake a model 'spin up' (Hancock et al., 2010). A spin up period allows a model to create a more representative and heterogeneous catchment grain size distribution as determined by 'baseflow' hydraulic conditions. In this study, this spin up was achieved by taking a five month long rainfall time series from a tipping bucket rain gauge within the catchment and applying this to the catchment four times to drive spatial changes in grain size distribution and ultimately decreases in sediment discharge (see Appendix A). The spin up period was limited by computational run times, with run times of over 100 hours. The resulting DEMs and grain size distributions were used as the initial conditions in the NFM implementation model scenarios.

3.2.3 Implementation of runoff attenuation features

The Environment Agency's WwNP potential area maps for runoff attenuation features were created by considering the key concept that areas of high flow accumulation from surface water flooding may be influenced by temporary storage. See the Mapping Technical Report for the methodological process (Hankin et al., 2018). Within the Eastburn Beck catchment, 274 locations were identified for the implementation of RAFs from the 1 in 100 year AEP potential area map (Figure 3.3).

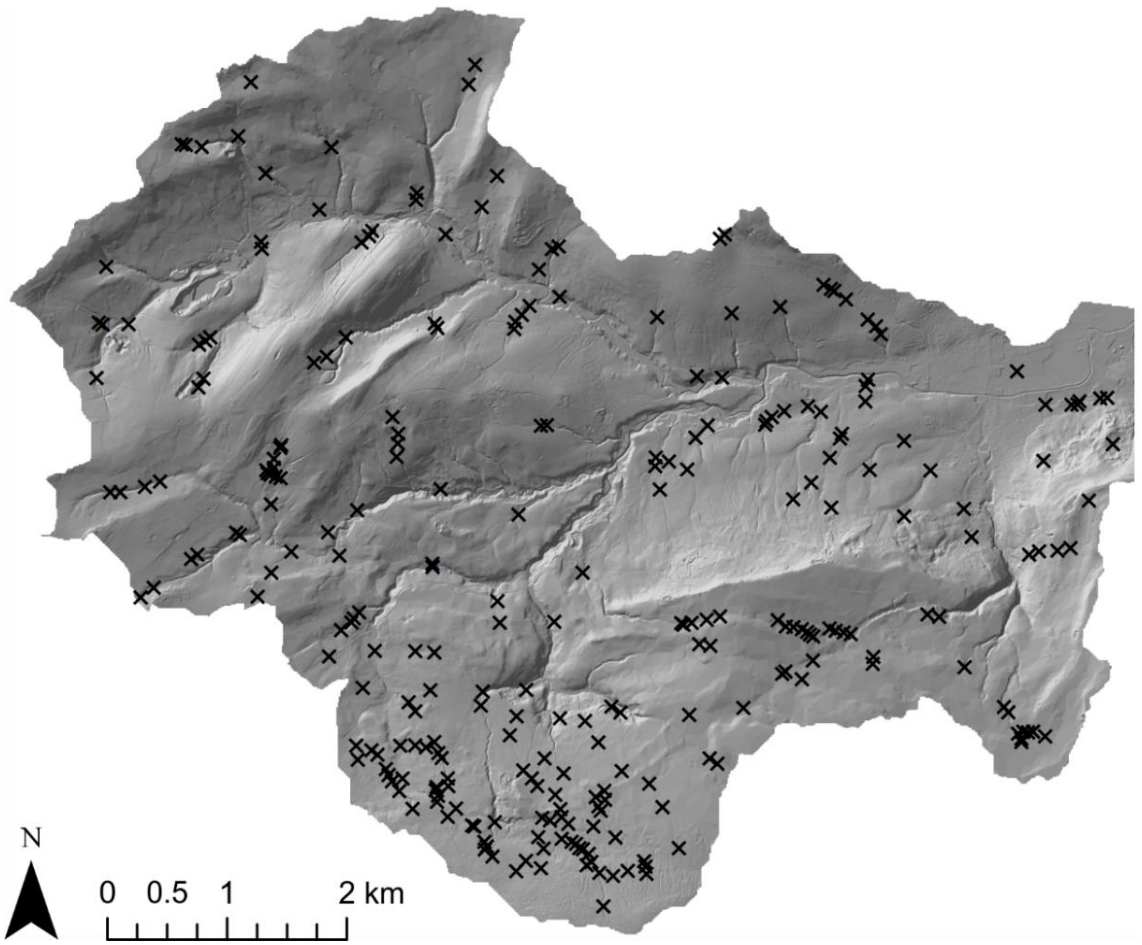

Figure 3.3: The 274 runoff attenuation feature locations as identified from the EA's WwNP potential area maps.

The designs of RAFs vary widely when built into a landscape. Therefore, this study aimed to look at the effect this variety has on the hydraulic and geomorphological response as represented within CAESAR-Lisflood. To do this, bunds were created downstream of the opportunities highlighted in the EA's WwNP potential area maps, as, linear and u-shaped RAFs to test shape, extended versions of these RAFs to test size, and using the original linear RAFs, a second bund was added approximately 20 m upstream wherever possible to test the effect of quantity, as shown in Figure 3.4. The size of the simulated bunds varied in relation to the size of the WwNP potential area. RAFs were 12 m to 40 m long when linear in design. The largest RAF was extended u-shaped in design and was 150 m long. RAFs were sized to be in line with those built in the real world. Quinn et al. (2013) highlight the cost of creating timber bunds up to 150 m long and earth bunds up to 50 m long. Timber bunds in Pickering were between 16.5 m and 57.5 m long (McAlinden, 2016) and one of the timber bunds in Belford was 100 m long (Wilkinson et al., 2010). Earth bunds constructed in Southwell were 86 to 132 m long (Wells, 2019).

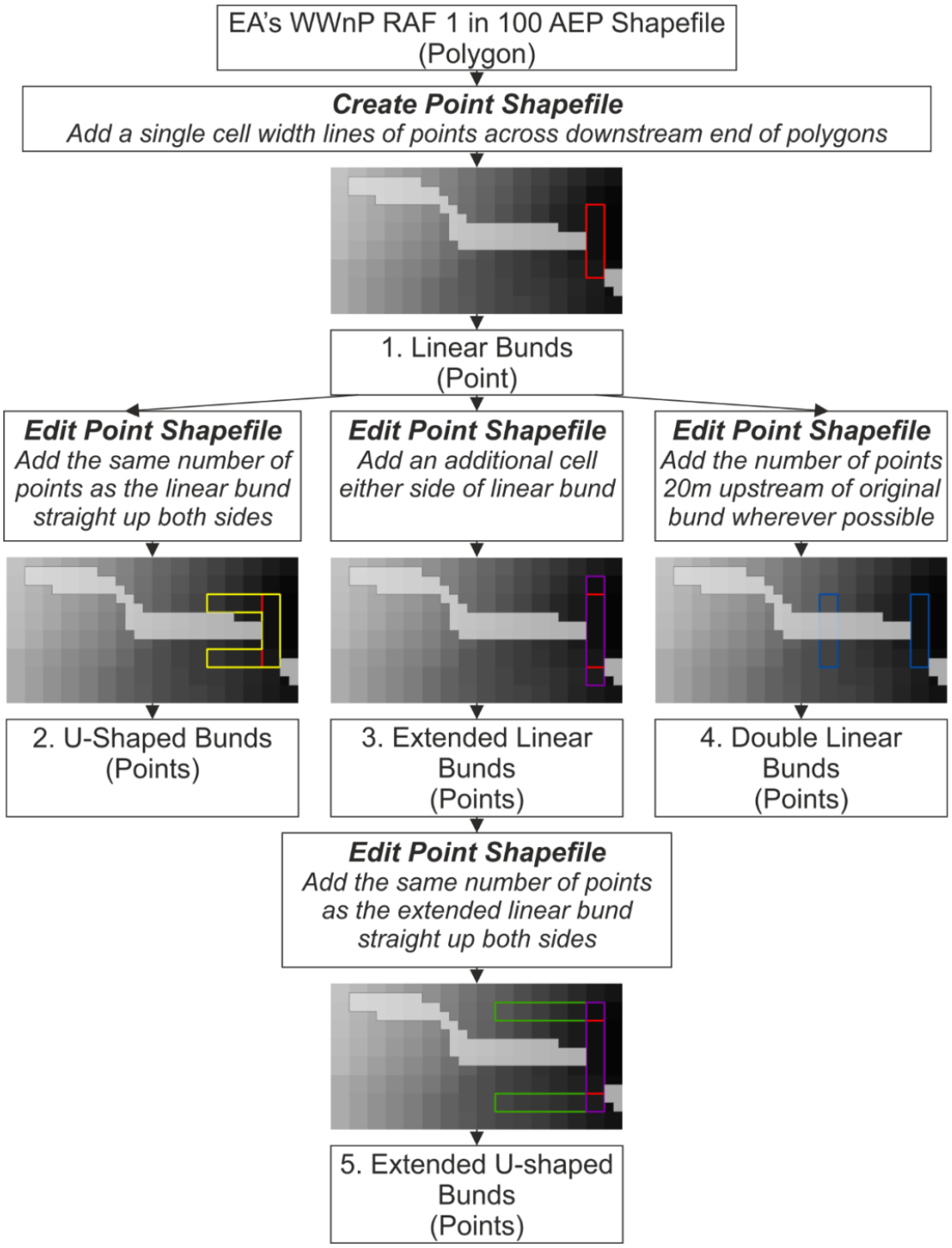

Figure 3.4: Geographic Information System (GIS) workflow followed for the creation of bund designs. Grey shaded polygon represents the EA WWnP RAF potential area. Coloured outline polygons represent the areas of increased elevation bund features.

The creation of the initial shapefiles of the different bund designs was followed by the topographic editing of the underlying DEM (Figure 3.5). The DEM cell values attributed to each point within the bund shapefiles were increased in elevation by 1 m because many features often built within NFM projects are small

in height. For example, a timber wall constructed as part of the scheme at Belford, Northumberland was 1 m in height at its maximum (Wilkinson et al., 2010) and timber bunds at the Pickering scheme were 1.5 m in height (Nisbet et al., 2017). The underlying bedrock elevation layer was left unaltered, therefore the features implemented were erodible. This implementation method enabled multiple designs of RAFs to be implemented across the catchment in an efficient, repeatable manner. It should be noted however that this method compromised the comparability with the behaviour of bunds implemented in the real world in two ways. Firstly, the method used in this study does not allow baseflow to be unimpeded if located in a channel, did not provide an outlet pipe for slow drainage if located offline and did not provide any direct “leakiness”. However, due to the spatial modelling resolution of 4 m, representing outlet pipes or “leakiness” within the DEM as gaps in the bund would make pipes or “leakiness” unrealistically large, greatly reducing the feature’s capacity to storage water. Secondly, once cells comprising the feature were identified, all cell values were increased by 1 m. Whether this is a correct representation of a feature depended on its location, such as when a feature is located within a channel, the RAF cells in the centre of the channel had a lower value than those on the banks. However, as the vast majority of locations identified within Eastburn Beck were offline (i.e. not in channels), the additional time needed to implement in-channel RAFs in a more complex manor would have limited capacity for the number of design scenarios or number of RAFs within the study.

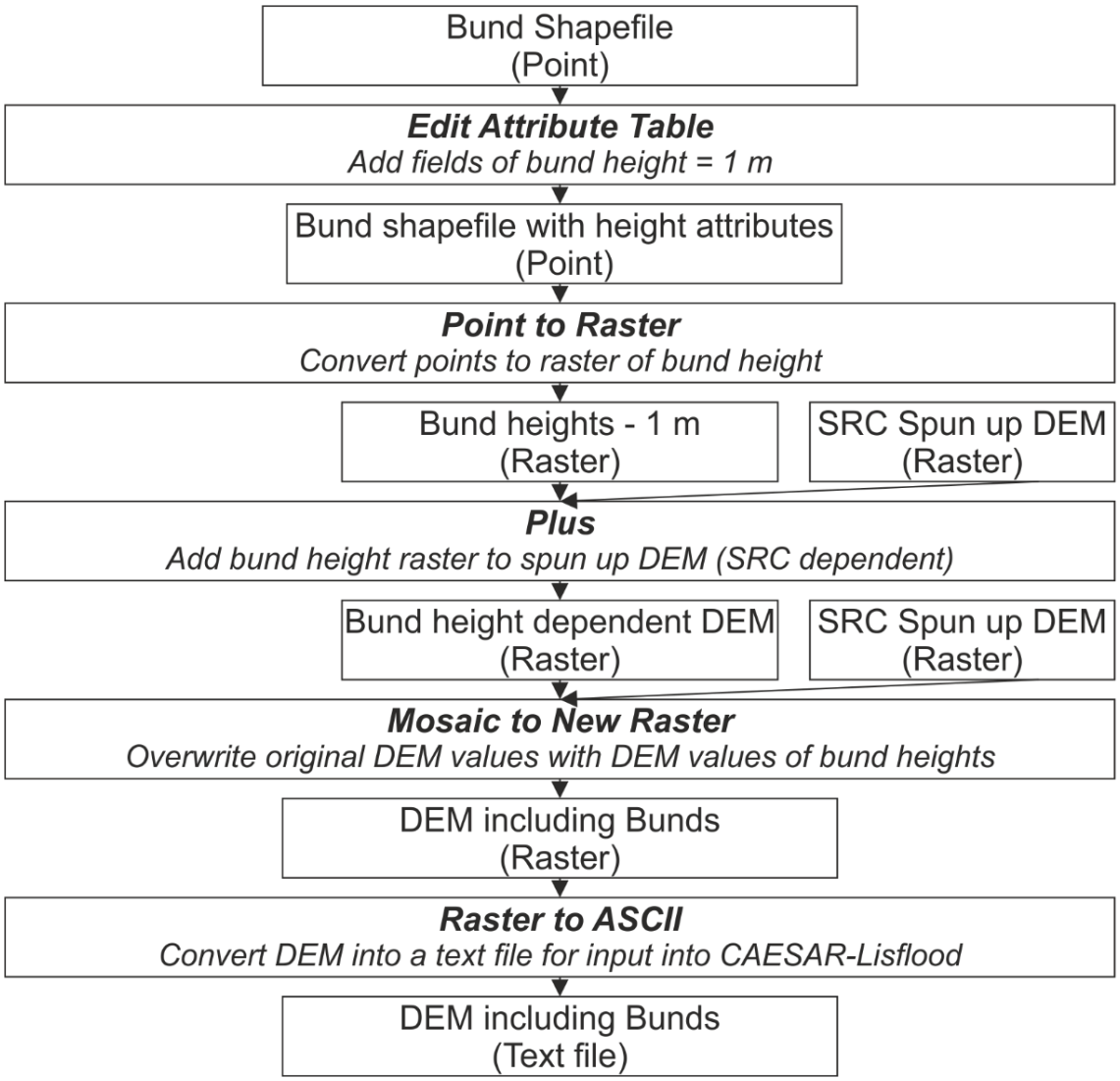

Figure 3.5: GIS workflow for the creation of bund implemented DEMs.

3.2.4 Data analysis

Comparisons between the baseline model scenarios and the RAF model scenarios were made for both hydrological and geomorphological model outputs. A total of 18 model scenarios were compared. For the three sediment response catchments, where the model's propensity to transport sediment was increased from minimum to median to maximum possible sediment yield, six scenarios were tested and compared:

- Baseline
- Linear RAFs
- U-shaped RAFs
- Extended linear RAFs
- Extended U-shaped RAFs
- Double linear RAFs

At the catchment outlet, water and sediment discharge were compared. For the catchment as a whole, spatially distributed outputs of water depth and elevation were exported from the model every half day, at a spatial resolution of 4 m. With regards to geomorphological change, the net elevation change was calculated between Day 24 and 28 to ensure the entirety of change occurring from the Boxing Day event was included within analysis. Prior to further analysis, a level of detection of 0.05 m was set for all water depths and net elevation changes. Water volume was also calculated through time using the water depth layers.

Change occurring within the vicinity, both up and downstream of the RAFs themselves was analysed using tools within ArcGIS's 'Zonal' toolbox, including 'Zonal Statistics' and 'Zonal Histograms'. Overtopping and bund erosion was calculated using the shapefiles of the bunds themselves (Figure 3.6). Water and sediment metrics were calculated for the areas immediately upstream and downstream of the RAFs (Figure 3.6). The upstream areas were created as the width of the RAF with the initial distance they extended to upstream created to be the same as the width. Distance upstream was then manually extended for each shapefile feature to ensure the backwater effect occurring at the peak of the event from all scenarios was included. The upstream areas were manually shifted to be placed immediately downstream of the RAFs to create the shapefiles for downstream analysis (Figure 3.6). Water volume and positive and negative volumetric elevation changes were calculated upstream. Positive and negative volumetric elevation change was also calculated downstream. Mean water height and velocity was calculated for both the areas upstream and downstream. Results were filtered to ensure correct statistical analysis including the calculation of volumes and means when using the ArcGIS tools. Filtering ensured all areas had at least two cells with values included.

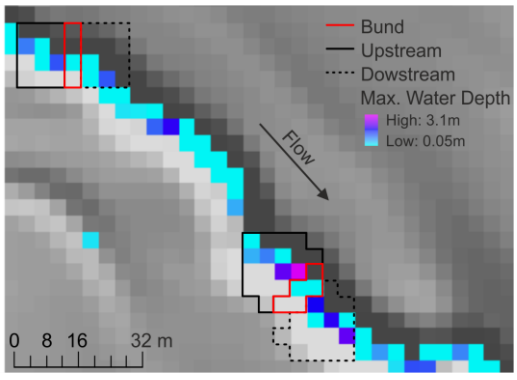

Figure 3.6: Examples of the shapefiles created for zonal statistical analysis for linear bunds. Background mapping is a hillshaded DTM for visualisation only.

Statistical analysis was undertaken on the mean upstream water depths and the positive and negative net elevation change to understand whether the five RAF designs were significantly different in terms of their hydrological and geomorphological effects. Anderson-Darling normality tests were taken prior to undertaking Kruskall-Wallis tests for the data per sediment response catchment in Minitab 18. Minitab 18 was subsequently used for post-hoc Dunn's Tests, with Bonferroni correction, to allow for greater understanding as to which designs were significantly different to the others (Minitab, 2019).

3.3 Results

3.3.1 Hydrological response of runoff attenuation features

3.3.1.1 Catchment outlet water discharge

Overall, there was little difference to the water discharge at the catchment outlet between any of the RAF modelled scenarios, with 13 of the 15 scenarios resulting in less than 2 % difference in either peak water discharge and flood volume. The notable exceptions were a 2.11 % decrease in flood volume for the minimum SRC when a u-shaped RAF was implemented and a 5.21 % decrease in flood volume for the minimum SRC when an extended u-shaped RAF was implemented (Table 3.2).

Table 3.2: Summary metrics of water discharge at the catchment outlet.

		Baseline	Linear	U-shaped	Extended Linear	Extended U-shaped	Double Linear
Minimum SRC	Peak Discharge (m^3s^{-1})	58.5	58.5	58.3	58.3	57.7	58.2
	% Change from baseline		**-0.13**	**-0.42**	**-0.46**	**-1.37**	**-0.64**
	Flood Volume (x 10^6 m^3)	4.14	4.14	4.06	4.13	3.93	4.07
	% Change from baseline		**-0.01**	**-2.11**	**-0.33**	**-5.21**	**-1.69**
Median SRC	Peak Discharge (m^3s^{-1})	58.0	58.4	58.1	58.2	58.1	58.0
	% Change from baseline		**0.71**	**0.11**	**0.23**	**0.17**	**0.03**
	Flood Volume (x 10^6 m^3)	4.23	4.21	4.20	4.21	4.19	4.21
	% Change from baseline		**-0.32**	**-0.55**	**-0.38**	**-0.99**	**-0.51**
Maximum SRC	Peak Discharge (m^3s^{-1})	59.1	58.7	58.8	58.7	58.9	58.7
	% Change from baseline		**-0.61**	**-0.49**	**-0.64**	**-0.28**	**-0.70**
	Flood Volume (x 10^6 m^3)	4.30	4.26	4.25	4.26	4.25	4.25
	% Change from baseline		**-0.87**	**-1.08**	**-1.01**	**-1.26**	**-1.12**

3.3.1.2 Whole catchment water volume

All RAF scenarios resulted in a greater cumulative water volume throughout the catchment than the baseline scenario (Figure 3.7a). The linear RAFs resulted in the lowest whole catchment cumulative water volume (1.39 – 3.17 x10^6 m^3) and the extended u-shaped RAFs resulted in the greatest whole catchment cumulative water volume (1.59 – 3.42 x10^6 m^3). Differences in RAF scenarios was greater after the peak of the event (Figure 3.7a). Cumulative water volume upstream of RAFs was greatest for the extended u-shaped RAFs (2.52 – 3.99 x10^5 m^3), followed by u-shaped, double linear and extended linear RAFs, the linear RAFs resulted in the lowest cumulative water volume upstream of RAFs (0.60 – 1.10 x10^5 m^3) (Figure 3.7b).

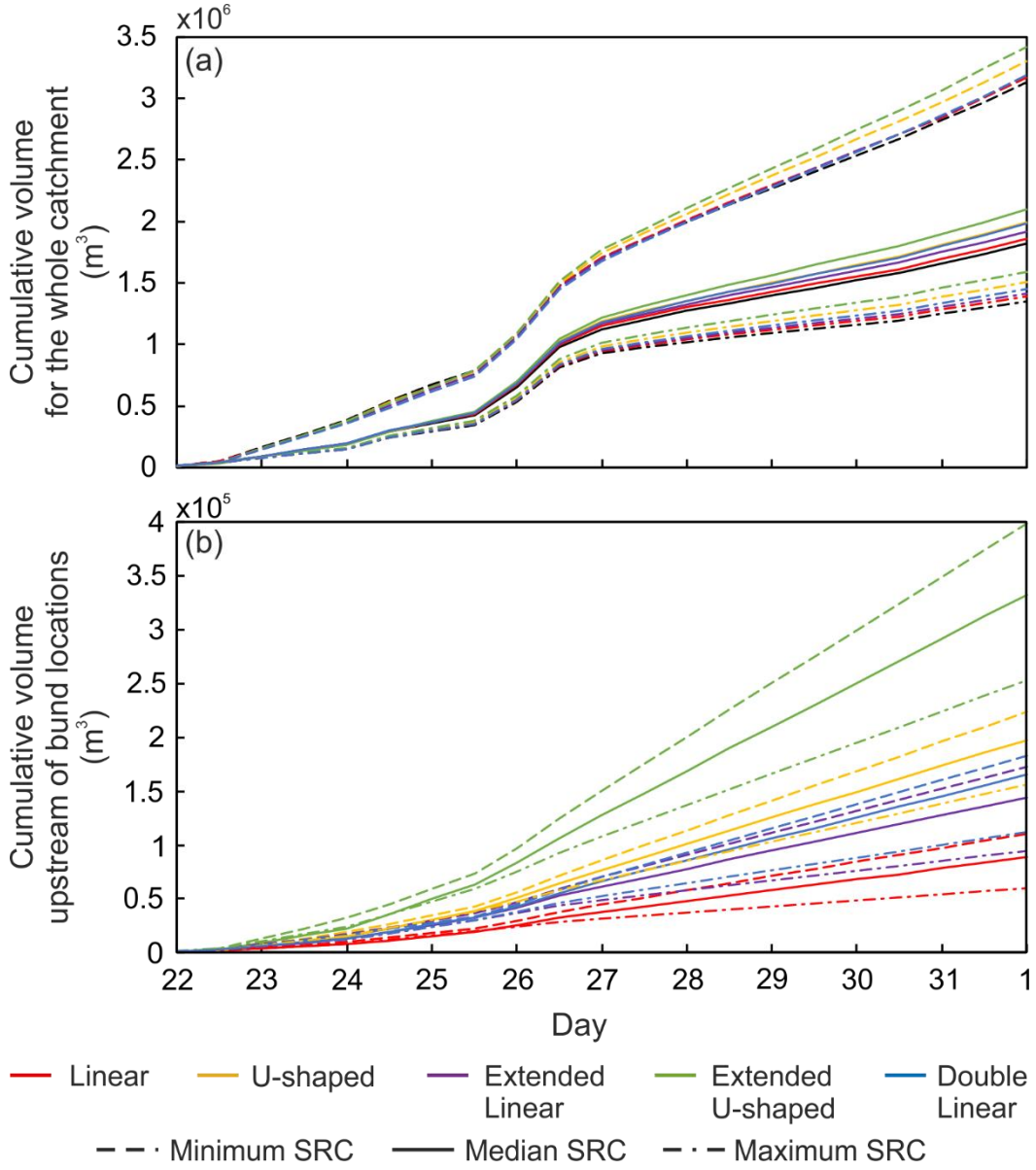

Figure 3.7: Cumulative volume of water through time for (a) the whole catchment and (b) the areas upstream of RAF locations.

3.3.1.3 Overall effect of RAFs on water retention

The fewest RAFs held water when they were linear in design, the most held water when they were extended u-shaped in design (Table 3.3). Changing the shape of the RAF from linear to u-shaped, increasing the size and increasing the quantity of RAFs increased the number of RAFs holding water. The maximum water volume held upstream was greatest for the extended u-shaped RAFs, apart from for the Maximum SRC, where a u-shaped RAF held the greatest water volume upstream (Table 3.3). Double linear RAFs resulted in the lowest maximum water volume. However, the most RAFs were overtopped when extended u-shaped in design with linear RAFs being overtopped the least (Table 3.3).

Table 3.3: Summary metrics of the hydrological performance of RAFs.

		Linear	U-shaped	Extended Linear	Extended U-shaped	Double Linear
Minimum SRC	Number of RAFs holding water	170	238	211	243	206
	Maximum volume for any RAF through time (m^3)	574.1	907.9	627.3	943.8	556.4
	Number of RAFs overtopped	27	50	46	66	42
Median SRC	Number of RAFs used holding water	171	236	212	243	221
	Maximum volume for any RAF through time (m^3)	491.0	956.0	586.3	975.6	473.9
	Number of RAFs overtopped	28	56	51	64	45
Maximum SRC	Number of RAFs used holding water	161	224	193	231	209
	Maximum volume for any RAF through time (m^3)	483.2	894.9	483.6	812	450.5
	Number of RAFs overtopped	28	65	50	78	45

3.3.1.4 Water volume held upstream of RAFs

Median water volume and the interquartile range (IQR) held upstream of RAFs was lower for the linear RAFs compared to the u-shaped RAFs throughout the simulation (Figure 3.8 a-c). At the peak of the event, the difference in median water volume was between 13.6 m^3 and 22.7 m^3 and the difference in the IQR

was between 9.54 m^3 and 18.5 m^3 depending on the SRC. Linear RAFs saw little difference in median water volume through time whereas for u-shaped RAFs, median water volume increased prior to the event peak and remained at an elevated level for the rest of the simulation (Figure 3.8 a-c).

Extending the linear RAFs resulted in increases of between 6.97 m^3 - 7.11 m^3 in the median water volume and of 13.2 m^3 - 20.5 m^3 to the IQR at the peak of the event (Figure 3.8 d-f). There was however, little difference (< 3.3 m^3) in the first quartile of water volumes between the linear and extended linear RAFs. Volume held upstream increased at a faster rate for the extended linear RAFs than for the linear RAFs. Extending the u-shaped RAFs increased the median water volume by between 18.3 m^3 and 31.5 m^3 and the IQR by 29.3 m^3 – 46.7 m^3 at the peak of the event (Figure 3.8 g-i). Both the u-shaped and extended u-shaped RAFs saw a dramatic increase in volume on the first day and continued to increase to the peak of the event, before there was little change to the end of the simulation.

Increasing the quantity of the linear RAFs resulted in an increase in median water volume of between 7.69 m^3 and 9.88 m^3 and in the IQR of between 18.7 m^3 and 25.4 m^3 at the peak of the event (Figure 3.8 j-l). These differences were of a similar magnitude to the differences between the linear and extended linear RAFs. Median water volume upstream of double linear RAFs increased at a greater rate than the linear RAFs before the peak of the event however for both RAF designs, median water volume remained at a similar level to the end of the simulation.

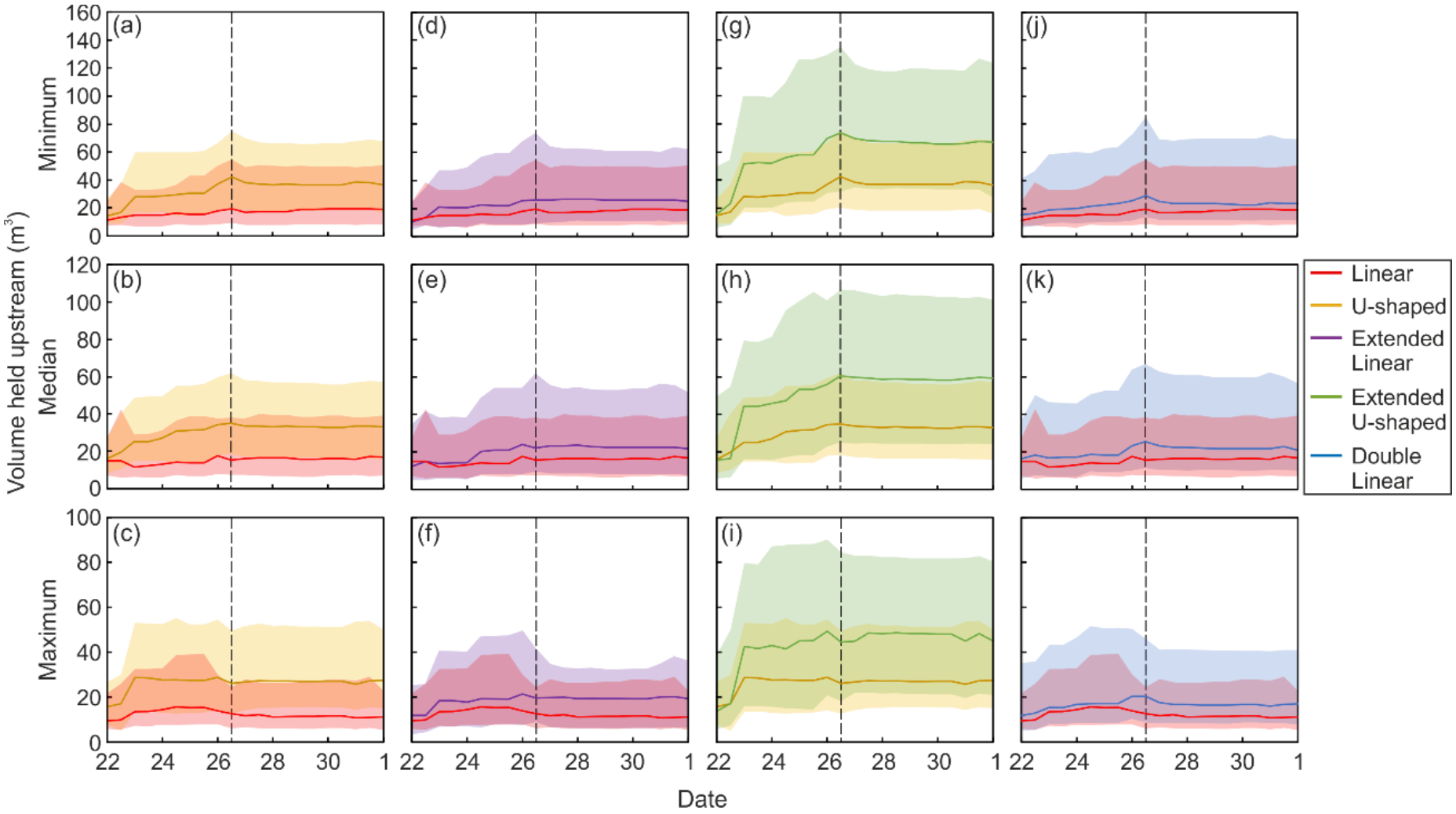

Figure 3.8: Median and shaded quartiles of water volume held upstream of RAFs through time for (a-c) linear and u-shaped RAFs, (d-f) linear and extended linear RAFs, (g-i) u-shaped and extended u-shaped RAFs and (j-l) linear and double linear RAFs.

3.3.1.5 Timing and duration of water retention

For the minimum SRC, of the RAF designs tested, the u-shaped design saw the greatest proportion of features where maximum water volume did not occur at the event peak (Table 3.4). 4.6 % of u-shaped RAFs saw the maximum water volume occur prior to the event peak and 10.1 % of u-shaped RAFs saw the maximum water volume occur after the event peak (Table 3.4). The u-shaped design also resulted in the highest proportion of RAFs retaining water for over half the simulation (97.1 %) (Table 3.4). For the median SRC, again the u-shaped design resulted in the highest proportion of RAFs experiencing maximum water volume before the peak of the event (22 %). The linear RAFs saw the greatest proportion of features result in the maximum water volume occurring after the event peak (11.1 %) (Table 3.4). The extended u-shaped design saw the largest proportion of RAFs with water being retained for over half the simulation (91.8 %) (Table 3.4). For the maximum SRC, the extended u-shaped design resulted in the largest proportion of features where maximum water volume occurred prior to the event peak (47.7 %) and the u-shaped design saw the greatest proportion of features where maximum water volume occurred after the event peak (9.6 %). The linear design resulted in the greatest proportion of RAFs where water was retained for longer than half the simulation time (50.3 %) (Table 3.4).

Table 3.4: Timing and duration metrics of water retention upstream of RAFs.

		Linear	U-shaped	Extended Linear	Extended U-shaped	Double Linear
Min. SRC	RAFs where maximum volume occurred not at event peak (Pre-peak/Post-peak) (%)	1.8/ 5.3	4.6/ 10.1	2.4/ 8.5	2.5/ 8.2	0.5/ 7.3
	RAFs where water was retained for over half the simulation (%)	84.1	97.1	86.7	96.7	93.2
Med. SRC	RAFs where maximum volume occurred not at event peak (Pre-peak/Post-peak) (%)	19.3/ 11.1	22.0/ 8.5	19.8/ 9.4	21.4/ 9.5	18.1/ 9.0
	RAFs where water was retained for over half the simulation (%)	75.4	91.5	82.5	91.8	90.0
Max. SRC	RAFs where maximum volume occurred not at event peak (Pre-peak/Post-peak) (%)	43.7/ 4.2	45.9/ 9.6	38.9/ 4.4	47.7/ 6.4	40.2/ 6.5
	RAFs where water was retained for over half the simulation (%)	50.3	24.9	46.3	29.4	37.9

3.3.1.6 Spatial variability of water retention

Figure 3.9 highlights the variation in volume held behind RAFs at the peak of the event throughout the catchment. Patterns can be seen in the south of the catchment, where changing the design from linear to u-shaped and from u-shaped to extended u-shaped overall increases the volume of water held, although volumes were smaller than in other areas of the catchment. In the west of the catchment, a number of linear RAFs held the most water of the designs tested. Various designs near the catchment outlet held the largest water volumes at the peak of the event, volumes which were greater than those in the upper reaches (Figure 3.9).

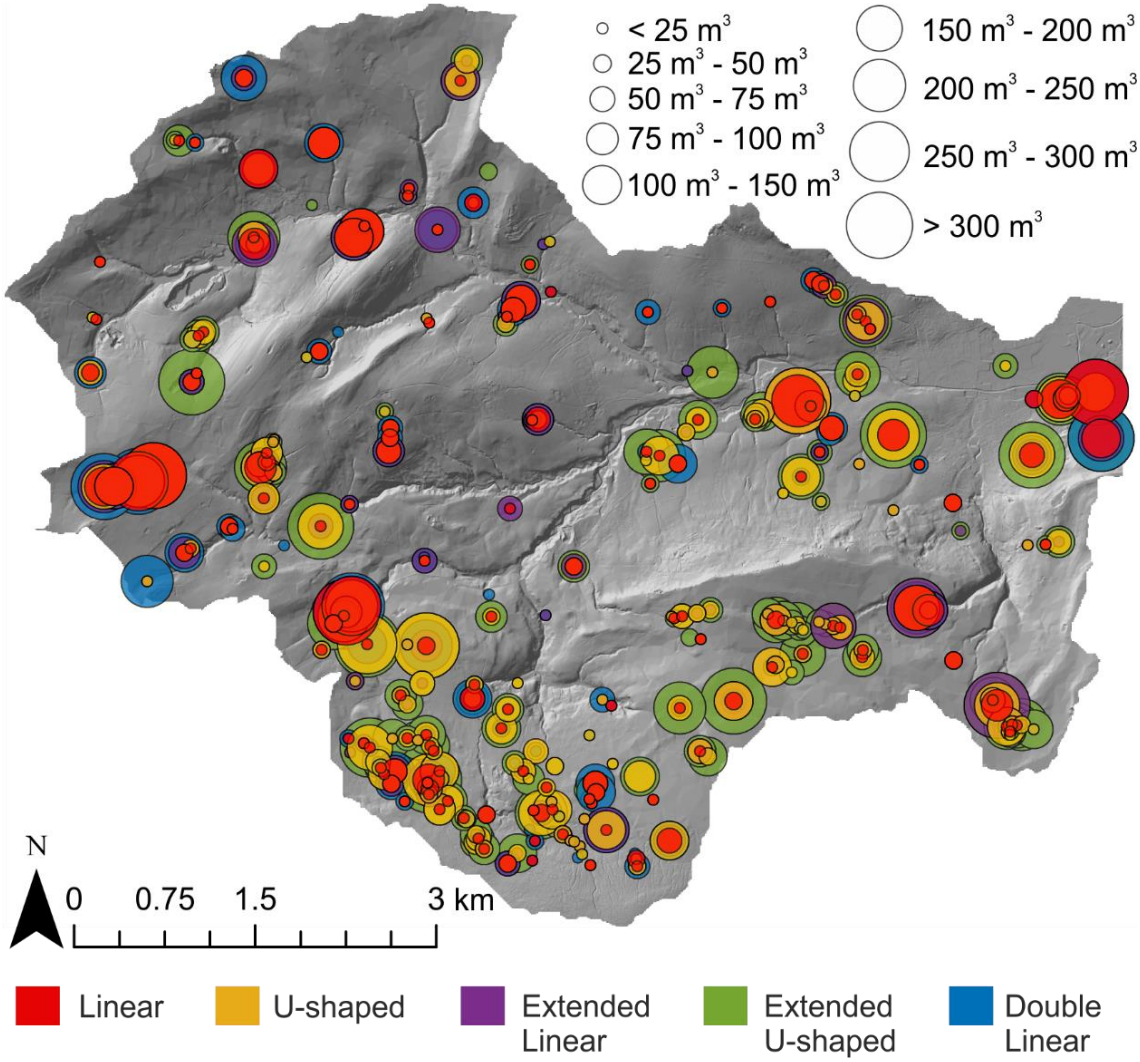

Figure 3.9: Graduated symbols of the water volume held behind RAFs for the median SRC. Background mapping is a hillshaded DTM for visualisation only. Separate figures available in Figure B.1.

3.3.1.7 Water depth and velocity

Regardless of design, mean water depth was greater upstream (median values between 0.15 and 0.38 m) compared to downstream (median values between 0.09 and 0.18 m), albeit with greater variation (IQR) upstream than downstream (Figure 3.10a). Mean water velocity was greater downstream (0.33 – 0.44 ms^{-1}) compared to upstream (0.09 – 0.35 ms^{-1}) in terms of the median, however the IQR was greater upstream compared to downstream (Figure 3.10b).

Upstream, u-shaped designs saw greater mean water depths (Figure 3.10a) and lower mean water velocities (Figure 3.10b) than linear designs albeit with no noticeable pattern between designs in the IQR. There was little difference in upstream mean water depth between the two u-shaped designs in terms of the median, however u-shaped RAFs saw a greater IQR compared to the extended u-shaped RAFs. The extended u-shaped RAFs saw greater mean velocities compared to u-shaped RAFs in terms of the median but also greater variation (IQR). For the linear designs, only small differences (< 0.05 m) were seen in upstream water depths (Figure 3.10a). However, mean velocity was lower for the double linear design compared to the two other linear designs (median values, Figure 3.10b). Fewer differences between designs were observed downstream, the only notable difference was the greater water depth and lower velocity for the double linear design.

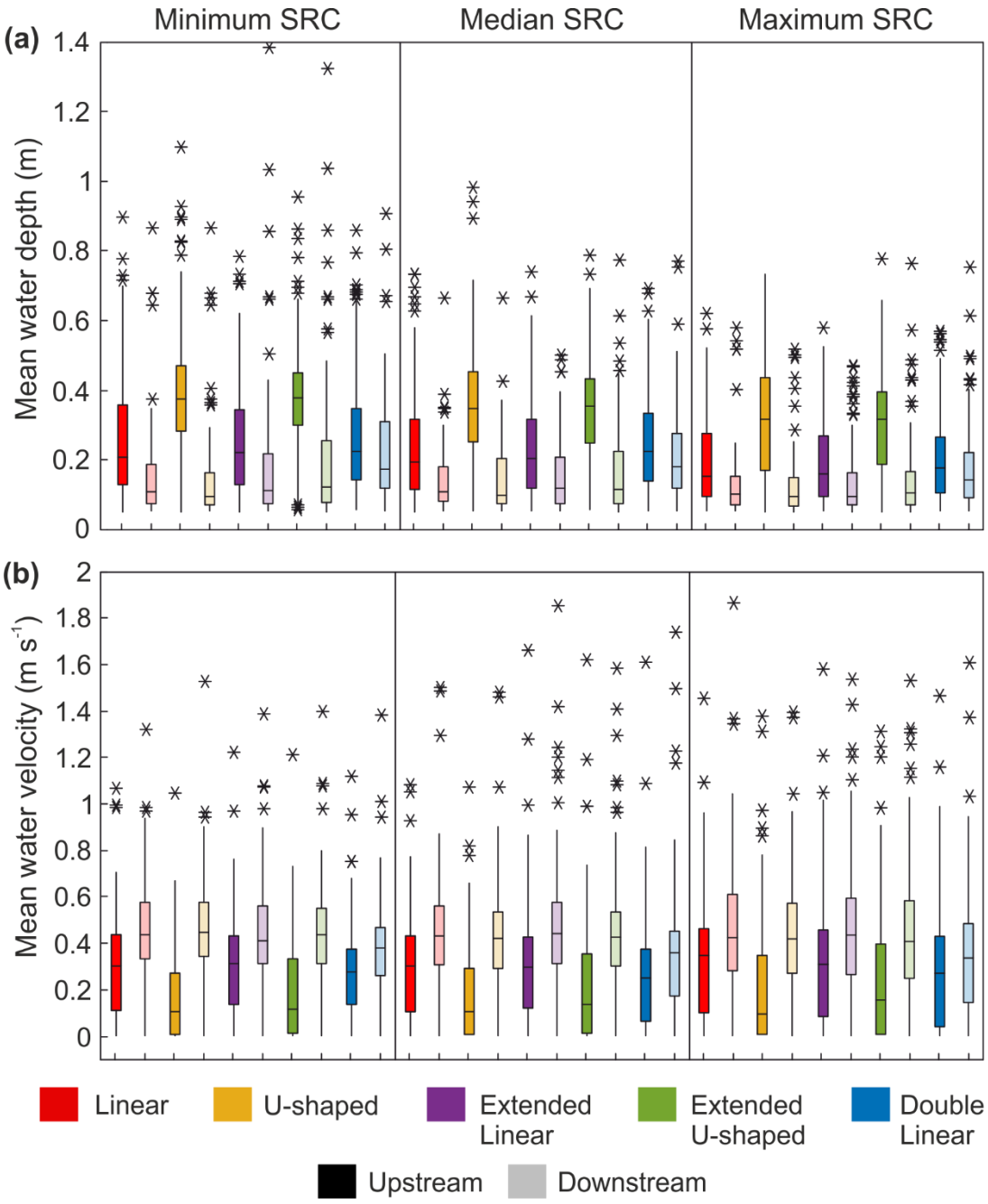

Figure 3.10: Boxplots of (a) mean water depth and (b) mean water velocity upstream (solid colour) and downstream (translucent colour) of RAFs at the peak of the event.

Mean upstream water depths were statistically significantly different (Table 3.5), between the RAF designs for all three sediment response catchments. Post-hoc testing showed, for all three sediment response catchments, the u-shaped design had statistically significantly greater water depths than the linear, extended linear and double linear designs (Table 3.6). The extended u-shaped design had significantly greater water depths than the three linear designs. The difference in depths were insignificant between the two u-shaped designs and again between the three linear designs (Table 3.6).

Table 3.5: Kruskall-Wallis statistical analysis results for mean water depth upstream of RAFs

Sediment Response Catchment	Kruskall-Wallis
Minimum	H=170.24, p<0.01
Median	H=145.91, p<0.01
Maximum	H=135.80, p<0.01

Table 3.6: Post-hoc Dunn's Test statistical analysis results for mean water depth upstream of RAFs. Z-values per SRC in italics below p-value, and are for the minimum, median and maximum SRC respectively.

	Linear	U-shaped	Extended Linear	Extended U-shaped	Double Linear
Linear		p<0.01 *z-values* *7.99,* *8.05,* *7.85*		p<0.01 *z-values* *8.46,* *7.67,* *7.37*	
U-Shaped			p<0.01 *z-values* *8.57,* *8.40,* *7.93*		p<0.01 *z-values* *7.61,* *7.20,* *7.25*
Extended Linear				p<0.01 *z-values* *9.07,* *8.00,* *7.43*	
Extended U-shaped					p<0.01 *z-values* *8.10,* *6.79,* *7.73*
Double Linear					

3.3.2 Geomorphological response to the implementation of runoff attenuation RAFs

3.3.2.1 Outlet sediment discharge

There was no clear pattern between the effects of RAF designs on sediment discharge at the catchment outlet (Figure 3.11). For the minimum SRC, percentage changes from the baseline scenario were less than 6 % for both changes to the peak sediment discharge and the sediment yield, the largest changes were increases to peak discharge (5.3 %) and sediment yield (3.4 %) for the u-shaped RAF (Figure 3.11a). For the median SRC, all RAF scenarios resulted in an increase to peak sediment discharge and sediment yield through time (Figure 3.11b). The greatest increase in peak discharge was observed for the linear RAF design (14.1 %) and the extended u-shaped RAFs saw the greatest increase in sediment yield (7.6 %). For the maximum SRC, all RAF scenarios resulted in an increase in peak discharge of up to 22.8 % (Figure 3.11c). Smaller differences were seen for sediment yield with the u-shaped and extended linear RAF scenarios resulting in a decrease in sediment yield (< 6.1 %), the other design scenarios saw increases of up to 7.6 % (Figure 3.11c).

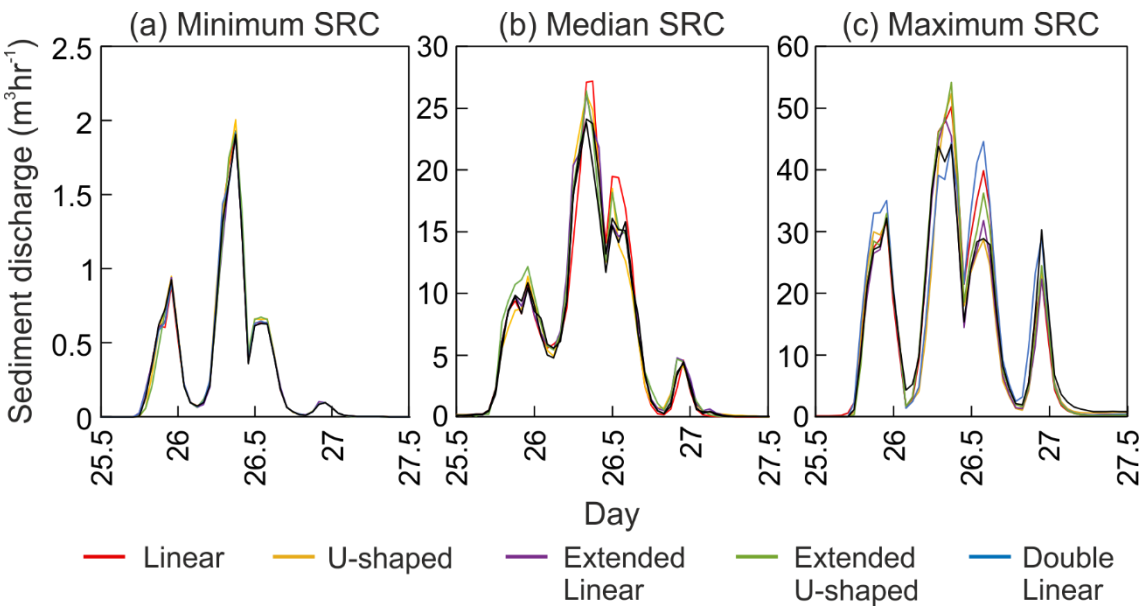

Figure 3.11: Catchment outlet sediment discharge for (a) the minimum, (b) the median and (c) the maximum SRCs.

3.3.2.2 Whole catchment net elevation change

In all scenarios, the catchment was deposition dominant (Figure 3.12). There was however very little difference in the internal geomorphology between RAF designs. For the minimum SRC, the greatest change was seen to the total geomorphologically active area, where a percentage increase of 18.4 % was observed between the smallest area (baseline, 1.25 x 10^5 m^2) and largest area (double linear, 1.48 x 10^5 m^2). For the median and maximum SRCs, the difference was less pronounced, with a percentage change between the smallest and

largest geomorphologically active areas of 2.8 % and 2.1 % respectively (Figure 3.12).

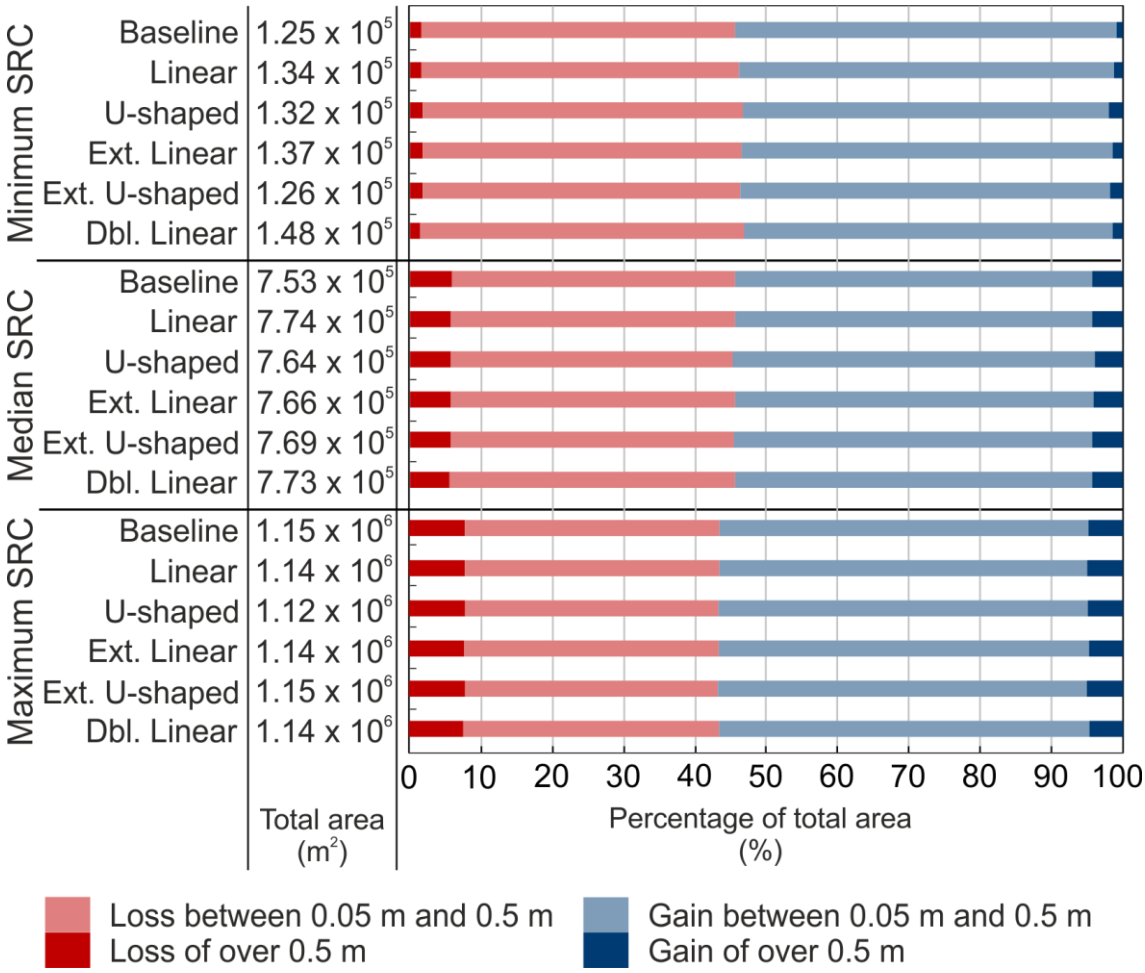

Figure 3.12: Ratios of magnitudes of net elevation change for the catchment as a whole and total geomorphically active areas for all scenarios.

3.3.2.3 Overall effect of RAFs on net elevation change

In the area immediately upstream of the RAFs, for the catchment as a whole, the total volume gained behind RAFs was greater than the total volume lost, with a greater number of RAFs experiencing deposition than erosion for all designs in all SRCs (Figure 3.13). The u-shaped RAF design resulted in the smallest sediment volume gained (50.3 – 1207.5 m^3) and smallest sediment volume lost (5.8 – 461.9 m^3) from behind the RAFs for all SRCs (Figure 3.13). The largest sediment volume gain occurred behind the double linear RAF design (253.7 – 2768.5 m^3) however the extended linear design resulted in the largest loss of sediment volume behind RAFs (80.2 – 1808.6 m^3) (Figure 3.13).

Immediately downstream of the RAFs, the sediment volume gained was greater than the sediment volume lost and a greater number of RAFs experienced

deposition downstream compared to those that experienced erosion downstream for all designs in all SRCs (Figure 3.13). Whether the volume lost or gained downstream was greater than the volume lost or gained upstream was both dependent on the RAF design and SRC (Figure 3.13). Overall the linear design tended to produce the smallest sediment volumes loss or gain downstream of the RAFs and the double linear and extended u-shaped designs resulted in the largest sediment volumes gained or lost downstream (Figure 3.13).

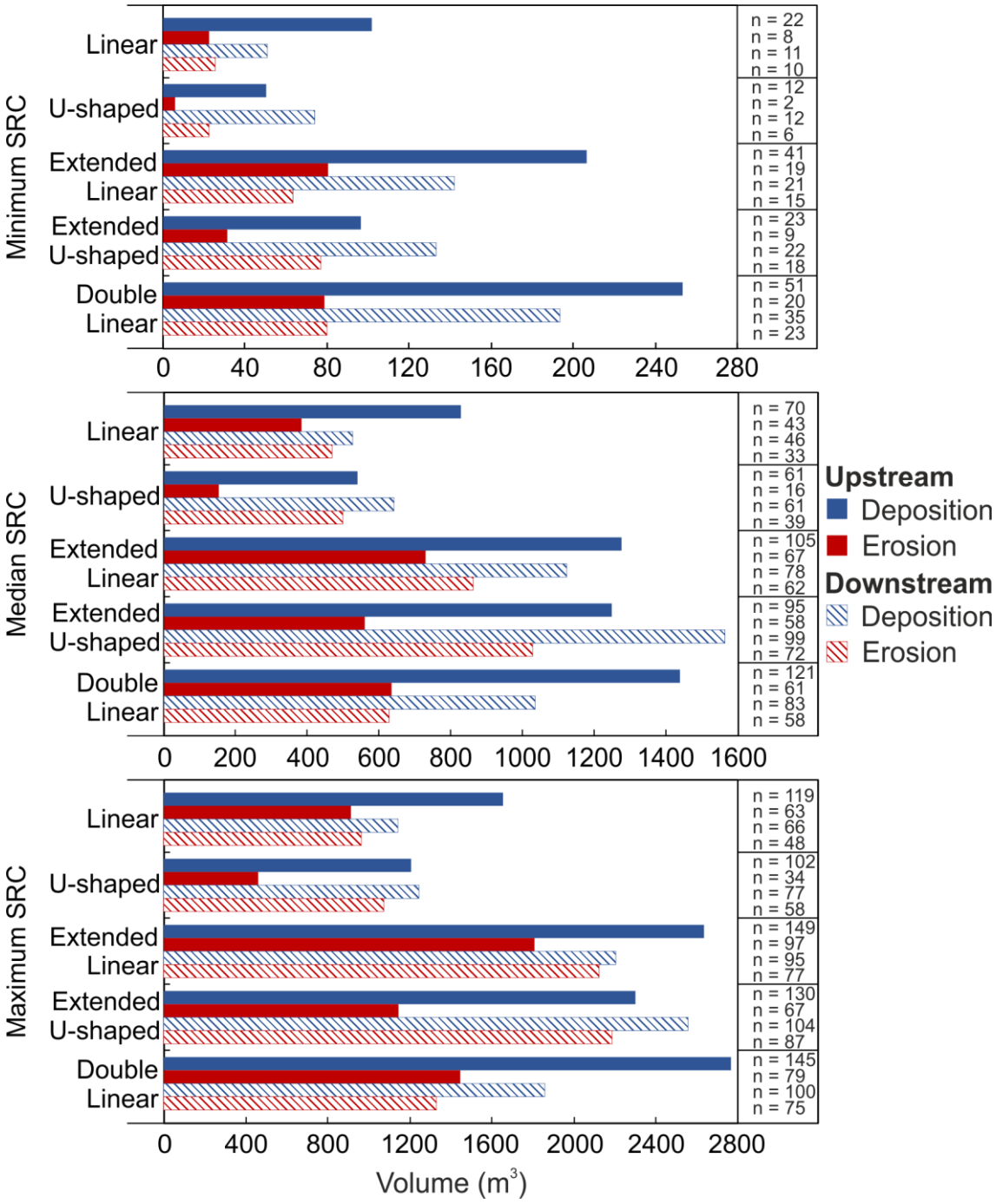

Figure 3.13: Total sediment volume lost or gained from areas upstream and downstream of RAFs with the associated count data.

Many RAFs experienced bund erosion, however the linear design was the least affected (12 – 54 RAFs) (Table 3.7). The design that was the most affected differed with the SRC. For the minimum SRC, the double linear design had the greatest number of bunds eroded (52 RAFs) and the for median and maximum SRCs, the extended u-shaped RAFs saw the greatest number of bunds eroded, with 115 RAFs and 131 RAFs eroded respectively (Table 3.7).

Table 3.7: Number of RAFs experiencing erosion to the bunds themselves.

	Linear	**U-shaped**	**Extended Linear**	**Extended U-shaped**	**Double Linear**
Minimum SRC	12	21	21	42	52
Median SRC	39	90	66	115	110
Maximum SRC	54	100	89	131	112

3.3.2.4 Net volumetric change occurring upstream of RAFs

Net negative volumetric change occurring upstream of RAFs was both dependent on design and SRC (Figure 3.14). For the minimum SRC, the extended linear design saw the greatest median negative volumetric change (-3.4 m^3) and the linear design saw the lowest median negative volumetric change (-2.2 m^3) and smallest IQR (2.0 m^3) (Figure 3.14a). For the median SRC, the u-shaped design saw the lowest median negative volumetric change of -4.1 m^3, the greatest being observed for the double linear design (5.3 m^3) (Figure 3.14b). For the median SRC, the greatest variation in negative volumetric change was seen for the extended linear design (IQR = 10.3 m^3). For the maximum SRC, the greatest median negative volumetric change was observed for the extended linear design (-8.42 m^3), the lowest was seen for the linear RAFs (-6.68 m^3) (Figure 3.14c). The largest variation in negative volumetric change was observed for the extended U-shaped RAFs (IQR = 19.7 m^3) (Figure 3.14c).

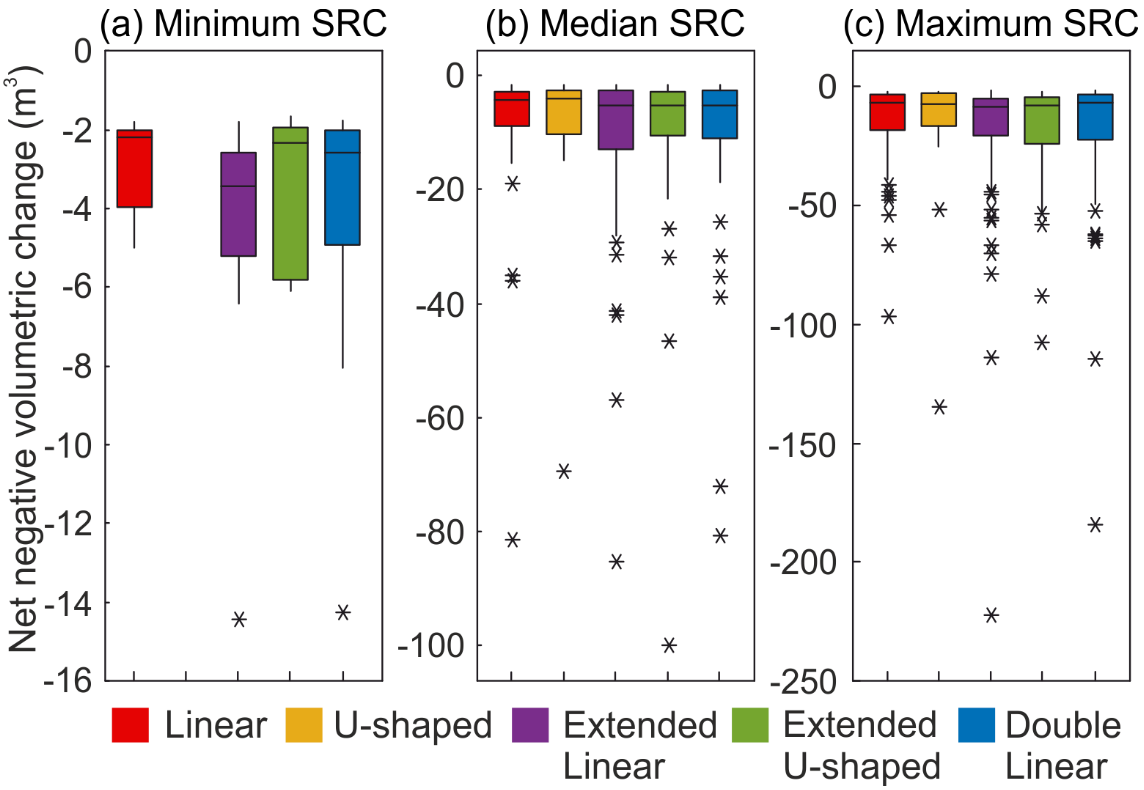

Figure 3.14: Boxplots of negative volumetric change occurring upstream of RAFs for (a) the minimum SRC, (b) the median SRC and (c) the maximum SRC. NB: Boxplot for u-shaped RAF in the Minimum SRC not applicable due to lack of samples (n = 2), see Figure 3.13 for all count data.

Net positive volumetric change was also dependent on the RAF design and SRC (Figure 3.15). The greatest median positive volumetric change occurred for the linear RAFs in the minimum SRC (4.2 m^3), double linear RAFs in the median SRC (7.2 m^3) and extended linear RAFs for the maximum SRC (11.0 m^3). The lowest median net positive volumetric change occurred for the extended u-shaped RAFs in the minimum and median SRCs (3.4 m^3 and 6.0 m^3 respectively) but for the u-shaped design in the maximum SRC (7.6 m^3). The largest variability in positive volumetric change occurred for the linear designs in the minimum and median SRCs (3.7 and 13.5 m^3) but for the double linear design in the maximum SRC (21.6 m^3) (Figure 3.15).

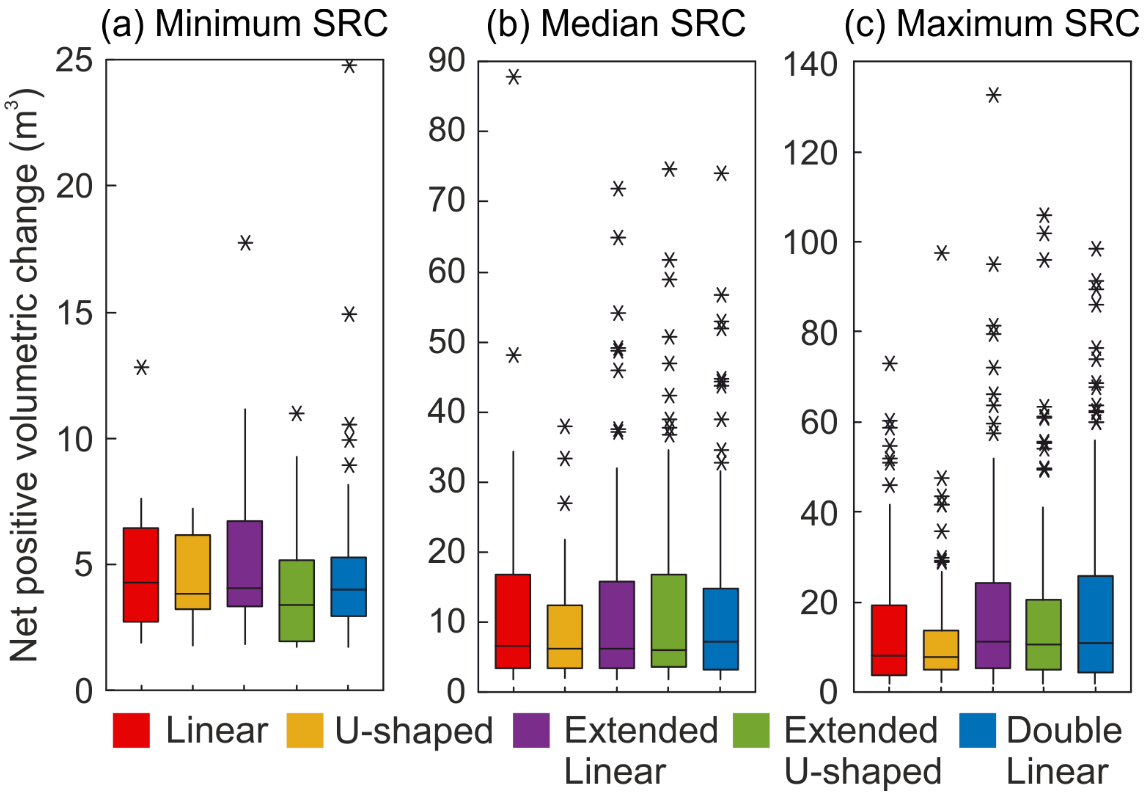

Figure 3.15: Boxplots of positive volumetric change occurring upstream of RAFs for (a) the minimum SRC, (b) the median SRC and (c) the maximum SRC.

Statistically, the minimum and median sediment response catchments showed no significantly different net elevation changes between RAF designs (Table 3.8). For the maximum sediment response catchment, only positive net elevation change was significantly different between the RAF designs (Table 3.8). There were significant differences in positive net elevation change between the linear and extended u-shaped design, u-shaped and extended u-shaped designs, and the linear and double linear designs (Table 3.9).

Table 3.8: Kruskall-Wallis statistical analysis results for net elevation change

SRC	Positive	Negative
Minimum	H=2.69, p=0.611	H=3.48, p=0.481
Median	H=1.39, p=0.846	H=1.07, p=0.899
Maximum	**H=13.8, p=0.008**	H=6.54, p=0.162

Table 3.9: Post-hoc Dunn's tests statistical analysis for maximum sediment response catchment

	Linear	U-shaped	Extended Linear	Extended U-shaped	Double Linear
Linear				p<0.01 z=2.90	p=0.02 z=2.41
U-Shaped				p<0.01 z=2.73	
Extended Linear					
Extended U-shaped					
Double Linear					

3.3.2.5 Spatial variability of net volumetric change

A noticeable proportion of RAFs experiencing both positive and negative net volumetric change were located in the south of the catchment in addition to a lack of RAFs experiencing volumetric change near the catchment outlet (Figure 3.16). Figure 3.16 highlights that fewer RAFs experienced negative volumetric change upstream compared to those experiencing positive volumetric change. There was no obvious catchment-wide pattern in RAF design for the size of positive volumetric change. In the northwest of the catchment, u-shaped designs resulted in lower positive volumetric change compared to other designs (Figure 3.16a). Fewer differences were observable in the south of the catchment. For negative volumetric change, the u-shaped design generally resulted in the lowest negative volumetric change throughout the catchment, spatial patterns were less discernible for other designs (Figure 3.16b).

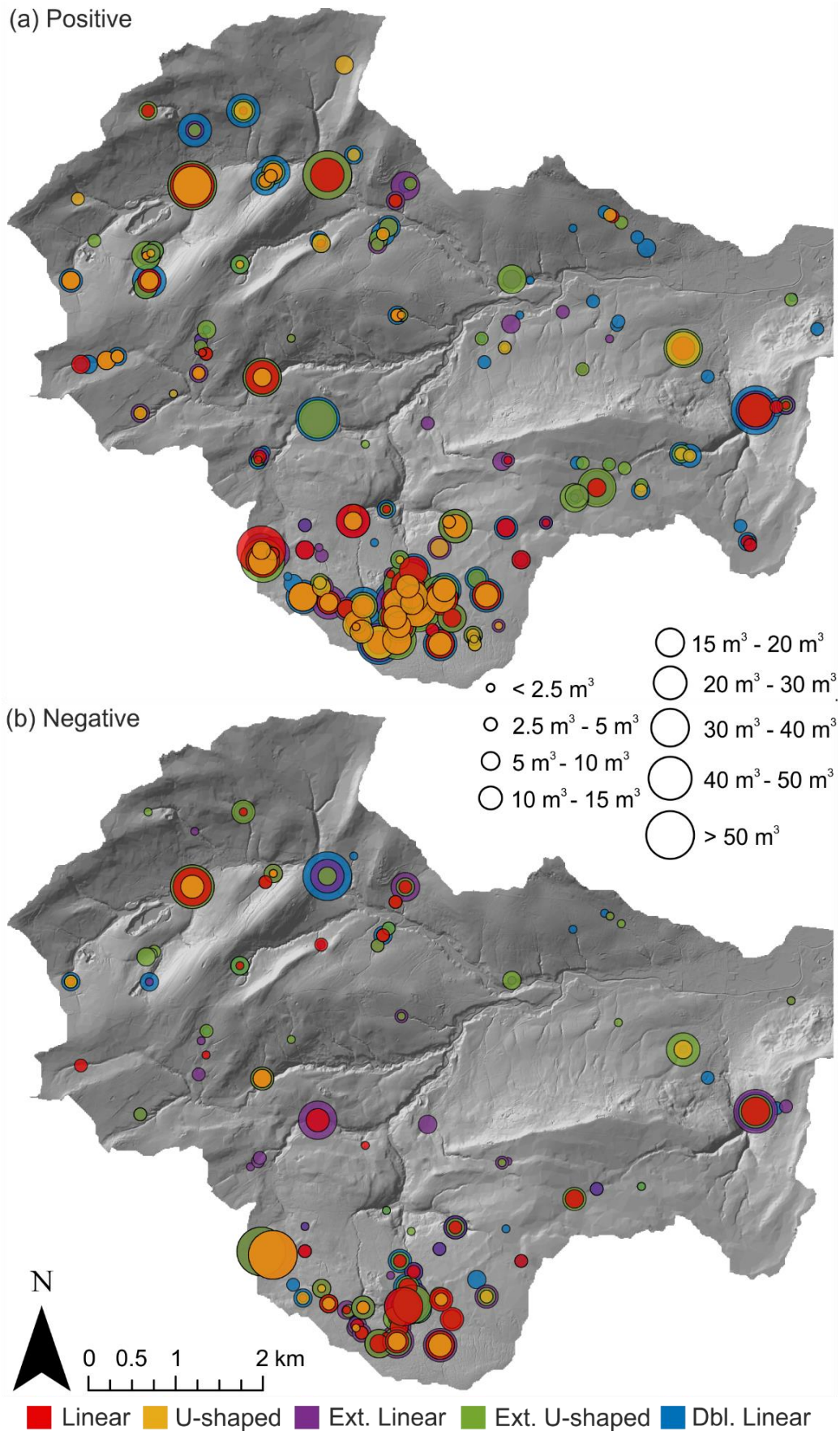

Figure 3.16: Graduated symbols of (a) positive volumetric change and (b) negative volumetric change for the median SRC. Background mapping is a hillshaded DTM for visualisation only. Separate figures available in Figure B.2 and Figure B.3.

3.3.3 The effect of the sediment response catchment

There was little difference to the catchment outlet water discharge and flood volume between the three SRCs (Table 3.2). However, when increasing the SRC, cumulative volume for the whole catchment decreased, with a difference from minimum SRC to maximum SRC of between 1.74 x 10^6 m^3 and 1.83 x 10^6 m^3 at the end of the simulation (Figure 3.7a). Cumulative volume behind RAFs also decreased for all RAF designs by between 5.1 x 10^4 m^3 and 1.46 x 10^5 m^3 at the end of the simulation (Figure 3.7b). Median water volume and the IQR of water volumes held behind RAFs decreased with increasing SRC at the peak of the event with a decrease of between 6.3 m^3 and 29.3 m^3 in the median water volume and 18.3 m^3 and 35.7 m^3 in the IQR (Figure 3.8). For other time steps, differences in the median and IQR varied depending on RAF design (Figure 3.8). The proportion of RAFs where peak water retention occurred before the peak of the event increased with increasing SRC by between 36.5 % and 45.2 % (Table 3.4)

As expected, increasing the SRC resulted in increases to the peak sediment discharge of up to 52 m^3hr^{-1} and increases in sediment volume of up to 682 m^3 at the catchment outlet (Figure 3.11). Increasing the SRC resulted in increases to the number of RAFs experiencing both erosion (increases between 90 and 108 RAFs) and deposition upstream (increases between 32 and 78 RAFs) (Figure 3.13). The total sediment volume lost from behind RAFs increased with increasing SRC by between 456 m^3 and 1728 m^3. Total sediment volume gained behind all RAFs also increased with increasing SRC by between 1157 m^3 and 2514 m^3 (Figure 3.13). An additional 42 to 89 RAFs experienced erosion to the feature itself between the minimum and maximum SRC (Table 3.7).

The median volume of erosion occurring upstream of RAFs increased with increasing SRC for all RAF designs by between 4.3 m^3 and 5.4 m^3. The IQR also increased for all RAF designs by between 13 and 15.9 m^3 (Figure 3.14). Median volume of deposition increased with increasing SRC for all RAF designs by between 3.6 m^3 and 7 m^3. IQR increased with increasing SRC by between 11.9 m^3 and 19.3 m^3 for all but the u-shaped RAFs, where the IQR was greatest for the median SRC (Figure 3.15).

3.4 Discussion

3.4.1 Key outcomes

Prior to a discussion about the effects of RAF design, the key outcomes of the modelling were:

- There was no notable impact of RAFs on the peak water discharge at the catchment outlet.
- There was greater variation in sediment discharge at catchment outlet when implementing RAFs, with little difference in the Minimum SRC, increases in sediment yield of up to 7.6 % for the Median SRC and either increases of up to 7.6 % (linear, extended u-shaped and double linear) or decreases of up to 6.1 % (u-shaped and extended linear) in sediment yield for the Maximum SRC.
- Linear RAFs were the least effective at storing water and extended u-shaped RAFs were the most effective at storing water with median water storage of 12.6 - 19.6 m^3 and 44.5 – 73.8 m^3 at the event peak respectively.
- Mean water depths upstream were statistically significantly higher for the two u-shaped designs compared to the three linear designs.
- U-shaped RAFs saw the lowest sediment volume lost and gained from upstream of RAFs.
- Double linear and extended linear RAFs saw the greatest volumes of sediment gained and lost from upstream of RAFs.
- The maximum sediment response catchment saw statistically significant differences in positive net elevation change between the linear and extended u-shaped designs, u-shaped and extended u-shaped, and linear and double linear designs.
- Extended u-shaped RAFs were most likely to be overtopped and linear the least.
- Linear RAFs were the least likely to experience erosion to the bund itself, with double linear RAFs being the most likely for the minimum SRC and extended u-shaped for the median and maximum SRCs.
- No notable RAF design differences with regards to timing of maximum water volume were observed, however the percentage of RAFs where

maximum volume occurred prior to the peak of the event increased with increasing SRC from between 0.5 – 4.6 % to 38.9 – 47.7 %.

3.4.2 Catchment scale

Despite the addition of 274 RAFs that were at least 12 m long and 1 m high, the effect of these in combination on the catchment outlet peak water discharge was negligible. The lack of an effect was the product of multiple factors; firstly, the ratio of storage capacity to catchment area was too small. Here in Eastburn Beck, the extended u-shaped RAFs resulted in a ratio of 683 m^3 of storage per km^2 of catchment area. In comparison, Metcalfe et al. (2018) used Dynamic TOPMODEL to simulate enhanced hillslope storage using a 1 m high barrier at the downstream boundary of the lumped hydrological response unit representing the enhanced storage in an eight hydrological response unit model. For a 223 km^2 Cumbrian catchment, providing a residence time of 10 hours, just over 10 million m^3 of storage was created, resulting in a median peak reduction of 5.8 % and a maximum peak reduction of 17.3 %. Metcalfe et al. (2018) had a storage to catchment size ratio of 44,843 m^3 per km^2. Secondly, peak discharge reduction decreases with increasing return period, as seen by Ahilan et al. (2019), who saw peak reduction of 85 % for a 5 year RP event decrease to 30 % reduction for a 100 year RP event for a single retention pond with a storage to catchment size ratio of 16,332 m^3 per km^2. It was therefore unlikely that an event as severe as that of Boxing Day 2015 would be affected by the relatively small storage capacity created with the bunds in the Eastburn Beck catchment. Finally, as the RAFs were not designed to be leaky, any attenuation benefits are unlikely at the peak of the event given that some features would have been full prior to the peak. Effective timing of storage has also been highlighted by Quinn et al. (2013).

A greater difference was seen in the catchment outlet sediment discharge than in water discharge, although whether the addition of RAFs of differing designs increased or decreased the outlet sediment discharge depended on the model's propensity to transport sediment. With minimal sediment transport, negligible effects were observed when implementing RAFs. When increasing the model's propensity for sediment transport, the addition of RAFs resulted in greater outlet sediment yield, with an increase of up to 8 %. For the maximum propensity for sediment transport, the addition of u-shaped and extended linear RAFs decreased the outlet sediment yield by up to 6.1 % whereas the other designs

resulted in an increase in sediment yield of up to 7.6 %. Suggesting that in a catchment where sediment is easily transported, some RAF designs act as local sediment traps, preventing the downstream passage of sediment to the catchment outlet. Berg et al. (2015) also related the increasing number of small farm ponds through time with a decrease in downstream sedimentation in reservoirs in seven small catchments (2 – 50 km^2) in Texas, relating this decrease to the sediment retention capacity of the ponds. However the contrasting response of one catchment, where sedimentation increased downstream with the inclusion of small ponds over time highlights that a number of factors may alter the downstream impact of the addition of features. This includes land use change, giving rise to local differences in sediment transport processes (Berg et al., 2015). Given in the Eastburn Beck model of this study, Manning's n (related to land use) was altered to change the catchment's propensity to transport material, the small changes to surface roughness across the catchment may have led to localised variations in sediment transport, altering the sediment yield exiting the catchment.

3.4.3 Local scale

3.4.3.1 The effect of RAF design on water

The linear RAF design was the least efficient with regard to the water held upstream. This inefficiency of the linear RAFs was likely the result of a lack of ability to store water without the aid of local topography as represented by the 4 m DTM. For effective storage behind a linear RAF, it would need to be located within and fully block the width of a channel (Figure 3.17a) to create a backwater effect. Thomas and Nisbet (2012) also saw a backwater effect when representing large woody debris dams using partial blockage functions in a hydraulic model and saw depth increase and velocity decrease behind their dams resulting in a 15 minute peak discharge delay for a 100 year RP event. Linear RAFs also work well when built at the edge of concavity in the topography such as a gully (Figure 3.17b) where they act as overland flow interceptors. Bunds working as overland flow interceptors have also been implemented in the Belford catchment and Nicholson (2013) recorded the water volume within an overland flow interception feature created as a soil and boulder bund over a natural field gully with a storage volume of 500 m^3. For a rainfall event where 28 mm fell within 12 hours, the bund

resulted in a peak overland flow reduction of over 50% and storage volumes of up to over 350 m^3.

However, if a linear RAF is placed on a hillslope, for such an extreme event as Boxing Day 2015, water flows to either side of the RAF, acting as a flow deflector rather than storage feature (Figure 3.17c). Robichaud, Wagenbrenner et al. (2008) also experienced a lack of runoff reduction for large rainfall events (over 2 year RP) for contour felled logs in post fire hillslope restoration project in the western US. They fitted regression models between treatment and control runoff of large and small rainfall events occurring over five sites and saw no reduction in treatment runoff compared to control runoff for large events but did see a reduction in treatment runoff for the small events. For the larger events, they observed runoff around the ends of the logs due to the limited storage capacity being exceeded. Therefore the efficiency of a linear RAF design is highly dependent on finding a suitable location, a factor known to be a limitation of the work of Metcalfe et al. (2018) and a concern for NFM features more widely as highlighted by Dadson et al. (2017).

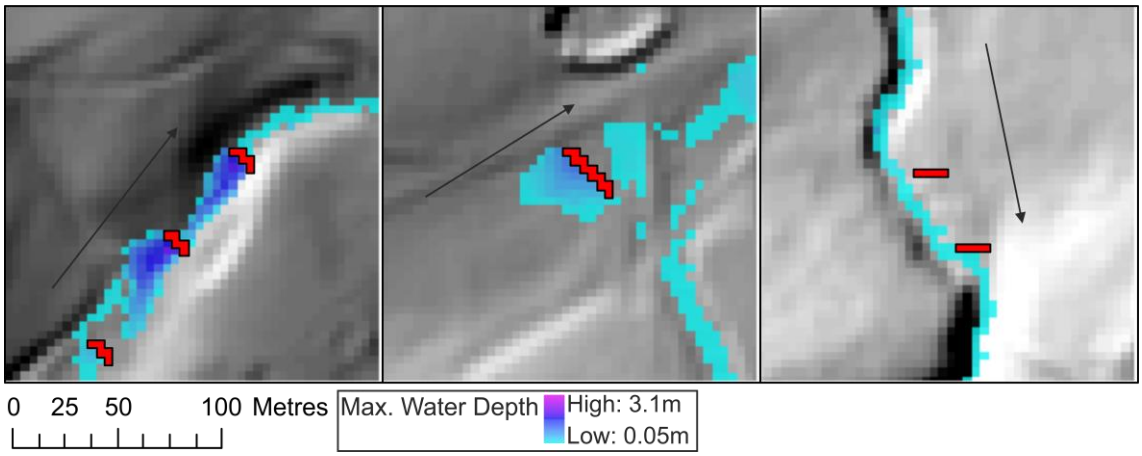

Figure 3.17: Examples of water depths behind linear RAFs. Background mapping is a hillshaded DTM for visualisation only.

Extended u-shaped RAFs were the most effective at retaining water upstream as they had the greatest ability of all designs to store water without reliance on local topography. When water flows into a u-shaped RAF, it is automatically stored within the confines of the bund itself (Figure 3.18a). The extended u-shaped RAF also enhances storage created by local topography as seen when comparing Figure 3.17b with a linear RAF and Figure 3.18b with an extended u-shaped RAF. It is unlikely that such comparisons between RAF designs can be seen in real-

world examples given two sites needed for direct comparison of designs are improbable in terms of, for example, contributing area, storage capacity arising from local topography and interaction with the main flow pathway. However, Wilkinson et al. (2010) built a curved timber barrier which, with the aid of the slope gradient, created a u-shaped type bund adjacent to the stream in Belford with a potential storage capacity of between 800-1000 m^3. During a 36 hour multi-peak rainfall event in 2008, the bund first stored surface runoff before stream runoff was partitioned into the RAF, resulting in approximately 75% of its capacity being filled as a maximum for the entire event (Wilkinson et al., 2010). However, the efficiency of extended u-shaped RAFs would likely decrease if located in channels (Figure 3.18c). This is due to the method in which the RAFs were implemented into the DEM, whereby the front end of the RAF would be significantly lower than the sides that sit on the floodplain, decreasing the storage capacity significantly.

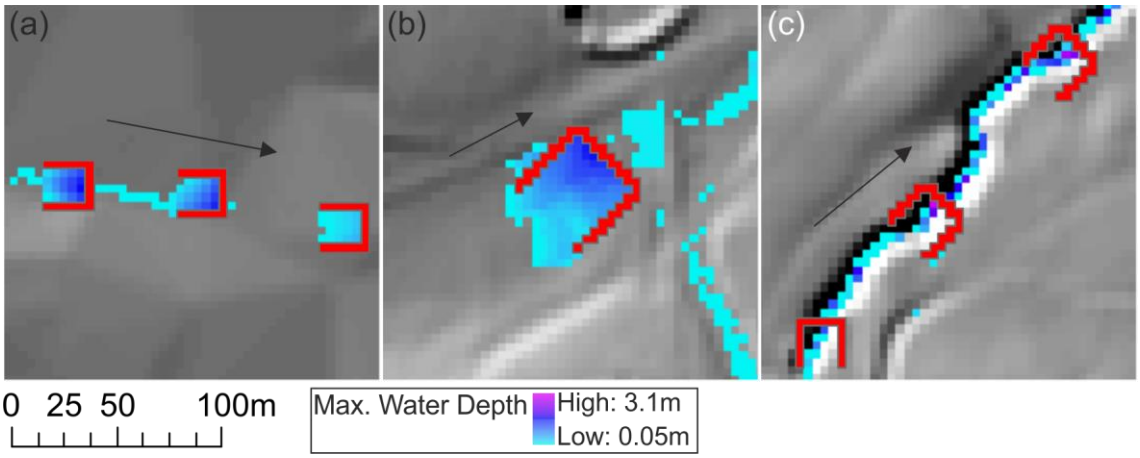

Figure 3.18: Examples of water depths behind extended u-shaped RAFs. Background mapping is a hillshaded DTM for visualisation only.

Interestingly, the double linear and extended linear RAFs held similar amounts of water upstream. In the double linear RAF scenario, the upstream bund holds the most water and if not overtopped, the downstream bund only uses a fraction of its capacity (Figure 3.19a). This produces a cascade effect as also seen by Nicholson et al. (2020) in a pond network model where each offline storage feature modelled was identical and the discharge output of the upper feature is the input discharge for the next feature in succession. The volume held between the two bunds in the double linear design equates to if the bund was slightly larger and placed in the downstream location as in the extended linear RAF scenario (Figure 3.19b). This poses an interesting management question, would

increasing the size of RAFs be more cost effective than adding multiple smaller RAFs? Implementing multiple RAFs in close succession is the predominant choice made within UK projects and a stipulation for certain UK funding streams (e.g. countryside stewardship) (Rural Payments Agency, 2017). However, this study has suggested that the efficiency of multiple bunds is much greater if either the upper bund is breached or there are significant inputs between the two bunds. Making small increases to a RAF's size would likely be more cost effective than building a second bund if located in areas where extending bunds was physically possible. Not building successive features in a network would also mean issues with cascade failure and the features classifying as reservoirs would be avoided (Wilkinson et al., 2013).

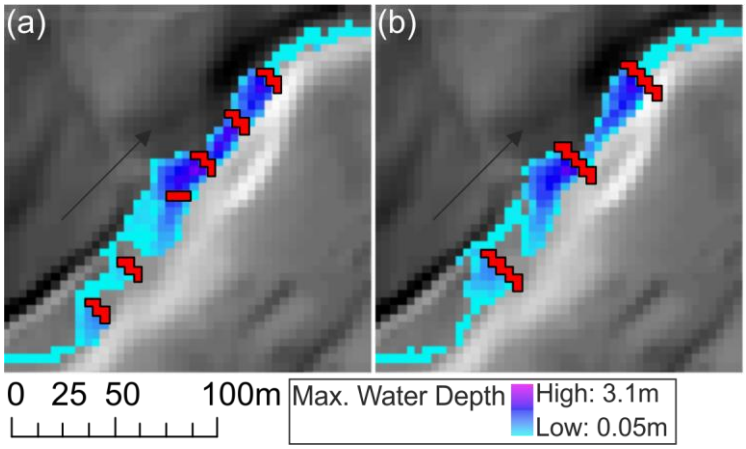

Figure 3.19: Examples of water depths behind (a) double linear and (b) extended linear RAFs. Background mapping is a hillshaded DTM for visualisation only.

3.4.3.2 The effect of RAF design on sediment

Between 30 % and 50 % of the RAFs produced no geomorphological effect regardless of design due to their upstream location. On hillslopes the lower roughness of the grass allows runoff to easily move towards the channels and the grass also protects the underlying material from being eroded. Within ephemeral channels, a lack of persistent flow and coarse sediment inhibits sediment transport. Of the RAFs within the headwaters experiencing geomorphological change, many were located in the south of the catchment on moorland, where hillslope material is more likely to be eroded due to the heather vegetation cover leaving soil below at risk from erosion, increasing the sediment supply available for deposition downstream.

Of the RAFs experiencing net elevation change upstream, up to 34 % (depending on the sediment response catchment and design) saw both erosion and

deposition occur upstream, a pattern also observed by Hilderbrand et al. (1998) for perpendicular wood dams placed on the stream bed, where scour, no change and fill were observed laterally across cross-sections 50 m upstream of the structures, measured as elevation change over a year. Hilderbrand et al. (1998) highlight the highly variable nature of the geomorphological impact of wood in rivers, with response depending on angle of the wood, whether the wood is placed as a dam or a ramp. Hilderbrand et al. (1998) also compared their results to those of Cherry and Beschta (1989) whose flume experiment focused on dowels placed to the mid-channel only, therefore allowing a proportion of flow to be unrestricted and unaffected by scour, highlighting wood length and placement across the channel bed as another factor influencing geomorphological response.

A greater proportion of RAFs experienced deposition rather than erosion upstream, which was to be expected as water accumulates and is stored behind bunds, the water depth increases and velocity decreases, increasing the likelihood of sediment deposition. Sedimentation upstream of bunds or in retention ponds is a frequently cited issue or at least concern in RAF studies (e.g. Quinn et al., 2013, Lane, 2017, Hankin et al., 2019). Retention ponds in Belgium have had between 625 and 4000 m^3 of sediment removed per year (Verstraeten and Poesen, 1999). RAFs at Belford Burn accumulated significant levels of silt through chronic runoff in small events, particularly at the inlet of the feature (Barber and Quinn, 2012). Erosion upstream may be the result of multiple mechanisms, with full channel obstructions creating a downwelling effect, where high-velocity water is forced to the channel bed, initiating scour (Buffington et al., 2002). Flow can also be accelerated around the ends of structures for a number of angles, causing scour immediately upstream and around ends of features (Cherry and Beschta, 1989).

With regard to RAF design, the double linear and the extended linear designs resulted in the greatest number of RAFs experiencing deposition upstream and the greatest volume of sediment gained upstream. They were also the designs that saw the highest number of RAFs experience erosion upstream and the greatest volume lost from upstream. Examples of the geomorphological response to these designs can be seen in Figure 3.20. Although sediment can be seen to be accumulating behind a proportion of the length of RAFs, the linear nature of the RAF results in a runoff pathway to one end. This creates a preferential flow

parallel to the RAF, increasing flow velocities, the likelihood of erosion and sediment transport ability of this concentrated flow pathway. The double linear design differs from the extended linear RAF whereby as water is stored behind the upstream of the two bunds, velocity decreases and the likelihood of deposition increases. If the upstream bund is overtopped and only a small quantity of water is moving from the upstream bund to the downstream bund, it is unlikely to have the power to be erosive and as the water gathers behind the downstream bund and depth increases and velocity decreases, the downstream bund will also most likely by depositional. This creates a longer trail of sediment deposition than compared to just a single larger RAF (Figure 3.20a and b i). The geomorphological impact is highly variable, such as for Figure 3.20a and b ii, where the extended linear RAF stores more water and leads to greater deposition than then double linear RAFs in the same location where water can more easily flow around the end of the structure, maintaining its power and decreasing the likelihood of deposition upstream. Erosion around the ends of features, such as those seen in Figure 3.20c has been also seen by Robichaud, Wagenbrenner et al. (2008) for post-fire hillslope restoration projects using contour felled logs, where greater localised erosion rates were experienced compared to if no treatment had been implemented. This is an even more prevalent issue if features are off-contour (i.e. not exactly perpendicular to slope) (Robichaud, Wagenbrenner et al., 2008). Due to a linear feature's naturally small storage capacity, their impact on erosion reduction decreases with increasing event size (Wagenbrenner et al., 2006, Robichaud, Wagenbrenner et al., 2008) with sediment laden runoff flowing around the ends of features once the capacity is full. However, Robichaud, Pierson et al. (2008) suggested the addition of end berms to contour-felled logs to create a u-shaped feature increased the sediment storage capacity of features at two sites by 10 and 16%, improving their ability to store as oppose to erode sediment.

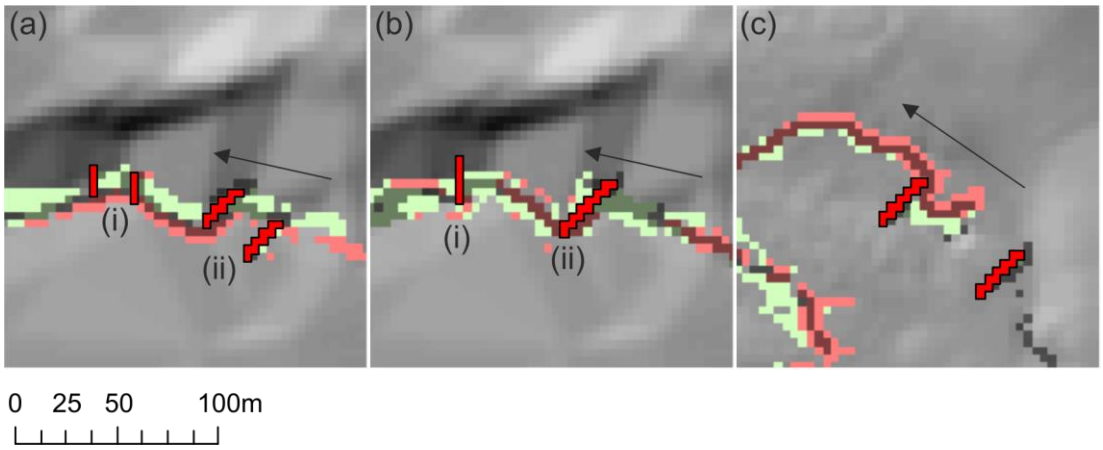

Figure 3.20: Examples of net elevation change behind (a) double linear and (b and c) extended linear RAFs, where red is erosion, green is deposition and the grey shaded areas are cells that were wet at the peak of the event. RAF locations (i) and (ii) are the same in (a) and (b). Background mapping is a hillshaded DTM for visualisation only.

The u-shaped design resulted in the lowest number of RAFs experiencing both erosion and deposition upstream and consequently the lowest volume of sediment gained and lost upstream. This was unexpected, however explained through the addition of the sides of the u-shaped RAFs altering where and how the flow enters the bund, with the geomorphological significance of this being dependent on location. A proportion of RAFs were fully inundated and in direct contact with the flow of the water, resulting in significant overtopping and erosion of the feature itself (Figure 3.21a), causing maximum water storage to occur prior to the event peak and draining of water by the event peak. Another proportion of RAFs saw the addition of the sides of the u-shaped bund force the water to be partitioned between the main flow pathway and the RAF (Figure 3.21b). With a smaller proportion of flow entering the bund, the water lacks power to erode, transport or deposit the coarse grained sediment prevalent in the upper reaches of the catchment. The RAF therefore stored water without significant changes to the local geomorphology for the rainfall event modelled. In a similar sense, Brainard and Fairchild (2012) found the presence of stream inflow into ten small ponds (volume between 366 – 6181 m^3) in an 840 km^2 catchment in Pennsylvania increased sediment accumulation due to the increased power streamflow has to move coarser grain sizes. This highlights the need for land managers to understand the influence of both the design and location on the likely accumulation of sediment behind RAFs.

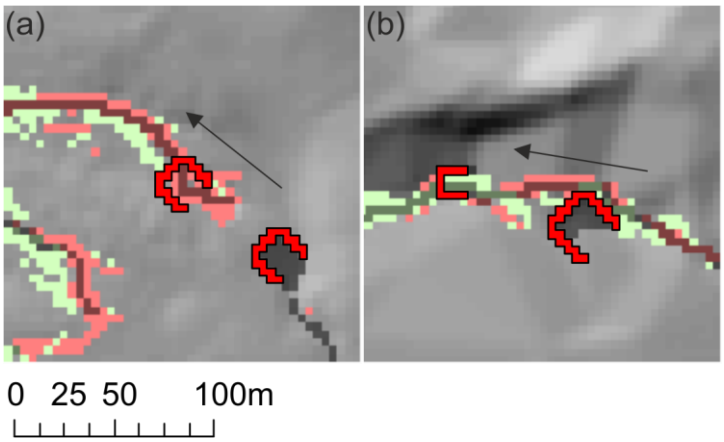

Figure 3.21: Examples of net elevation change behind u-shaped RAFs, where red is erosion, green is deposition and the grey shaded areas are cells that were wet at the peak of the event. Background mapping is a hillshaded DTM for visualisation only.

3.4.3.3 Overtopping and bund erosion

Several RAFs were overtopped, regardless of design (Figure 3.22a), however, linear RAFs were overtopped the least and extended u-shaped RAFs the most. This is primarily the result of the difference in their shape. As discussed previously, linear RAFs are likely to fill behind, then spill to the sides (Figure 3.22b upper, e.g. Robichaud, Pierson et al., 2008), whereas due to the addition of sides to the extended u-shaped RAFs, water is likely to spill over the front of the bund if slope gradient results in the front of the bund being lower than the sides of the bund (Figure 3.22b, lower). RAFs which are full and overtopping have been seen to result in less effective flow attenuation due to a lack of velocity reduction (Wilkinson et al., 2019) and loss of flow pathway lengthening. Although the main reason behind a lack of catchment outlet response to the RAFs was the amount of storage compared to the size of the event, overtopping leading to a reduction in attenuation will likely affect larger rainfall events down to when overtopping does not occur.

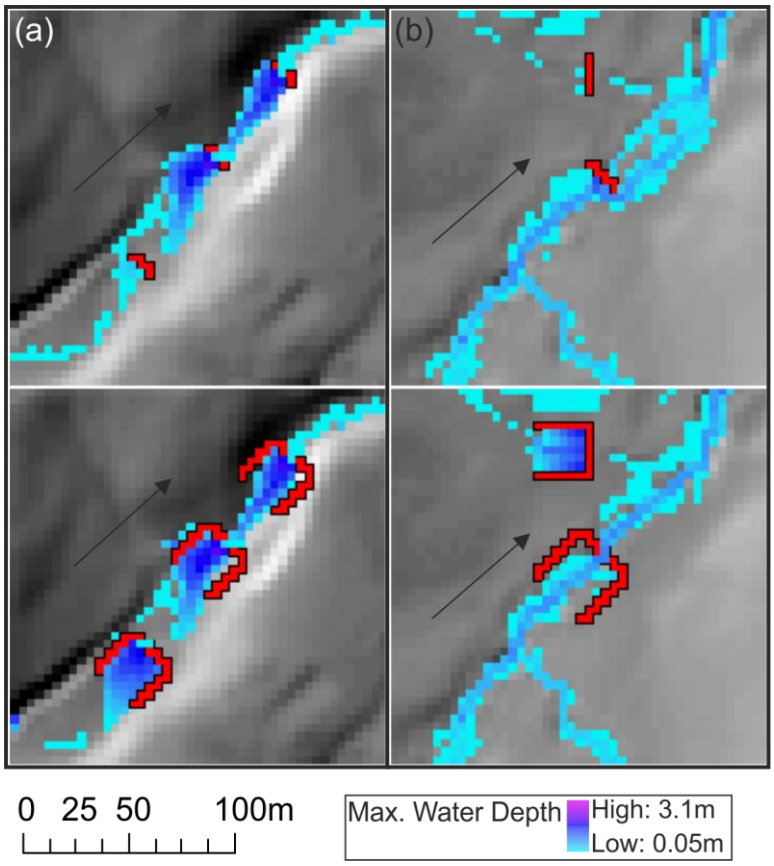

Figure 3.22: Examples of overtopping of linear RAFs (upper pane) and extended u-shaped RAFs (lower pane) at the peak of the event. NB: some flow pathways may not be shown if water depth was under 0.05 m. Background mapping is a hillshaded DTM for visualisation only.

Due to the water flowing over the RAFs, bund erosion was observed to some extent for all designs and sediment response catchments. The difference in general followed the pattern of overtopping, whereby the linear design resulted in the fewest RAFs experiencing bund erosion and the double linear and extended u-shaped designs resulted in the greatest number of RAFs experiencing bund erosion. Erosion occurred to both the crest of the bund as water flowed over the top (Figure 3.23a) and to the bund sides given the diversion of flow around the ends of the bunds (Figure 3.23b).

Differences in the timings of peak water storage were observed resulting from bund erosion. The percentage of RAFs where maximum water volume occurred prior to the peak of the event increasing from between 0.5 – 4.6 % for the minimum SRC to 38.9 – 47.7 % for the maximum SRC. Given there was no implementation of an outlet pipe, as the catchment's propensity for geomorphological change increased, once the RAFs were overtopping, they were more likely to be eroded by less powerful flows, decreasing the storage

available prior to the peak of the event. These simulations highlight the need for reinforcement of outlet pathways, which is often pre-empted in many NFM projects, with control structures such as outlet pipes or bund crests being constructed out of unerodible material (Quinn et al., 2013). More naturally, once vegetated, correctly designed compacted soil bunds have the potential to last indefinitely (Nicholson et al., 2017). However if reinforcement is required, the cost increases, as seen in Pickering, where Nisbet (2017) changed the type of feature implemented to a highly engineered large storage area at the bottom of the catchment, due to the unfeasibility of more natural solutions.

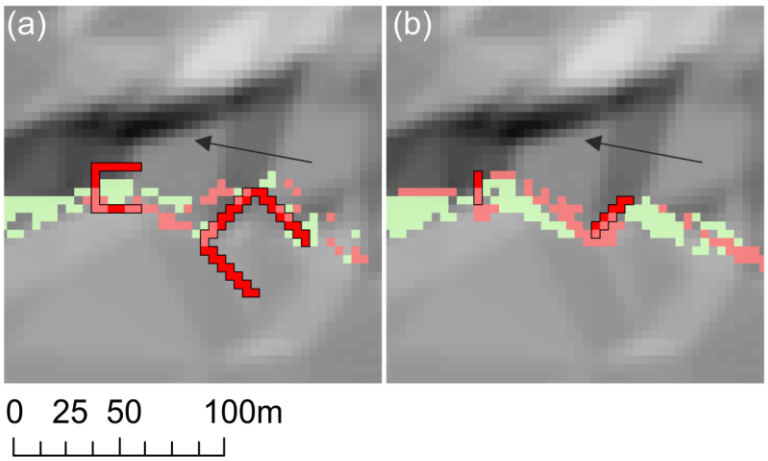

Figure 3.23: Examples of bund erosion of (a) extended u-shaped RAFs and (b) linear RAFs where red is erosion, green is deposition. Background mapping is a hillshaded DTM for visualisation only.

Once overtopping, compared to upstream, water depth was lower and velocity was higher downstream of RAFs, suggesting RAFs behaved similarly to that of more traditional weirs. Kitts (2010) observed similar hydraulic behaviour for an accumulation of in-channel wood with a high blockage ratio, where a 0.5 m step in water level was observed and for floodplain inundation to occur, a discharge of only 0.2 m^3s^{-1} was required upstream, increasing to 0.94 m^3s^{-1} downstream of the accumulation. The increase in velocity downstream increased the number RAFs experiencing erosion downstream compared to upstream for the majority of the simulations, with scour downstream of barriers such as large woody debris being a common occurrence in empirical and modelling studies (e.g. Smock et al., 1989, Hilderbrand et al., 1998 and Haschenburger and Rice 2004).

RAFs not experiencing erosion downstream are likely not due to their location within the catchment, land cover or grain size. A proportion of RAFs which are in the very upper headwaters of the catchment are unlikely to have the stream

power to erode even with the advantage of greater velocities compared to upstream. Those located on vegetated surfaces may lack the power to overcome the additional protection the vegetation gives against erosion. A proportion which are further down the river network where sediment sizes are much greater may again not have the power to erode the larger gravels and cobbles. There were few design differences in the water depth and velocity downstream of the RAFs, with only the double linear design resulting in higher downstream water depths and lower velocities compared to other designs. The proximity of the two bunds within the double linear design would mean the backwater effect of the downstream bund would increase the water depth and decrease the water velocity of the area immediately downstream of the upstream bund.

3.4.4 Implications for the management of NFM projects

During this study a number of points have arisen which have implications for NFM projects. Firstly, when locating RAFs, local knowledge and detailed site-specific analysis of runoff pathways will aide placement to ensure efficient use. If RAFs are placed aside from a flow pathway, their water retention potential may be reduced. However as seen with the u-shaped RAFs, off-centre bunds may still hold water without negative geomorphological impacts such as sedimentation upstream. If available, modelling RAFs, however simply, would lead to ensuring their effective use throughout a catchment prior to their implementation as the balance between water storage and geomorphological impact as discussed above, may influence the location of RAFs (Hankin et al., 2020).

The design of RAFs has an effect on their hydrological and geomorphological functioning. Overall, creating storage that is larger and does not depend on local topography (i.e. u-shaped designs) will result in greater water retention but could also result in greater geomorphological impact due to the larger quantities of water being stored and potential energy of the water if the RAF were overtopped, causing erosion of the feature itself, loss of its retention capacity, therefore allowing water to pass quickly downstream. Therefore, although some designs are more beneficial than others, decisions should be made on a feature-by-feature basis depending on factors which will affect their performance and risk of failure such as slope and the availability and propensity to transport sediment alongside the overarching goals of the NFM project.

Several RAFs experienced deposition of sediment upstream and erosion to the bunds themselves, therefore RAFs should be constructed out of material that can tolerate erosion, or weak areas, such as the bund crest and ends should be reinforced with unerodible materials. The need for reinforcement of bund spillways has also previously been highlighted by Quinn et al. (2013). Although reinforcement would reduce the “naturalness” of the RAF, it is important to ensure long-term effective use and reduce the risk of failure without the need for frequent monitoring and management. Monitoring would however be needed to ensure sedimentation upstream of RAFs does not heavily reduce their storage capacity. Quinn et al. (2013) suggest bunds on arable land may need sediment removal annually, but also highlight the benefits sedimentation may have on water quality. Therefore the long term management of RAFs is site specific and will need to be in line with the goals of the NFM project.

Suggestions so far have all been with respect to the local, feature-scale aspect of a project, however as found in this study, a large, likely to be unachievable number of features would be required to see a positive flood risk impact at the downstream catchment boundary for such an extreme event as on Boxing Day 2015. For example, the volume of water exiting the catchment over the four day period encompassing the Boxing Day event was 4.23 million m^3 in the median SRC baseline scenario, to reduce this volume by half, 2,169 RAFs would have to be implemented based on the design which held the most water (975 m^3 - extended u-shaped). The actual number required would be even higher given this quick calculation does not take into account inefficiency based on location and temporal differences in water volume stored (e.g. storage at event peak). Finding physically suitable locations for such a large quantity of RAFs is unlikely. When factoring in challenges such as landowner permission, cost of construction (£2.2 mil based on a cost of £1 k per feature (see Quinn et al. (2013) for estimated costs of different RAFs)) and a lack of governance (Wells et al., 2020), the use of RAFs for effective flood attenuation for such an extreme event at small-catchment scale is highly unlikely, if not impossible. With the likelihood of increased river flow levels and flood magnitude with climate change (Environment Agency, 2016), these challenges are only likely to increase. Therefore RAFs should be used in small catchments, where properties are at risk from small, frequent floods, such as at Belford (Wilkinson et al., 2010; Nicholson et al., 2020).

3.4.5 Future work

Given a difference in hydrological and geomorphological response has been observed from different RAF designs, higher resolution modelling (in terms of space and time) of RAFs implemented in the real-world would be beneficial to validate the findings of this study. Monitoring data would provide an invaluable insight into the interactions between the RAF, water and sediment however data for such extreme events as Boxing Day 2015 will be difficult given the rarity by which they occur (Metcalfe et al., 2018). This gap in the monitoring of the whole system needs to be addressed however higher resolution modelling efforts may provide greater insight whilst the monitoring challenge is being solved.

The effectiveness of RAFs is proportional to the size of the event and here, no hydrological benefits at the catchment outlet were observed for the Boxing Day 2015 event. Therefore the hydrological and geomorphological response to RAF design needs to be assessed for smaller events to gain an understanding of whether RAFs can provide flood risk reduction and the associated management that may be required to ensure storage capacity is maintained. Once the effect of a range of event sizes has been established, estimations of the impact of increasing flood flows from climate change could be assessed. Similarly, studies have suggested an increase in the frequency and magnitude and changes to seasonal cycles of flooding with climate change. (e.g Reynard et al., 2001 and Kay et al., 2006). Therefore the impact of multiple events of different magnitudes returning at different frequencies in different seasons needs to be assessed to understand longer term management issues. With a compromise between spatial and temporal resolution to avoid impractical computer run times, CAESAR-Lisflood has the capacity to estimate long term effects of NFM and should be the focus of the use of CAESAR-Lisflood in modelling the impacts of NFM in the future.

3.5 Conclusions

Despite the addition of 274 RAFs of varying design there was no flood attenuation effect at the catchment outlet. This lack of an effect was due to the ratio of the number of RAFs compared to the catchment size (40.8 km^2) and the severity of the event. The retention capacity of the RAFs simply did not compare to the

volume of water flowing through the system in the extreme event of Boxing Day 2015.

This study has however provided insight into differences relating to design and implementation of RAFs into a landscape evolution model to assess geomorphological impact. Firstly, larger RAFs that do not necessarily need to rely on local topography (e.g. u-shaped) can store the most water. They are however, also the most likely to suffer from scour to the front of the bund as a result of the RAF filling fully, then overtopping, therefore reducing their capacity and ability to store water at the peak of the event.

Linear designs are the least effective at storing water, with those located anywhere other than to fully block a channel acting as flow deflectors rather than storage features. The implication of this design is that flow is often preferentially channelled alongside the feature, causing erosion immediately upstream and around the end of the bunds.

Geomorphologically, the catchment response to the addition of RAFs was complex. Both erosion and deposition occurred upstream of many RAFs, although deposition was more common than erosion. With regard to design, unexpectedly, the smaller u-shaped design resulted in the fewest geomorphological changes upstream, partly due to the partitioning of a smaller proportion of less powerful flow from the main channel.

Linear designs were more geomorphologically impactful, with double linear and extended linear RAFs resulting in the greatest sedimentation and greatest scour upstream of the five designs tested.

Increasing propensity for sediment transport resulted in a greater proportion of RAFs seeing their maximum storage occur prior to the event peak as a result of increases to the number of RAFs experiencing erosion. This meant capacity to store the water at and after the peak of the event was reduced.

Future work should assess the impact of smaller rainfall events to establish whether RAFs can result in wider-scale retention. Differences occurring from the method of implementation needs to be investigated including comparing to other popular methods (e.g. using hydraulic structures) alongside validation with field data and higher resolution (spatial and temporal) modelling to more precisely establish the localised processes and impacts of the RAFs including differences

in design. The true advantage of using a landscape evolution model should also be utilised to assess the effect of many RAFs over much longer timescales than feasible in other models and empirical studies.

Chapter 4
Can geomorphological processes be estimated without recourse to morphodynamic models?

4.1 Introduction

The use of hydraulic models for flood risk mapping is a well-established practice in industry and academia. Common practice is to predict inundation depth, velocity and extent for a number of events based on their occurrence frequency (Hansson et al. 2008). Models used in flood risk mapping typically solve a full or simplified form of the shallow water equations (Hunter et al. 2008) and output includes inundation extent, water depth and flow velocity. Sediment transport is virtually ignored in flood risk mapping studies, although is considered more often in engineering studies such as risk of scour to infrastructure. Furthermore, flood risk maps are only valid for a single scenario. Maps will need to be revised due to climate and land-use changes, with climate change affecting the magnitude and probability of flood events and land use change affecting the risk of a particular flood. Constant improvements in computational ability and understanding of how to model the physical processes will also result in advancements in the prediction of flood risk.

Perhaps of most immediate concern is that flood risk mapping typically assumes no morphological change during or between flood events. However, flood events can produce profoundly important morphological changes that affect the water level during and after the event and can impact local infrastructure, suggesting some measurement of morphological changes should be incorporated into flood risk assessment (Neuhold et al. 2009). Flood risk assets, be that natural or built defences, are also affected by geomorphological processes. Deterioration resulting from significant scour or channel movement and channel capacity reduction due to siltation are key issues for those managing watercourses. Not only can the inclusion of fluvial geomorphology in flood risk estimation improve prediction, it can also allow for original and holistic flood risk reduction, river management and restoration strategies (Arnaud-Fassetta et al. 2009).

Hydromorphodynamic models are very complex, accounting for non-linear processes associated with turbulent flow and how these interact with moving sediment (e.g. Coulthard et al. 2013, Asahi et al. 2013 and Nicholas 2013). They

therefore in general, do not have the capability to perform simulations on the spatial and temporal resolutions that can be accommodated within hydraulic models, if they do, run times are often too long to be practical. Conversely, hydraulic models necessarily have an (often gross) simplification of geomorphological processes within them (Arnaud-Fassetta et al. 2009) and adding in these processes would increase model uncertainty (Neuhold et al. 2009).

Nonetheless, if it is appreciated that hydraulic models often represent shallow water flood flows more precisely than morphodynamic models, then it can be suggested that outputs such as depth and velocity from these hydraulic models could be used with a level of confidence to calculate other metrics to more widely represent the riverine system. These metrics can include stream power and shear stress, the latter having importance for the estimation of erosion and deposition. A precedent for this type of analysis at small scales was given by Reid et al. (2019), who demonstrated (subject to understanding the limitations of the approach) that even without incorporating sediment dynamics, a 2D flow model could be useful in gaining insights about channel evolution in a complex system of gravel bars. Here, I test this idea at a much larger scale.

Therefore the aim of this study is to compare a hydraulic model derived geomorphological output with the change occurring from a cellular automaton landscape evolution model to assess whether the hydraulic model data can be used as a valuable resource for those interested in the effects of sediment dynamics without the need for expensive monitoring campaigns or extensive morphodynamic modelling efforts.

4.2 Methodology

4.2.1 Site description and rainfall event

Lothersdale is a small, steep-sided upland catchment (12.9 km^2) in northern England consisting of sheep grazed pasture, natural grassland and heath, overlying glacial till deposits (Figure 4.1). The Lothersdale catchment feeds into the Eastburn Beck catchment (40.8 km^2) (Figure 4.1), which has known sediment issues, with a sediment trap regularly infilling at the catchment outlet. Lothersdale was chosen over other sub-catchments due to it having the highest percentage

of tree coverage free channel, allowing for the maximum areal comparison between modelled results and aerial imagery. Eastburn Beck feeds into the larger River Aire catchment flowing through Leeds, Yorkshire, UK.

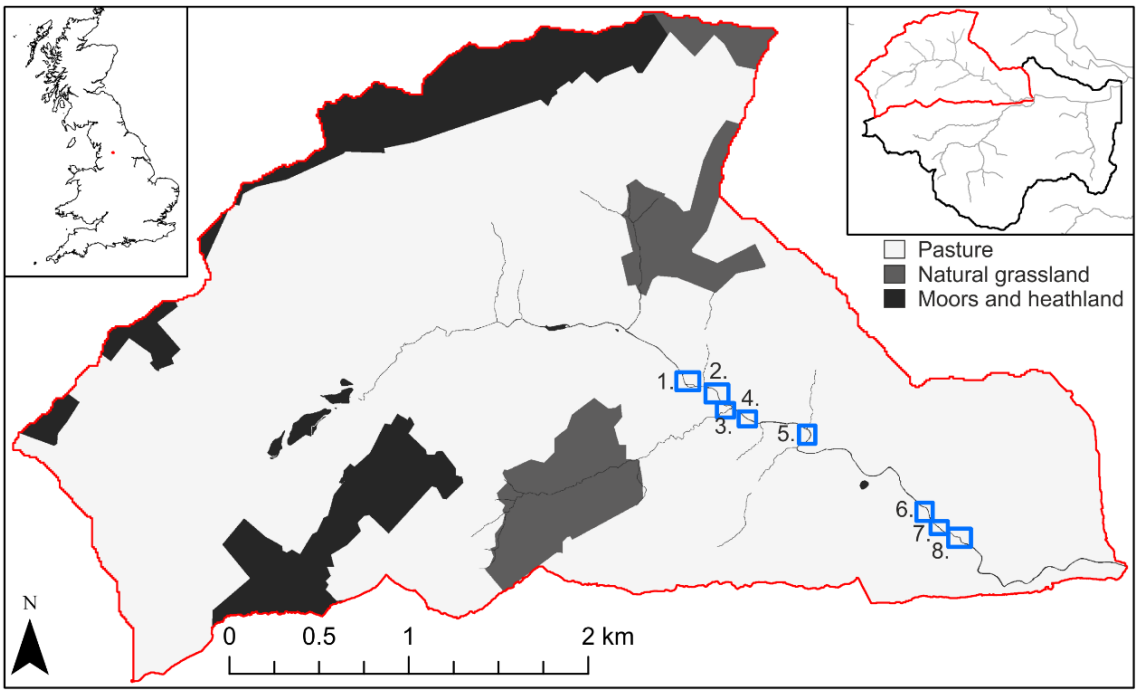

Figure 4.1: Lothersdale catchment location with areas for model comparison highlighted in blue.

The village of Lothersdale has been affected by flooding in the past, with multiple houses being affected by the Boxing Day 2015 flood which affected large parts of the region. The Boxing Day 2015 event was hydrologically exceptional in the UK (Barker et al. 2016). Having followed drier conditions through autumn, three named storms in November caused saturated soils and elevated river levels by the beginning of December (Barker et al. 2016). Extreme rainfall totals on the 25th and 26th December of 100-120 mm falling over the southern Pennines resulted in many rivers recording new maxima, including the River Aire. The closest gauge station to Lothersdale is at the outlet of the larger Eastburn Beck catchment, which was no exception to the extremes of the Boxing Day 2015 event, where a discharge of 54.4 m^3s^{-1} was reached (NRFA, [no date]), which was the highest discharge recorded since records began, estimated to be of an 120 year return period.

The Boxing Day 2015 event was a multiple peak event but for simplicity a Revitilised Flood Hydrograph method (Kjeldsen et al. 2005) rainfall time series was designed of a similar magnitude (120 year RP) and duration (47 hour) as the Boxing Day 2015 event using the catchment descriptors available.

4.2.2 Model set up

CAESAR-Lisflood (Coulthard, et al. 2013) is a landscape evolution model which has been combined with the Lisflood-FP hydrodynamic flow model (Bates et al. 2010). The model simulates flow, erosion and deposition in river catchments and reaches over timescales ranging from thousands of years to hours. This is achieved through the model's four components:

- The hydrological model is adapted from TOPMODEL (Beven et al. 1979), allowing for the generation of run-off given the rainfall input.
- Run-off is routed through the flow model, Lisflood-FP, a conservation-based inertial formulation of the shallow water equations following the method of Bates et al., (2010).
- The fluvial erosion and deposition model, which allows for a choice of sediment transport equations, Einstein (1950) or Wilcock and Crowe (2003). Wilcock and Crowe (2003) was developed with coarser gravel field and laboratory data, whereas Einstein (1950) was developed with sand based laboratory data. Due to the nature of the upland catchment, the method of Wilcock and Crowe (2003) was chosen for this study.
- The slope processes model, whereby sediment inputs from slopes are calculated based on a critical slope threshold.

Meadows (2014) provided an in-depth discussion of different modelling options to assess long-term sediment management plans for a catchment influenced by Mount St. Helens, USA. Issues with physically-based spatially distributed models such as SHETRAN, WEPP, EUROSEM and LISEM include their added complexity and computational demands to solve physically-based equations. This means there is a need to lump small scale physics into larger model grids to enable whole catchment representation and they also have large input parameter requirements. For these reasons, landscape evolution models are preferable over physically-based spatially distributed models (Meadows, 2014).

Meadows (2014) goes further to suggest why the use of CAESAR-Lisflood is beneficial over other landscape evolution models (e.g. SIBERIA, CASCADE and CHILD) due to CAESAR-Lisflood's:

- Implementation of a derivative of the LISFLOOD-FP flow model for greater representation of water movement between cells.

- Use of a 9-fraction grain size distribution including the potential for suspended sediment in the representation of erosion, transport and deposition of sediment, including lateral erosion allowing for meandering and braiding to be represented.
- Ability to use high temporal resolution input data (hourly) to allow the representation of separate storm events which cause erosion.

A CAESAR-Lisflood model was set up using a 2 m resolution composite LiDAR DTM and model parameters optimised based on a wider sensitivity analysis (See Appendix A) and knowledge following site visits to the catchment. This resolution was higher than most previous studies using CAESAR-Lisflood, however, previous studies such as Walsh et al. (2020) have used a higher resolution (1m) over a smaller area (2.1ha). Therefore this model scale was deemed acceptable and necessary to model detailed change occurring across the channel. The model was 'spun-up' to create a more realistic catchment wide sediment distribution and DTM using 5 months of 15 minute tipping bucket rainfall gauge (TBR) data from within the catchment, repeated four times to observe changes to the grain size distribution and decreases in sediment discharge.

The hydraulic model used for comparison in this study was HEC-RAS 2D, which has been developed to include 2D flow routing for unsteady flow analysis. The floodplain and channel are represented by flow areas, comprising of a structured or unstructured grid for numerical calculations, overlaid on a DTM. HEC-RAS 2D has sub-grid capabilities, whereby hydraulic tables are created for each numerical cell face based on the higher resolution sub-grid topography, speeding up computational time. There is a choice of governing equations of either the full 2D Saint-Venant equations, or 2D diffusive wave equations which ignore the inertial terms. The diffusive wave equation set was chosen for this study.

Both the CAESAR-Lisflood and HEC-RAS 2D models were set up to explore how the methods for estimating geomorphological change differed as opposed to being used to predict geomorphological change within Lothersdale. Instead Lothersdale was used as a basis to collect data for model set up.

Shustikova et al. (2019) provide a detailed comparison between the diffusive wave solver in HEC-RAS 2D and the Lisflood-FP flow model (Bates et al., 2010) used in CAESAR-Lisflood. As the two models differ in their complexity,

Shustikova et al. (2019) compared the two models using spatial resolutions of between 25 and 100 m and both included and excluded the sub-grid capabilities of HEC-RAS 2D. Flood extent accuracy compared to an observed flood outline was between 77 - 81 % for the two models and the RMSE of observed to simulated maximum water levels were found to be between 0.61 and 0.84 m. When including sub-grid capabilities, HEC-RAS 2D understandably outperformed Lisflood-FP in terms of spatial distribution details. The authors therefore highlighted the need for accurate representation of complex terrain to ensure correct flood wave propagation and inundation for both models.

To ensure both the HEC-RAS 2D model and CAESAR-Lisflood model were set up as equally as possible, the HEC-RAS 2D model was set up using the 2 m DEM produced from the spun-up CAESAR-Lisflood model as the sub-grid topography with a 20 m structured computational grid. Manning's n was implemented in both models using a 2 m grid, with Manning's n values depending on land cover (Table 4.1). It should be noted however that due to the sub-grid functionality in HEC-RAS 2D, if two values of Manning's n occurred across one computation grid cell face, the mode value was chosen. Manual investigation in areas across the catchment, focusing particularly on the channels, suggested that where a computational cell face encompassed both the channel and bank, the channel Manning's n was most often used. To represent Manning's n more accurately, a finer computational grid would have been required, increasing computational run times. Given the small difference in Manning's n between the pasture and channel and that the majority of the watercourses are located within the pasture land cover type (Figure 4.1), this limitation was deemed acceptable.

Table 4.1: Manning's n values implemented into both CAESAR-Lisflood and HEC-RAS 2D.

Land Cover	**Manning's n**
Channel	0.035
Pasture	0.032
Natural grassland	0.024
Moors and heathland	0.04

4.2.3 Data processing

The CAESAR-Lisflood elevation data from the end and the beginning of the model simulation were differenced to create net elevation change. A level of

detection of ± 0.05 m was removed as such small changes in elevation would not be observed in aerial imagery and may be the result of inherent model uncertainty. The remaining cells were reclassified as deposition for positive change (1) and negative change as erosion (-1).

The HEC-RAS 2D maximum depth and velocity data from over the simulation was taken and maximum shear stress was calculated using Equation 4.1 (Lane and Ferguson 2005, Reid et al., 2019).

$$\tau = \frac{\rho g n^2 u^2}{d^{\frac{1}{3}}} \qquad \text{Equation 4.1}$$

where ρ = density; g = gravity; n = Manning's roughness; U = depth-averaged velocity; and d = depth.

A value for critical shear stress was estimated for the grainsize of bed-material present (Equation 4.2), this critical shear stress was used to define areas of erosion (areas with a shear stress above the critical value) and deposition (shear stresses below the critical value).

$$\tau_{ci} = \tau^*_{c_{50}} \rho_s g D_{50} \qquad \text{Equation 4.2}$$

where $\tau^*_{c_{50}}$ = Shields parameter; ρ_s = rock density; g = gravity; D_{50} = median grain size.

A number of the parameters in both Equation 4.1 and Equation 4.2 are dependent on the model simulation and are therefore potential sources of sensitivity within the results. Therefore sensitivity testing was undertaken and is detailed in Table 4.2.

Table 4.2: Rationale and values used for sensitivity testing of shear stress equations.

Parameter	Rationale	Values Tested
Manning's n (Equation 4.1)	Spatially distributed Manning' n values based on land cover are used in both the CAESAR-Lisflood and HEC-RAS 2D models.	**0.024 – 0.07 $s^{-1}m^{1/3}$** Same values based on land cover as used in both CAESAR-Lisflood and HEC-RAS 2D **0.05 $s^{-1}m^{1/3}$** Manning's n value used for the river channels **0.032 $s^{-1}m^{1/3}$** Manning's n value used for pasture- the main land cover in the catchment
Shields parameter (Equation 4.2)	A number of values have been previously stated within the literature.	**0.045** More recent common value (Yalin and Karahan 1979) **0.06** Original value (Shield 1936) **0.03** Lowest value found (Lavelle and Mofjeld 1987) **0.086** Highest value found (Buffington and Montgomery 1997)
Median grain size **(Equation 4.2)**	Median grain size calculated by CAESAR-Lisflood model at the end of spin up, taken as a catchment average.	**0.031 m** CAESAR-Lisflood catchment average **0.025 m and 0.037 m** ± 20% of catchment average **0.016 m and 0.047 m** ± 50% of catchment average

4.2.4 Data analysis

The F coefficient (Horritt and Bates 2001), a metric to compare binary patterns of modelled and observed data, was altered to compare the difference in cells of erosion or deposition between the two models (Equation 4.3). Values range from 0 for no agreement to 1 for perfect agreement. Values of the F coefficient were

calculated for the catchment as a whole and for the individual comparison areas as shown in Figure 4.1.

$$F = \frac{CL1HEC1}{(CL1HEC1+CL1HEC0+CL0HEC1)} \quad \text{Equation 4.3}$$

where CL1HEC1 = number of erosion/deposition cells in both models; CL1HEC0 = number of erosion/deposition cells in CAESAR-Lisflood but not HEC-RAS 2D; CL0HEC1 = number of erosion/deposition cells in HEC-RAS 2D but not CAESAR-Lisflood.

Visual comparisons were made between the two model outputs alongside aerial imagery taken in April 2015 and June 2018. A field visit was also undertaken in early March 2020 following a wet February where on three separate occasions, stage data at the Eastburn Beck catchment outlet showed levels of over 1.3 m. In perspective, the maximum stage of the Boxing Day event was 1.8 m and stage has only exceeded 1.3 m in eight events since records began (National River Flow Archive, [no date]). Although not the Boxing Day event itself, recent geomorphic change was apparent and geotagged photos were taken wherever possible. This enabled a comparison to be made between model results where tree coverage meant channel geomorphology was not visible in the aerial imagery.

4.3 Results

4.3.1 Hydrological response

The hydrological response from the CAESAR-Lisflood model and HEC-RAS 2D model to the ReFH model rainfall time series showed a similar magnitude of discharge at the catchment outlet and both model responses were similar to the ReFH model direct runoff (Figure 4.2). A difference of less than 1 % was observed between the peak discharge from the ReFH and HEC-RAS 2D models (Table 4.3). The CAESAR-Lisflood model resulted in a 4.3 % decrease in peak discharge compared to the ReFH model. The timing of the peak discharge was two hours earlier for the HEC-RAS 2D model compared to the ReFH model and 0.25 hours later for the CAESAR-Lisflood model. Both HEC-RAS 2D and CAESAR-Lisflood resulted in smaller flood volumes compared to ReFH, with a difference of -7.2 % and -9.6 % respectively (Table 4.3).

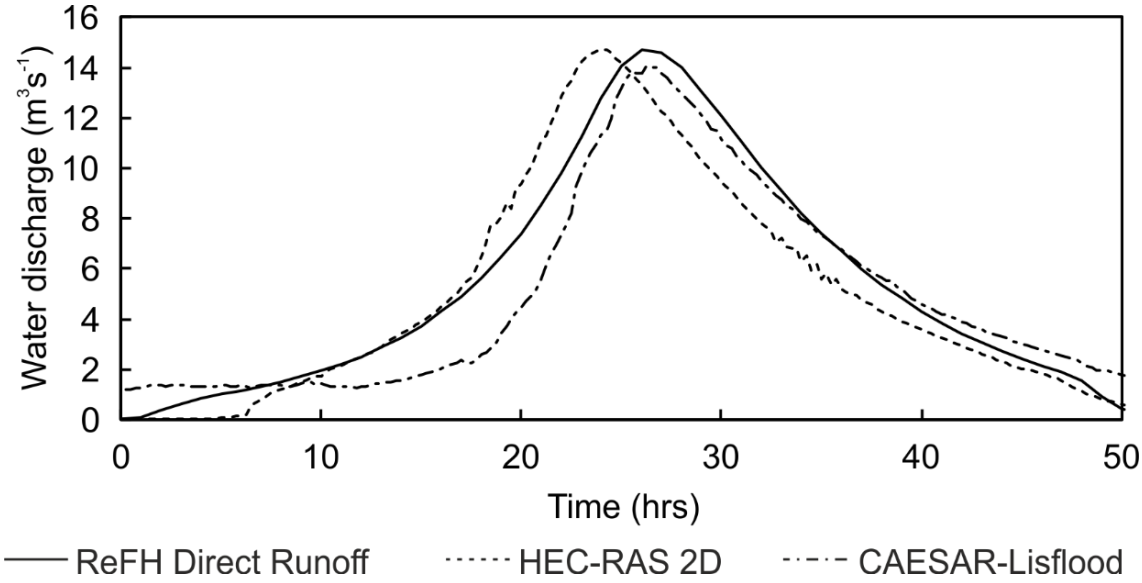

Figure 4.2: Hydrological response of CAESAR-Lisflood and HEC-RAS 2D in comparison with ReFH Direct Runoff.

Table 4.3: Hydrograph summary metrics for ReFH, HEC-RAS 2D and CAESAR-Lisflood models.

Model	**Peak discharge (m^3s^{-1})**	**Time of peak discharge (hr)**	**Flood volume (m^3)**
ReFH Direct Runoff	14.68	26	986,251
HEC-RAS 2D	14.71	24	914,832
Percentage change from ReFH (%)	*0.17 %*	*- 7.7 %*	*- 7.2 %*
CAESAR-Lisflood	14.05	26.25	891,840
Percentage change from ReFH (%)	*- 4.3 %*	*1.0 %*	*- 9.6 %*

4.3.2 Parameter sensitivity

Figure 4.3 highlights a clear overestimation of the total area of deposition for all parameter values tested in the HEC-RAS 2D method (2.75 – 4.64 x 10^5 m^2) compared to the CAESAR-Lisflood model (9.48 x 10^4 m^2). The total area of erosion was closer to that of the CAESAR-Lisflood model, with some parameter values resulting in a total area of erosion within 10% of that of the CAESAR-Lisflood model (between 3.38 x 10^4 and 2.23 x10^5 m^2 compared to 9.1 x 10^4 m^2). The spatial n and 0.032 lumped n model run resulted in similar areas of erosion (9.63 x 10^4 m^2 and 8.35 x 10^4 m^2 respectively) and deposition (4.02 x 10^5 m^2 and

4.15 x 10^5 m^2 respectively). The 0.05 lumped n model run decreased deposition and increased erosion (2.75 x 10^5 m^2 and 2.23 x 10^5 m^2 respectively). Increasing the Shield's parameter increased the area of deposition from 3.4 x 10^5 m^2 to 4.64 x10^5 m^2 and decreased the area of erosion from 1.58 x 10^5 m^2 to 3.38 x 10^5 m^2. Increasing the grain size decreased the area of erosion from 1.95 x 10^5 m^2 to 5.01 x 10^4 m^2 and increased the area of deposition from 3.03 x 10^5 m^2 to 4.48 x 10^5 m^2 (Figure 4.3).

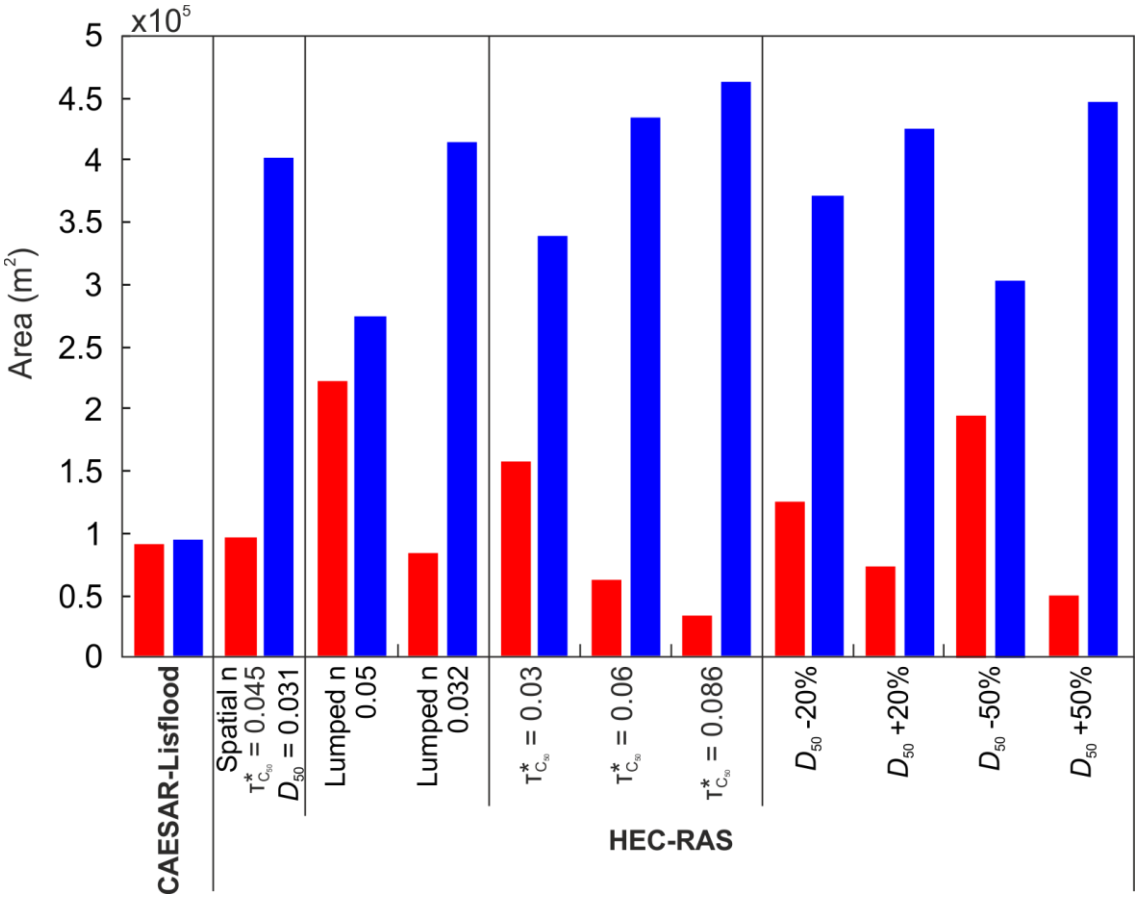

Figure 4.3: Total area within the model estimated to be erosion (red) and deposition (blue) for the CAESAR-Lisflood and HEC-RAS 2D models including parameter sensitivity.

The chosen parameter set had the most similar average F coefficient scores between erosion (0.25) and deposition (0.23) (Figure 4.4). The 0.032 lumped n run decreased the model agreement for erosion (0.21), and marginally increased the agreement for deposition (0.24), whereas the 0.05 lumped n run increased the agreement for erosion (0.28), however exhibited very little agreement for deposition (0.04). Increasing the Shield's parameter decreased the agreement for erosion (0.28 to 0.18) and increased the agreement for deposition (0.13 to 0.32). Increasing grain size decreased the agreement for erosion (0.28 to 0.22),

but to a greater extent increased agreement for deposition (0.08 to 0.31) (Figure 4.4).

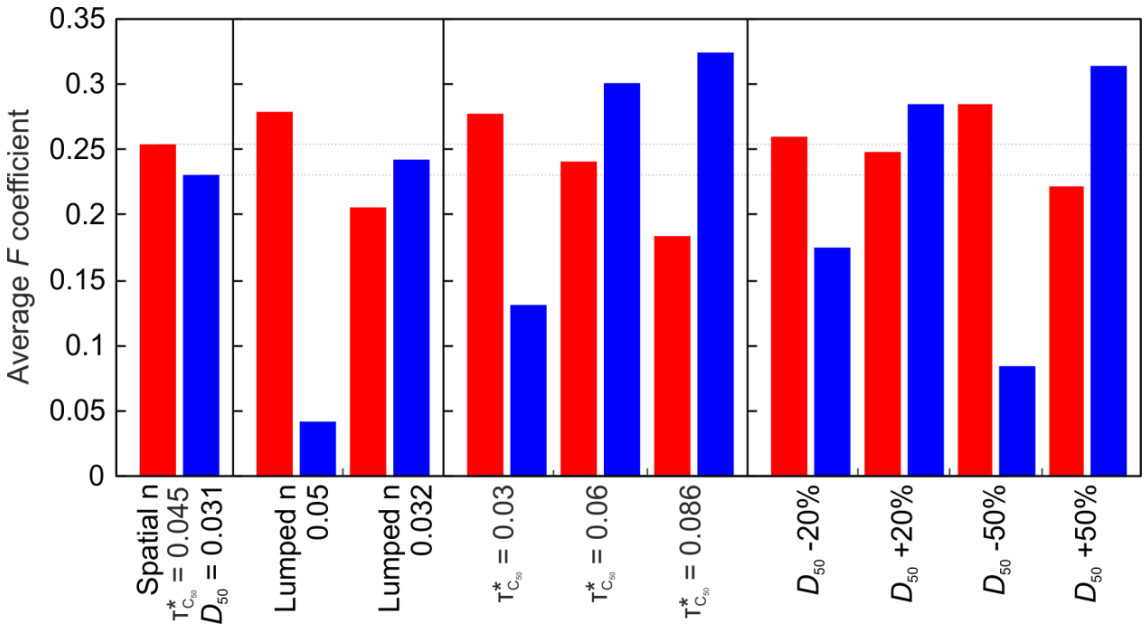

Figure 4.4: Average F coefficients for erosion (red) and deposition (blue) over the eight comparison areas for the parameters tested for sensitivity.

4.3.3 Evaluation against aerial imagery and field photos

Figure 4.5 shows fair agreement between the two models in the upper part of the comparison area, with erosion to the left hand bank and deposition to the right hand floodplain. However a lack of clarity around the secondary channel, which can be identified in Figure 4.5d was also apparent. The large area of deposition in both models down the right hand floodplain was plausible given it is low lying and that patches of sand deposition were identified on the field visit (Figure 4.5, Photo 1). In the lower part of the comparison area, CAESAR-Lisflood identified the correct geomorphological processes given the evidence in the field photos, however it does appear to slightly over-exaggerate the lateral extent (Figure 4.5a). No process complexity around the secondary channel was apparent in the HEC-RAS 2D model, where only erosion was estimated (Figure 4.5b). Overall, agreement was greater for erosion than deposition (F = 0.38 and 0.24 respectively).

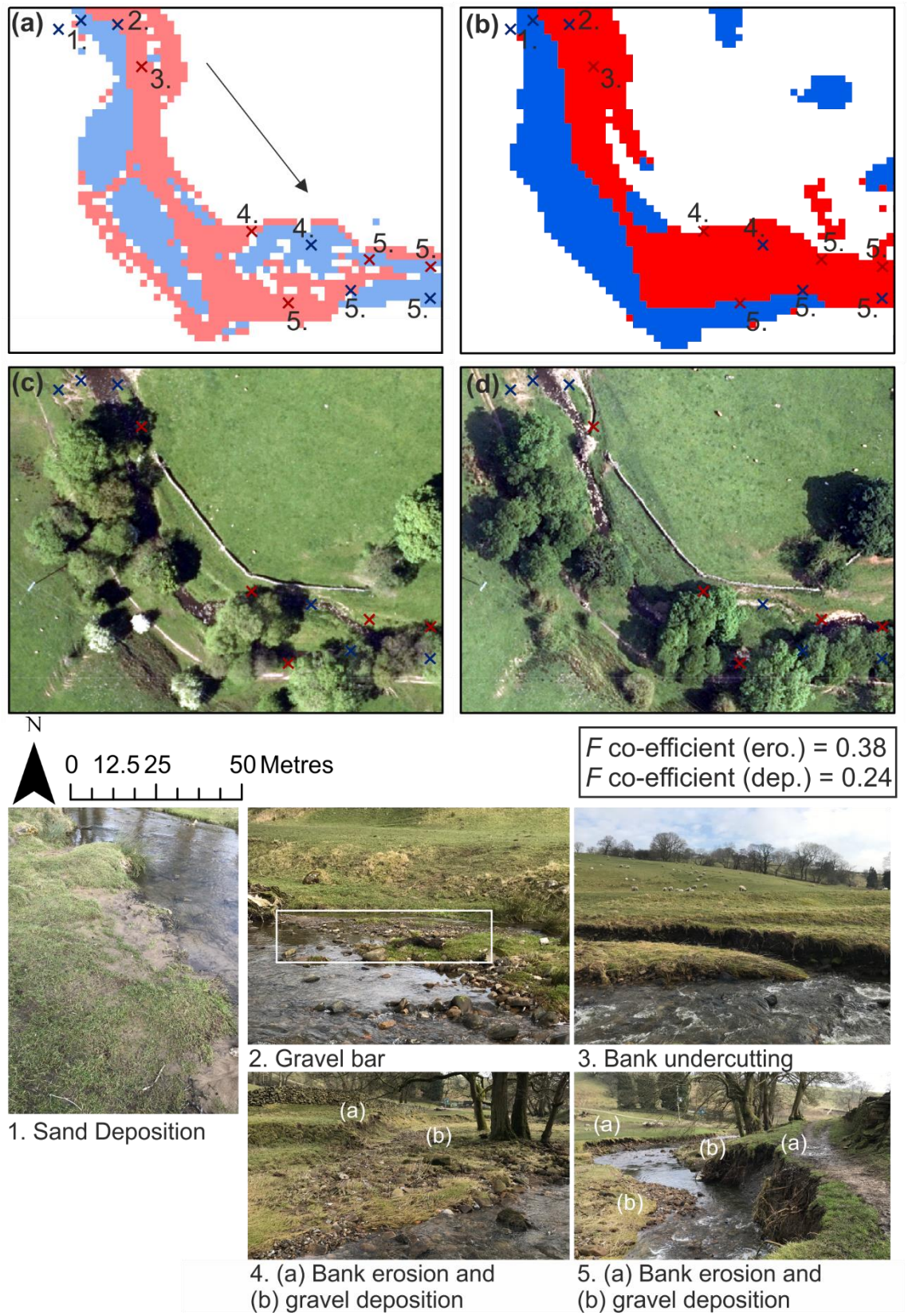

Figure 4.5: Comparison area 1 with modelled outputs for (a) CAESAR-Lisflood and (b) HEC-RAS 2D and aerial imagery in (c) 2015 and (d) 2018. Red shows erosion and blue shows deposition. Numbered annotations (with associated colour for geomorphological process) correspond with field photographs below taken in March 2020. Arrow highlights flow direction.

An overestimation of erosion and deposition by HEC-RAS 2D compared to CAESAR-Lisflood was apparent in Figure 4.6, aiding the F coefficient values of 0.25 and 0.3 respectively. The area was characterised by eroding banks and a low lying floodplain on the right hand side where sand deposition was seen (Figure 4.7). CAESAR-Lisflood defined the erosion within the channel and banks well and although HEC-RAS 2D also estimated erosion in the same areas, the channel definition is less clear. The greatest difference between the two models was on the floodplain, where erosion was estimated when using HEC-RAS 2D and no processes or deposition was estimated in CAESAR-Lisflood.

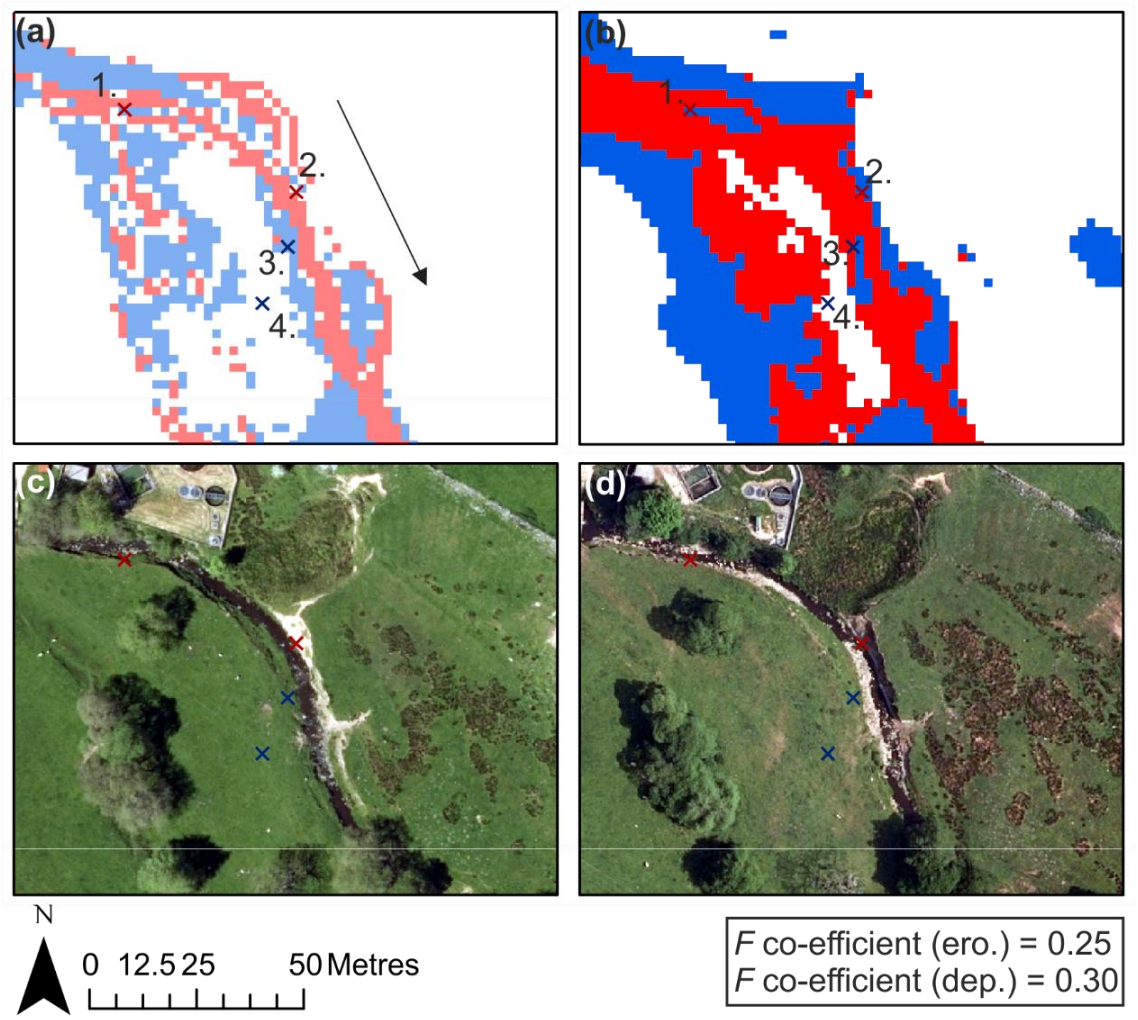

Figure 4.6: Comparison area 2 with modelled outputs for (a) CAESAR-Lisflood and (b) HEC-RAS 2D and aerial imagery in (c) 2015 and (d) 2018. Red shows erosion and blue shows deposition. Numbered annotations (with associated colour for geomorphological process) correspond with field photographs below taken in March 2020 in Figure 4.7. Arrow highlights flow direction.

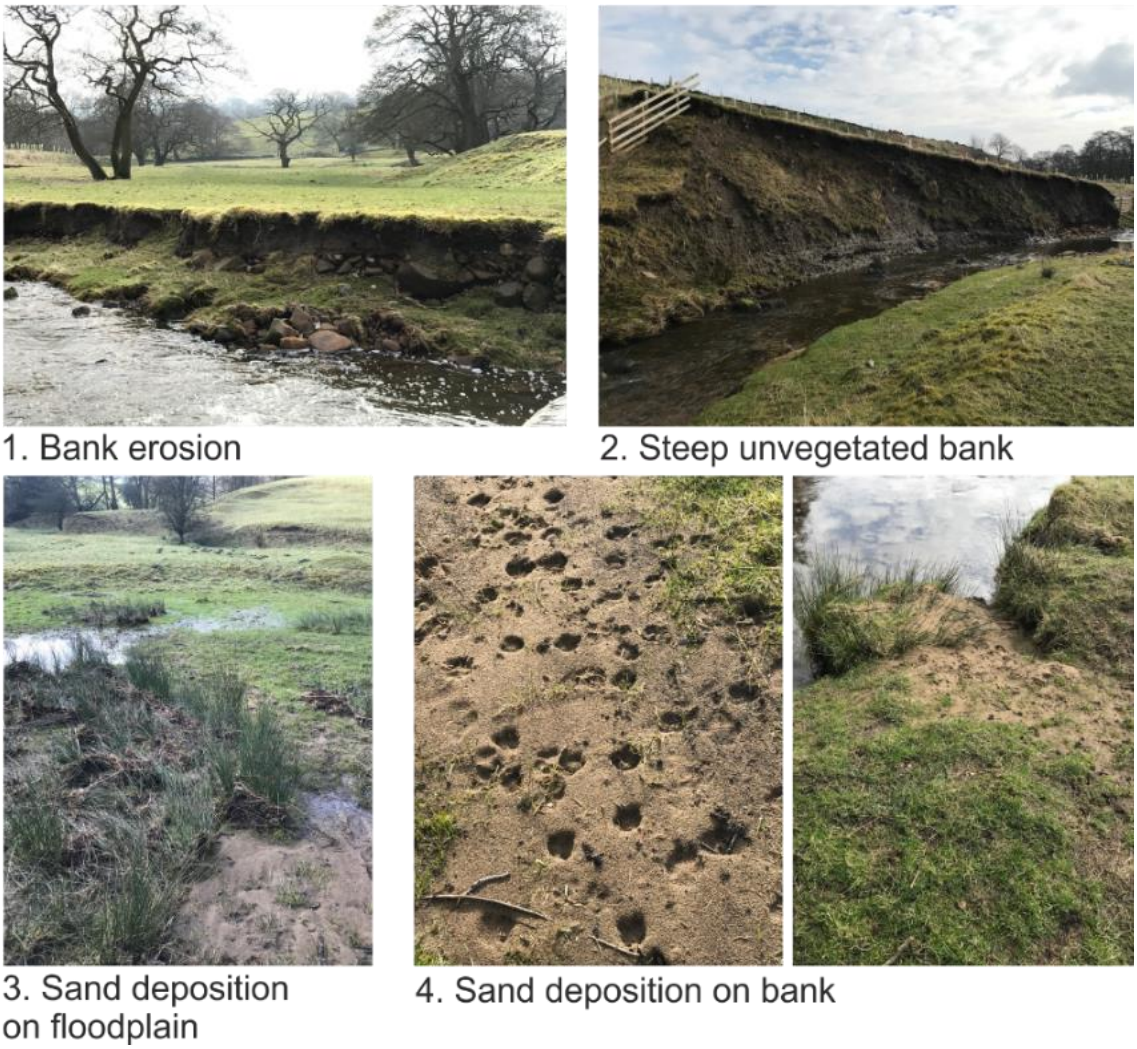

Figure 4.7: Field photos taken in March 2020 in comparison area 2.

In comparison area 3, both models appeared to exaggerate the extent of apparent geomorphological processes from both aerial imagery and from field photos (Figure 4.8). Deposition on the floodplain in the top left corner of Figure 4.8a and b was evidenced by the sand deposition in the foreground of Photo 1. However there was no evidence for the erosion estimated in both models on the floodplain. Gravel deposition within Photo 1 and the erosion in Photo 2 were not apparent in either model, however both were relatively small, less than 1 m in width. On the tributary coming in from the bottom left corner in Figure 4.8, both bank erosion and gravel deposition was apparent within the field photos, however this was not translated into either model, with a lack of clarity for CAESAR-Lisflood and in HEC-RAS 2D no processes were suggested for the erosion to the steep bank as shown in Photo 3.

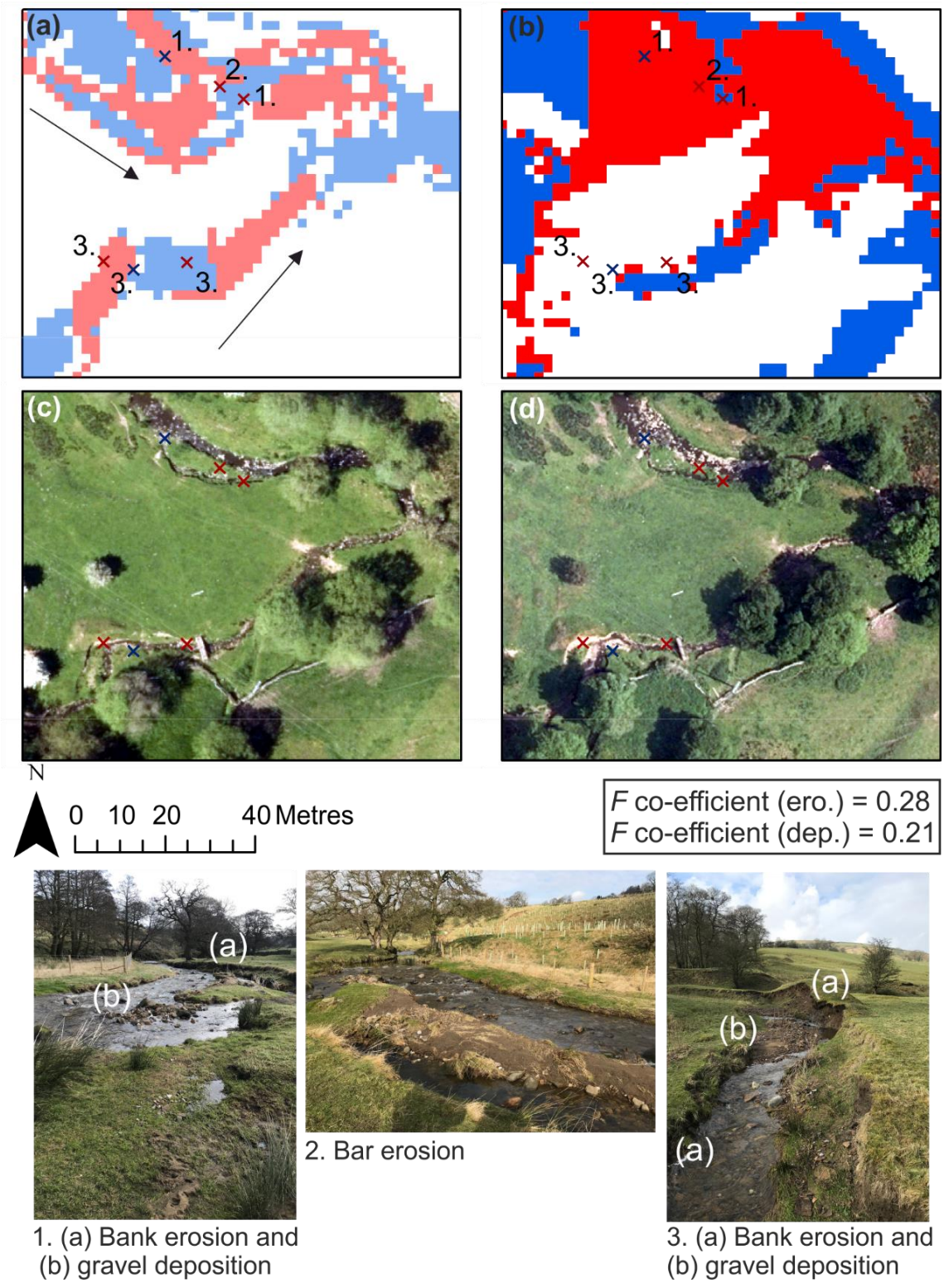

Figure 4.8: Comparison area 3 with modelled outputs for (a) CAESAR-Lisflood and (b) HEC-RAS 2D and aerial imagery in (c) 2015 and (d) 2018. Red shows erosion and blue shows deposition. Numbered annotations (with associated colour for geomorphological process) correspond with field photographs below taken in March 2020. Arrow highlights flow direction.

The F coefficient for area 4 for both erosion and deposition was the lowest of any comparison area (Figure 4.9). Processes on the left and right hand floodplains did not correspond between the two models well, with areas of deposition in CAESAR-Lisflood predicted as erosion in HEC-RAS 2D on the left hand floodplain and the opposite for the right hand floodplain. However no evidence was found in the field photos to suggest either erosion or deposition was occurring on the floodplain. Both models did represent an erosive channel, particularly in the upper part of the comparison area.

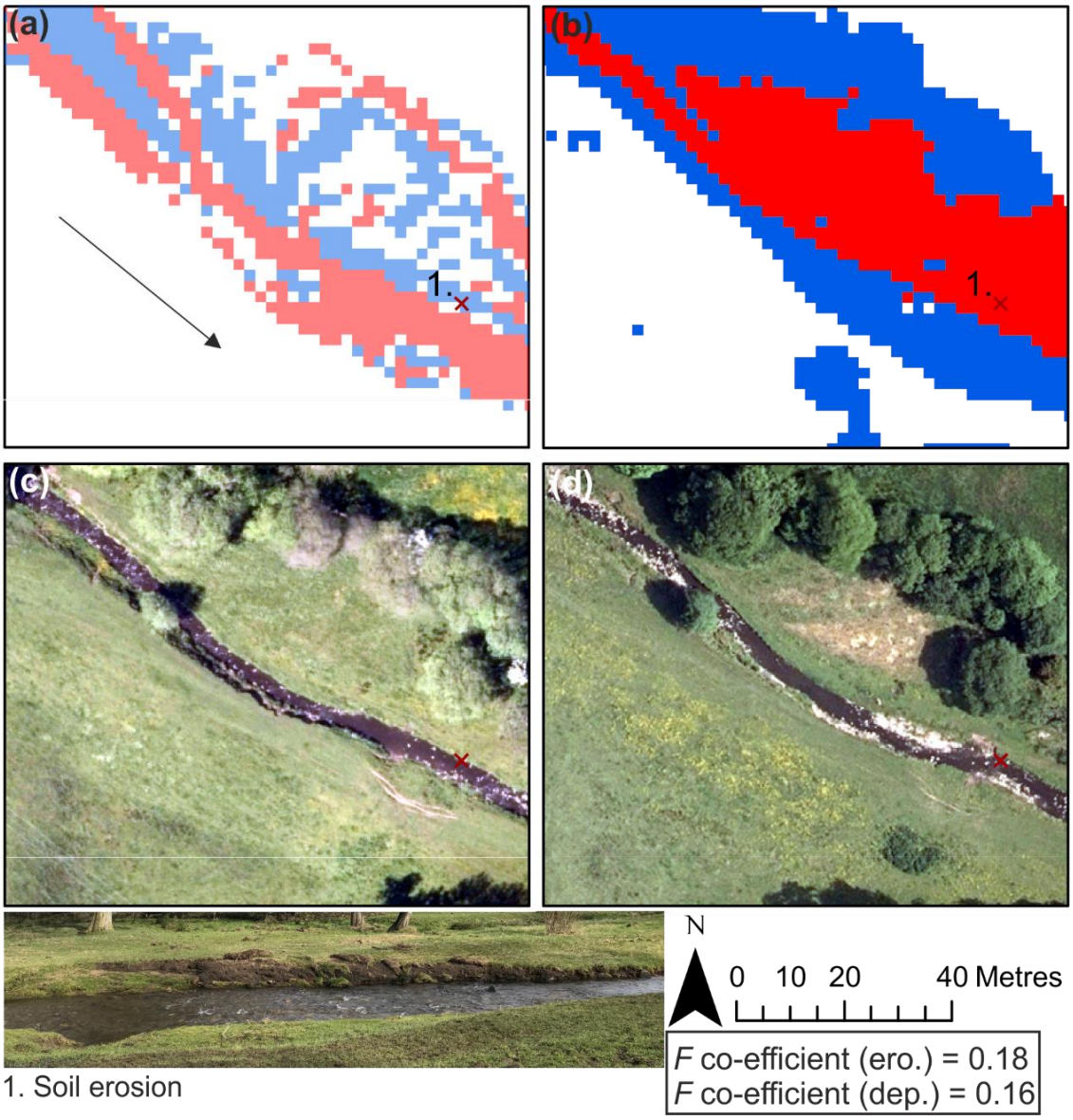

Figure 4.9: Comparison area 4 with modelled outputs for (a) CAESAR-Lisflood and (b) HEC-RAS 2D and aerial imagery in (c) 2015 and (d) 2018. Red shows erosion and blue shows deposition. Numbered annotations (with associated colour for geomorphological process) correspond with field photographs below taken in March 2020. Arrow highlights flow direction.

Figure 4.10 shows that within comparison area 5, there appears to be little agreement between the two models with regards to erosion, made evident by the low F coefficient for erosion (0.18). The field photo shows a gravel bar located at the start of the meander which was estimated within both models although definition was not clear. The removal of a tree and grass between 2015 and 2018 and the creation of what appears to be a gravel bar (Figure 4.10c and d), were depicted in the CAESAR-Lisflood model as a large area of deposition with a small outline of erosional cells on the inner curve of the meander. The equivalent area in HEC-RAS 2D was estimated to be entirely erosional. CAESAR-Lisflood appeared to represent floodplain deposition, bank erosion and a depositional channel bed at the downstream limit of the comparison area (Figure 4.10a) although tree cover within aerial imagery and a lack of access to the site inhibited knowing whether this was a true representation.

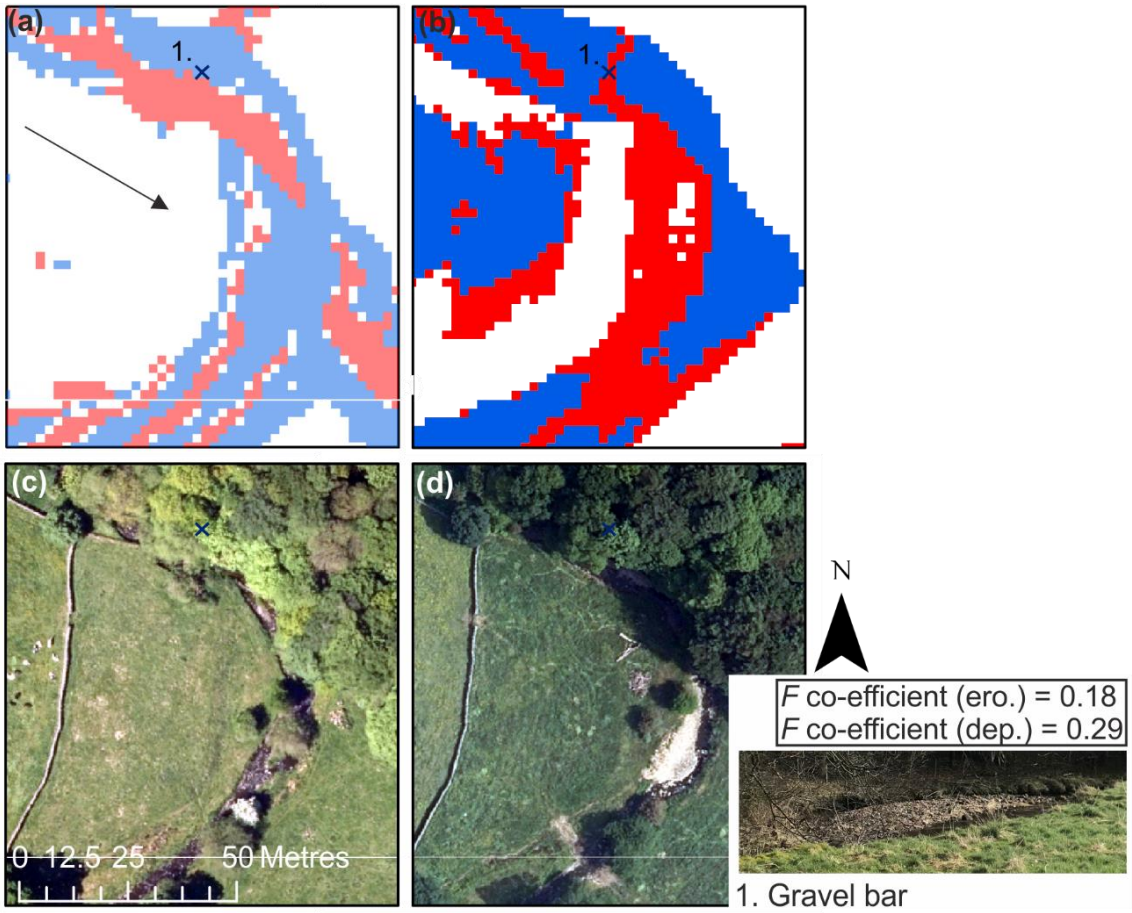

Figure 4.10: Comparison area 5 with modelled outputs for (a) CAESAR-Lisflood and (b) HEC-RAS 2D and aerial imagery in (c) 2015 and (d) 2018. Red shows erosion and blue shows deposition. Numbered annotations (with associated colour for geomorphological process) correspond with field photographs below taken in March 2020. Arrow highlights flow direction.

Comparison area 6 was characterised by lateral movement of the channel and a subsequent large area of deposition that appeared between the 2015 and 2018 aerial imagery (Figure 4.11c and d). CAESAR-Lisflood did represent this movement, although the erosional line of cells running from the top left corner of Figure 4.11a were matched to the channel location in 2015 but not once the migration apparent in 2018 had occurred. HEC-RAS 2D also identified the area of deposition and erosion although greatly overestimated the lateral extent of both.

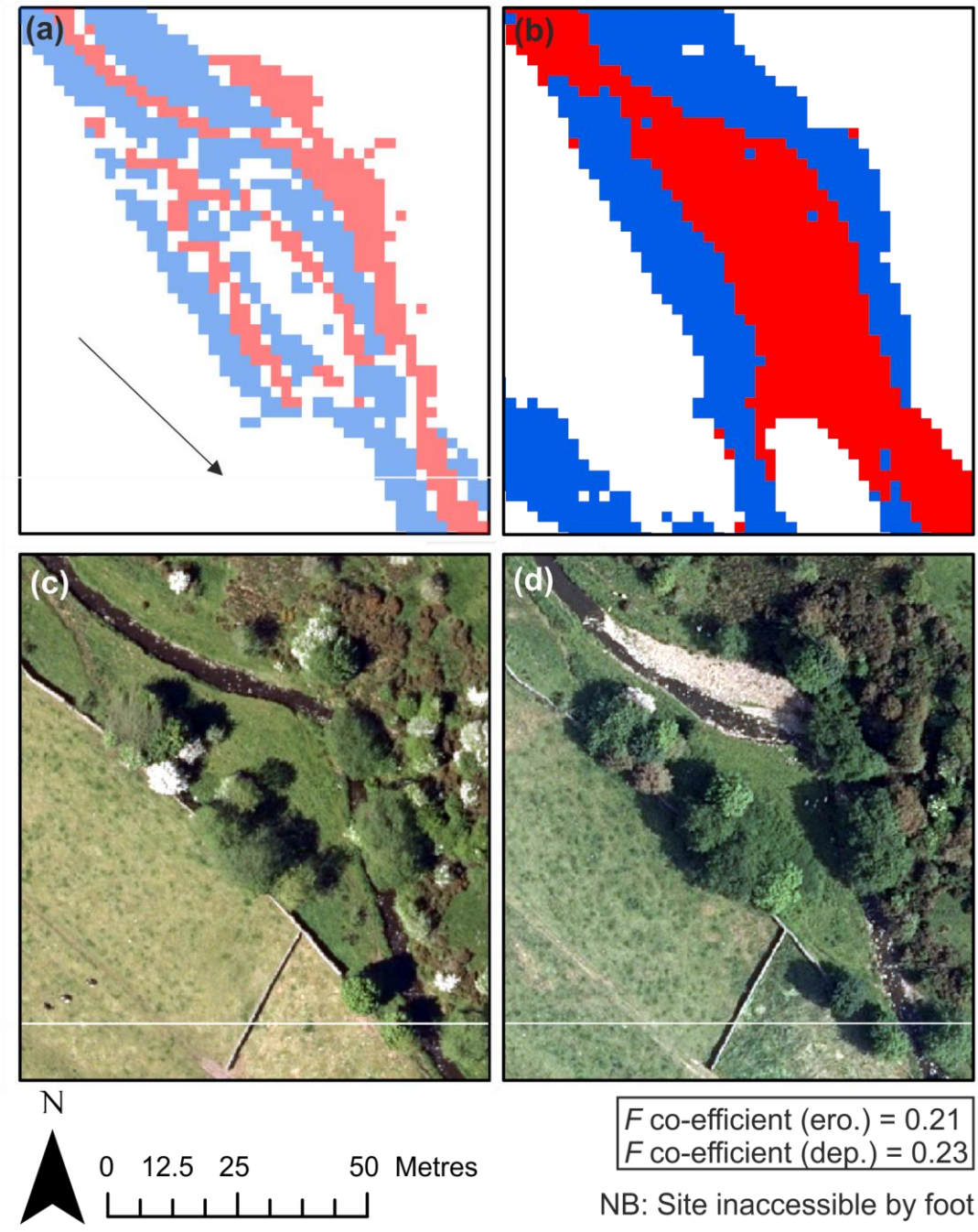

Figure 4.11: Comparison area 6 with modelled outputs for (a) CAESAR-Lisflood and (b) HEC-RAS 2D and aerial imagery in (c) 2015 and (d) 2018. Red shows erosion and blue shows deposition. Arrow highlights flow direction.

An erosive line of cells in CAESAR-Lisflood aligned with the channel location in the aerial imagery and a long-distance photo taken also showed bank erosion occurring down the reach in comparison area 7 (Figure 4.12). What was less apparent in the modelling results was the slight channel migration near the downstream boundary of the comparison area. HEC-RAS 2D also identified erosion within the channel, although a lack of definition was apparent. The greater extent to geomorphological change particularly extending to the right hand side of the channel observed in both models was not apparent in the aerial imagery. A small flow pathway can be seen in the background of picture 1 in Figure 4.12, however geomorphological processes were not identifiable.

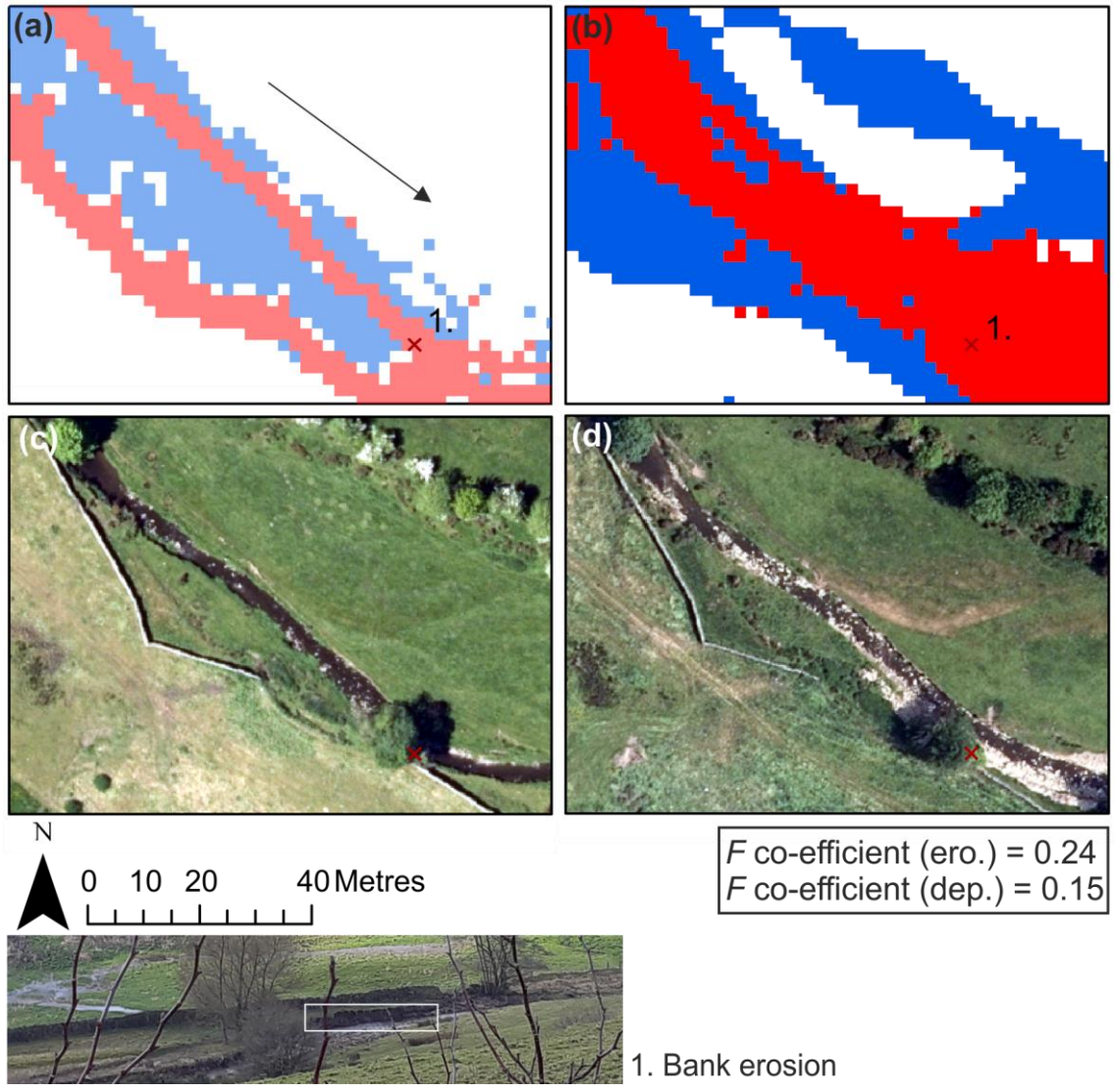

Figure 4.12: Comparison area 7 with modelled outputs for (a) CAESAR-Lisflood and (b) HEC-RAS 2D and aerial imagery in (c) 2015 and (d) 2018. Red shows erosion and blue shows deposition. Numbered annotations (with associated colour for geomorphological process) correspond with field photographs below taken in March 2020. Arrow highlights flow direction.

The greatest change within the aerial imagery was observed in comparison area 8 (Figure 4.13). Both models suggested a central line of erosion with deposition occurring either side, however what appeared to be less accurate was the location of the central line of erosion. CAESAR-Lisflood suggested that erosion occurred to the outer bend visible in the 2015 imagery although this did not appear to be what happened given the evidence in the aerial imagery. Although HEC-RAS 2D seemingly more accurately represented what occurred to the left hand bank compared to CAESAR-Lisflood, to the right, extent of both erosion and therefore the outer deposition was over-estimated.

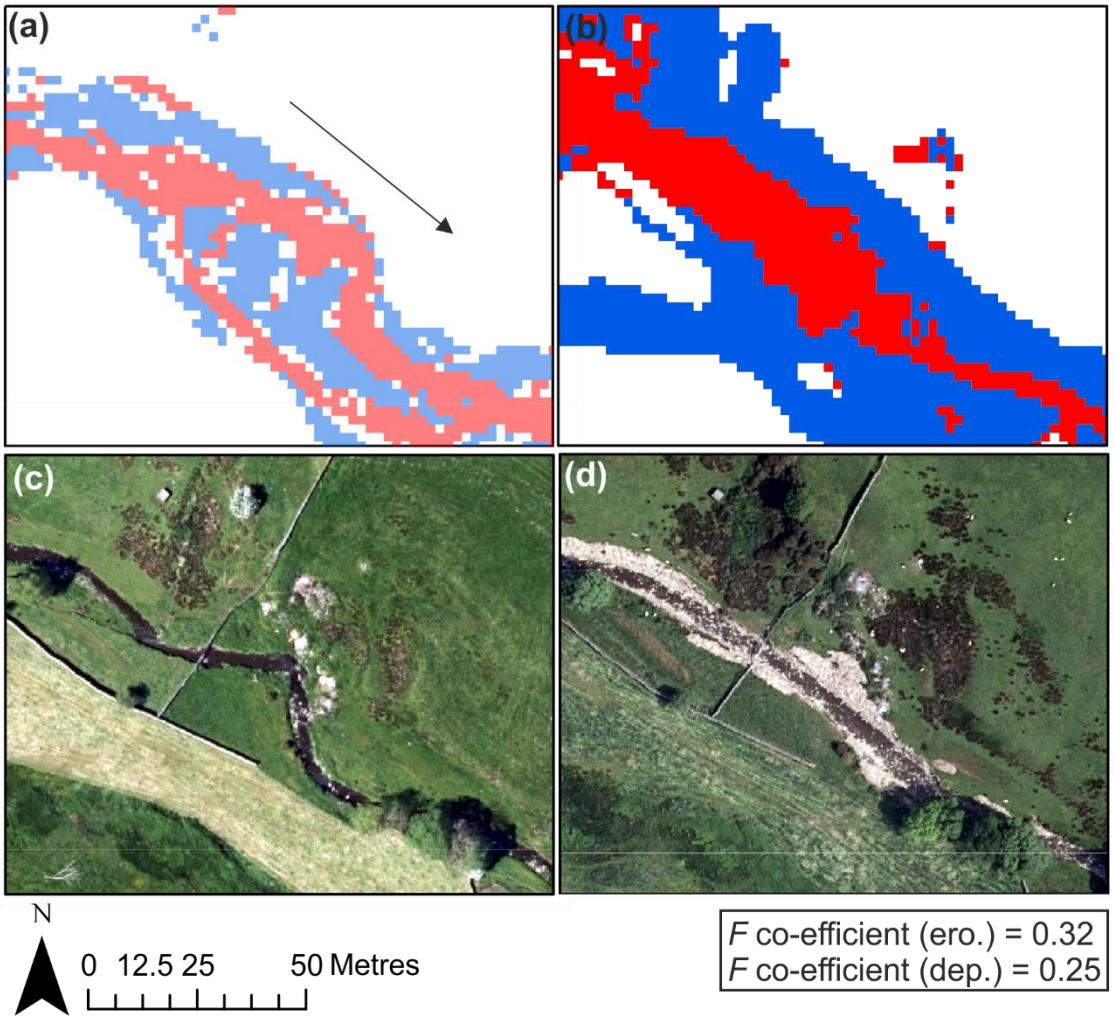

Figure 4.13: Comparison area 8 with modelled outputs for (a) CAESAR-Lisflood and (b) HEC-RAS 2D and aerial imagery in (c) 2015 and (d) 2018. Red shows erosion and blue shows deposition. Arrow highlights flow direction.

4.4 Discussion

4.4.1 Model comparison

Sensitivity of the model agreement metric (*F* coefficient) to the parameter value choice within the method for estimating geomorphological processes from shear stress grids highlighted the need for careful selection of the Manning's n, Shield's parameter and median grain size (D_{50}) (Figure 4.4). Both Manning's n and the median grain size are assessable with knowledge of the catchment and therefore uncertainty arising from these two parameters can be reduced through field visits and careful use of the many available land-use related tables of Manning's n values. Although the Shield's parameter is less related to catchment descriptions, a vast amount of literature is available for those seeking a justifiable value. As the Shield's parameter is used within the calculation of the critical shear stress, grids of shear stress can be quickly and simply reclassified with different critical shear stress values within GIS software to assess the effect in relation to aerial imagery, field knowledge or other modelling results for any given area of interest.

The comparison between CAESAR-Lisflood and HEC-RAS 2D highlighted that generally, longitudinal patterns of erosion and deposition were qualitatively the same in both models. Quantitatively, the low values (< 0.32) for the *F* coefficient do suggest the two models were less agreeable. This was expected due to the high resolution, cell-by-cell basis of such spatial goodness-of-fit metrics. Slight differences in the methodology for the two models may have also factored into the low *F* scores for the erosion and deposition.

Firstly, HEC-RAS 2D cannot account for change occurring to the shear stress from environmental changes such as the energy losses through the movement of sediment through time. CAESAR-Lisflood however, calculates sediment transport, bed elevation and changes to grain size per time step. Changes may include those to the bed elevation, grainsize and sediment availability. This is important for a true representation of the complexity of sediment transport. This will limit the applicability of the shear stress methodology to simple sediment problems over short time periods where geomorphological processes are transport and not sediment limited. This limitation echoes that highlighted by Reid et al. (2019) who used the same shear stress approach at a small finer spatial resolution to evaluate gravel bar reworkings. It is most likely to be unsuitable for

estimating geomorphic change for systems where sediment waves are apparent (Lisle et al. 2001), bed armouring develops (Gomez 1983) and where anthropogenic influences, such as grazing and vehicle use, will cause bank failure and compaction.

Secondly, the HEC-RAS 2D erodibility output is derived from the maximum values occurring at any time. Instead, the CAESAR-Lisflood output is derived from the event as a whole, providing a truer picture of the system response to a flood event. Sediment deposition often occurs after the peak of a flood event, the HEC-RAS 2D methodology may therefore underestimate the amount of deposition, resulting in a low *F* score for deposition. In this sense, the resulting map of geomorphological processes from the HEC-RAS 2D methodology can be thought of an “erosion worst-case scenario”.

Both models appear to exaggerate the extent of geomorphological activity compared to the aerial imagery and the field evidence. In HEC-RAS 2D this is the result of the method defining each wet cell as being geomorphologically active. Therefore if the flood extent is over-estimated, large areas of deposition would be expected in the shallower peripheries of the flood extent. It is also improbable to assume that every cell is geomorphologically active, particularly in systems which are sediment- as opposed to transport-limited. The exaggerated extent within CAESAR-Lisflood is likely to be due to the modelled outputs being reclassified into binary maps, thus all magnitude of change is shown as a single value. In reality, much change would not be observable from aerial imagery, where only large differences are visible e.g. bar formation and channel migration. Spatial overestimation has also been observed in CAESAR-Lisflood by Feeney et al. (2020), who observed an overestimation of the size of meanders when using CAESAR-Lisflood to model decadal changes of UK river reaches.

4.4.2 Implications for NFM projects

With careful consideration of the methodological assumptions as previously discussed and alongside aerial imagery or site walk overs, hydraulic models can be used to evaluate geomorphological dynamics within areas of a catchment. HEC-RAS 2D produces general longitudinal patterns of erosion and deposition, though CAESAR-Lisflood appeared far more realistic, particularly for variability across the channel and within a reach. These findings are important for guidance

for future studies, particularly for NFM projects where a morphodynamic modelling study is often unfeasible in terms of cost.

Many NFM projects cover too large a catchment at too high a resolution for morphodynamic modelling. Results from this study show larger projects are able to estimate geomorphological processes based on the calculation of shear stress. This would aid projects where previously a geomorphological assessment would not have been possible to acknowledge the impact geomorphological processes may have and how this may affect performance and management of NFM implemented. The findings of this study are also important for projects where open access depth and velocity grids already exist, as they do for the entire country for a set of design events at 2 m as part of the national surface water flood risk modelling and mapping project. The re-use of the depth and velocity grids to evaluate geomorphological processes provides a very cost effective methodology – especially for national scales, which previously would not have been possible without costly morphodynamic modelling or extensive field surveying.

4.4.3 Future work

Currently, geomorphological outputs derived from hydraulic models cannot be used without reference to real-world data such as repeat aerial imagery, site walkovers or field measurements of geomorphological change. Therefore more examples of the accurate prediction of geomorphological change from hydraulic models is needed for varying magnitude events and for catchments of different sedimentological characteristics. These early uses of hydraulically derived geomorphological outputs can however guide practitioners as to where to collect more detailed datasets to further validate the hydraulic model outputs. Once there is more evidence that hydraulically modelled shear stress can accurately predict erosion and deposition in a number of differing scenarios, the methodology may be used on large pre-existing datasets of depth and velocity grids available as part of nationwide flood risk mapping efforts. This would result in an efficiently created, unprecedented estimation of geomorphological change at a national scale for multiple return period events at a high resolution.

The advantage of using a hydraulic model is their ability to simulate hydraulic structures. Future studies may look to take advantage of this to examine how

these structures affect the shear stress and hence potential erosion and deposition as the current suite of morphodynamic models available are not able to simulate such complex flow dynamics. Such applications are important, particularly if one may choose to simulate nature-based flood management solutions such as woody debris dams (e.g. Keys et al. 2018). An acknowledgement of a structure's geomorphological impact is critical for their design and long term management, whereby event dependent trade-offs between hydraulic function and scour or in-filling will be needed.

4.5 Conclusions

This study has aimed to establish whether geomorphological change due to episodic river floods can be estimated without the use of morphodynamic models. For the first time, it has been established that patterns of erosion and deposition can be efficiently estimated by comparing shear stress calculated from a HEC-RAS 2D model with the net elevation change calculated from a CAESAR-Lisflood model for an extreme rainfall-induced flood event in a small upland catchment.

Qualitatively, field evidence validated the longitudinal patterns of geomorphological processes estimated using HEC-RAS 2D to provide a catchment-wide picture on a scale that would have previously required the use of a morphodynamic model.

Quantitatively, goodness-of-fit metrics suggested a poorer agreement between the outputs derived from HEC-RAS 2D and CAESAR-Lisflood. Such metrics however, are high resolution and can therefore over-emphasise cell-by-cell process misrepresentations whilst both models estimate the correct "bigger picture" of longitudinal changes in geomorphological processes.

Given this study provides an initial insight into the re-purposing of a hydraulic model's depth and velocity grids, it is advised therefore that more studies need to be undertaken on a wide range of rainfall events, catchments varying in sedimentological characteristics and at a finer spatial scale. If future studies show a fair comparison between modelled and observed geomorphological change, there is the potential for refinement of the methodology using filtering or machine learning. The methodology would then allow for the re-purposing of pre-existing nationwide datasets to achieve a high resolution analysis of potential geomorphic change occurring for differing return period events for all watercourses included

within national flood risk mapping efforts. This would provide invaluable insight without the great expense of creating individual morphodynamic models.

Chapter 5

The hydrological and geomorphological impact of leaky barrier design with event magnitude at reach scale

5.1 Introduction

Flooding is one of the most damaging natural hazards in the UK. For example, the winter floods of 2015 to 2016 resulted in estimated costs of £1.6 billion (Environment Agency, 2018a). Within just four months from November 2019 to February 2020, three major flooding events occurred in the UK, inundating and damaging houses, businesses and farmland, blocking travel routes and causing loss of life. These floods and their impacts could be a sign of the future, because the frequency and magnitude of flooding is likely to increase with changing precipitation under future climate change scenarios, including more intense summer storms (Kendon et al., 2014). Additionally, continuing urbanisation and intensification of farming may increase surface water runoff pathways and soil erosion, impacting flood risk, river morphology, water quality and biodiversity (O'Connell et al., 2007 and Jacobson, 2011).

The Pitt Review which followed the widespread UK flooding in 2007 suggested that a catchment-based, holistic approach of structural and non-structural measures was needed (Pitt, 2008). Natural flood management (NFM) measures are one set of non-structural approaches that have been increasingly implemented (Dadson et al., 2017). NFM has seen an increase in awareness and funding, particularly since the Environment Agency's "Working with Natural Processes" evidence directory was published in 2017 (Burgess-Gamble et al., 2017), alongside £15m of funding from the UK government department, DEFRA. NFM aims to reinstate or improve natural catchment processes previously affected by human activities to reduce flooding (Dadson et al., 2017). NFM has added non-flood risk benefits including improved water and soil quality, habitat creation and improved biodiversity (Dadson et al., 2017). NFM measures include leaky barriers, soil management, woodland planting, floodplain reconnection and run-off attenuation features (Burgess-Gamble et al., 2017).

Leaky barriers are a popular NFM measure, commonly added into UK watercourses. Their uptake has been aided by funding opportunities under the Countryside Stewardship scheme (Rural Payments Agency, 2020). They are

engineered to reduce flow velocities, increase channel friction and to simulate the natural process of trees falling into and semi-blocking a river channel. Leaky barrier structures vary widely in terms of design. The majority allow for baseflow under the structure to be unimpeded and some water to pass through the structure at higher flows. Most water is stored temporarily within the channel, with water also being encouraged onto the floodplain. The variability in leaky barrier design (Figure 5.1) arises from differences in cost, location and what materials are available at the location, but most importantly there is no overarching design criteria and only a few design suggestions (e.g. Figure 5.2, Rural Payments Agency 2021; YDRT, 2018a). The difficulty in monitoring such leaky barriers in the field including the dependency on different magnitude rainfall events and a lack of monitoring data overall has added to the lack of unity in design. There is therefore an opportunity for numerical modelling of leaky barriers to contribute to guidelines for their design (e.g. CIRIA, 2018).

Figure 5.1: Variability in leaky barrier types. Modified diagram (names added) from JBA Trust (2020), p.2.

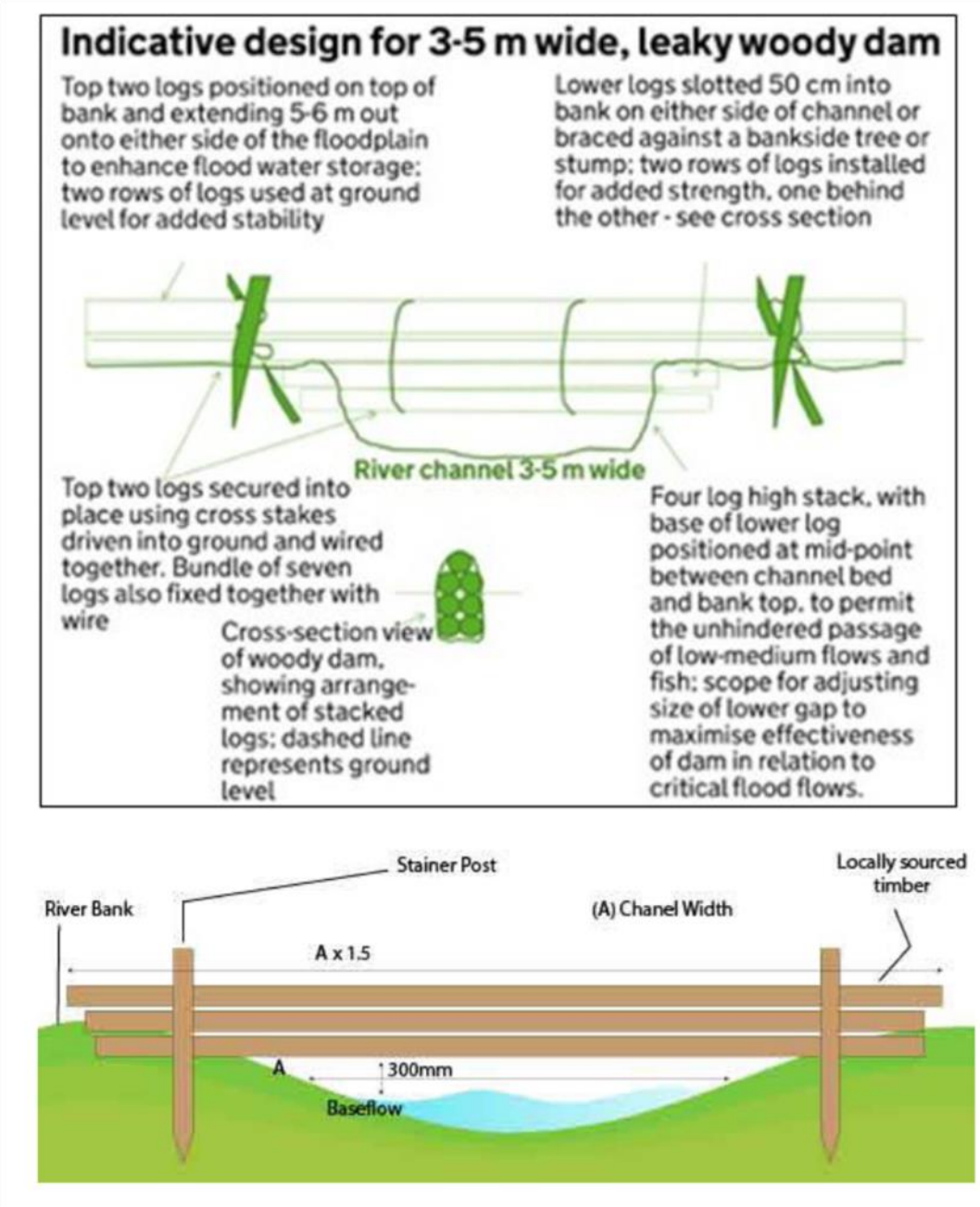

Figure 5.2: Diagram of indicative leaky barrier designs for (a) funding under Higher Tier Countryside Stewardship “large leaky woody dam” (Rural Payments Agency, 2021) and (b) from Yorkshire Dales Rivers Trust Leaky Dam guidance (2018).

To date there are very few studies detailing the impact of altering specific design aspects such as the height and length of a leaky barrier. Furthermore, no universal leaky barrier specific models, additional model modules or capabilities exist, a problem not just for NFM but also for naturally occurring large woody debris too. Despite this, leaky barriers have been represented within numerical models in a number of ways to simulate the hydrological and hydraulic impact of barriers (see the recent review of Addy and Wilkinson, 2019). Representations

include partial channel blockage (e.g. Thomas and Nisbet, 2012; Pinto et al., 2019) and the use of hydraulic structures that behave in a similar manner to a leaky barrier, such as a weir with a culvert (e.g. Metcalfe et al., 2017, Metcalfe et al., 2018). Keys et al., (2018) used a weir and randomly placed orifices to represent large woody debris and showed increased floodplain connectivity. Leakey et al., (2020) modelled leaky barriers using a hydraulic structure and validated their efforts using evidence from flume experiments.

The focus to date for modelling leaky barriers, has been their impact on local hydrology and hydraulics. However, field evidence shows naturally occurring large wood has an important role in the geomorphological response to a flood event (Gurnell, 2012). As a result, there have been calls for additional research into modelling the effects that both naturally occurring large wood and engineered wood structures can have on fluvial geomorphology (Keys et al., 2018; Addy and Wilkinson, 2019).

Given the lack of evidence surrounding the hydrological and geomorphological response to leaky barrier design, particularly for large flood events (Burgess-Gamble et al., 2017), the aim of this chapter is to examine how changing design aspects of a common leaky barrier style (Figure 5.2) affect the hydrological and geomorphological response to differing magnitude and seasonality flood events both.

5.2 Methodology

5.2.1 Study Area

The Lothersdale catchment (12.9 km^2) is a small typically steep-sided upland gravel-bed river catchment in northern England (Figure 5.3). The catchment sits within the Eastburn Beck catchment, details of the wider Eastburn Beck catchment can be found in Chapter 2, Section 2.1. The catchment is underlain by till superficial deposits and the Hodder Mudstone Formation bedrock with associated slowly permeable soils. Land use within the catchment consists of sheep grazed pasture, natural grassland and heath (Figure 5.3).

A reach within the upper Lothersdale catchment with a contributing area of 2.89 km^2 was chosen due to the floodplain which extended up to 30 m either side of the channel. The reach extended 264 m downstream, with a channel width at

baseflow of approximately 2 m and elevation decreasing from 213 m to 205 m downstream. The modelled reach is used currently as pasture for sheep grazing.

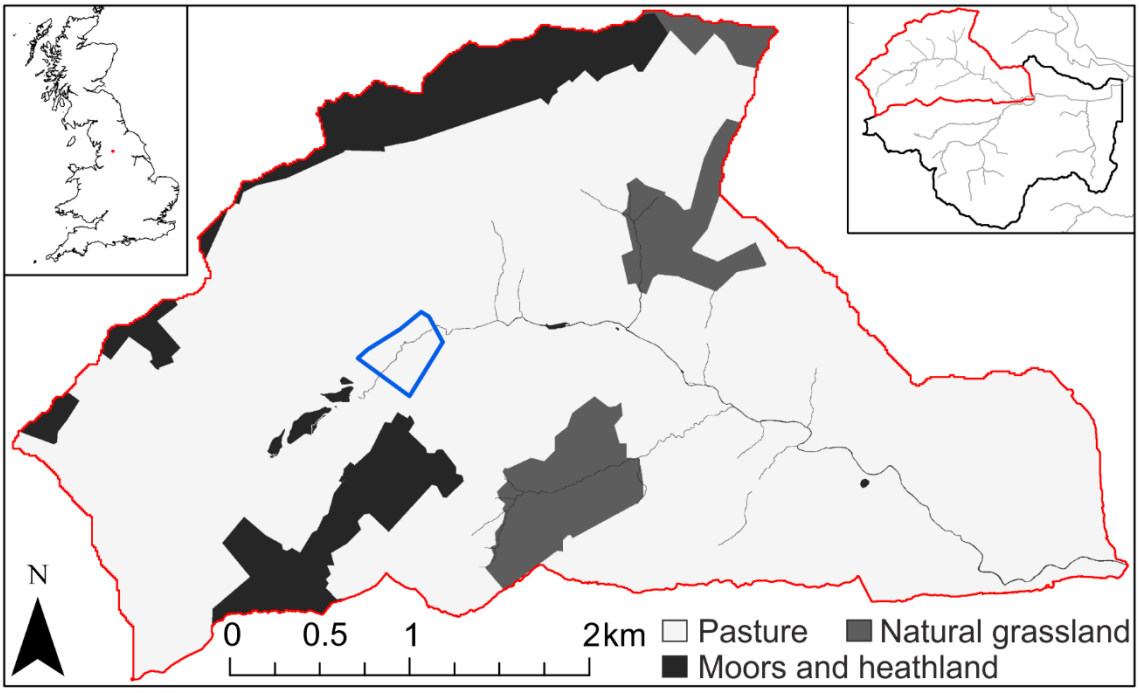

Figure 5.3: Lothersdale catchment location, highlighting modelled reach location within the catchment (blue).

5.2.2 Model selection and set up

The HEC-RAS hydraulic modelling software was chosen due to its capabilities to model the specified reach in 2D with a choice of governing equations. A 2D modelling approach was required for accurate representation of flow over the floodplain located within the model domain (Figure 5.4). HEC-RAS solves the 2D Saint-Venant equations for the conservation of mass and the conservation of momentum in the x and y directions.

HEC-RAS also benefits from sub-grid capabilities resulting in shorter model run times where the computational grid can be unstructured and of a much larger resolution than the underlying topographic data. An exploratory model based on data collected from the wider Lothersdale catchment was set up using a 2016 LiDAR 0.5 m Digital Terrain Model (DTM). The model was not expected to be predictive, instead data from Lothersdale was used as an example to allow for scenario testing of leaky barrier design. An initial computational grid with 5 m cell spacing was created. Breaklines, with a finer grid spacing of 2 – 4 m, were enforced along the channel centreline and tops of slopes to improve model accuracy in the channel and around terrain features such as ridges on the

floodplain (Figure 5.4). Grid refinement resulted in unstructured computational cells within and surrounding the channel (Figure 5.4). Manning's n roughness was set within the model domain at a 0.5 m resolution and was based on land use with a value of 0.032 being used to represent grassed areas. A higher value of 0.05 was used to represent the coarse, cobbled nature of the upland catchment sediment present on the channel bed.

Regarding governing equations, the small spatial extent of the model domain allowed for short enough run times to apply the full shallow water equations solver. Computation time step was set to 0.1 seconds so as to avoid model instability. These two choices led to model run times of approximately an hour.

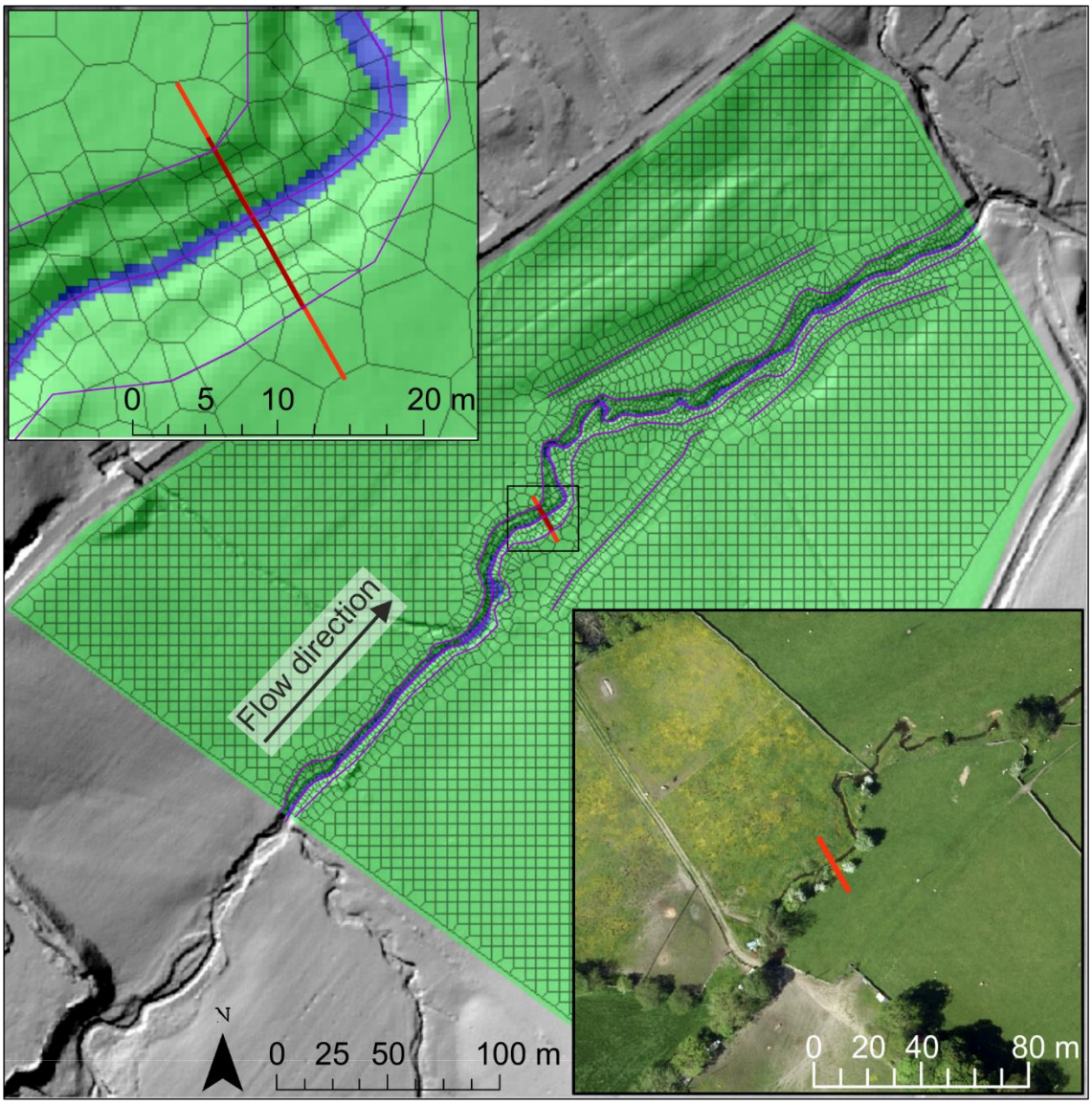

Figure 5.4: Model domain set up in HEC-RAS highlighting the computational grid, difference in Manning's n (green for grass, blue for channel), breaklines (purple) and barrier location (red).

5.2.2.1 Event Choice

The Revitalised Flood Hydrograph (ReFH) method was used to estimate the discharge of single flood events for the reach. Catchment descriptors utilised in the parameterisation of the ReFH model are available for all catchments larger than 0.5 km^2 in the UK (Bayliss, 1999). This ReFH usage allowed for storm hydrographs to be estimated for the ungauged small modelled reach based on the associated contributing area and catchment descriptors for the Lothersdale catchment. The ReFH model was used to create storm hydrographs for 2-, 5-, 10-, 30-, 100- and 1000- year return periods for the recommended rainfall duration of 3.5 hours (Figure 5.5).

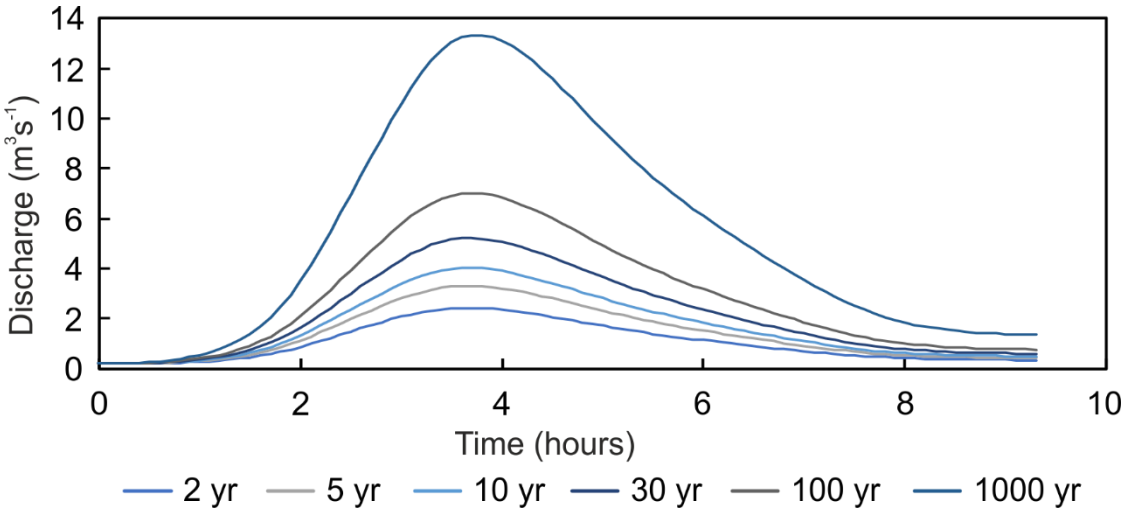

Figure 5.5: Storm hydrograph scenarios input as discharge at model's upper boundary condition.

5.2.2.2 Leaky barrier implementation and scenario testing

Many previous modelling studies have focused on the implementation of leaky barriers by using partial blockage functions (Thomas and Nisbet, 2012, Pinto et al., 2019). This method typically partially blocks the channel laterally, such as how a flow deflector is situated in a channel, whereas in this study, the aim was to partially block the channel vertically. Therefore the leaky barrier was simulated using a weir function in the HEC-RAS 2D model with a culvert placed at the bottom of the channel to represent the gap under the barrier (Figure 5.6). A similar method was used by Keys et al. (2018) where a weir and randomly placed orifices were implemented and Leakey et al. (2020) concluded that representing leaky barriers using a similar traditional hydraulic structure was valid.

The rise of the culvert (height) was chosen based on design guidelines available – 0.3 m (YDRT, 2018a; Figure 5.6a) and knowledge from leaky barriers in-situ

across the north of England – 0.05 m (Figure 5.6b). Culvert width was calculated to span the entire width of the base of the channel when the culvert height was set to 0.3 m (Figure 5.6a). It should be noted that HEC-RAS 2D solves the flow through a culvert using the specified rectangular dimensions (rise and span) regardless of whether there is underlying topography cutting through the culvert (Figure 5.6). This is an overestimation of the flow capacity under the barrier. It was assumed that this overestimation instead could account for the leakiness of the barrier, which is not otherwise explicitly represented. With this assumption, it should also be acknowledged that the “leakiness” would be utilised much earlier in the storm hydrograph than if gaps between individual tree trunks had been modelled.

A scenario without the leaky barrier and a scenario with a barrier but without the culvert were also created to assess both the effect of the barrier in its entirety and the effect the “leakiness” had, respectively. A third set of barrier dimensions were tested based on an extension of the barrier onto the floodplain by both increasing the height and length of the barrier, but maintaining the 0.3 m high culvert (Figure 5.6c). For all barriers, the weir efficiency was reduced to 1.5 and Manning’s n for the culvert was increased to 0.1 to simulate the roughness of the wood compared to smoother surfaces (e.g. concrete) that would typically be modelled using these parameters in a hydraulic structure representation.

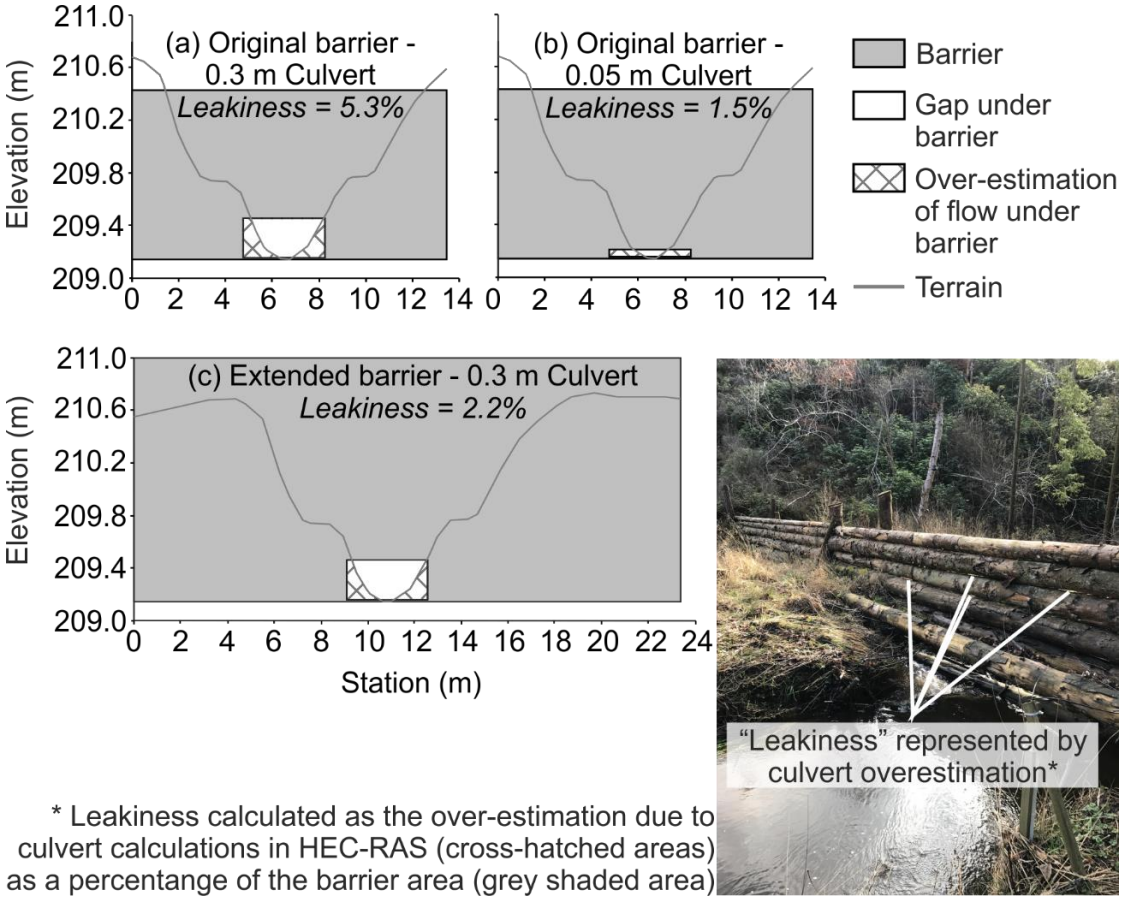

Figure 5.6: Visualisation of leaky barrier dimensions.

5.2.3 Data analysis

The combination of event choice and barrier dimension scenarios (Table 5.1) necessitated 30 model runs. The model domain was classified into zones to assess differences between areas within the channel and on the floodplain. The channel was also separated into 50 m long sections starting at the barrier location going upstream for one 50 m section and downstream to the end of the model domain (Figure 5.7).

Table 5.1: Factors tested within scenarios.

Return period (years)					
2	5	10	30	100	1000
Barrier dimensions					
No barrier	Barrier 0.3 m culvert *(H) 1.3 m* *(W) 11.1 m* *(CulvH) 0.3 m* *(CulvW) 3.5 m*	Barrier 0.05 m culvert *(H) 1.3 m* *(W) 11.1 m* *(CulvH) 0.05 m* *(CulvW) 3.5 m*	Barrier no culvert *(H) 1.3 m* *(W) 11.1 m*	Extended barrier 0.3 m culvert *(H) 1.8 m* *(W) 23.4 m* *(CulvH) 0.3 m* *(CulvW) 3.5 m*	

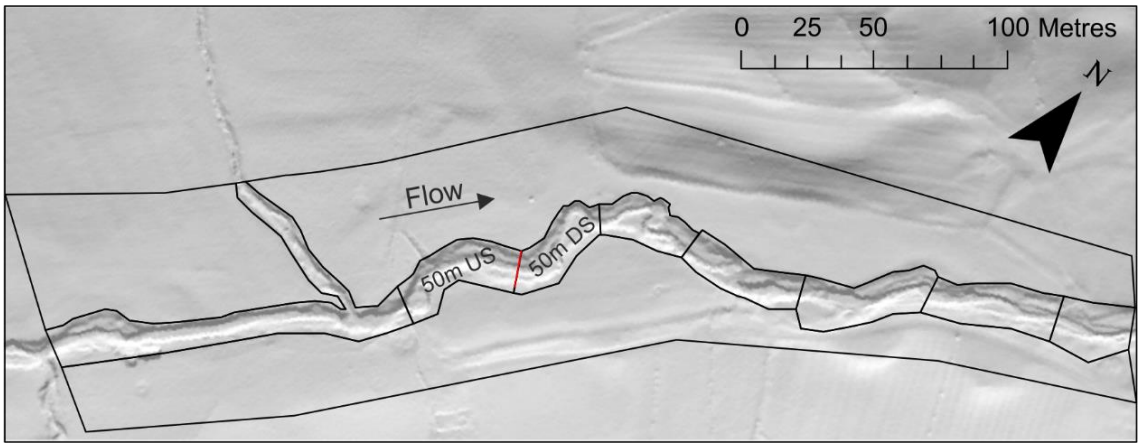

Figure 5.7: Zonal separation of the modelled reach for the purpose of testing longitudinal and lateral differences.

5.2.3.1 Hydrological assessment

Water discharge through time was extracted from HEC-RAS 2D at multiple points within the model. Reduction in peak discharge was calculated at 10 m, 100 m and 200 m downstream of the barrier. Discharge was also taken at the barrier, separated into culvert and weir flow depending on the barrier design. Total inundation extent was calculated based on the maximum water depth, which included both within channel and floodplain water. To evaluate the additional temporary water storage of each scenario, maximum water volume was calculated for the within channel area up to 50 m upstream of the barrier location. Water volume was also calculated for both the left- and right-hand floodplain, the floodplain was not separated longitudinally downstream.

5.2.3.2 Geomorphological assessment

The maximum value for depth and for velocity experienced by each 0.5 m topographic cell was exported as a grid for each scenario. Both the maximum depth and velocity grids were taken and shear stress was calculated using Equation 5.1 (Lane and Ferguson, 2005) and spatially distributed values of Manning's n of 0.032 for the grass and 0.05 for the bed of the channel.

$$\tau = \frac{\rho g n^2 U^2}{d^{\frac{1}{3}}} \qquad \text{Equation 5.1}$$

where, ρ = density; g = gravity; n = Manning's roughness; U = depth-averaged velocity; and d = depth.

To classify shear stress into “erodibility”, a value for critical shear stress was estimated based on an assumed grain size of the present bed-material and a value of the Shield’s parameter using Equation 5.2. The value for D_{50} was taken to be the same as the value implemented as part of the model comparison in Chapter 4 of this thesis. The Shield’s parameter value was chosen to be the more recent common value from the literature of 0.045 (Yalin and Karahan, 1979). Resulting in a critical shear stress of 22.3 Nm^{-2}, over which it was assumed erosion may occur, under which, deposition.

$$\tau_{ci}=\tau^{*}_{c_{50}}\rho_s g D_{50} \qquad \text{Equation 5.2}$$

where $\tau^{*}_{c_{50}}$ = Shields parameter; ρ_s = rock density; g = gravity; D_{50} = median grain size.

The rasterised shear stress was converted into a point shapefile, with each point being classified into the zones seen in Figure 5.7. Both count data for the erodibility classification and median shear stress were calculated for each zone. A second zonal classification was made to evaluate the effect of the culvert on shear stress, where all points within a 0.5 m buffer of the polyline associated with the culvert were taken and median shear stress was calculated. Median shear stress was used following a sub-sample of datasets being tested for normality, where Anderson-Darling normality tests were undertaken and $P < 0.05$. Therefore the data was non-parametric and median values were more suitable descriptive statistics.

5.2.4 The effect of seasonality- Annualisation

The seasonality of flooding is important for river basin management, infrastructure operation and forecasting (Cunderlik et al., 2004). With the intensity of summer storm events potentially increasing with climate change (Kendon et al., 2014), the possible differences flood seasonality may have on the different barrier designs was estimated. The barrier design scenarios and analysis detailed above were repeated for equivalent “summer” return period events using the seasonality difference in the ReFH model (Figure 5.8). Seasonality within the ReFH model was taken into account in the rainfall estimates using the approach of Kjeldsen et al. (2006), with the seasonal correction factors of 0.83 and 0.94 for winter and summer respectively. The seasonal design rainfall estimates were calculated by multiplying the rainfall estimates from the Flood Estimation

Handbook Depth-Duration-Frequency (FEH DDF) model by the corrective factor (Faulkner, 1999).

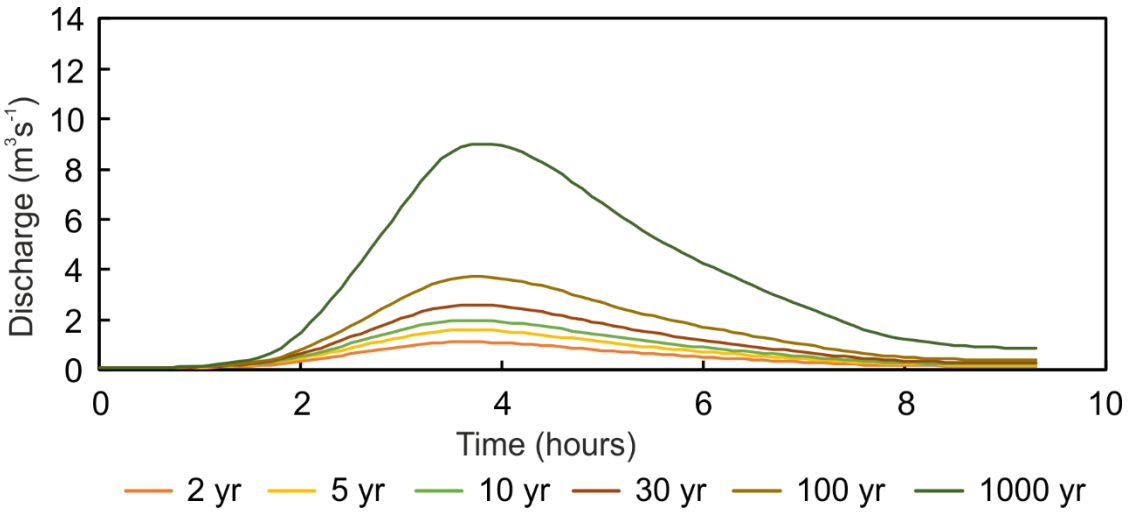

Figure 5.8: Upstream discharge inputs for summer events.

The effects of barrier design and seasonality were summarised quantitatively by accounting for differences occurring per event probability (or return period) using annualisation. The methodology was modified from one often used to calculate flood damages (Olsen et al., 2015). Metrics chosen to be annualised for the winter and summer events included peak magnitude reduction, water volume held upstream of the barrier, inundation extent, floodplain water volume, area of estimated deposition and area of estimated erosion. The annual average was calculated for these metrics using Equation 5.3. The probability of event occurrence was taken into account through the extreme events having a lower weighting than those of the more frequent events. Contribution per each return period event was calculated, before all event contributions were summed to be the annual average value.

$$\frac{1}{2}\sum_{i=1}^{n}\left(\frac{1}{RP_i}-\frac{1}{RP_{i+1}}\right)(V_i+V_{i+1}) \qquad \text{Equation 5.3}$$

where RP = return period and V = metric value.

5.3 Results

5.3.1 Hydrological response to the addition of a barrier

5.3.1.1 Peak flow reduction

The addition of a leaky barrier showed no peak discharge reduction at the model's downstream boundary (Figure 5.9). The largest differences in discharge at the downstream boundary were observed at the beginning of the simulation. Water discharge was first identified at the downstream boundary in the same time-step for all except the no culvert barrier scenario. The no culvert barrier caused a short sharp increase in discharge ~15 minutes later, after which, discharge was the same as the no barrier scenario (Figure 5.9b). The downstream discharge occurring as a result of implementing the 0.05 m high culvert barrier was initially similar to the no barrier simulation. After ~ 15 minutes, the 0.5 m high culvert barrier saw a slower rise in discharge compared to the no barrier scenario. Once discharge reached approximately 0.27 m^3s^{-1}, a rapid increase up to the same discharge as the no barrier scenario was observed (Figure 5.9b).

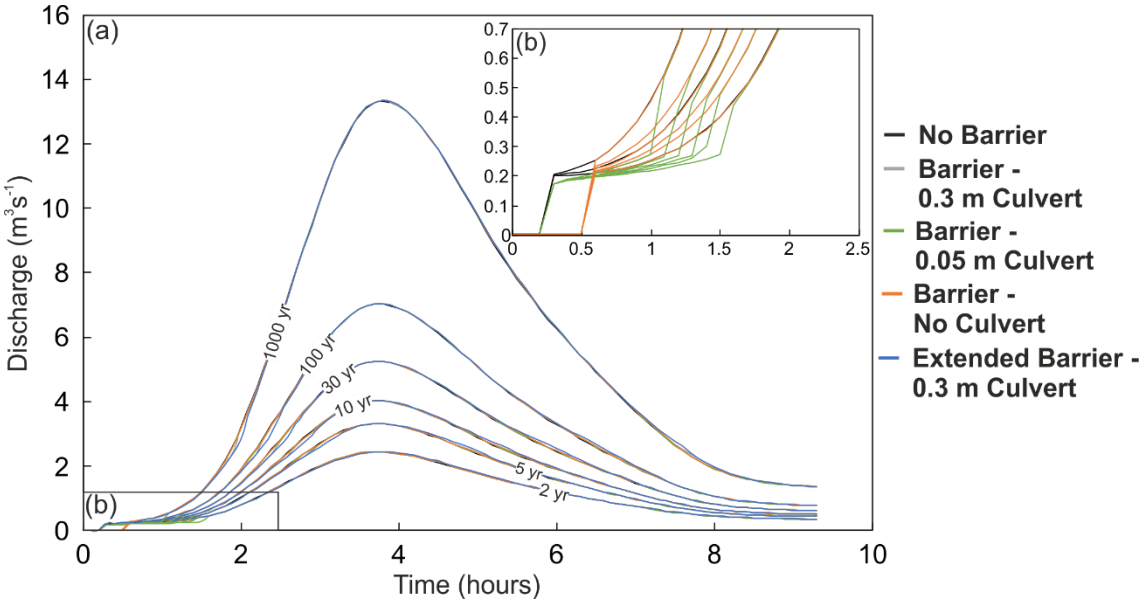

Figure 5.9: Discharge at the downstream boundary condition for barrier scenarios for (a) the entire flood event and (b) with a focus on the start of the simulation.

Increasing the size of the culvert decreased the reduction in peak discharge for all return period events (Figure 5.10a). This effect reduced with distance downstream (Figure 5.10b and c). For a number of events, there was no peak reduction observed when the culvert was 0.3 m high even immediately downstream of the structure (Figure 5.10a). The largest peak reductions were

observed for the 1000 year event, 10 m downstream with a reduction of -43.7 %, -42.5 %, and -31.5 % for the no culvert, 0.05 m high culvert and 0.3 m high culvert barrier designs respectively, dropping to -3.48 %, -3.41 % and -2.83 % at a point 200 m downstream (Figure 5.10c). It should also be highlighted that there was little difference in peak reductions for the no culvert and 0.05 m high culvert barriers.

There was no impact of extending the barrier for the 2 year RP event (Figure 5.10a). For all other events, extending the barrier resulted in largest reductions of peak magnitude of any barrier design. The largest reduction in peak magnitude resulted from the 1000 year event (-74 %), 10 m downstream (Figure 5.10a). Further downstream, the reduction in peak magnitude for the extended barrier tailed off, particularly for the largest of events. Where an 18.5 % additional reduction was seen from the 100 to 1000 year events 10 m downstream, this reduced to 3 % 100 m downstream (Figure 5.10b) and at 200 m downstream a decrease in the reduction was observed of 1.43 % compared to the original barrier with a 0.3 m high culvert (Figure 5.10c).

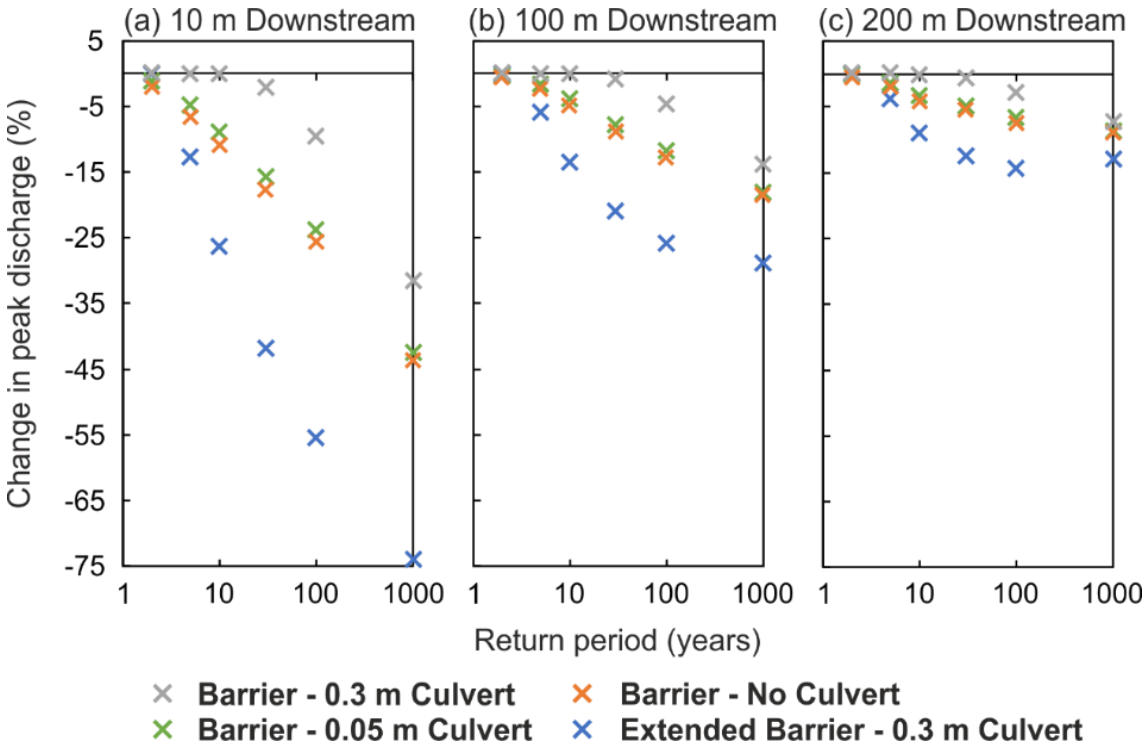

Figure 5.10: Percentage change in peak discharge from the no barrier scenario, (a) 10 m downstream, (b) 100 m downstream and (c) 200 m downstream.

5.3.1.2 Flow over the barrier

Overtopping (utilisation of the weir) decreased with increasing culvert height (Figure 5.11a). Overtopping occurred 96 % of the time for the no culvert barrier for all events, decreasing to between 84 % and 89 % for the 0.05 m high culvert barrier. The 0.3 m high culvert barrier was also overtopped for all events but for shorter amounts of time, with overtopping occurring for between 4 % and 62 % of the time and extending the barrier resulted in overtopping only occurring for the 1000 year event for 20 % of the simulation time (Figure 5.11a).

The mean discharge over the weir, or top of the barrier, decreased with increasing culvert height but increased with increasing return period for all culvert heights (Figure 5.11b). The no culvert barrier resulted in a mean discharge from 1.03 m^3s^{-1} to 3.5 m^3s^{-1} with increasing return period. Mean discharge was between 0.15 m^3s^{-1} and 0.24 m^3s^{-1} lower for the 0.05 m high culvert barrier compared to the no culvert barrier and up to 1.1 m^3s^{-1} lower for the 0.3 m high culvert barrier compared to the 0.05 m high culvert barrier. Due to the lack of weir utilisation, the extended barrier resulted in no mean discharge for all but the 1000 year event (0.013 m^3s^{-1}) (Figure 5.11b).

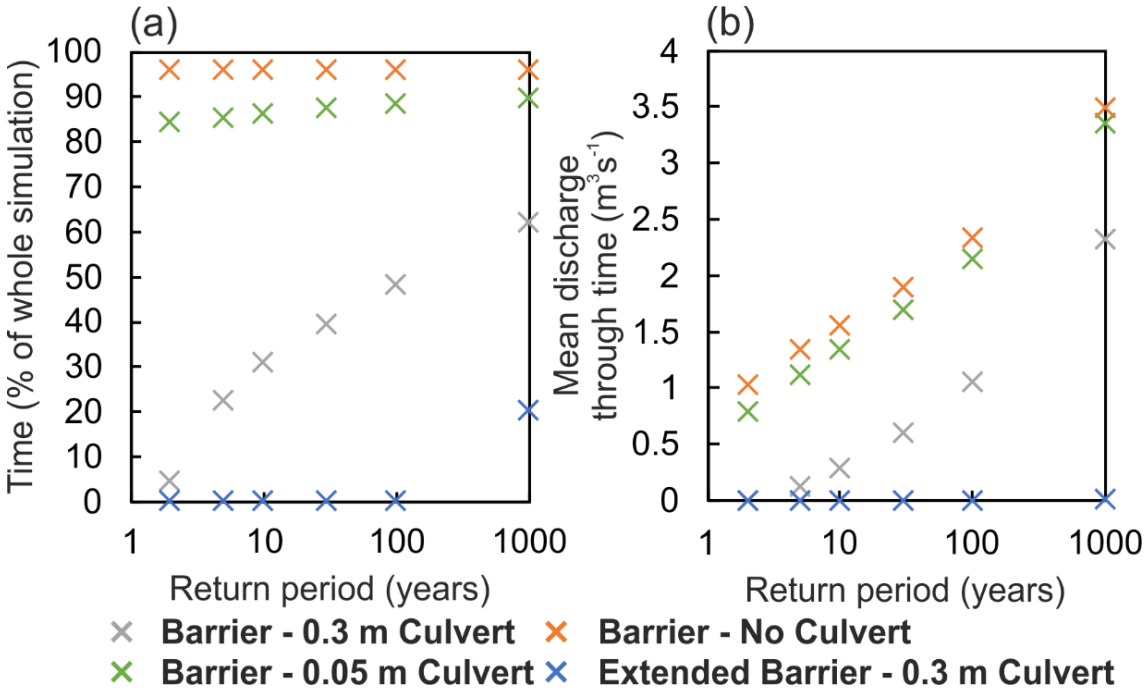

Figure 5.11: Weir utilisation for all events, (a) percentage of the simulation time that overtopping/utilisation of the weir occurred for, (b) mean weir discharge through time.

5.3.1.3 Flow beneath the barrier

For the leaky barrier designs which allowed flow underneath the barrier via the culvert, discharge was dependent on both design and return period. Mean discharge through the culvert remained similar for all return period events (~0.23 m^3s^{-1} and ~0.25 m^3s^{-1}) for the 0.05 m high culvert barrier (Figure 5.12a), highlighted by Figure 5.12b showing an almost constant discharge throughout the simulation for both the 2 and 1000 year events. Mean discharge for the 0.3 m high culvert barrier and the extended barrier increased with increasing return period, with the extended barrier increasing at a higher rate than the 0.3 m high culvert barrier up to maximum mean discharges of 2.3 m^3s^{-1} and 1.9 m^3s^{-1} respectively (Figure 5.12a). Through time, for the 2 year RP event, the 0.3 m high culvert barrier and extended barrier exhibited the same discharge (Figure 5.12b). For the 1000 year event, culvert discharge for the extended barrier was higher than for the 0.3 m high culvert barrier, for both of which discharge levelled off at around 3 m^3s^{-1} and 2.5 m^3s^{-1} respectively for approximately 5 hours (Figure 5.12b).

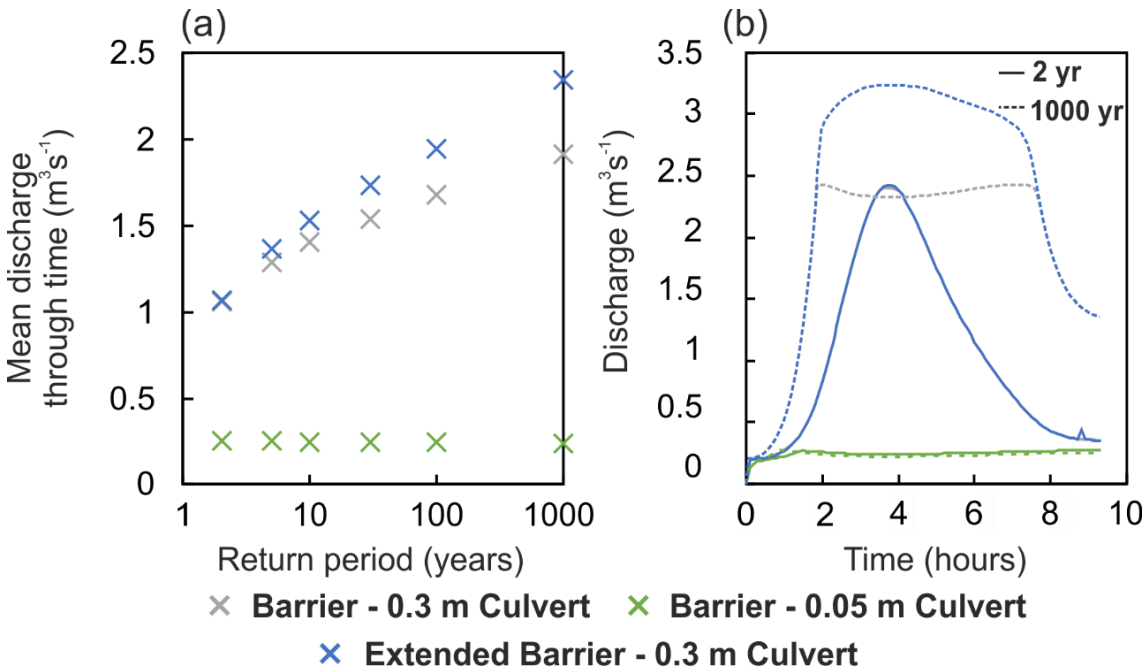

Figure 5.12: Culvert discharge (a) mean culvert discharge, (b) discharge through time.

5.3.1.4 Water volume and depth upstream of barrier

When implementing a leaky barrier, between 147 m^3 and 275 m^3 of additional water storage was achieved in the 50 m upstream of the barrier with storage increasing with return period (Figure 5.13a). The difference in storage occurring from culvert height decreased with return period, with small decreases in upstream volume between the no culvert and 0.05 m culvert designs of up to 7.36 m^3. Larger differences in volume of between 13 m^3 and 96 m^3 were observed between the 0.05 m and 0.3 m high culvert designs (Figure 5.13a). For the 2 year event, there was little difference between the original and extended barrier (4.55 m^3). The largest difference of 89.6 m^3 was observed between the two barriers for the 5 year event. The difference then decreased with increasing return period, however the extended barrier still held over 58 m^3 of additional water upstream compared to the original barrier (Figure 5.13a).

At a point 10 m upstream of the barrier, mean water depth over time increased with return period (Figure 5.13b). Increasing the culvert height decreased the mean depth, with the difference decreasing with return period and the difference being larger between the 0.05 m and 0.3 m high culverts compared to the no culvert and 0.05 m high culvert designs. Mean depth upstream remained the highest for the no culvert design for all return periods (1.22 m - 1.39 m), this decreased for the 0.05 m high culvert to between 1.12 m and 1.32 m. A larger difference due to return period was observed for the 0.3 m high culvert of between 0.45 m and 1.02 m (Figure 5.13b). The extended barrier resulted in increased mean depth compared to the original barrier of between 0.08 m and 0.17 m (Figure 5.13b).

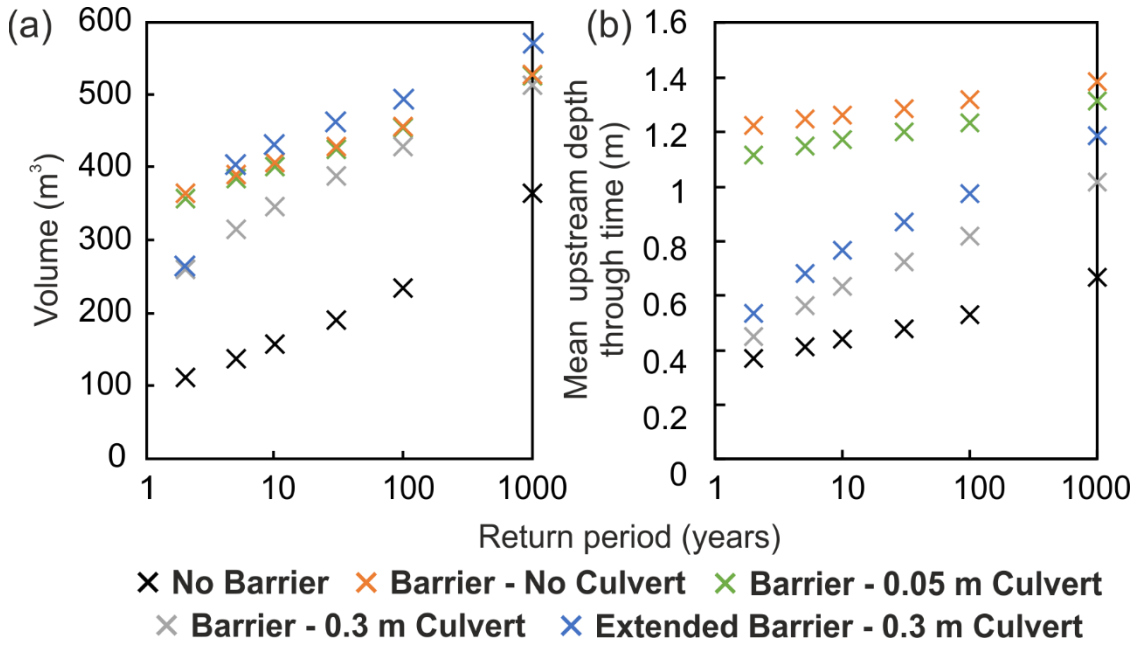

Figure 5.13: (a) Maximum volume of water held within the 50 m upstream of the barrier location and (b) Mean upstream depth through time at a point 10 m upstream of the barrier location.

5.3.1.5 Inundation extent and floodplain utilisation

Inundation extent increased with increasing return period (Figure 5.14a). When no barrier was implemented, inundation extent increased gradually before over doubling in size for the 1000 year event (Figure 5.14a). There was only a minor difference in inundation extent between the no culvert and 0.05 m high culvert barriers. Both increased innundation extent by between 19 % and 33 % for each event, before increasing in size again between the 100 year and 1000 year events, up to inundation extents of 12,886 m^2 and 12,908 m^2 for the 0.05 m high culvert and no culvert designs respectively (Figure 5.14a). Increasing the culvert height from 0.05 m to 0.3 m caused smaller inundation extents, this difference increased up to the 30 year event before decreasing up to the 1000 year event, where there was little difference in inundation extent for any barrier (Figure 5.14a). For the 2 year event, there was little difference between the original and extended barriers. Up to the 10 year event, the difference between the original and extended barrier increased by up to 89 %. For events larger than this, the difference between the two barriers decreased up to a difference of only 7 % for the 1000 year event (Figure 5.14a).

Spatially, differences in inundation extent between designs for the 100 year event occurred due to differences on the floodplain, with inundation being greater to the left than to right of the channel (Figure 5.14c). The floodplain was only utilised for

the 1000 year event when no barrier was implemented (Figure 5.14b). Only the 0.05 m high culvert and no culvert barriers resulted in floodplain use for the 2 year event. Both of these designs resulted in an increase in the floodplain water volume with increasing return period, with up to 735 m^3 of water storage for the 1000 year event. The 0.3 m high culvert barrier caused little floodplain water storage for events up to the 100 year event, with a large increase in floodplain use between the 100 and 1000 year event of 518 m^3. The extended barrier did not cause floodplain use for the 2 year event, but resulted in the greatest floodplain use compared to the other barrier designs for all other return period events, with 967 m^3 of floodplain water volume for the 1000 year event (Figure 5.14b).

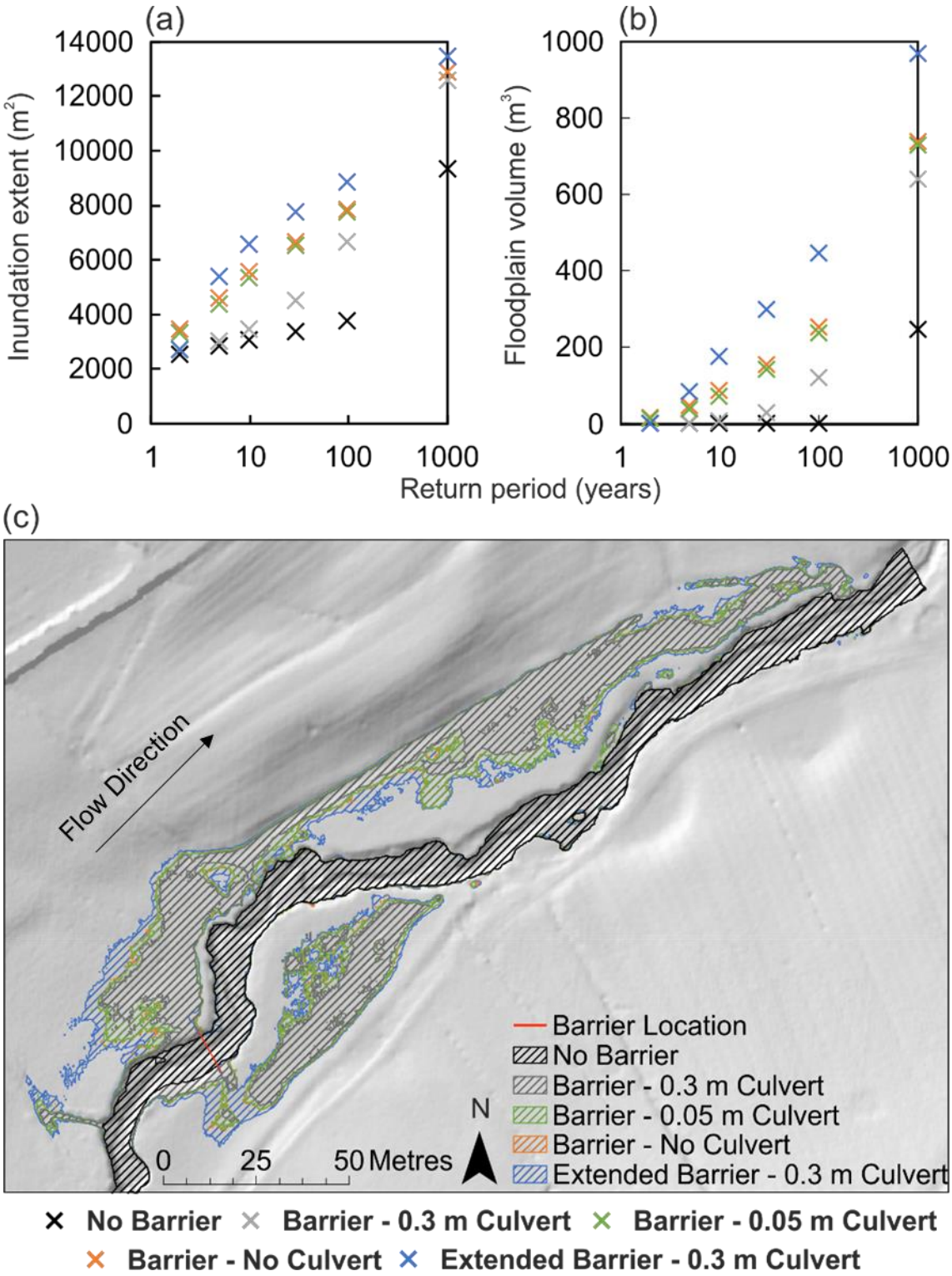

Figure 5.14: Spatially distributed hydrological results (a) inundation extent for all barriers and events, (b) floodplain volume for all barriers and events, (c) individual extents for each barrier scenario for the 100 year RP event.

5.3.2 Geomorphological response to the addition of a barrier

5.3.2.1 Erodibility

For the 50 m extending upstream of the barrier location, the area of estimated erosion increased with return period when there was no barrier added into the model (Figure 5.15a). The barrier with a 0.05 m high culvert and the no culvert barrier behaved similarly, with little erosion being estimated for the less extreme events (up to ~25 m^2), but for the 100 year and 1000 year events, larger increases were observed of up to ~90 m^2 and ~210 m^2 respectively. The 0.3 m high culvert barrier resulted in a larger area of estimated erosion upstream compared to the other two culvert options, the difference decreasing with increasing return period (Figure 5.15a). The original barrier with a 0.3 m high culvert and the extended barrier behaved similarly, with a small decrease in the area of estimated erosion, before this increased for the larger storms (Figure 5.15a).

Without a barrier, the area estimated as deposition upstream of the barrier remained similar with increasing return period (~125 m^2) (Figure 5.15b). The no culvert barrier and the 0.05 m high culvert barrier both showed a small increase in depositional area of up to 26 m^2 up to the 30 year event. A decrease in depositional cells was observed after this point of up to ~120 m^2. The 0.3 m high culvert barrier exhibited smaller areas of deposition upstream of the barrier compared to the other culvert designs. An increase of 108 m^2 was seen up to 100 year event before a decrease of 75.5 m^2 between the 100 year and 1000 year events. The extended barrier resulted in larger areas of deposition compared to the original barrier for all return periods, the largest difference between the two of 124 m^2 was seen for the 2 year event. The extended barrier saw a small decrease between the 2 and 5 year events, the only design that this decrease occured for. After this, the area of estimated deposition increased up to the 30 year event, before decreasing again (Figure 5.15b).

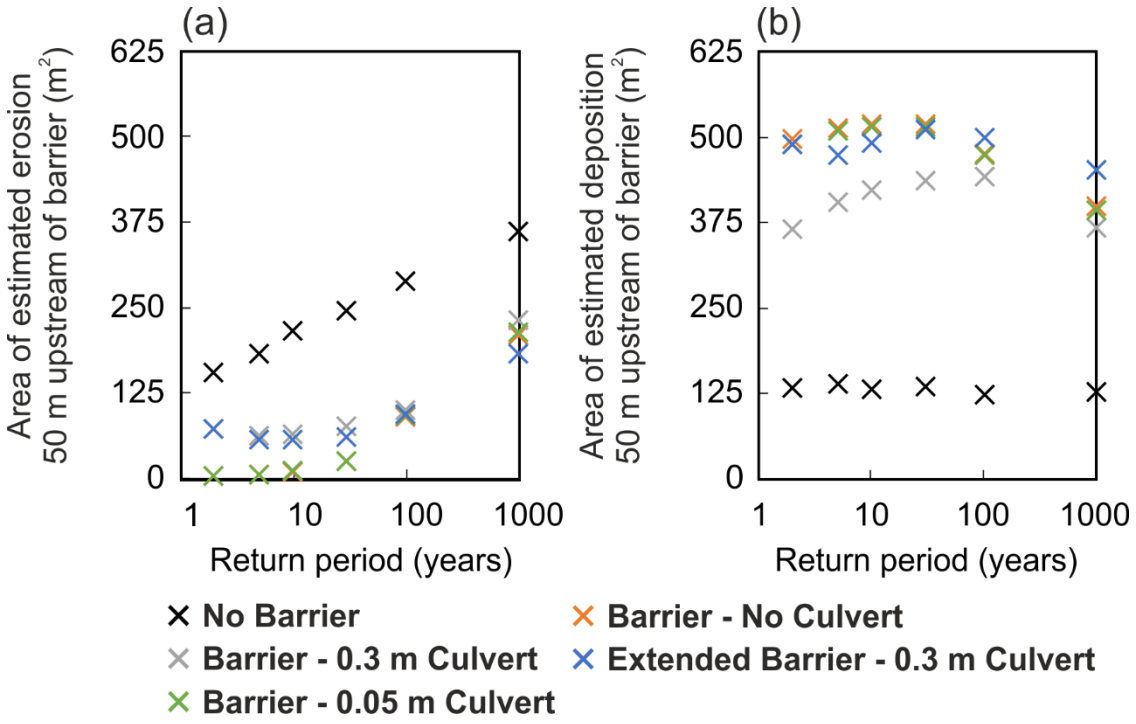

Figure 5.15: Erodibility around the barrier with the area estimated to be (a) erosional and (b) depositional up to 50m upstream of the barrier.

In the area up to 50 m downstream of the barrier, there were only small differences in the areas of estimated erosion for the barriers with different culvert heights compared to the baseline no barrier scenario, with the area of estimated erosion increasing with return period up to ~276 m^2 (Figure 5.16a). The extended barrier saw an increase in erosion with increasing return period, however these increases were much smaller than for the other scenarios up to a maximum of 160 m^2 (Figure 5.16a).

A decrease in the area of estimated deposition was seen for all scenarios when increasing the return period for all but the extended barrier scenario (Figure 5.16b). The no barrier scenario resulted in the smallest areas of estimated deposition. There were small differences between the 0.3 m high, 0.05 m high and no culvert scenarios, the 0.3 m high culvert barrier resulted in marginally lower levels of deposition (up to 9.75 m^2) compared to the other two culvert designs. The extended barrier behaved differently, an increase in deposition of 10.25 m^2 was seen between the 2 and 5 year events. A small decrease (4.25 m^2) was seen to the 10 year event, at which point there was little change before a small increase (3.5 m^2) was seen between the 100 and 1000 year events (Figure 5.16b).

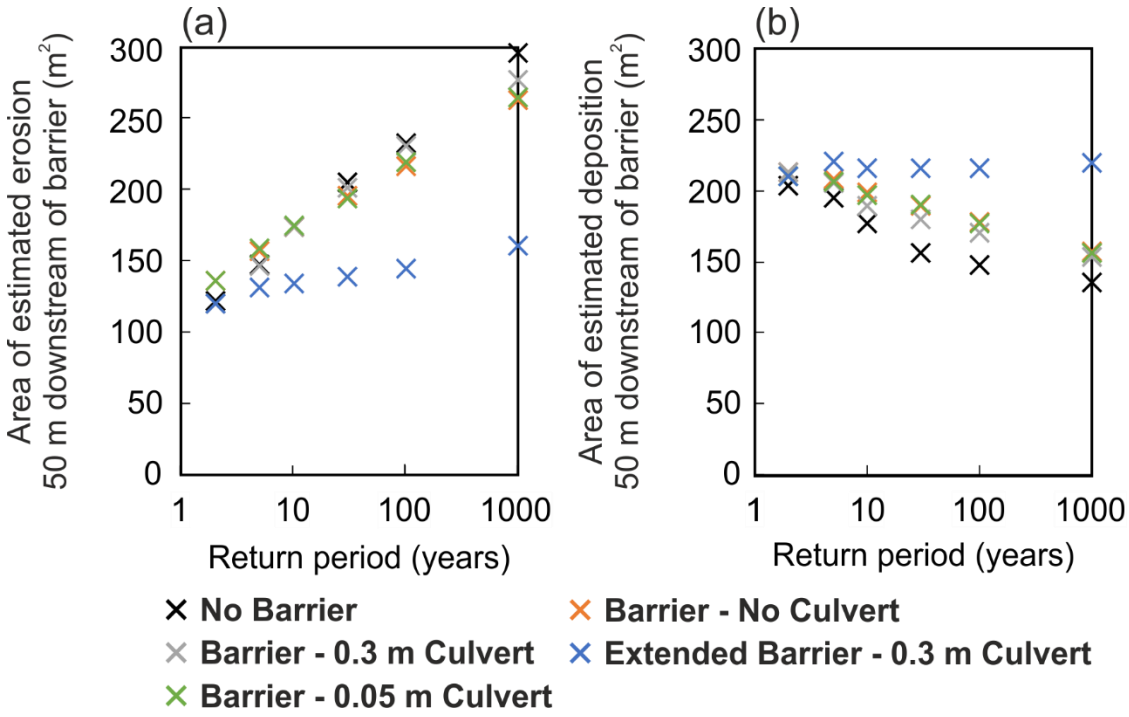

Figure 5.16: Erodibility around the barrier with the area estimated to be (a) erosional and (b) depositional up to 50m downstream of the barrier.

5.3.2.2 Shear Stress

Large differences in median shear stress were observed within a 0.5 m buffer of the culvert location between the leaky barrier designs (Figure 5.17). The 0.05 m high culvert barrier resulted in the lowest median shear stresses, which increased with return period from 9.4 to 13.9 Nm^{-2}, whereas the 0.3 m high culvert barrier resulted in a median shear stress of around 28.8 Nm^{-2} that varied very little with return period. There was little difference between the original barrier and extended barrier for the 2 year event, however larger events, the extended barrier resulted in much higher median shear stress of around 41 Nm^{-2} (Figure 5.17).

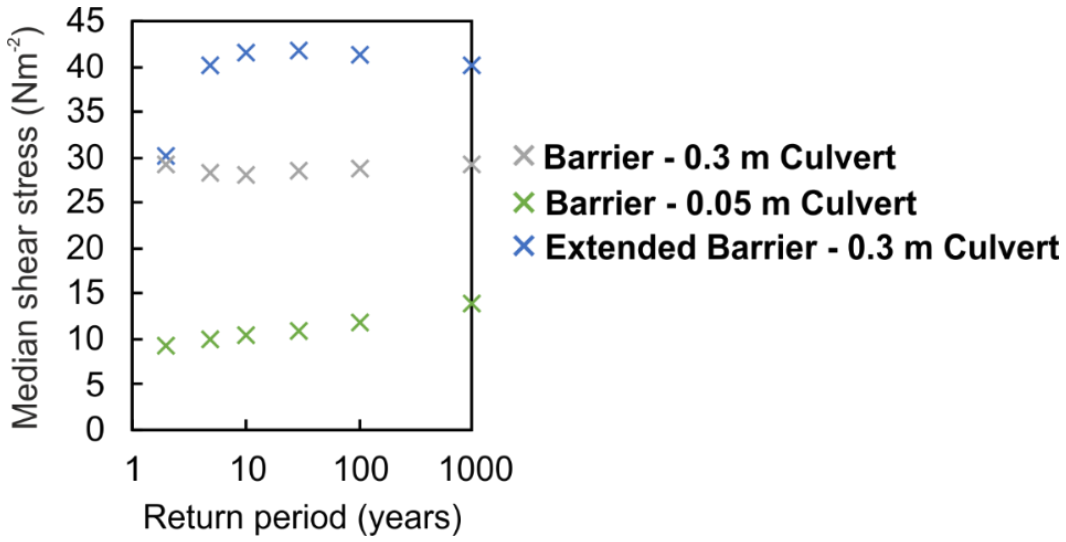

Figure 5.17: Median shear stress for the 0.5 m buffer of the culvert location.

Looking at the spatial distribution of shear stress, for the 2 year event, the addition of a barrier with no culvert and with a 0.05 m high culvert resulted in a large area of low shear stress upstream of the barrier (Figure 5.18ai and bi). Two small areas of erosional shear stress occurred immediately downstream of the barrier on the left and right of the channel, with shear stress decreasing in the centre of the channel (Figure 5.18ai and bi). At the culvert location, the 0.05 m high culvert barrier did result in an additional small area of erosional shear stress (Figure 5.18bi). A larger difference was observed when increasing the culvert height to 0.3 m (Figure 5.18ci). Shear stress was higher for a wider area in the centre of the channel upstream of the barrier and the culvert, a larger area of higher shear stress was apparent that appeared to extend slightly upstream and downstream from the structure. When extending the barrier, there was very little difference with the original barrier for the 2 year event (Figure 5.18di).

For the 100 year event, increasing the culvert height and extending the barrier increased the shear stress around the culvert itself (Figure 5.18ii). Compared to the 2 year event, shear stress on the left hand side of the channel was higher for the 100 year event, for all barrier designs. The no culvert, 0.05 m high culvert and extended barrier designs also resulted in an area of erosional shear stress on the floodplain (Figure 5.18aii, bii, dii). For the 0.3 m high culvert barrier, a new area of erosion on the right hand side of the channel immediately downstream of the barrier was apparent (Figure 5.18cii). Overall, all three culvert height designs tested resulted in more extensive erosional shear stress downstream of the feature, however there was little change downstream for the extended barrier design (Figure 5.18dii).

For the 1000 year event, little difference could be seen between the no culvert and 0.05 m high culvert barriers (Figure 5.18aiii and biii). For both, more intense and wide spread erosional shear stress was observed on the left and right hand floodplain and shear stress was higher within the channel upstream of the barrier, with a particular increase in the centre compared to the 100 year event. The changes occurring were similar for the 0.3 m high culvert barrier, with erosional shear stresses observed on the floodplain for the first time and an overall increase in shear stress in the channel too (Figure 5.18ciii). The extended barrier resulted in the largest areas of erosional shear stress of any of the barrier designs on the left floodplain (Figure 5.18diii). Very low shear stress remained immediately

upstream of the barrier, extending more laterally compared to the 100 year event and the other barriers (Figure 5.18diii).

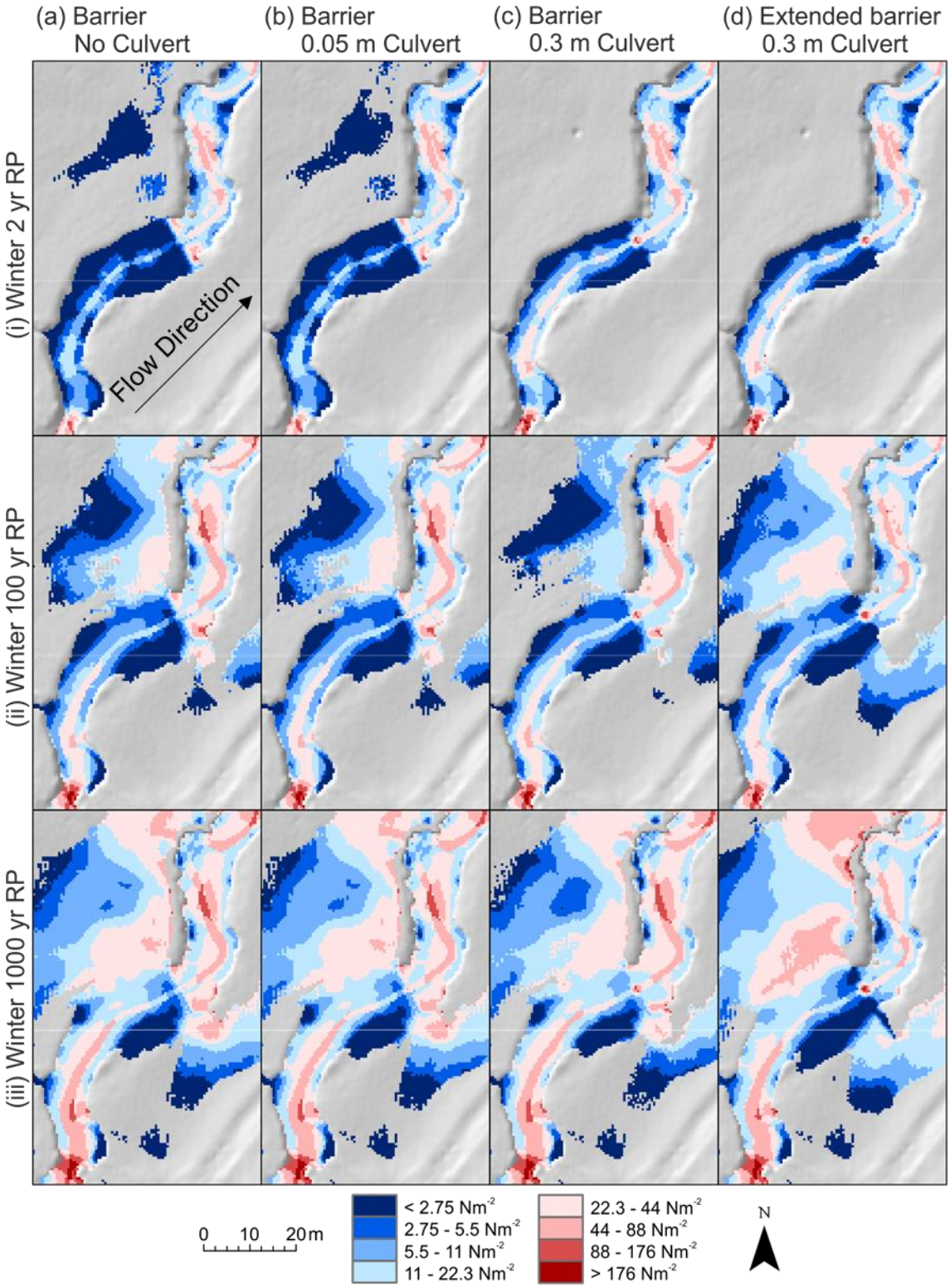

Figure 5.18: Shear stress distribution within the channel and immediate floodplain for (a) the no culvert barrier, (b) the 0.05 m high culvert barrier, (c) the 0.3 m high culvert barrier and (d) the extended barrier for (i) the 2 year RP event, (ii) the 100 year RP event and (iii) the 1000 year RP event.

The median shear stress on the floodplain for any given event and any given barrier design did not exceed 13 Nm^{-2} and was therefore depositional (Figure 5.19), however median shear stress did increase with return period for all scenarios. Increasing the culvert height decreased the floodplain median shear stress, with differences of up to 4.5 Nm^{-2} between the 0.3 m and 0.05 m high culvert barriers. The extended barrier exhibited higher median shear stress for any given event compared to the original barrier, with differences of up to 3.4 Nm^{-2} (Figure 5.19).

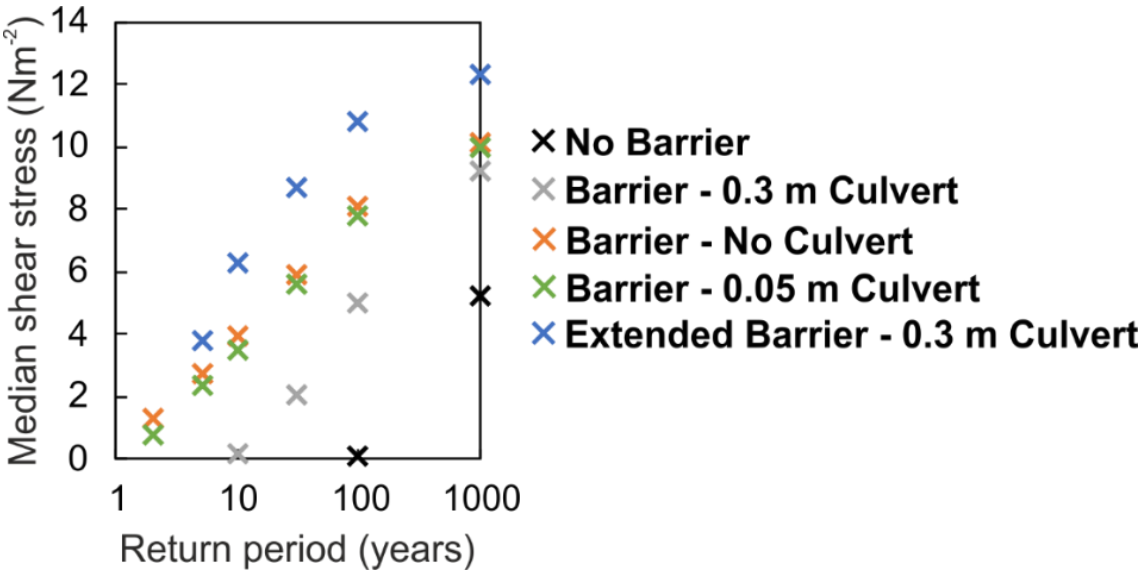

Figure 5.19: Median shear stress for the floodplain. Median shear stress was calculated for those events where floodplain inundation occurred.

There were few discernible differences spatially in floodplain shear stress for the no culvert and 0.05 m high culvert barriers (Figure 5.20a and b). Both exhibited a secondary pathway on the left floodplain, which for its majority, was depositional. A small area of erosional shear stress was apparent near the downstream boundary of the reach, spanning between the floodplain and channel. Compared to the 0.05 m high culvert barrier, the 0.3 m high culvert barrier resulted in a narrower secondary pathway of lower shear stress and a depositional connection between the floodplain and channel near the downstream boundary (Figure 5.20c). The extended barrier resulted in higher shear stresses being maintained further down the secondary pathway. Near the downstream boundary, two connections between the channel and floodplain were observed, the first, a small erosional pathway and the second was a larger depositional pathway (Figure 5.20d).

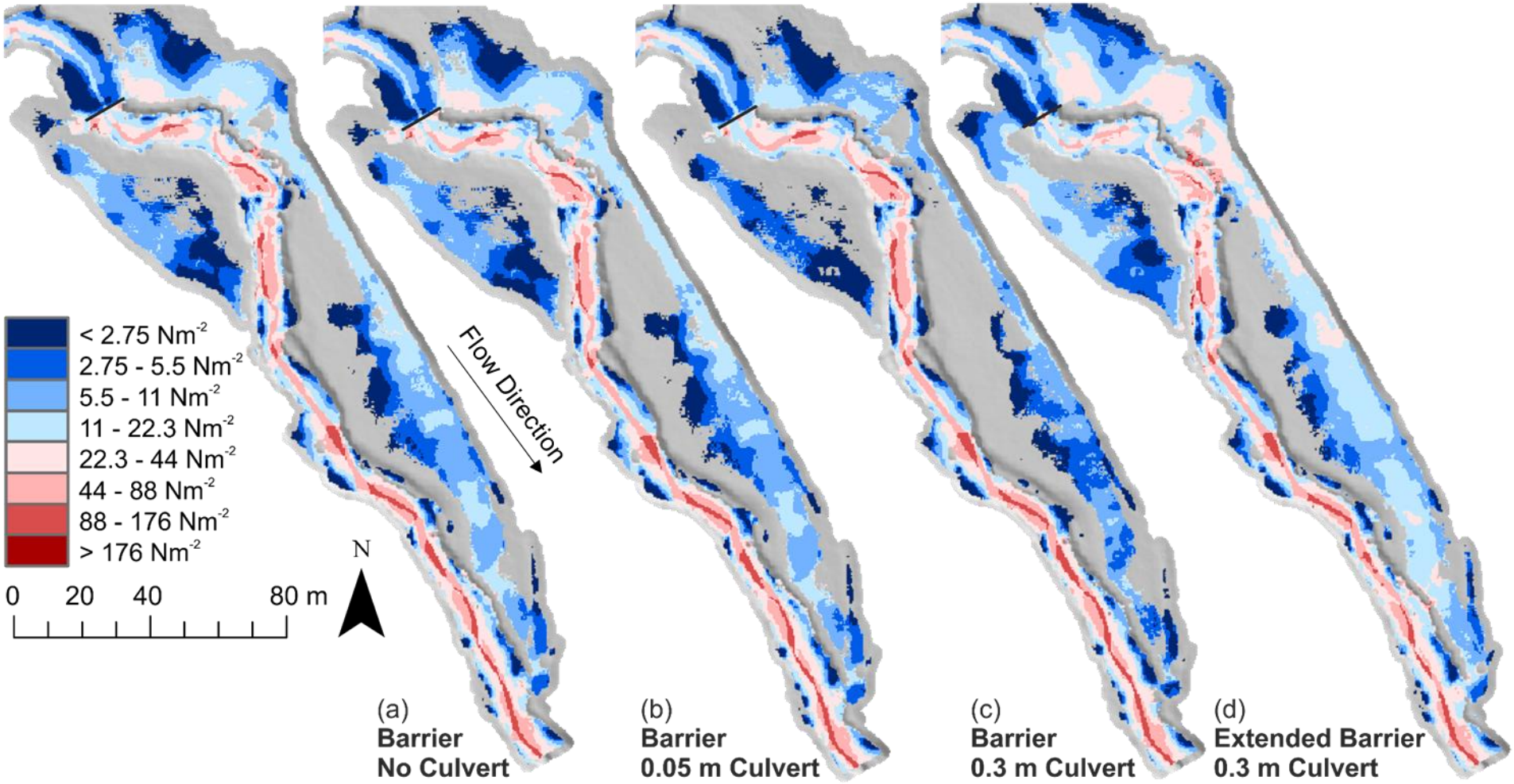

Figure 5.20: Shear stress distribution on the floodplain resulting from the 100 year RP event for (a) the no culvert barrier, (b) the 0.05 m high culvert barrier, (c) the 0.3 m high culvert barrier and (d) the extended barrier.

5.3.3 Annualisation – the effect of seasonality

The annualised value for peak reduction 10 m downstream of the barrier location was an order of magnitude lower for all barriers for the summer events compared to the winter events (Table 5.2). The largest difference between the two seasons was seen for the extended barrier (7.3 %). The seasonal difference in annualised water volume held upstream was dependent on barrier design, with the 0.3 m high culvert barrier and the extended barrier resulting in much greater differences (> 130 m^3) compared to the no culvert and 0.05 m high culvert barriers, however these did also see a reduction in volume held upstream (< 50 m^3). Inundation extent was lower for summer events compared to winter events for all barrier designs, with the difference being smallest for the 0.3 m high culvert design (700 m^2) and greatest for the extended culvert (1573 m^2). Utilisation of the floodplain was also lower for the summer events than the winter events, with again, the smallest difference being for the 0.3 m high culvert barrier (5.63 m^3) and the largest for the extended barrier (51.5 m^3).

The annualised area estimated to be depositional was also lower for the summer events compared to the winter events (Table 5.2). The difference between barriers showed that the extended barrier resulted in the largest decrease with 199 m^2 less deposition in summer, followed by the 0.3 m high culvert barrier with 128 m^2. The 0.05 m high culvert and no culvert barriers resulted in the smaller decreases of 17 m^2 and 25 m^2 respectively in summer compared to winter.

With regards to the estimated area of erosion, overall, the areas of erosion were smaller than areas of deposition and with this, smaller differences between the seasons were observed (Table 5.2). The first increases were observed when comparing winter to summer events, with the 0.3 m high culvert barrier and the extended barrier both showing increases in the areas of erosion for with summer events (< 10 m^2). The 0.05 m high culvert and no culvert barriers resulted in decreases in the area of erosion of 5.75 m^2 and 5.5 m^2 respectively (Table 5.2).

Table 5.2: Annual averaged metrics for the barrier designs

	Season	Barrier No Culvert	Barrier 0.05 m Culvert	Barrier 0.3 m Culvert	Extended Barrier 0.3 m Culvert
Peak reduction 10 m downstream of barrier (%)	Winter	4.47	3.46	0.401	7.94
	Summer	0.38	0.54	0.05	0.67
Water volume held in the area up to 50 m upstream of barrier (m^3)	Winter	286.1	281.6	222.4	254.0
	Summer	238.8	246.2	87.6	90.8
Inundation extent (m^2)	Winter	3,277	3,150	2,353	3,277
	Summer	1,890	1,968	1,644	1,704
Water volume held on the floodplains (m^3)	Winter	37.3	31.9	7.00	57.0
	Summer	4.23	5.69	1.37	5.49
Area estimated to be depositional up to 50 m upstream of the barrier location (m^2)	Winter	377	373	290	364
	Summer	352	356	162	165
Area estimated to be erosional up to 50 m upstream of the barrier location (m^2)	Winter	7	7	53	50
	Summer	1.5	1.25	60	60

5.4 Discussion

5.4.1 The effect of barrier design

5.4.1.1 Culvert height

Culvert height was increased based on real examples to assess the impact of the size of the gap between the channel bed and leaky barrier. As culvert height was increased from 0.05 m to 0.3 m, the reduction in peak discharge decreased by up to 14 % (10 m downstream of the barrier, Figure 5.10), overtopping of the barrier decreased by between 28 % and 80 % (difference decreasing with increasing return period, Figure 5.11), and water volume held on the floodplain and upstream of the barrier decreased by up to 118 m^3 and 96 m^3 and respectively (Figure 5.14; Figure 5.13). These results were all to be expected as the larger the culvert, the more discharge it would convey. As culvert height

increased, the ratio of the cross section unavailable for the movement of water decreased, allowing a higher proportion of water to flow freely before being impeded by the barrier, decreasing the size of the backwater effect. Kail (2003) also identified a strong correlation between pool volume and blockage ratio whilst monitoring six streams with naturally occurring wood accumulations in. Hydrological benefits identified by decreasing the gap underneath the barrier suggests the commonly used 0.3 m gap used in UK leaky barrier guidance (e.g. YDRT, 2018a) may be resulting in reduced hydrological effectiveness. Whether it is feasible to decrease the gap beneath the leaky barrier will however, depend on whether this will inhibit fish passage, an uncertainty known in the current use of wood in river restoration (Grabowski et al., 2019).

Including a gap beneath the leaky barrier also produced geomorphological differences despite large depositional areas being observed upstream. Increasing the size of the culvert, or gap beneath the leaky barrier from 0.05 m to 0.3 m resulted in an increase of up to 68 m^2 in the area estimated to be erosional with a subsequent decrease of up to 124 m^2 in the area estimated to be depositional upstream (Figure 5.15). As less flow was impeded with increasing culvert height, velocity would be higher and depth lower resulting in an increase in shear stress and potential for erosion. Muhawenimana (2019) also saw a decrease in depth upstream when adding porosity to channel-spanning structures of different designs within flume experiments. Muhawenimana (2019) suggested that the gap below the structure would result in high flow, high shear stress and the potential for scour. The same erosion potential was seen in this study at the culvert location, where increasing the culvert height from 0.05 m to 0.3 m increased the shear stress at the culvert by up to 20 Nm^{-2} (Figure 5.17). Therefore a compromise between the hydraulic benefits and implications of added bed scour potential underneath the barrier and sedimentation upstream of the barrier when altering the height of the gap beneath the barrier may need to be sought on a site by site basis.

5.4.1.2 Barrier extension onto the floodplain

There were few hydraulic differences between the original and extended barriers for the smallest event (2 year RP) due to the “leakiness” or culvert conveying all flow downstream. However, once the magnitude of the event was large enough that the flow interacted with the barrier, water backed up and volume held

upstream of the barrier increased sharply, with the extended barrier storing up to 90 m^3 more water upstream than the original barrier (Figure 5.13). Unlike the original barrier, the extended barrier forced water onto the floodplain before the barrier was overtopped due to the additional height of the barrier providing additional floodplain connectivity, resulting in up to 330 m^3 of additional water on the floodplain (Figure 5.14). Floodplain volume was seen to increase with increasing return period for both the original and extended leaky barrier designs (Figure 5.14). This differed slightly from the findings of Keys et al. (2018) who found connectivity decreased with increasing return period as a result of the barrier no longer being the primary mechanism for controlling floodplain flow. No decrease in floodplain connectivity was observed in this study as the barrier remained the primary mechanism controlling floodplain flow given the reach was heavily incised. Due to this incision, flow typically remained in-channel even for the more extreme events when the original barrier was implemented. The degree of floodplain connectivity and the subsequent flow attenuation benefits is therefore highly site-specific.

Although the extended barrier increased floodplain flow, once water re-entered the channel further approximately 200 m downstream (Figure 5.14), there was no reduction in water discharge past this point. Therefore although the floodplain was utilised, the amount of water re-entering the channel resulted in no attenuation or peak reduction at the downstream reach boundary (Figure 5.9). Water re-entering the channel from the floodplain and the subsequent lack of reduction to the peak magnitude of a flood was also reported by Thomas and Nisbet (2012) when modelling instream wood. Thomas and Nisbet (2012) did however, observe a small delay in the time of the peak discharge. Such a delay in peak discharge was not seen in this study, likely due to only having implemented a single leaky barrier. Localised peak reduction effects indicate that it is important to consider the location of a leaky barrier and the relation this has to where measurements are taken when identifying the hydrological benefits of any given leaky barrier. Reduction in peak discharge was only seen in close proximity to the leaky barrier (< 200 m downstream), suggesting there is limited hydrological benefit of a leaky barrier as a single feature within a reach.

There was little difference in the area estimated as erosional upstream of the barrier between the original and extended leaky barrier designs, however

extending the leaky barrier did increase the area estimated to be depositional by up to 124 m^2 (Figure 5.15). The difference between the two designs is likely the result of the backing up effect of water behind the barrier. As water pooled behind the barrier, depth increased and velocity decreased, reducing the power of the water increasing the number of depositional cells. Given the additional 0.5 m of height of the extended barrier, the backwater effect would be expected to be greater than for the original barrier design. The facilitation of deposition through the backing up of water behind in-channel wood is well understood in relation to natural large wood in rivers (Wohl, 2013) and would have impacts on the ecological functioning of the site, with habitat and nutrient loadings likely to be altered (Hilderbrand et al., 1997, Sawyer et al., 2011).

Floodplain flow started for smaller flood events for the extended leaky barrier (5 year RP) compared to the original leaky barrier design (10 year RP) (Figure 5.14). The additional floodplain usage of the extended barrier influenced the channel up to 50 m downstream. The extended barrier resulted in a decrease of up to 104 m^2 in erosion and an increase of up to 63 m^2 in deposition compared to the original barrier design (Figure 5.16). Further than 50 m downstream was unaffected by changes to barrier design with regard to erosion and deposition (Figure 5.20).

Regardless of design, erosional cells were observed on the bank where water was exiting and re-entering the channel. Bank erosion resulting from large naturally occurring ‘valley jams’, where wood has a greater width than bankfull channel, has also been observed by Abbe and Montgomery (2003) in field surveys of the Queets river basin, Washington, USA.

Shear stress on the floodplain was mainly depositional for both the extended and original leaky barrier designs. This was expected given water on a floodplain is often very shallow and lacking in power and therefore the deposition of sediment is encouraged. Jeffries et al., (2003) also observed floodplain deposition in their monitoring of a naturally occurring woody debris dam in the New Forest, England. When the proportion of overbank flow was higher, as seen for the extended leaky barrier design, erosional shear stresses were reached (Figure 5.20) which may have the potential to form secondary channels through erosion. Such potentials for floodplain channel creation was observed by Sear et al. (2010) in a New Forest river catchment with naturally occurring debris dams. The additional

encouragement of floodplain use by the extended barrier may also be beneficial in terms of barrier stability as it promotes a limit in flow depth associated forces that may mobilise wood at higher discharges (Wohl, 2011) and increase the habitat diversity of the floodplain resulting from the sediment and flow dynamics as seen by Davis et al. (2007).

5.4.1.3 A summary of the impact of leaky barrier design

To summarise, barrier design does influence both the hydrological and geomorphological response to a flood event. Key differences and their wider implications are:

- Increasing the height between the bed and the bottom of a barrier decreased the retention capacity behind the barrier.
- Increasing the height between the bed and the bottom of a barrier allowed for more free flowing water and therefore maintained higher shear stresses which may have implications for bed scour below the barrier and for footings securing the barrier in place.
- Increasing the height between the bed and the bottom of a barrier allows for more easy fish passage and maintains flow levels and therefore habitat downstream.
- Extending the barrier onto the floodplain increased floodplain use, although if water was allowed to re-enter the channel, reductions in downstream flood magnitude were lost.
- Extending the barrier onto the floodplain increased the risk of bank erosion where water left and re-entered the channel, however it also increased the heterogeneity of shear stress on the floodplain.
- Extending the barrier may ease pressure on the barrier itself, reducing the likelihood of failure and the water partitioned onto the floodplain may increase habitat diversity through differing water depths, the deposition of fine sediment and the creation of secondary channels.

5.4.2 The effect of increasing return period

Burgess-Gamble et al. (2017) identified that there is currently limited evidence on the impact of leaky barriers for large flood events. Therefore, this project sought to quantify the differences in the hydrological and geomorphological response with increasing flood event return period. For the original leaky barrier design,

which had a gap beneath the barrier of 0.3 m, a total height of 1.3 m and a width of 11.1 m, at a point 100 m downstream, a reduction in peak discharge of 4.6 % and 13.8% was achieved for the larger 100 year and 1000 year RP events, respectively (Figure 5.10). This reduction in peak discharge was surprising given the common perception that leaky barriers will only attenuate flow for smaller flood events (Lane, 2017). There are, however, a couple of factors that could explain this unexpected finding. Firstly, as previously discussed in Section 5.4.1.1, the gap beneath the leaky barrier will influence the downstream reduction in peak discharge. A larger gap has the ability to convey more water freely through the barrier, decreasing the need for overtopping and decreasing the reduction in peak discharge downstream. Secondly, when the floodplain flow pathway is utilised, as it was for the larger 100 and 1000 year RP events (Figure 5.14), a proportion of the total flow is removed from within the channel, resulting in a reduction in peak discharge (Section 5.4.1.2).

Peak discharge reduction benefits of leaky barriers for larger flood events have also been reported by Ferguson and Fenner (2020) who identified ~ 30 % reduction for events with return periods up to 100 years. Ferguson and Fenner (2020) implemented leaky barriers through increasing the Manning's n of suitable channels in a HEC-RAS model of the 48 km^2 River Asker catchment. However, both the study of Ferguson and Fenner (2020) and this study are limited by the lack of simulation of leaky barrier failure, which would be expected to be more likely in extreme flood events (Hankin et al., 2020). This study is also limited by having only simulated a single leaky barrier and it should not simply be assumed that leaky barriers will result in a reduction in peak discharge for larger flood events at larger spatial scales. Potential flood risk reduction through the use of leaky barriers should hence be calculated on a case-by-case basis.

Geomorphologically, for the original leaky barrier design, an initial decrease in the upstream area estimated to be erosional between the 2 and 5 year RP events (10 m^2) was observed. For the larger flood events (> 100 year RP), there was a large increase in the area estimated to be erosional (Figure 5.15). The largest increase in erosional area was observed between the 100 year and 1000 year event (132 m^2), with erosional shear stress being maintained in the centre of the channel in closer proximity to the leaky barrier (Figure 5.18). Higher shear stress in the centre of the channel would be expected given the additional quantity of

water flowing through the channel for the larger events and the highest velocity occurring in deepest part in the centre of the channel. Practitioners should therefore be aware of the potential risk of scour upstream of a leaky barrier if a large flood event was to occur. Awareness is also needed as to where transported sediment would likely be deposited after the event.

Depositional areas were observed directly upstream of the leaky barrier adjacent to the location of the gap beneath the barrier (Figure 5.18). However, erosional shear stresses were maintained through the gap beneath the barrier (Figure 5.17). The shear stress through the gap beneath the barrier remained similar with increasing return period for the original leaky barrier design (~ 28-29 Nm^2, Figure 5.17). The lack of difference in shear stress through the gap beneath the leaky barrier with increasing return period was expected given the HEC-RAS 2D model cannot simulate movement or changes to the leaky barrier itself in response to an increase in discharge as the gap beneath the barrier will remain set at a constant size and therefore discharge through it is limited. This representation of an unchangeable gap is of course a simplification of reality. Given erosional shear stress is maintained through the gap beneath the barrier (Figure 5.17), scour would be expected if the bed was moveable. The work from Schalko et al. (2019) highlights that wood accumulations can cause bed scour. Their physical model representation of wood accumulations with a moveable bed resulted in bed scour both directly below and within the immediate upstream and downstream locality of the wood accumulation (Schalko et al., 2019).

Leaky barriers are often thought of to be depositional features (Addy and Wilkinson, 2016; Burgess-Gamble et al., 2017), this remains to be true (Figure 5.18). However, this project has also highlighted the importance of a consideration of the risk of scour both upstream and beneath the leaky barrier being implemented. Practitioners should be aware of this risk and the repercussions additional scour of material will have on the quantity of sediment which will be subsequently deposited in low flows elsewhere.

5.4.3 The effect of seasonality

The smaller peak magnitude and subsequent flood volume for the summer events (Figure 5.8) resulted in smaller hydrological effects for all barriers compared to the winter events. The annualised reduction in peak discharge 10 m downstream

of the barrier was an order of magnitude lower for the summer events compared to the winter events (Table 5.2). Summer flood events are often the result of short-lived but intense convective storms. Catchment responses are dependent on the previous hydrological conditions and catchment characteristics such as the permeability of the catchment as seen in the 2012 summer flood event in the UK (Parry et al., 2013). As this study used the total flow calculated by the ReFH model, the short, intense rainfall of the summer event had already been routed and partitioned within the ReFH model, prior to its use within the HEC-RAS 2D model. The catchment descriptors used within the ReFH model would have affected the flow output and the resulting discharges (Figure 5.8) suggest that within the small contributing area upstream of the modelled reach (2.89 km^2), rainfall was still able to infiltrate into the soil, resulting in lower magnitude events compared to the winter events where soil would more likely be saturated from longer, but less intense rainfall events.

The impact of a leaky barrier would likely have been different if the catchment was less permeable and the antecedent conditions had been more extreme with continued rainfall resulting in saturation of the catchment prior to an intense summer rainfall event. Such conditions were seen in the 2007 summer flood events in the UK (Marsh and Hannaford, 2007). High levels of overland runoff would have likely resulted in the flood discharge occurring as a short sharp peak. A leaky barrier would not interfere with the flow for as long due to the short nature of the event, reducing the leaky barrier's ability to attenuate flow.

The greater pace of an intense, short summer flood wave would have implications for the geomorphological response. Higher shear stresses occurring upstream of the barrier would increase the risk of bank erosion and scour underneath the structure. Increased erosion may ultimately result in the failure of the structure, leading to the potential of flood surges. Such wood related geomorphological processes were observed following a flash flood in a mountainous watershed in Slovenia in 2007 (Marchi et al., 2009). Floodplain utilisation in a short, intense summer event would likely aid in the dissipation of flood wave energy, easing the pressure on the main channel and reducing the risk of the structure failing and additional erosion occurring. Wohl (2011) observed such a threshold within the Colorado Front Range, where floodplain utilisation was a "safety valve", where increases in flow depth and forces that would mobilise wood were limited as

discharge increased. Practitioners therefore need to consider the different types of rainfall event which a leaky barrier may exposed to and the implications this would have on the structural integrity of the leaky barrier and the repercussions of total failure of a barrier.

5.4.4 Implications for wider use

5.4.4.1 Scaling and the impact on locating features

A well-known disadvantage of leaky barriers is that many are needed to affect the downstream flood volume (Thomas and Nisbet, 2012, Dixon et al., 2016). Based on the designs tested in this study, Table 5.3 highlights the number of leaky barriers needed to reduce flood volume down a given return period. Funding for leaky barriers in the UK through Countryside Stewardship stipulates that leaky barriers need to be built in series with a spacing of between 5 to 7 times the channel width to be funded (Rural Payments Agency, 2020). For the headwaters of the Lothersdale catchment modelled here, assuming a channel width of 2 m, each dam would need to be 10 m apart. To provide a 30 year RP level of protection when implementing the original 0.3 m high culvert leaky barrier design, 197 leaky barriers would need to be built, requiring 1.97 km of channel length (Table 5.3). A brief flow accumulation analysis alongside the use of aerial imagery showed only 5.5 km of channel length exists upstream of the downstream boundary of the modelled reach. Although the given example scenario is possible, providing the highest level of protection (1000 year RP) would not be (Table 5.3).

Table 5.3: Number of barriers require to hold the increase in flood volume for any given increase in return period. Calculations based on volume held behind each barrier for the larger of the two events. Channel length required based on guidance available in the literature for leaky dam placement (YDRT, 2018a).

	Difference in flood volume between return periods (m^3)	Number of barriers needed to reduce flood volume between return periods			
		No Culvert	0.05 m Culvert	0.3 m Culvert	Extended Barrier
5 yr – 2 yr	11,671	47	48	66	44
10 yr – 5 yr	9,544	39	40	51	35
30 yr – 10yr	15,783	67	68	80	58
100 yr – 30 yr	23,798	108	109	123	92
1000 yr – 100 yr	83,243	510	515	561	403
Total (1000 yr – 2 yr)	**101,326**	**467**	**474**	**766**	**641**
Channel length required (km)		**4.36**	**4.42**	**7.15**	**5.98**

The aforementioned estimation of channel length required to support the number of leaky barriers needed to provide any given level of protection does not take into account the need to remove sections of channel that would be inappropriate for barrier placement. Such locations include steep slopes, common in upland headwater catchments, which would limit the backwater effect and thus efficiency of a leaky barrier and main arterial channels which would increase the risk of barrier failure (Hankin et al., 2020). An understanding of the physical location limitations of these barriers stipulated in funding channels also need to be considered. As part of the Countryside Stewardship grants, funding for leaky barriers are given based on a number of requirements including that barriers should be located on slow flowing reaches with an average of 2 m of floodplain either side of the channel and that they should not be located directly upstream of pinch points where back up flows are likely to occur (Rural Payments Agency, 2020). In this study, the largest of leaky barrier designs, the extended leaky barrier, was shown to hold the most water upstream and utilise the floodplain efficiently to reduce downstream peak discharge. The extended barrier held the most upstream water and increased floodplain utilisation due to its additional 0.5 m of height. However, this barrier was over 23 m wide. Its dimensions would therefore limit how many would be possible within the catchment. In general there would be few places where such a large barrier would be possible and in addition to this, there would be no guarantee the barrier would behave in a similar way, particularly with regard to the floodplain utilisation.

5.4.4.2 The impact of climate change

The Environment Agency's (2019) Climate Impacts Tool estimated that under a 4 °C global mean temperature warming scenario, extreme rainfall intensity may increase by up to 40% by the 2080s. An analysis of peak rainfall within the ReFH model used in this chapter suggests a similar 40% increase was found for the peak rainfall between the 30 year and 100 year winter events. This suggests that the present day 30 year rainfall extremes, by 2080 could be similar to the present day 100 year rainfall extremes. Implications of this may for example include, for a leaky barrier of the extended design, a 13.7 % increase in peak reduction immediately downstream of the structure, an increase of 32 m^3 in water held upstream and an increase of 146 m^3 in floodplain water volume (Section 5.3.1). Geomorphologically, a 13 m^2 decrease in the area upstream estimated to be

depositional and a 33 m^2 increase in the area upstream estimated to be erosional would be expected. An increase in event severity would result in an increase in the number of leaky barriers needed to provide the same level of protection in the future. An additional ~ 100 barriers would need to be implemented now to ensure the same 30 year RP standard of flood protection in the future (Table 5.3). Not only does increased flood severity affect the level of flood protection the barriers bring, but also added concerns over the increase in shear stress and therefore possible erosion that may cause the barrier to fail need to be taken into account.

5.4.5 Future work

Only localised hydrological and geomorphological effects were observed for the leaky barrier implemented in this study. Therefore future work should seek to repeat a similar exercise of implementing leaky barriers as hydraulic structures but at catchment scale to assess whether the localised effects can be scaled up to provide wider flood risk reduction. Leaky barriers should be implemented in triplets as defined by advice for practitioners (YDRT, 2018a), in numerous locations around the catchment to begin to aim towards the number of leaky barriers required to provide a level of flood protection (Table 5.3). The addition of leaky barriers which extend across the lateral extent of the floodplain may aid attenuation by inhibiting flow pathways back into the channel. This study used a simple representation of a leaky barrier and provides a way of estimating geomorphological impacts based on the calculation of shear stress that could be used in any hydraulic model with 2D flow and hydraulic structure representation, providing a flexible method to test many scenarios over many scales.

The extreme weather in the early part of 2020 in the UK has highlighted the need to examine the effect flood frequency and sequencing has on leaky barriers and the geomorphological implications multiple extreme events may have. With the additional pressure of multiple extreme events, a barrier's likelihood to fail also needs to be assessed. Due to the added complexity using a morphodynamic model to simulate leaky barriers requires, efforts could be made to approximate the geomorphological effect a leaky barrier has through monitoring, prior to implementing these effects within a hydraulic model. An example being, that if a specified area and depth of deposition or erosion was observed, the topography within the hydraulic model could be altered, before running the model again to see the effect this change would have on the subsequent event in terms of flood

risk and geomorphological approximation. Such a study would require real-world examples to ensure geomorphological change was of a representative magnitude.

It should be noted that this study does not address the shortcomings of representing leaky barriers in hydraulic models such as those stated in Addy and Wilkinson (2019). It does however, provide a novel example of the combination of a commonly used leaky barrier representation (hydraulic structure) with an estimation of the geomorphological impact through the calculation and subsequent partitioning of shear stress, which was suggested by Addy and Wilkinson (2019) as a possible alternative to morphodynamic modelling. Therefore, in line with previous calls for more accurate representation of leaky barriers within hydraulic models (Addy and Wilkinson, 2019), future work should not only look at more accurately representing a leaky barrier's hydraulic effects, but also the geomorphological effects, and not just in hydraulic models, but in numerical models more widely, including morphodynamic models. For such ambitious model improvements to be made, efforts should also focus on disseminating the importance of geomorphological effects of different barrier designs to practitioners and landowners implementing such features as part of flood reduction schemes.

5.5 Conclusions

Very few studies have looked explicitly at the design of leaky barriers which are currently being implemented widely as part of natural flood management schemes with little to no specific guidance on design. Here, a numerical model (HEC-RAS 2D) was used to experimentally analyse differences occurring from two design aspects, firstly the size of the gap between the channel bed and bottom of the leaky barrier and secondly the extension of a leaky barrier onto the floodplain.

With regard to the height between the bed and barrier, there was little difference in the hydrological and geomorphological effects of different flood events for a solid barrier and a barrier with only a small 0.05 m gap between the channel bed and lower limit of the barrier. For such barrier designs, reductions in peak discharge were observed, alongside water storage upstream and floodplain inundation. However, with a small gap beneath the leaky barrier, it was often

overtopped, even for the smallest of flood events. A larger 0.3 m gap resulted in reduced hydrological benefits including a smaller reduction in peak discharge and a smaller volume of water held upstream of the barrier. Hydrological differences were the result of differing ratios of flow being unimpeded by the different barrier sizes. Although there are hydrological benefits to a smaller gap beneath the structure, care should be taken when designing specific features to allow for fish passage and freely flowing baseflow which would maintain a healthy watercourse.

Geomorphologically, the larger 0.3 m gap beneath the leaky barrier resulted in more erosion and less deposition upstream alongside a higher median shear stress underneath the barrier. As less flow was impeded, upstream depth was lower and velocity was greater, increasing the shear stress and decreasing the pooling of water and loss of energy behind the barrier. It should however be noted that regardless of barrier design, deposition dominated the area upstream of the barrier location, which would likely result in a sediment management issue.

Extending the barrier so that it intersected the floodplain saw the largest hydrological benefits, including the largest reduction in peak magnitude and greatest volume held upstream of the barrier. The extension of the barrier also saw greater inundation extent and floodplain water volume. It should also be noted that the extended barrier was seldom overtopped, whereas the original barrier was overtopped for all events tested. The benefits of the extended barrier were the result of the additional height required for it to intersect the floodplain and its partition of water onto the floodplain.

There was little difference in the area estimated to be erosional upstream when extending the leaky barrier, however a larger area of deposition was observed. Greater differences were seen downstream of the barrier where the extended barrier saw less erosion and more deposition than its original counterpart. This was the result of a proportion of the total flow being diverted onto the floodplain, therefore there was less flow with less power within the channel. Floodplain shear stress was greater for the extended barrier as a greater proportion of the flow was routed down the floodplain, increasing its power. With this knowledge, wherever possible, hydrological benefits may be greater if leaky barriers were to be made more substantial so they divert a significant proportion of the flow onto the floodplain.

Increases to the intensity of the flood event resulted, for all barrier designs, in an increase in the reduction of peak discharge and an increase in volume held upstream of the barrier. Increases of estimated erosion were also seen in addition to decreases in deposition. The increasing hydrological benefits with increasing return period were surprising given it is often assumed leaky barriers will not provide protection against more extreme flood events. However, only a single barrier was analysed and it cannot be assumed that benefits from one barrier can be scaled up and achieved for multiple barriers across a wider spatial scale. Although not modelled in this study, increasing event magnitude will also increase the risk of barrier failure and the downstream movement of wood may have implications for downstream infrastructure or other NFM features. Therefore, natural flood management features should be considered as a whole system, rather than in isolation.

Most importantly, despite each barrier design resulting in localised changes to the hydrology and geomorphology of flood events, significant numbers of barriers would be required to hold the volume of water needed to reduce the severity of any given return period event. Such large quantities of barriers is unlikely to be achievable due to physical limitations on their location. In addition to this, as storm severity is likely to increase with climate change, such scaling issues will only prove more challenging as flood events grow larger and more frequent.

Future NFM numerical modelling work should seek to implement many more leaky barriers as hydraulic structures within a catchment setting to gain an understanding of the hydrological benefits in addition to an estimation of the geomorphological implications leaky barriers have at a wider scale. Efforts could also be made to implement accurate representations of leaky barriers, including their potential failure, into morphodynamic models to allow for longer term geomorphological change to be modelled. A longer-term outlook would provide a vital understanding of the impacts of successive flood events and future management needs.

Chapter 6
Discussion

Given the individual research chapters in this thesis have independent discussions, this chapter brings together their work to synthesise the outcomes in relation to the two evidence gaps identified at the beginning of the thesis:

- Design – There is limited evidence available for design specifications and the impacts changes to design have for RAFs apart from indicative guidance to qualify for certain funding for leaky barriers.
- Scale – There is limited evidence for the effectiveness of RAFs at catchment scale for large flood events and how RAFs perform when scaling up from an individual feature to catchment scale and from small to large flood magnitudes.

Findings are discussed in relation to their impact on the management of NFM projects and to climate change. The chapter ends by considering future directions for the use of RAFs and geomorphological modelling in NFM projects.

6.1 Geomorphological and hydrological impacts of RAFs

6.1.1 The influence of design

6.1.1.1 Size and shape

This thesis has established that the local hydrological and geomorphological impacts of runoff attenuation features are affected by specific design considerations. This thesis therefore highlights that until engineering design standard guidance is published, many projects will continue to be inhibited by uncertainty regarding design (Waylen et al., 2018).

With regards to hydrological impacts, and as to be expected, the larger the size of individual features, be that in length or height, the greater the storage capacity (Table 3.3; Figure 5.13). For example, increasing the length of linear RAFs by 8 m increased the maximum storage capacity by up to 95 m^3 for a 120 year return period event (Table 3.3). Increasing the height of a leaky barrier by 0.5 m and extending the barrier onto the floodplain, resulting in a 12.3 m increase in length, increased water storage by 90 m^3 for 5 year return period flood (Figure 5.13). In addition to size, decreasing the reliance on local topography to aid in creating

storage by implementing u-shaped RAFs rather than linear RAFs also increased the maximum water storage by up to 465 m^3 for a 120 year return period event (Table 3.3).

However, it should be noted that effective performance of RAFs in reducing runoff is not a given, with up to 41 % of linear RAFs not storing any water during the event scenario tested in this thesis (Table 3.3). A lower percentage of RAFs were not storing water when they were larger and linear in design (30 %), u-shaped (18 %) and larger and u-shaped (16 %) (Table 3.3). Under-utilisation of potential storage of RAFs has also been identified by Quinn et al., (2013), Metcalfe et al., (2017), Metcalfe et al., (2018) and Hankin et al., (2020), but this project has additionally identified that greater under-utilisation of RAFs can be caused by specific design aspects including the size and shape of a feature. Practitioners should therefore aim to increase the potential storage of any given RAF either through an increase in size or decrease on the reliance on local topography. They should also be aware that storage should be designed to be used effectively, taking water from the peak of the event as opposed to when the river is still rising.

Geomorphological responses to changes in size and shape of RAFs were more varied than the hydrological impacts. However, it should first be noted that between 30 % and 50 % of RAFs, regardless of design, resulted in no geomorphological change upstream (Figure 3.13). This was due to their headwater location reducing deposition occurring upstream due to a lack of sediment within the water column. Many RAFs were also sited on grassed hillslopes, which would be less susceptible to erosion than bare soil (Section 3.4.3.2).

Increasing the size of linear RAFs by 8 metres increased the number experiencing deposition upstream from 70 to 105 (Median SRC, Figure 3.13). An increase in deposition with leaky barrier size was also observed in Chapter 5, where the extended barrier resulted in increases in the area of deposition upstream by up to 124 m^2 compared to the original barrier (Figure 5.15). Deposition upstream of naturally occurring large woody debris is well understood due to the backwater effect the channel blockage produces (Wohl, 2013). This thesis has however also identified the differences in deposition occurring from changes in the size of engineered leaky wooden barriers (Figure 5.15) in addition to RAFs more generally (Figure 3.13). The differences between a natural

blockage of large woody debris compared to an engineered leaky barrier include longitudinal extent of the wood, with a natural blockage extending further downstream compared to a leaky barrier. Within the natural blockage there is much greater complexity to the flow pathways the water needs to take compared to a leaky barrier. These two differences reduce the velocity and increase the likelihood of deposition over a greater extent in naturally occurring large woody debris, compared to a large, in terms of height, but short in terms of length, blockage and potential deposition behind an engineered leaky barrier.

With regard to erosion, the larger, linear RAFs resulted in the greatest number of features (up to 97) experiencing erosion upstream (Figure 3.13) as their locations on hillslopes caused preferential flow pathways to one side of the feature and therefore an increased risk of erosion. Erosion to a preferred pathway was also seen by in field observations by Robichaud, Wagenbrenner et al. (2008) for contour log post-fire erosion control measures. This thesis has therefore shown that despite increasing the size of RAF increasing the water stored, practitioners should also consider the additional increase in risk of deposition when increasing the size and increase in risk of erosion if larger linear RAFs are located on hillslopes.

When altering the shape of the RAFs from linear to u-shaped, fewer saw erosion (43 to 16 RAFs) and deposition (70 to 61 RAFs) occur immediately upstream of the RAF (Median SRC, Figure 3.13). U-shaped RAFs were seen to partition the flow pathway (Figure 3.21), reducing the stream power within a feature and thus its ability to erode or transport material (Bizzi and Lerner, 2015). However, some u-shaped RAFs which were located directly across powerful channel flows resulted in erosion upstream (Figure 3.21). The channel blockage caused by the RAF likely forced water downwards towards the bed, resulting in bed scour. Abbe and Montgomery (1996) also observed scour immediately upstream albeit of naturally occurring large woody debris when located in the centre of a channel. This thesis has therefore highlighted the importance of RAF shape on geomorphology, where if placed carefully, u-shaped features reduce the geomorphological response.

A number of the RAFs simulated in Chapter 3 were overtopped and subsequently suffered from scour to the RAFs themselves (Table 3.7). Increasing the size of a linear RAF increased the number of RAFs experiencing scour by 27 (Median

SRC, Table 3.7). Altering the shape of the RAF from linear to u-shaped also increased the likelihood of scour, with an additional 51 RAFs experiencing scour (Median SRC, Table 3.7). Practitioners therefore need to ensure critical infrastructure, such as the crest of a RAF, are protected from erosion which will likely occur regardless of RAF size or shape (Quinn et al., 2013). This could be achieved through the use of unerodible materials (e.g. on the crest of the bund) or careful choice of revegetation species (e.g. around the ends of bunds), combined with regular monitoring to ensure early mitigation if erosion was occurring. However, this thesis has shown that particular focus should be on protecting larger, u-shaped RAFs from scour.

6.1.1.2 Floodplain connectivity

When within-channel structures, such as the leaky barrier tested in Chapter 5 are increased in size, involving a 0.5 m increase in height and 12.3 m increase in length, so that they extend onto the floodplain and encourage floodplain inundation (Wohl, 2013), greater decreases in downstream peak discharge can be observed (Figure 5.10). For example, at a point 10 m downstream of the leaky barrier, the extended barrier design resulted in a 74 % decrease in peak discharge, compared to a 44% decrease for the original barrier design for a 1000 year return period event (Figure 5.10). Highlighted by Quinn et al. (2013) as an advantage of RAFs, when they allow for flow across the floodplain, attenuation potential is increased given the “tortuous” path which is taken.

To fully take advantage of the additional peak discharge reduction from extending the leaky barrier onto the floodplain, the water needs to remain on the floodplain for as long as possible. Once water was allowed to re-enter the channel from the floodplain, no further peak discharge reduction was seen for either the extended or original leaky barrier designs (Figure 5.9). Thomas and Nisbet (2012) also identified floodplain water re-introduction as a limitation to downstream attenuation for fully within-channel leaky barriers. However, this thesis has additionally identified that even if a leaky barrier is increased in size to purposely increase floodplain connectivity, the advantage the extension onto the floodplain has on downstream peak discharge reduction diminishes when water is allowed to re-enter the channel.

It has also been identified, in this thesis, that at the point of re-entry, bank erosion may occur. This has also been seen by Sear et al. (2010) who saw head cutting where floodplain channels re-entered the main channel, with head cutting being maximised when the floodplain is not drowned out in flood. Comparisons here can also be made to the geomorphological processes occurring at confluences of channels with uneven bed depths, where the shallower channel flow can re-circulate towards the banks and bed as the shallower channel meets the deeper channel (De Serres et al, 1999). Practitioners should be made aware of this and management of leaky barriers which utilise the floodplain should extent to where water re-enters the channel, at least in terms of monitoring for geomorphological change. Risk maybe reduced by adding material or rougher vegetation to the floodplain to slow floodplain flows even further to reduce the risk of scour at re-entry points, where natural bank protection, such as through the use of living willow, would reduce the risk further.

Given the additional 0.5 m of height required to enable the leaky barrier modelled in Chapter 5 to be extended onto the floodplain, an understanding needs to be gained surrounding the additional force of water resulting from the increase in water depth upstream of the barrier of up to 0.17 m due to the increase in barrier height (Figure 5.13). Additional hydraulic load on the leaky barrier may increase the likelihood of failure, but HEC-RAS 2D cannot explicitly represent leaky barrier failure. Previous research by Wohl (2011) suggested that floodplain inundation causes a limit to the water depth and associated forces which may cause mobilisation of naturally occurring woody debris dams. Wohl's (2011) findings may hold true for engineered equivalents, however, to date, there has been little emphasis on calculating the likelihood of the failure of systems of leaky barriers (Hankin et al., 2020). Areas of low shear stress immediately upstream of the extended leaky barrier design (Figure 5.18) suggest pressure on the extended barrier was limited due to the floodplain connectivity despite the increase in barrier height and increase in headwater stage.

The extension of the leaky barrier onto the floodplain not only resulted in an increase in floodplain inundation adjacent to the barrier of up to 89 % compared to the original leaky barrier design (Figure 5.14), the extended barrier also increased the variability of shear stress experienced on the floodplain (Figure 5.20). Heterogeneity of floodplain flows may lead to an intrinsic network of

secondary channels and areas of deposition (Jeffries et al., 2003; Sear et al., 2010). Subsequently, habitat diversity on the floodplain may also increase (Davis et al., 2007). The evidence in this thesis has suggested that extending a leaky barrier onto a floodplain to increase floodplain connectivity benefits peak discharge reduction and floodplain shear stress heterogeneity without increasing the risk of leaky barrier failure. Therefore, this thesis has, for the first time from a hydro-geomorphological perspective, therefore highlighted that practitioners in the future should aim to design leaky barriers to be extended onto the floodplain with the intention of increasing floodplain connectivity. However, it should be noted that there is evidence in the literature that floodplain flow may, in some cases, be a more efficient flow path than within channel flow (Anderson et al., 2006). Practitioners should be aware that attenuation benefits from floodplain utilisation may be lost if the floodplain is hydraulically smooth (e.g. heavily grazed improved grassland) and additional floodplain vegetation may be needed to increase the hydraulic roughness and increase the likelihood of flow attenuation.

6.1.1.3 Leakiness

The inclusion of a representation of leakiness and/or control structures such as inflow and outflow pipes of RAFs within the model implementation has been shown to be important. Inclusion of a gap underneath the leaky barrier in Chapter 5 alone, and also the size of the gap, influenced both the hydrological and geomorphological functioning of the leaky barrier. As the gap below the barrier was increased from 0.05 m to 0.3 m, water volume upstream decreased by between 13 m^3 and 96 m^3 from the 1000 year to 2 year return period events (Figure 5.13), alongside a decrease in the reduction of peak flow downstream of up to 14 % (Figure 5.10). This would be expected given the lower blockage ratio of the channel and has also been identified for naturally occurring woody debris dams (Kail, 2003).

Geomorphologically, when increasing the gap beneath the barrier from 0.05 m to 0.3 m and therefore decreasing the blocking ratio, the area upstream of the leaky barriers with both 0.05 m and 0.3 m high gaps remained depositional, but the 0.05 m gap resulted in a larger area of deposition than the 0.3 m gap. An additional 124 m^2 of deposition was identified for the 2 year return period event, which decreased to 27 m^2 for the 1000 year event (Figure 5.15). Increasing the size of the gap from 0.05 m to 0.3 m high did increase the shear stress directly

below the barrier by approximately 20 Nm^2. This increase in shear stress resulted in possible erosion when the 0.3 m gap was implemented (Figure 5.17). Although erosion was only estimated in this thesis, the potential for scour below a leaky barrier has also been identified by Muhawenimana (2019) and Schalko et al. (2019). Comparisons can also be made to the geomorphological impacts of culverts, erosion, creating a scour hole at the outlet of culverts is well understood (Rajaratnam and Berry, 1977; Liriano et al., 2002), however, given their construction material (e.g. concrete, plastic), it is unlikely that erosion will occur in a traditional culvert. Crookston and Tullis (2012) observed the geomorphological processes in a flume with a bottomless arch culvert for pressurised and non-pressurised flows. They identified that scour occurred most severely at the inlet of the culvert and along the downstream half of the culvert itself, scour was also observed at the culvert outlet. This thesis goes further than previous leaky barrier studies to suggest that the size of the gap beneath a leaky barrier will increase the potential risk of bed scour. As leaky barrier design guidance in the UK often states a set 0.3 m gap between the bed and leaky barrier should be aimed for (YDRT, 2018a), practitioners therefore need to be aware that this may result in an increased potential for scour beneath the leaky barrier compared to a smaller gap.

6.1.2 The influence of scale

Burgess-Gamble et al. (2017) highlighted the need to understand the effectiveness of NFM measures at a range of catchment scales and for a range of return periods. The 274 implemented RAFs in the ~41 km^2 Eastburn Beck catchment model in Chapter 3 showed negligible reduction to peak discharge at the catchment outlet for a 120 year return period event, despite individual RAFs storing up to 975 m^3 of water (Extended u-shaped design, Table 3.3). Increasing the quantity of RAFs in the catchment model by adding, wherever possible, an identical linear RAF 20 m upstream of the originally implemented linear RAF, resulting in 541 features overall, did not result in a substantial reduction in peak discharge at the catchment outlet (Table 3.2). Despite almost doubling the number of RAFs within the catchment, water storage did not greatly increase per location despite two RAFs being implemented. As such the maximum water storage volume for the original linear design of RAFs was 491 m^3, compared to

the double linear RAF scenario where maximum volume stored upstream of the RAFs totalled 474 m^3 (Median SRC, Table 3.3).

As 274 RAFs storing up to 975 m^3 of water each (equivalent to each RAF storing 0.0002 % of the total flood volume) did not affect the catchment outlet discharge, the ratio between available storage and catchment size needs to be much greater than what was achieved in Eastburn Beck of 683 m^3 per km^2. A downstream flood peak reduction has been observed of up to 17.3 % from a modelling exercise by Metcalfe et al. (2018). Their larger catchment (223 km^2) did however have a storage to catchment size ratio of 44,843 m^3 per km^2. Combining available data from this project and others in the literature to identify a relationship between available storage and catchment size will allow for an understanding of the level of protection that could be provided using RAFs for downstream communities.

Projected numbers of RAFs to achieve a reduction in downstream flood volume were identified in both Chapter 3 and Chapter 5. In Chapter 3, based on the extended u-shaped design of RAFs which had a maximum storage volume of 975 m^3, 2,169 features would be required to reduce the flood volume produced by the 120 year flood event simulated by half in the ~41 km^2 catchment (Section 3.4.4). Similarly in Chapter 5, to reduce the flood volume occurring from the 100 year return period event to the flood volume of the 30 year return period event, an additional 123 leaky barriers, of the original design with a 0.3 m gap underneath the barrier, would be required in the 2.89 km^2 contributing area upstream of the modelled reach (Section 5.4.4.1). However, it should be noted that these projections of the number of features required to reduce downstream flood volume, set out in Chapter 3 and Chapter 5 are estimations and therefore do not take into account under-utilisation as discussed in Section 6.1.1.1 of this discussion or the availability of feasible locations (Section 5.4.4.1). For example, in the 2.89 km^2 contributing area upstream of the modelled reach in Chapter 3, 5.5 km of channel exists. UK guidance for the implementation of leaky barriers states individual leaky barriers should built with a spacing of between 5 to 7 times the channel width (Rural Payments Agency, 2020). To reduce the flood volume occurring from the 1,000 year return period event to the flood volume occurring from the 2 year return period event, 766 leaky barriers of the original design with a 0.3 m gap underneath the barrier would be required. To accommodate the 766 barriers, 7.15 km of channel length would be required and thus, the watercourses

upstream of the modelled reach in Chapter 5 are simply not long enough to support such a large number of features. The projections for the number of features required to reduce downstream flood volume that have been estimated in this thesis therefore suggest that RAFs will most likely be unable to achieve flood volume reduction for larger return period events (> 100 year return period).

Up to 115 RAFs experienced scour to the features themselves in Chapter 3 (Median SRC, Table 3.7). Therefore the risk of geomorphological processes affecting the stability of the features themselves is significant. Subsequently, the potential reduction in storage volume if scour and failure was to occur should also be taken into account both when designing RAFs individually and when projecting how many RAFs would be needed to reduce downstream flood volume. The average cost of a RAF, depending on type and size, is between £100 and £5,000 (Quinn et al., 2013). Necessary maintenance, to ensure the structural integrity of RAFs will only add to the cost of the project (Metcalfe et al., 2018, Hankin et al., 2020). Accounting for the number of RAFs required to reduce flood volume alongside the cost per RAF, they are likely to only be feasible as a standalone solution for highly localised flood issues. RAFs alone have been shown to work at Belford (5.7 km^2), where the 45 RAFs constructed have a total storage capacity of 12,000 m^3 (Nicholson et al., 2017) and provide protection for a small pocket of the community (25 properties) who were affected by small return period events (2 year return period) (Wilkinson, Quinn and Welton, 2010; Nicholson et al., 2020). This thesis has highlighted that RAFs alone will unlikely be able to provide a high standard of protection for downstream communities, even in relatively small catchments. Such communities may benefit from a combined solution, like the scheme at Pickering, where RAFs and wider NFM contribute prior to the larger more engineered structure located more closely to the town itself (Nisbet, 2017). Using a varied approach to alleviate flood risk was also highlighted by Nicholson et al. (2020) as a potential solution for larger catchments.

6.2 Implications for management

6.2.1 The use of RAFs

The size, shape and leakiness of a RAF, alongside it's ability to connect the channel with the floodplain, will affect the amount of potential water storage, the local reduction in peak discharge, the likelihood of sediment erosion and

deposition upstream and the integrity of the RAF itself. Therefore an understanding of the hydrological and geomorphological impact of a feature's design at the planning phase of a project will decrease the risk of failure and thus the negative potential impacts on flood risk, ecological functioning and the cost of removing washed out material. It will also assist in decreasing the uncertainty of potential future management needs, allowing for budget to be set aside if management is deemed necessary.

With regards to scale, the very large number of RAFs required to significantly decrease downstream flood risk will require widespread and enthusiastic landowner uptake. Engagement as early into a project as possible will aid this, alongside tangible local case studies and evidence where NFM has been shown to not only work but not negatively impact the owner's land (Howgate and Kenyon, 2009; Wilkinson et al., 2019; Wells, 2019). Modelling outputs such as inundation maps can be used to increase landowner engagement and subsequently, landowners can provide their own knowledge to refine the design process (Hankin et al., 2016).

6.2.2 The use of geomorphological numerical modelling

This thesis has highlighted the use of both CAESAR-Lisflood (Chapter 3) and HEC-RAS 2D (Chapter 5) in assessing the geomorphological response to different RAF design aspects. Both models could be used in the planning phase of a project proposal, the choice between the two models will depend on its intended use and the catchment being described. A summary of potential uses for both HEC-RAS 2D and CAESAR-Lisflood in relation to natural flood management is discussed in further detail below and can be found in Table 6.1.

The shear stress methodology used to estimate geomorphological processes in HEC-RAS 2D as part of Chapters 4 and 5 has been shown in this thesis to have the potential, albeit with a need for added methodological validation, to be used with depth and velocity data from pre-existing nation-wide flood risk maps (Section 4.4.2). This would allow for an understanding of geomorphological processes across England at a 2 m resolution. The depth and velocity grids could be used to identify suitable locations of features in their original form to evaluate where water is currently being attenuated within the catchment. Subsequently, the calculation and classification of shear stress using the depth and velocity grids

could be used to evaluate the area's current geomorphological state (e.g. Hankin et al., 2019). Providing a ready-to-use national database of estimated geomorphological processes will be useful for projects where numerical modelling is unfeasible due to the associated high costs or expertise required. Finding geomorphologically suitable locations for RAFs, particularly for bunds, is important given this thesis has identified that the location of a feature will impact its ability to store water (Section 3.4.3.1), the risk of scour and thus structural integrity (Section 3.4.3.3). A suitable location to benefit both water storage and reduce potential scour risk may be on a relatively shallow gradient overland flow pathway, which is introduced into the system in larger rainfall events, this will reduce the potential for chronic suspended sediment inputs, as identified by Barber and Quinn (2012), but store water when it is most needed. Consideration to the soil properties and vegetation cover should also be given in reducing risk of erosion, particularly if the feature was full and water started moving around or over the top of the bund, it would start to erode the soil more widely. Identifying geomorphologically suitable locations should also therefore reduce longer term management needs.

As HEC-RAS 2D is able to represent NFM interventions such as leaky barriers and bunds through the creation of a hydraulic structure (Leakey et al., 2020), the model can also be used in the design phase of a project to assess changes occurring from differences in a structure's design. Such a process was undertaken in Chapter 5 which highlighted differences in the reach scale response both hydrologically and geomorphologically given increases in the height of the gap below a leaky barrier and increases to the total height of the barrier. Given the benefits observed in both Chapter 3 and Chapter 5 from small changes in RAF design, projects should look to maximise water storage and localised peak flow reductions, with HEC-RAS 2D being able to do this relatively simply through the use of a weir and culvert to simulate the barrier and associated leakiness.

However, given the HEC-RAS 2D methodology is not morphodynamic, its use as a location and design planning tool should be avoided for catchments where temporal changes in bed elevations are frequent, such as in braided systems. The methodology is also likely to be inappropriate for catchments where sediment transport is supply limited and catchments where grain size cannot be accurately

represented through the use of D_{50} (Section 4.4.1). Using a non-morphodynamic model to estimate geomorphological processes in such catchments will result in the under- or over- estimation of sediment transport and subsequent increases in NFM project management costs due to sedimentation upstream of RAFs or scour to the RAFs themselves.

The aforementioned highly active catchments would benefit from the use of CAESAR-Lisflood. CAESAR-Lisflood provides the user with the ability to input a range of grain sizes and has been used previously in more active catchments (e.g. Ziliani et al., 2020). As with the HEC-RAS 2D methodology, CAESAR-Lisflood can be used as a location planning tool to find hydrologically and geomorphologically suitable locations, albeit with greater modelling requirements such as parameter calibration and model spin up such as the process followed in Appendix A and summarised in Chapter 2. However, as CAESAR-Lisflood is yet to be able to accurately represent small-scale NFM features at a high resolution, design considerations such as the effect of leakiness identified in Chapter 5 would not be able to be assessed at the current time. Scale limitations for the application of CAESAR-Lisflood were also identified by Ziliani et al. (2020) and an alternative morphodynamic model would need to be found for accurate representation of NFM interventions such as leaky barriers.

Given CAESAR-Lisflood's origins as a landscape evolution model, using it as a long term management tool would be advantageous to assess the longevity of, in particular, the larger NFM interventions such as floodplain reconnection and river restoration. These interventions rely largely on topographic changes, which are easily implemented into CAESAR-Lisflood through the use of an altered DEM and are also those more likely to alter the local morphodynamics of the watercourse. An example would be the application to dam removal by Poeppl et al., (2019). Large scale interventions also have the potential to cause the greatest long term geomorphological changes such as the reintroduction of meandering. Therefore their possible future impacts should be understood as best as possible prior to construction, which could be done using CAESAR-Lisflood and designs should be refined to decrease local risk to infrastructure, flooding and habitat, if required.

Table 6.1: Suggested uses for CAESAR-Lisflood and HEC-RAS 2D in relation to catchment and NFM types.

Model	**Catchment type**	**NFM types**	**Available implementation**	**Model outputs of interest specific to the given model**
CAESAR-Lisflood	Stable to highly active systems Permeable soils	River restoration Floodplain restoration Woodland	Topographic alteration *(Can be made unerodible by increasing height of bedrock layer to height of feature implemented)* Roughness alteration Soil infiltration alteration	Sediment discharge per set time interval at downstream boundary condition (including suspended) Spatially distributed elevation and D_{50} per set time interval
HEC-RAS 2D	Relatively stable systems Impermeable soils Topographically complex *(Use breaklines to ensure no inaccurate leakage through topography)* Inclusion of infrastructure (e.g. bridges, culverts)	Leaky barriers River restoration Floodplain restoration Offline storage areas Woodland	Hydraulic structures Topographic alteration Roughness alteration	Time series data per set time interval (discharge, depth, velocity) for any modelled point Flow/Stage data for hydraulic structures and downstream boundary condition Animated velocity vectors and particle tracking

6.3 Implications for climate change

Alongside the challenges faced when implementing NFM now (Wells et al., 2020), climate change provides the need for additional resilience planning (Environment Agency, 2018b). Climate change projections are uncertain, but government adaptation planning is being progressed on the basis of predicted higher peak river levels and increases in rainfall intensity (Environment Agency, 2019b). Increases to river levels and rainfall intensity will increase the flood impacts for a given flood volume and thus result in an increase in the number of RAFs required

to store additional flood water. As such, the Climate Impacts Tool (Environment Agency, 2019b) was used in Chapter 5 to suggest that an additional ~100 leaky barriers (of any of the designs tested) would be required to account for a shift in flood volume from the current day 30 year return period event to what the 2080 30 year return period event may look like (Section 5.4.4.2). However, the leakiness or inflow/outflow infrastructure of features should also be correctly designed to allow effective storage of storm water (Quinn et al., 2013; Hankin et al., 2020), but allow baseflow to be unimpeded or drain freely given monthly river flow levels are likely to decrease in future climate change predictions (Environment Agency, 2019b). This suggests that adaptive management may be required into the future to alter the height of inflow/outflow infrastructure of a RAF or the level of blockage a leaky barrier causes depending on the level of protection desired for each structure.

With resilience planning accounting for an increase in the extremity of events (Environment Agency, 2019b), more extreme geomorphological change may also occur (Death et al., 2015). Features should therefore be designed to withstand an increased likelihood of erosion (Figure 5.18) through the reinforcement of critical infrastructure such as inflows, outflows and spillways. Locating features in succession may reduce the negative downstream impacts of the risk of failure and washout. Thomas and Nisbet (2012) and Hankin et al. (2020) showed washed out wood material from leaky barriers was retained by the next downstream barrier, increasing its own resilience. Additional management will also likely be required to inspect features after events to check structural integrity and levels of sedimentation (Quinn et al., 2013).

6.4 Recommendations for future direction

6.4.1 The future for RAFs

This discussion chapter has highlighted the different factors, including design, location and number of features which need to be considered before implementing RAFs and has added to the evidence that they may not be suitable to provide flood risk alleviation at larger catchment scales (~ > 10 km^2, Sections 3.4.2 and 5.4.4.1). A lack of larger catchment flood risk alleviation does not however, need to be a negative outcome for their future use. RAF implementation should be focused on catchments with similar flood risk issues as Belford, where

they have been shown to reduce flood peaks (Wilkinson, Quinn and Welton, 2010; Nicholson et al., 2020). RAFs may provide small communities at risk from fairly frequent floods a cost-effective solution which they may not otherwise have been able to have if relying on more traditional management options due to the poor cost-benefit ratio of hard engineering approaches in such small catchments (Wilkinson, Quinn and Welton, 2010). Smaller catchments (< 10 km^2), suffering from frequent flooding are therefore where NFM research and projects should focus their attention for RAFs specifically. Careful RAF placement in the catchment will reduce project costs (Hankin et al., 2020), making them an even more viable flood risk reduction option. A greater understanding does need to be gained regarding how to protect the RAFs, which work to protect communities from small floods, against larger floods which may cause damage to the features themselves, as shown by scour to RAFs in Chapter 3. Building up more case studies of their beneficial use in small catchments to enhance wider implementation will help communities across the UK who may not believe there is another solution to their flooding problems.

For larger catchments (> 10 km^2), the number of RAFs required to impact downstream flood risk will increase with catchment size as highlighted by the greater number of features required to reduce flood volume of a 120 year event by half in Chapter 3 (> 2,000 features, Section 3.4.4) compared to those needed to reduce the flood volume of a 100 year event to the flood volume of a 30 year event in Chapter 3 (~ 100 features, Section 5.4.4.1). It is therefore more than likely that RAFs will not reduce flood risk alone in larger catchments (Dadson et al., 2017). Future work should consequently focus on the use of a combined approach with RAFs being coupled with more traditional flood defence works, as also highlighted in recent work by Nicholson et al., (2020). Pickering provides the evidence that combinations of measures can work, where leaky barriers, timber bunds and a large flood storage area provided protection in the Boxing Day 2015 event (Slowing the Flow Partnership, 2016). However, given the added complexity of such a combined approach, including finding funding for the different types of flood alleviation and finding a large number of landowners happy to implement NFM on their own land (Wells et al., 2020), it is understandable that not more case studies are available. Therefore, alongside the practical side of future research, focus on tackling the barriers to uptake of NFM overall is also

needed. Wells et al. (2020) provide useful summaries of issues highlighted by practitioners and landowners, with those being cited the most including a lack of evidence, governance and funding, in addition to perceptions of NFM and land manager interactions. Decreasing uncertainty regarding legislation, funding, liability and maintenance will ease implementation of more complex, larger projects.

Common paths forwards for the use of RAFs in both small and large catchments include a need to increase understanding of the hydrological and geomorphological response to cascades of RAFs given they will most likely be needed to increase the overall number of features within a catchment, but are also a stipulation in some English funding streams (e.g. Rural Payments Agency, 2020). The latest network modelling research by Hankin et al. (2020) suggests main arterial routes in the stream network may not necessarily be the preferred locations for cascades of leaky barriers due to an increase in the risk of failure. However, there is an overall lack of reporting of leaky barrier failure, which needs to be addressed to improve our knowledge of the resilience of systems of RAFs prior to an increase in RAF implementation.

In addition to the physical considerations, imperative for the future use of RAFs, is the need for increased landowner engagement to implement as many features as possible. As seen in Belford, an increase in landowner understanding led to more RAFs being implemented (Nicholson, 2013). Landowners will not want to give up productive land, with surveys by Holstead et al. (2017) suggesting over half of participants believe land was too valuable in its current form for NFM. Focusing on RAFs like offline ponds which are primarily dry unless in flood and increasing the understanding of geomorphological processes that may affect any feature implemented will also ease wider community uncertainty regarding potential failure or additional long term management that may be required, including the removal of sediment.

6.4.2 The future for geomorphological numerical modelling in NFM

Previous discussions have highlighted the likely future uses of the CAESAR-Lisflood and HEC-RAS 2D methodologies for NFM projects (Section 6.2.2). This section looks to consider potential issues or compromises that will need to be

addressed in the future when using CAESAR-Lisflood or HEC-RAS 2D to assess geomorphological effects of RAFs.

Chapter 4 provided the first known comparison between the geomorphological outputs of a landscape evolution model (CAESAR-Lisflood) and the estimated geomorphological processes calculated using shear stress from depth and velocity outputs from a hydraulic model (HEC-RAS 2D) to assess whether geomorphological understanding can be gained without the use of a morphodynamic model. The comparison showed longitudinal changes in geomorphological patterns of erosion and deposition were similar between both models, albeit qualitatively. However, quantitative agreement between CAESAR-Lisflood and HEC-RAS 2D was low (< 25 % agreement, Figure 4.4). The spatial extent of geomorphological processes was also overestimated due to the shear stress methodology assuming each wet cell had an associated geomorphological process and the CAESAR-Lisflood methodology assuming all net elevation change was of the same magnitude. Such assumptions for each methodology will therefore result in “worst-case scenario” interpretations which may be unrepresentative of the real world. The geomorphological outputs from both numerical models should therefore be validated. Data to do this should be from monitored catchments, with erosion pins, sediment mats, bedload pressure sensors and repeat high resolution topographic surveying providing possible validation data. Once greater understanding of model disagreement and spatial overestimation of geomorphological processes has been established, the shear stress methodology used in Chapter 4 can be refined through the use of machine learning to more accurately represent geomorphological processes over wider spatial scales. Such refinement would require easily accessible validation data across wider spatial scales at high resolution through the use of repeat topographic surveys and aerial imagery to enable validation with less field effort.

As mentioned previously, the lack of morphodynamics in HEC-RAS 2D and other hydraulic models will limit the applicability of the shear stress methodology and will likely be unsuitable in highly active systems (Section 6.2.2). A limitation also highlighted by Reid et al. (2019) who used a similar shear stress methodology to assess gravel bar reworking. This assumption however, is yet to be fully tested and future work should look at the applying the shear stress methodology to a wide range of catchment types and catchment sizes. If additional evidence can

be gained to validate the HEC-RAS 2D methodology's ability to assess geomorphological processes across a range of settings, it will open up the aforementioned opportunity to assess indicative geomorphological change from a standardised process through the re-purposing of model outputs created as part of the national flood maps.

This thesis has focused on single flood events, but in reality the response of the fluvial system to a rainfall event depends on external factors too. Floods frequently have multiple peaks and multiple flood events can occur over short periods of time for which the response of RAFs will differ to the response to a single flood peak (Metcalfe et al., 2017). Understanding the response over longer time scales (e.g. multiple years) has also been highlighted by Addy and Wilkinson (2019) for in-stream wood. Chapter 5 highlighted the hydrological and geomorphological impacts of increasing magnitudes of a single flood event on a single leaky barrier. It would therefore be expected that multiple events or multi-peaked events with different peak flow discharges, durations and recovery times would result in a complex geomorphological response with multiple phases of sediment erosion and deposition occurring through time (Garcia et al., 2000). Therefore to fully understand the capability of the HEC-RAS 2D shear stress methodology, but also CAESAR-Lisflood to accurately predict the geomorphological response to RAFs, increasing the complexity of the rainfall events simulated would be beneficial.

Additionally, geomorphological change outside of major flooding events should be considered. As shown by Barber and Quinn (2012), suspended sediment deposition occurred between flood events. Validating the models' ability to capture these smaller, more frequent contributions will allow for a more well-rounded understanding of their application to assess possible long term management needs including the removal of sediment build up through time.

This thesis has utilised a number of different grid resolutions in its models and so has also provided an interesting discussion point around the most suitable resolution to efficiently model NFM measures (Table 6.2). Lower modelling resolutions are likely to be needed, particularly for larger catchments, where computational efficiency and issues with increased data requirements may compromise the level of detail that can be achieved without unnecessarily large uncertainties (Lane, 2017). The work of Chapter 3, where RAFs were simulated

as topographic changes in a 4 m resolution DTM was the lowest model resolution used to model the entire ~41 km^2 Eastburn Beck catchment. Topographic modifications at a 4 m resolution may be thought of as an over-simplification given the inability to represent leakiness and with the width of the simulated RAFs (4 m) being greater than some types constructed in the real world (e.g. logs used in leaky barriers are < 1 m in diameter, Linstead and Gurnell (1999)). Further testing is therefore needed to assess the impact of such simplified topographic representations of RAFs, without the ability to represent leakiness, particularly on the timing of storage. Having available flood water storage coincide with the peak of the flood event is important to ensure effective use of an individual RAF (Nicholson et al., 2020).

The highest resolution tested in this project was used in the modelled reach (0.11 km^2) of Chapter 5, at 0.5 m resolution. Here detailed differences, such as the increase in shear stress within a 0.5 m radius of the culvert location occurring from increasing the height of the gap underneath the leaky barrier and the heterogeneity of shear stress across the floodplain could be identified. Using a hydraulic structure representation of a leaky barrier at a high model resolution could be used in future projects to aid understanding of specific elements of a feature's design, as it has been used in this project. Design elements to consider using this methodology for include the size and height of inflow/outflow infrastructure, levels of leakiness or changes needed for extension onto the floodplain. Future work should therefore look into the compromise between detailed representation of NFM measures, the increased model resolution required, the subsequent reduction in catchment size able to be modelled and potential increases in uncertainty in modelling outputs (Vaze et al., 2010). This analysis could be aided by the use of 3D flow hydraulics to identify important processes, particularly relating to the representation of NFM measures, to have a greater understanding of the effects of decreasing the complexity of the modelling.

Table 6.2: Model resolution, spatial extent and run times as a guide for future model applications.

Model	**CAESAR-Lisflood**			**HEC-RAS 2D**	
DEM resolution (m)	2	4	10	0.5	2
Spatial extent (km^2)	15	50	50	0.15	15
Approximate time taken to simulate 1 hour (h)	0.77	0.11	0.009	0.11	0.23
	(lower value = more efficient)				
Machine used	OEGStone CS-B x64-based PC, with an Intel® Core™ i7-4790 @ 3.60GHz processor, 16GB RAM and 250GB SSD Hard drive NB: Run times increase with increasing geomorphological activity			Lenovo X1 Carbon x64-based Laptop with an Intel® Core™ i7-6600U @ 2.60GHz processor, 8GB RAM and 250GB SSD Hard drive NB: Lower resolution computational grid (5 m for 0.5 m DEM and 20 m for 2 m DEM) increases run time efficiency	

Finally, ambitious improvements could be made to both models, caveated with the need for greater computational efficiency in relation to the resolution compromises previously discussed. For HEC-RAS 2D and hydraulic models as a whole, the difficult task of including validated 2D morphodynamics without severely compromising model efficiency will revolutionise their use for geomorphological appraisal of projects, both for NFM and more traditional flood defence works. Not only would this increase their use in highly active catchments but also the accuracy to predict geomorphological change resulting from multi-peaked and complex series of rainfall events.

For CAESAR-Lisflood, the inclusion of functionality to simulate infrastructure such as inflow/outflow pipes and leakiness would provide a methodology that would more accurately represent the behaviour of RAFs constructed in real life. Including infrastructure would also allow for traditional structures such as culverts, bridges and weirs to be modelled. Improvements to model run times for higher resolution models would allow a greater understanding of larger catchments without losing the detail needed for smaller NFM measures.

For both models, one of the apprehensions surrounding wood in rivers is its risk of failure and subsequent movement downstream (Grabowski et al., 2019).

Models such as that of Ruiz-Villanueva et al. (2014) have shown simulating wood transport is possible. Providing such means of representing wood transport would increase understanding of the system as a whole and implications wood transport may have on local infrastructure (e.g. culverts and bridges) and would allow for the geomorphological impact of fallen or transported wood to be assessed, with novel applications to not just flood risk related projects but to ecological projects. The inclusion of dynamic movement of wood in models has also been cited as a knowledge gap by Addy and Wilkinson (2019).

6.5 Concluding remarks

Research untaken in this thesis has highlighted that geomorphology is important in natural flood management. Individual RAFs will both affect and be affected by the geomorphological response following their construction. Practitioners should be aware that changes in design of RAFs may result in increased erosion and deposition upstream, erosion to the feature itself, erosion to the bed below a feature and erosion and deposition on the adjacent floodplain. The relative importance of the geomorphological response will depend on the scale of any investigation as with the hydrological response, the geomorphological response is localised and impact decreases with distance downstream.

Using modelling to assess geomorphological response will depend on a project's size in terms of the actual catchment, of the RAFs themselves and quantity of the RAFs required. Modelling needs will also depend on a project's aims as to whether they are local or catchment focused and whether assessment is being made solely for flood risk purposes or more holistically. Practitioners are advised to use HEC-RAS 2D, or a similar hydraulic model, for localised, highly detailed problems for single flood events. CAESAR-Lisflood, or a similar morphodynamic model, should be used for all problems in highly active catchments, in larger scale catchments and larger scale NFM problems (e.g. river restoration) and if long term management needs are important. Both types of models would provide invaluable insight into effective locations for NFM measures. The use of geomorphological modelling has been shown to and should be continued to be used in the evidence of the geomorphological response to NFM. Greater understanding will be important to decrease the uncertainty of NFM impact on the surrounding area and will hopefully subsequently increase engagement and

uptake as a substantial number of interventions will be required to aim towards decreasing flood risk in a climate resilient way.

Chapter 7
Conclusions

This thesis as a whole has aimed to gain an understanding of the hydrological and geomorphological impact of runoff attenuation features through the use of numerical modelling across a number of spatial scales. The need for this work was underpinned by evidence gaps highlighted in the Environment Agency's WwNP Evidence Directory (Burgess-Gamble et al., 2017). The report identified that additional knowledge was needed regarding the design of RAFs and specifically (i) the response of RAFs to extreme events and (ii) the effects of RAFs at larger catchment scales. This chapter firstly summarises the major findings of this thesis and then provides conclusions with an outlook for future work.

7.1 Research summary

7.1.1 What are the hydrological and geomorphological impacts of runoff attenuation features implemented within a morphodynamic model at catchment scale?

The implemented RAFs were unable to reduce extreme flood risk at catchment scale (120 yr RP event in a ~41 km^2 catchment). A reduction in extreme flood risk would be an unlikely achievement without greatly increasing the storage to catchment size ratio to well beyond 10,000 m^3 of storage per km^2 of catchment. Implementing such large volumes of storage within a catchment adds challenges such as landowner agreement and increased project cost and management.

However, localised hydrological and geomorphological impacts were observed, with differences occurring as a result of changes made to RAF design. Firstly, increasing the size of a RAF increased the water volume stored upstream. A greater size of RAF also increased the likelihood of that feature being overtopped. Geomorphologically, an increase in RAF size resulted in increases both to the likelihood of erosion and deposition occurring upstream and the sediment volume being eroded or deposited. However, it should be noted that despite the hydrological benefits of increasing a RAF's size, an increase in the likelihood of erosion to the RAF itself was also identified.

Secondly, changing the shape of a RAF from linear to u-shaped also increased the water volume stored upstream and the likelihood of overtopping.

Geomorphologically, less erosion and deposition was seen upstream of RAFs when u-shaped in design compared to linear. However, the risk of erosion to the features themselves was greater for u-shaped RAFs than linear RAFs.

Thirdly, increasing the quantity of linear RAFs resulted in only small increases in water volume stored upstream. The double linear RAF scenario saw increased risk of overtopping alongside an increased risk in erosion to the features themselves. Increasing the quantity of RAFs also resulted in increases to both erosion and deposition occurring upstream of the RAFs.

Despite the lack of impact at catchment scale, practitioners should be aware of the localised geomorphological implications of altering the design of a RAF with the intention of increasing water storage and thus potential flood risk reduction. Increases to the likelihood of both erosion and deposition upstream of a feature should be considered, alongside the risk of erosion to a feature itself. Practitioners should voice these considerations to landowners, paying particular attention to the geomorphological impacts, alongside the risk of failure of a feature and possible implications failure may have to their land.

7.1.2 Can geomorphological processes be estimated without recourse to morphodynamic models?

Longitudinal changes in geomorphological processes were reproduced relatively well in HEC-RAS 2D through the calculation and classification of shear stress. Visual comparisons could be seen between the outputs from the HEC-RAS 2D shear stress methodology and CAESAR-Lisflood, alongside repeat aerial imagery and field evidence. Bed and bank erosion, floodplain deposition and gravel bars were all identifiable in both the geomorphological outputs calculated from HEC-RAS 2D and CAESAR-Lisflood.

However, quantitative assessment showed poor model agreement (< 25 %) between the geomorphological outputs from HEC-RAS 2D and CAESAR-Lisflood. This was perhaps due to the cell-by-cell nature of the metric calculation and differences in the two model methodologies. Differences included that firstly, the shear stress methodology used for HEC-RAS 2D does not take into account the fluvial system’s response to environmental changes occurring during a flood event. Changes to grain size, bed elevation and sediment availability will all influence the spatial patterns of geomorphological processes through time.

Secondly, the shear stress methodology used for HEC-RAS 2D uses the maximum depth and velocity values through time whereas CAESAR-Lisflood accounts for geomorphological changes for the event as a whole. In this respect the shear stress methodology can be thought of as an “erosion worst-case scenario” and may underrepresent deposition occurring whilst river levels return to baseflow conditions. The spatial extent of geomorphological processes was also overestimated in both models due to for HEC-RAS 2D each wet cell being assigned a geomorphological process and in CAESAR-Lisflood, all magnitudes of net elevation change being classified as one.

A high quantitative agreement may not be necessary for a lot of applications, however, the aforementioned methodological differences and discrepancies in spatial extent warrant further validation to ensure both numerical models can accurately represent geomorphological processes. Observations from field evidence or monitoring data should be used for a number of catchment types and flood events in favour of a comparison with a morphodynamic model. Once more validation evidence has been gathered, the shear stress methodology can be used on national flood risk map depth and velocity grids, providing a wealth of geomorphological information across the country.

7.1.3 How does leaky barrier design affect the hydrological and geomorphological impact at increasing event magnitudes at reach scale?

Firstly, with regard to leaky barrier design, increasing the height of the gap beneath a leaky barrier resulted in a decrease in localised peak discharge reductions, reduced water volume held upstream and reduced floodplain inundation. However, overtopping of the leaky barrier decreased with increasing height of the gap beneath the leaky barrier. Geomorphologically, increasing the gap beneath the barrier resulted in an increase in erosion and decrease in deposition upstream of the leaky barrier in addition to a decrease in shear stress on the floodplain. Increasing the height of the gap beneath the leaky barrier also increased the shear stress underneath the barrier.

The second design adjustment was to the size of the leaky barrier to allow for extension onto the floodplain. This resulted in increases to the localised reductions in peak discharge, increases to the volume of water held upstream

and increased floodplain inundation alongside a decrease in barrier overtopping. There was little difference in erosion upstream, but an increase in deposition was seen when extending the leaky barrier. Downstream, the extended leaky barrier resulted in less erosion but more deposition than the original barrier design. On the floodplain, shear stress increased when the leaky barrier was extended. For the gap underneath the leaky barrier, extending the leaky barrier increased the shear stress observed.

Hydrological and geomorphological impacts were also seen when increasing flood magnitude. Local peak discharge reductions were seen to increase, as did water volume held upstream and on the floodplain. Geomorphologically, there was little difference in erosion upstream of the leaky barrier for the smaller flood events, but erosion increased for the larger magnitude events (> 100 yr RP). Deposition increased with increasing flood magnitude before decreasing for the largest event tested (1000 yr RP). There was little difference for shear stress underneath the barrier, but floodplain shear stress increased with increasing flood magnitude. Findings should be scaled up with caution given only a single barrier was tested and peak discharge reductions were only observed up to 300 m downstream of the leaky barrier.

The previously highlighted hydrological and geomorphological differences resulting from changes in leaky barrier design suggests that guidance for practitioners should firstly encourage extension of leaky barriers onto the floodplain and secondly include a flexible approach when deciding on the height of the gap beneath a leaky barrier. Awareness should also be raised for the risk of leaky barrier failure, given it was not simulated but does naturally occur yet is often underreported.

7.2 Implications and recommendations for future NFM projects

7.2.1 Use of RAFs

RAFs are unlikely to provide flood risk reduction for extreme events or for larger catchments because they are too small and hence an often unfeasibly high number are required to reduce extreme flood risk. This thesis has shown that the number of RAFs required to reduce flood risk needs to take into account less than 100 % effectiveness of the RAFs due to a lack of suitable locations, less than 100 % utilisation of potential storage from individual features and geomorphological

change decreasing efficiency or undermining individual features causing their failure. Additional concerns due to a need for large numbers of RAFs include landowner uptake and a lack of clear governance and funding opportunities. Given the large numbers of RAFs needed for extreme events or larger catchments, practitioners will likely need to combine NFM measures with more traditional flood defence works to achieve the desired standard of protection. The use of RAFs alone is most likely to be possible in small catchments, with small contributing areas, where flood risk is characterised by small return period events. For such situations, previously studies have shown RAFs to be able to reduce flood risk (e.g. Belford). When using RAFs, consideration should be made to the implications a change in design may have not just hydrologically, but also geomorphologically. This thesis has quantified the response to changes in a RAF's shape, size, quantity, leakiness and ability to allow floodplain connection and can be used as a guide for what differences may be likely given a change in design.

Future research should look to provide a greater number of real world examples of where RAFs have made a positive difference to flood risk in smaller catchments. Synthesising current knowledge alongside an increase in the number of real world examples will allow for a threshold of potential storage required per catchment size to be gained whereby after a point, RAFs will likely not reduce flood risk alone and should be combined with other defence works. Providing such evidence will help projects understand their needs of a mixture of NFM and defence works. Given the increase in cost of constructing more traditional defences, future research should look to identify the most cost-effective combinations of NFM and traditional defences with consideration of the additional holistic benefits of NFM including increased habitat heterogeneity and cultural appeal.

7.2.2 Use of numerical modelling

The use of numerical modelling to estimate geomorphological impacts of NFM will depend on the type and size of catchment and the types of NFM being constructed. The CAESAR-Lisflood methodology should be used for larger catchments applying larger scale, primarily topographic changes such as river restoration or floodplain reconnection. CAESAR-Lisflood could also be used to assess long term management needs.

The HEC-RAS 2D methodology should be used for smaller catchments with detail specific problems, including changes to design. HEC-RAS 2D should however, be avoided for highly active catchments where bed elevation and channel morphology changes rapidly. Here, CAESAR-Lisflood should be used.

Future numerical modelling of NFM measures should aim towards greater validation of a model's geomorphological outputs. The use of erosion pins, sedimentation mats and bedload pressure sensors can provide point based sediment transport validation data. Successive high resolution topographic surveying campaigns can provide net geomorphological change data for an event or longer timescales for larger spatial extents.

Ambitious improvements to both CAESAR-Lisflood and HEC-RAS 2D could be made to more accurately represent NFM in the real world. For CAESAR-Lisflood, the ability to simulate leakiness or inflow/outflow structures such as through the ability to implement hydraulic structures would notably improve the accuracy of representing RAFs, particularly at higher spatial resolutions. For HEC-RAS 2D, the difficult task of including a computationally efficient representation of morphodynamics would allow for more accurate applications in a wider range of catchments. In both models, simulation of wooden structure failure (e.g. leaky barriers) through a statistical probability relationship would decrease uncertainty in the understanding of when a structure might fail. However the additional complexity of representing the physical processes of wood movement would also allow for an understanding of the implications the transported material would have on downstream flood risk.

7.2.3 Climate change

Climate change should be accounted for when designing NFM projects if they are to maintain the same standard of protection in the future with more features being needed to provide additional flood storage. Future work could also look into the innovation of adaptive designs including how to alter the size of the gap beneath a leaky barrier over time to account for longer term changes in river levels. Community engagement will also be essential to increase awareness of the necessity of additional features now to allow us to provide climate resilience for the future.

References

Abbe, T.B. and Montgomery, D.R. 1996. Large woody debris jams, channel hydraulics and habitat formation in large rivers. *Regulated Rivers: Research and Management*. **12**(2-3), pp.201-221.

Abbe, T.B. and Montgomery, D.R. 2003. Patterns and processes of wood debris accumulation in the Queets river basin, Washington. *Geomorphology*. **51**(1-3), pp.81-107.

Adams, R., Quinn, P., Barber, N. and Reaney, S. 2018. The role of attenuation and land management in small catchments to remove sediment and phosphorus: A modelling study of mitigation options and impacts. *Water*. **10**(9), pp.1-18.

Addy, S. and Wilkinson, M.E. 2016. An assessment of engineered log jam structures in response to a flood event in an upland gravel-bed river. *Earth Surface Processes and Landforms*. **41**(12), pp.1658-1670.

Addy, S. and Wilkinson, M.E. 2019. Representing natural and artificial in-channel large wood in numerical hydraulic and hydrological models. *Wiley Interdisciplinary Reviews: Water*. **6**(6), pp. 1-20.

Ahilan, S., Guan, M., Wright, N., Sleigh, A., Allen, D., Arthur, S., Haynes, H. and Krivtsov, V. 2019. Modelling the long-term suspended sedimentological effects on stormwater pond performance in an urban catchment. *Journal of Hydrology. **571***, pp.805-818.

Anderson, B.G., Rutherfurd, I.D. and Western, A.W. 2006. An analysis of the influence of riparian vegetation on the propagation of flood waves. *Environmental Modelling & Software*. **21**(9), pp.1290-1296.

Arnaud-Fassetta, G., Astrade, L., Bardou, E., Corbonnois, J., Delahaye, D., Fort, M., Gautier, E., Jacob, N., Peiry, J.L., Piégay, H. & Penven, M.J. 2009. Fluvial geomorphology and flood-risk management. *Géomorphologie: Relief, Processus, Environnement*. **15**(2), pp. 109-128.

Arnell, N.W. and Gosling, S.N. 2016. The impacts of climate change on river flood risk at the global scale. *Climatic Change*. **134**(3), pp.387-401.

Asahi, K., Shimizu, Y., Nelson, J. & Parker, G. 2013. Numerical simulation of river meandering with self-evolving banks. *Journal of Geophysical Research: Earth Surface*. **118**(4), pp. 2208-2229.

Barber, N.J. 2013. *Sediment, nutrient and runoff management and mitigation in rural catchments.* PhD Thesis, Newcastle University.

Barber, N.J. and Quinn, P.F. 2012. Mitigating diffuse water pollution from agriculture using soft-engineered runoff attenuation features. *Area*. **44**(4), pp.454-462.

Barker, L., Hannaford, J., Muchan, K., Turner, S. & Parry, S. 2016. The winter 2015/2016 floods in the UK: a hydrological appraisal. *Weather*. **71**(12), pp. 324-333.

Bates, P.D., Horritt, M.S. and Fewtrell, T.J. 2010. A simple inertial formulation of the shallow water equations for efficient two-dimensional flood inundation modelling. *Journal of Hydrology.* **387**(1-2), pp.33-45.

Bayliss, A. 1999. *Flood Estimation Handbook: Catchment Descriptors*. Wallingford: Institute of Hydrology.

Berg, M.D., Popescu, S.C., Wilcox, B.P., Angerer, J.P., Rhodes, E.C., McAlister, J. and Fox, W.E. 2016. Small farm ponds: overlooked features with important impacts on watershed sediment transport. *Journal of the American Water Resources Association*, **52**(1), pp.67-76.

Beschta, R.L. 1983. The effects of large organic debris upon channel morphology: a flume study. In*: Proceedings of D.B. Simons Symposium on Erosion and Sedimentation, Fort Collins, CO*, pp. 8-63-8-78.

Beven, K.J. & Kirkby, M.J. 1979. A physically based, variable contributing area model of basin hydrology/Un modèle à base physique de zone d'appel variable de l'hydrologie du bassin versant. *Hydrological Sciences Journal.* **24**(1), pp. 43-69.

Beven, K. 1997. TOPMODEL: a critique. *Hydrological Processes*. **11**(9), pp.1069-1085.

Bizzi, S. and Lerner, D.N. 2015. The use of stream power as an indicator of channel sensitivity to erosion and deposition processes. *River Research and Applications*, **31**(1), pp.16-27.

Blanc, J., Wright, G. and Arthur, S. 2012. *Natural Flood Management (NFM) knowledge system: The effect of NFM features on the desynchronising of flood peaks at a catchment scale*. Aberdeen: Centre of Expertise for Waters.

Brainard, A.S. and Fairchild, G.W. 2012. Sediment characteristics and accumulation rates in constructed ponds. *Journal of soil and water conservation*, **67**(5), pp.425-432.

Brunner, G.W. 2016. HEC-RAS River Analysis System 2D Modeling User's Manual. California: U.S. Army Corps of Engineers.

Buffington, J.M., Lisle, T.E., Woodsmith, R.D. and Hilton, S. 2002. Controls on the size and occurrence of pools in coarse-grained forest rivers. *River Research and Applications*, **18**(6), pp.507-531.

Burgess-Gamble, L., Ngai, R., Wilkinson, M., Nisbet, T., Pontee, N., Harvey, R., Kipling, K., Addy, S., Rose, S., Maslen, S. and Jay, H. 2017. *Working with Natural Processes–Evidence Directory, Report No. SC150005*. Bristol: Environment Agency.

Cabinet Office. 2016. *National Flood Resilience Review*. London: Cabinet Office.

Chatterton, J., Clarke, C., Daly, E., Dawks, S., Elding, C., Fenn, T., Heck, E., Miller, J., Ogunyoye, F. and Salado, R. 2016. *The costs and impacts of the winter 2013 to 2014 floods*. Bristol: Environment Agency.

Chatterton, J., Viavattene, C., Morris, J., Penning-Rowsell, E.C. and Tapsell, S.M. 2010. *The costs of the summer 2007 floods in England*. Bristol: Environment Agency.

Cherry, J. and Beschta, R.L. 1989. Coarse woody debris and channel morphology: a flume study. *Journal of the American Water Resources Association*. **25**(5), pp.1031-1036.

Chow, V.T. 1959. *Open-channel Hydraulics* (Vol. 1). New York: McGraw-Hill.

CIRIA. 2018. *CIRIA proposal- Guidance on natural flood management RP1094*. [Online]. [Accessed 7 May 2020]. Available from: https://www.ciria.org/Research/Projects_underway2/Guidance_on_natural_flood_management_RP1094.aspx

Coulthard, T.J. 2018. Error found in suspended sediment calculation. Versions 1.2 -1.9f. 14 October 2018. *CAESAR-Lisflood*. [Online]. [Accessed 7 December

2018]. Available from: https://groups.google.com/forum/#!topic/caesar-lisflood/LaojBr-13io

Coulthard, T.J. and Skinner, C.J. 2016. The sensitivity of landscape evolution models to spatial and temporal rainfall resolution. *Earth Surface Dynamics.* **4**(3), pp.757-771.

Coulthard, T.J. and Van De Wiel, M.J. 2006. A cellular model of river meandering. *Earth Surface Processes and Landforms.* **31**(1), pp.123-132.

Coulthard, T.J. and Van De Wiel, M.J. 2017. Modelling long term basin scale sediment connectivity, driven by spatial land use changes. *Geomorphology.* **277**, pp.265-281.

Coulthard, T.J., Neal, J.C., Bates, P.D., Ramirez, J., de Almeida, G.A. and Hancock, G.R. 2013. Integrating the LISFLOOD-FP 2D hydrodynamic model with the CAESAR model: implications for modelling landscape evolution. *Earth Surface Processes and Landforms*. **38**(15), pp.1897-1906.

Crookston, B.M. and Tullis, B.P. 2012. Scour prevention in bottomless arch culverts. *International Journal of Sediment Research*. **27**(2), pp.213-225.

Csiki, S. and Rhoads, B.L. 2010. Hydraulic and geomorphological effects of run-of-river dams. *Progress in Physical Geography*. **34**(6), pp.755-780.

Cunderlik, J.M., Ouarda, T.B. and Bobée, B. 2004. Determination of flood seasonality from hydrological records. *Hydrological Sciences Journal*. **49**(3), pp.511-526.

Dadson, S.J., Hall, J.W., Murgatroyd, A., Acreman, M., Bates, P., Beven, K., Heathwaite, L., Holden, J., Holman, I.P., Lane, S.N. and O'Connell, E. 2017. A restatement of the natural science evidence concerning catchment-based 'natural' flood management in the UK. *Proceedings of the Royal Society A: Mathematical, Physical and Engineering Sciences.* **473**(2199), pp.1-19.

Daniels, R.B. and Gilliam, J.W. 1996. Sediment and chemical load reduction by grass and riparian filters. *Soil Science Society of America Journal.* **60**(1), pp.246-251.

Davis, R.J. and Gregory, K.J. 1994. A new distinct mechanism of river bank erosion in a forested catchment. *Journal of Hydrology.* **157**(1-4), pp.1-11.

Davis, S.R., Brown, A.G. and Dinnin, M.H. 2007. Floodplain connectivity, disturbance and change: a palaeoentomological investigation of floodplain ecology from south-west England. *Journal of Animal Ecology*. **76**(2), pp.276-288.

De Serres, B., Roy, A.G., Biron, P.M. and Best, J.L. 1999. Three-dimensional structure of flow at a confluence of river channels with discordant beds. *Geomorphology.* **26**(4), pp.313-335.

Death, R.G., Fuller, I.C. and Macklin, M.G. 2015. Resetting the river template: The potential for climate-related extreme floods to transform river geomorphology and ecology. *Freshwater Biology*, **60**(12), pp.2477-2496.

DEFRA. 2005. *First Government response to the autumn 2004 making space for water consultation exercise*. London: DEFRA.

DEFRA. 2017. *New £1 million flood competition to protect more communities.* [Online]. [Accessed 27 April 2020]. Available from: https://www.gov.uk/government/news.

DEFRA. 2017. *Schemes across the country to receive £15 million of natural flood management funding*. [Online]. [Accessed 29th June 2020]. Available from: https://www.gov.uk/government/news/schemes-across-the-country-to-receive-15-million-of-natural-flood-management-funding

Dixon, S.J., Sear, D.A., Odoni, N.A., Sykes, T. and Lane, S.N. 2016. The effects of river restoration on catchment scale flood risk and flood hydrology. *Earth Surface Processes and Landforms*. **41**(7), pp.997-1008.

Dodd, J.A., Newton, M and Adams, C.E. 2016. *The effect of natural flood management in-stream wood placements on fish movement in Scotland*. Aberdeen: CREW.

Downs, P.W. and Gregory, K.J. 2004. *River channel management: Towards sustainable catchment hydrosystems*. London: Arnold.

Ebert, E.E., Janowiak, J.E. and Kidd, C. 2007. Comparison of near-real-time precipitation estimates from satellite observations and numerical models. *Bulletin of the American Meteorological Society*. **88**(1), pp.47-64.

Einstein, H.A. 1950. *The bed-load function for sediment transportation in open channel flows. Technical Bulletin No. 1026*. Washington D.C.: Department of Agriculture.

England, J., Skinner, K.S. and Carter, M.G. 2008. Monitoring, river restoration and the Water Framework Directive. *Water and Environment Journal*. **22**(4), pp.227-234.

Environment Agency. [no date]. *Long term flood risk.* [Online]. [Accessed 29 August 2021]. Available from: https://flood-warning-information.service.gov.uk/long-term-flood-risk

Environment Agency. 2001. *Lessons learned- Autumn 2000 floods*. Bristol: Environment Agency.

Environment Agency. 2009. *Flooding in England: A national assessment of flood risk*. Bristol: Environment Agency.

Environment Agency. 2012a. *Greater working with natural processes in flood and coastal erosion risk management*. Bristol: Environment Agency.

Environment Agency. 2012b. *Rural sustainable drainage systems (RSuDS).* Bristol: Environment Agency.

Environment Agency. 2016. *Adapting to Climate Change: Advice for Flood and Coastal Erosion Risk Management Authorities*. Bristol: Environment Agency.

Environment Agency. 2017. *Working with natural processes to reduce flood risk*. [Online]. [Accessed 29 June 2020]. Available from: https://www.gov.uk/government/publications/working-with-natural-processes-to-reduce-flood-risk

Environment Agency. 2018a. *Estimating the economic costs of the 2015 to 2016 winter floods*. Bristol: Environment Agency.

Environment Agency. 2018b. *Climate change impacts and adaptation.* Bristol: Environment Agency.

Environment Agency. 2019a. *Flood and coastal erosion risk management: long-term investment scenarios*. [Online]. [Accessed 16 September 2020]. Available from: https://www.gov.uk/government/publications/flood-and-coastal-risk-management-in-england-long-term-investment

Environment Agency. 2019b. *Climate Impacts Tool: Understanding the risks and impacts from a changing climate*. Bristol: Environment Agency.

Environment Agency. 2020. *National Flood and Coastal Erosion Risk Management Strategy for England*. Bristol: Environment Agency.

Environment, Food and Rural Affairs Committee (EFRA). 2014. *Winter floods 2013-2014*. London: House of Commons.

Farming and Wildlife Advisory Group (FWAG) South West. 2018. *Hills to Levels Information Sheet 11: Leaky woody dams*. Wellington: FWAG South West.

Faulkner, D. S. 1999. *Rainfall Frequency Estimation. Flood Estimation Handbook, Volume 2.* Wallingford: Institute of Hydrology.

Feeney, C.J., Chiverrell, R.C., Smith, H.G., Hooke, J.M. and Cooper, J.R. 2020. Modelling the decadal dynamics of reach-scale river channel evolution and floodplain turnover in CAESAR-Lisflood. *Earth Surface Processes and Landforms.* **45**(5), pp. 1273-1291.

Ferguson, C. and Fenner, R. 2020. Evaluating the effectiveness of catchment-scale approaches in mitigating urban surface water flooding. *Philosophical Transactions of the Royal Society A.* **378**(2168), p.20190203.

Fiener, P., Auerswald, K. and Weigand, S. 2005. Managing erosion and water quality in agricultural watersheds by small detention ponds. *Agriculture, Ecosystems and Environment*. **110**(3-4), pp.132-142.

Foulds, S.A. and Macklin, M.G. 2016. A hydrogeomorphic assessment of twenty-first century floods in the UK. *Earth Surface Processes and Landforms.* **41**(2), pp.256-270.

Fowler, H.J. and Ekström, M. 2009. Multi-model ensemble estimates of climate change impacts on UK seasonal precipitation extremes. *International Journal of Climatology.* **29**(3), pp.385-416.

Gao, J., Holden, J. and Kirkby, M. 2015. A distributed TOPMODEL for modelling impacts of land-cover change on river flow in upland peatland catchments. *Hydrological Processes*. **29**(13), pp.2867-2879.

Gao, J., Holden, J. and Kirkby, M. 2017. Modelling impacts of agricultural practice on flood peaks in upland catchments: An application of the distributed TOPMODEL. *Hydrological Processes.* **31**(23), pp.4206-4216.

Garcia, C., Laronne, J.B. and Sala, M. 2000. Continuous monitoring of bedload flux in a mountain gravel-bed river. *Geomorphology*. **34**(1-2), pp.23-31.

Ghimire, S., Wilkinson, M. and Donaldson-Selby, G. 2014. Application of 1D and 2D numerical models for assessing and visualizing effectiveness of Natural Flood Management (NFM) measures. In: *11th International Conference on Hydroinformatics, 17-21 August 2014, New York.* New York: CUNY Academic Works.

Gippel, C.J. 1995. Environmental hydraulics of large woody debris in streams and rivers. *Journal of Environmental Engineering*. **121**(5), pp.388-395.

Glendell, M. 2013. *Evaluating an ecosystem management approach for improving water quality on the Holnicote Estate, Exmoor*. PhD Thesis, University of Exeter.

Gomez, B. 1983. Temporal variations in bedload transport rates: the effect of progressive bed armouring. *Earth Surface Processes and Landforms*. **8**(1), pp. 41-54.

Grabowski, R.C., Gurnell, A.M., Burgess-Gamble, L., England, J., Holland, D., Klaar, M.J., Morrissey, I., Uttley, C. and Wharton, G. 2019. The current state of the use of large wood in river restoration and management. *Water and Environment Journal*. **33**(3), pp.366-377.

Graf, W.L. 2008. Sources of uncertainty in river restoration research. In: Darby, S. and Sear, D. eds. *River Restoration: Managing uncertainty in restoring physical habitat*. Chichester: Wiley, pp.15-21.

Grimaldi, S., Petroselli, A., Alonso, G. and Nardi, F. 2010. Flow time estimation with spatially variable hillslope velocity in ungauged basins. *Advances in Water Resources*. **33**(10), pp.1216-1223.

Gurnell, A. 2012. Wood and river landscapes. *Nature Geoscience*. **5**(2), pp.93-94.

Habib, E., Krajewski, W.F. and Kruger, A. 2001. Sampling errors of tipping-bucket rain gauge measurements. *Journal of Hydrologic Engineering.* **6**(2), pp.159-166.

Hancock, G.R. and Coulthard, T.J. 2012. Channel movement and erosion response to rainfall variability in southeast Australia. *Hydrological Processes*. **26**(5), pp.663-673.

Hancock, G.R., Lowry, J.B.C., Coulthard, T.J., Evans, K.G. and Moliere, D.R. 2010. A catchment scale evaluation of the SIBERIA and CAESAR landscape evolution models. *Earth Surface Processes and Landforms*. **35**(8), pp.863-875.

Hankin, B., Burgess-Gamble, L., Bentley, S. and Rose, S. 2016. *How to model and map catchment processes when flood risk management planning*. Environment Agency: Bristol,

Hankin, B., Chappell, N., Page, T., Kipling, K., Whitling, M. and Burgess-Gamble, L. 2018. *Mapping the potential for Working with Natural Processes – technical report, Report No. SC150005/R6.* Bristol: Environment Agency.

Hankin, B., Hewitt, I., Sander, G., Danieli, F., Formetta, G., Kamilova, A., Kretzschmar, A., Kiradjiev, K., Wong, C., Pegler, S. and Lamb, R. 2020. A risk-based network analysis of distributed in-stream leaky barriers for flood risk management. *Natural Hazards and Earth System Sciences.* **20**(10), pp.2567-2584.

Hankin, B., Metcalfe, P., Beven, K. and Chappell, N.A. 2019. Integration of hillslope hydrology and 2D hydraulic modelling for natural flood management. *Hydrology Research*. **50**(6), pp.1535-1548.

Hankin, B., Metcalfe, P., Craigen, I., Page, T., Chappell, N., Lamb, R., Beven, K. and Johnson, D. 2017. Strategies for testing the impact of natural flood risk management measures. In: Hromadka, T and Rao, P. eds. *Flood risk management*. Rijeka, Croatia: Intech, pp.1-39.

Hansson, K., Danielson, M. & Ekenberg, L. 2008. A framework for evaluation of flood management strategies. *Journal of Environmental Management*. **86**(3), pp. 465-480.

Harman, J., Bramley, M.E. and Funnell, M. 2002. Sustainable flood defence in England and Wales. *Proceedings of the Institution of Civil Engineers - Civil Engineering*. 1**50**(5), pp.3-9.

Harrison, D.L., Norman, K., Pierce, C. and Gaussiat, N. 2012. Radar products for hydrological applications in the UK. *Proceedings of the Institution of Civil Engineers-Water Management*, **165**(2), pp. 89-103.

Haschenburger, J.K. and Rice, S.P. 2004. Changes in woody debris and bed material texture in a gravel-bed channel. *Geomorphology*. **60**(3-4), pp.241-267.

Hester, N., Rose, S., Hammond, G. and Worrall, P. 2017. *Case study 20, From Source to Sea: the Holnicote experience, SC150005*. Bristol: Environment Agency.

Hilderbrand, R.H., Lemly, A.D., Dolloff, C.A. and Harpster, K.L. 1998. Design considerations for large woody debris placement in stream enhancement projects. *North American Journal of Fisheries Management*. **18**(1), pp.161-167.

Hilderbrand, R.H., Lemly, A.D., Dolloff, C.A. and Harpster, K.L. 1997. Effects of large woody debris placement on stream channels and benthic macroinvertebrates. *Canadian Journal of Fisheries and Aquatic Sciences*. **54**(4), pp.931-939.

Hogan, D.L. 1986. *Channel morphology of unlogged, logged and debris torrented streams in the Queen Charlotte Islands. British Columbia Ministry of Forests and Lands, Land Management Report 49*. Victoria BC: Research Branch, Ministry of Forests and Lands.

Holden, J., Gascoign, M. and Bosanko, N.R. 2007. Erosion and natural revegetation associated with surface land drains in upland peatlands. *Earth Surface Processes and Landforms.* **32**(10), pp.1547-1557.

Holden, J., Shotbolt, L., Bonn, A., Burt, T.P., Chapman, P.J., Dougill, A.J., Fraser, E.D.G., Hubacek, K., Irvine, B., Kirkby, M.J. and Reed, M.S. 2007. Environmental change in moorland landscapes. *Earth-Science Reviews.* **82**(1-2), pp.75-100.

Holstead, K.L., Kenyon, W., Rouillard, J.J., Hopkins, J. and Galán-Díaz, C. 2017. Natural flood management from the farmer's perspective: criteria that affect uptake. *Journal of Flood Risk Management*. **10**(2), pp.205-218.

Horritt, M.S. & Bates, P.D. 2001. Effects of spatial resolution on a raster based model of flood flow. *Journal of Hydrology*. **253**(1-4), pp. 239-249.

Howgate, O.R. and Kenyon, W. 2009. Community cooperation with natural flood management: a case study in the Scottish Borders. *Area*, **41**(3), pp.329-340.

Hunter, N.M., Bates, P.D., Neelz, S., Pender, G., Villanueva, I., Wright, N.G., Liang, D., Falconer, R.A., Lin, B., Waller, S. & Crossley, A.J. 2008. Benchmarking 2D hydraulic models for urban flood simulations. *Proceedings of the Institution of Civil Engineers-Water Management*. **161**(1), pp. 13-30.

Jacobson, C.R. 2011. Identification and quantification of the hydrological impacts of imperviousness in urban catchments: A review. *Journal of Environmental Management*. **92**(6), pp.1438-1448.

JBA Trust. 2020. *Developing Best Practice Guidance for Leaky Barriers*. [Online] Skipton: JBA Trust. [Accessed 11 July 2021]. Available from: https://www.jbatrust.org/wp-content/uploads/2020/01/Sam-Bailey-summary-poster.pdf

Jeffries, R., Darby, S.E., Sear, D.A. 2003. The influence of vegetation and organic debris on flood-plain sediment dynamics: Case study of a low-order stream in the New Forest, England. *Geomorphology.* **51**(1-3), pp.61-80.

Jones, P.D. and Conway, D. 1997. Precipitation in the British Isles: an analysis of area-average data updated to 1995. *International Journal of Climatology*. **17**(4), pp.427-438.

Kail, J. 2003. Influence of large woody debris on the morphology of six central European streams. *Geomorphology*. **51**(1-3), pp.207-223.

Kalyanapu, A.J., Burian, S.J. and McPherson, T.N., 2009. Effect of land use-based surface roughness on hydrologic model output. *Journal of Spatial Hydrology*, **9**(2).

Kay, A.L., Davies, H.N., Bell, V.A. and Jones, R.G. 2009. Comparison of uncertainty sources for climate change impacts: flood frequency in England. *Climatic change.* **92**(1-2), pp.41-63.

Kay, A.L., Jones, R.G. and Reynard, N.S. 2006. RCM rainfall for UK flood frequency estimation. II. Climate change results. Journal of Hydrology. **318**(1-4), pp.163-172.

Kendon, E.J., Roberts, N.M., Fowler, H.J., Roberts, M.J., Chan, S.C. and Senior, C.A. 2014. Heavier summer downpours with climate change revealed by weather forecast resolution model. *Nature Climate Change.* **4**(7), pp.570-576.

Kendon, M. and McCarthy, M. 2015. The UK's wet and stormy winter of 2013/2014. *Weather*. **70**(2), pp.40-47.

Keys, T.A., Govenor, H., Jones, C.N., Hession, W.C., Hester, E.T. and Scott, D.T. 2018. Effects of large wood on floodplain connectivity in a headwater Mid-Atlantic stream. *Ecological Engineering*. **118**, pp.134-142.

Kjeldsen, T.R., Prudhomme, C., Svensson, C. and Stewart, E.J. 2006. A shortcut to seasonal design rainfall estimates in the UK. *Water and Environment Journal*. **20**(4), pp.282-286.

Kjeldsen, T.R., Stewart, E.J., Packham, J.C., Folwell, S. & Bayliss, A.C. 2005. *Revitalisation of the FSR/FEH rainfall-runoff method. Defra R&D Technical Report FD1913/TR*. Wallingford: CEH Wallingford.

Lane, S.N. & Ferguson, R.I. 2005. Modelling reach-scale fluvial flows. In P.D. Bates, S.N. Lane & R.I. Ferguson (eds), *Computational Fluid Dynamics: Applications in Environmental Hydraulics*. Chichester: Wiley-Blackwell, pp. 215-269.

Lane, S.N. 2017. Natural flood management. *Wiley Interdisciplinary Reviews: Water*. **4**(3), p.1211.

Lane, S.N. and Ferguson, R.I. 2005. Modelling reach-scale fluvial flows. In: P.D. Bates, S.N. Lane and R.I. Ferguson (eds), *Computational Fluid Dynamics: Applications in Environmental Hydraulics*. Chichester: Wiley-Blackwell, pp. 215-269.

Lavelle, J.W. and Mofjeld, H.O. 1987. Do critical stresses for incipient motion and erosion really exist? *Journal of Hydraulic Engineering.* **113**(3), pp.370-385.

Law, A., McLean, F. and Willby, N.J. 2016. Habitat engineering by beaver benefits aquatic biodiversity and ecosystem processes in agricultural streams. *Freshwater Biology.* **61**(4), pp.486-499.

Lawley, R. 2012. *User Guide: Soil Parent Material 1 Kilometre dataset (OR/14/025)*. Nottingham: British Geological Survey.

Leakey, S., Hewett, C.J., Glenis, V. and Quinn, P.F. 2020. Modelling the impact of leaky barriers with a 1D Godunov-type scheme for the shallow water equations. *Water.* **12**(2), pp1-28.

Linstead, C. and Gurnell, A.M. 1999. *Large woody debris in British headwater rivers, physical habitat role and management guidelines. R&D Technical Report W181*. Bristol: Environment Agency.

Liriano, S.L., Day, R.A. and Rodney White, W. 2002. Scour at culvert outlets as influenced by the turbulent flow structure. *Journal of Hydraulic Research*. **40**(3), pp.367-376.

Lisle, T.E., Cui, Y., Parker, G., Pizzuto, J.E. & Dodd, A.M. 2001. The dominance of dispersion in the evolution of bed material waves in gravel-bed rivers. *Earth Surface Processes and Landforms*. **26**(13), pp. 1409-1420.

Marchi, L., Borga, M., Preciso, E., Sangati, M., Gaume, E., Bain, V., Delrieu, G., Bonnifait, L. and Pogačnik, N. 2009. Comprehensive post-event survey of a flash flood in Western Slovenia: observation strategy and lessons learned. *Hydrological Processes.* **23**(26), pp.3761-3770.

Marks, S.D. and Rutt, G.P. 1997. Fluvial sediment inputs to upland gravel bed rivers draining forested catchments: potential ecological impacts. *Hydrology and Earth System Sciences Discussions*. **1**(3), pp.499-508.

Marsh, T.J. and Hannaford, J. 2007. *The summer 2007 floods in England and Wales–a hydrological appraisal*. Wallingford: Centre for Ecology & Hydrology.

Marsh, T.J., Kirby, C., Muchan, K., Barker, L., Henderson, E. and Hannaford, J. 2016. *The winter floods of 2015/2016 in the UK - a review*. Wallingford: Centre for Ecology and Hydrology.

McAlinden, B. 2016. Slowing the Flow at Pickering. [Online]. [Accessed 26 October 2020]. Available from: https://www.ice.org.uk/knowledge-and-resources/case-studies/slowing-the-flow-at-pickering

McHugh, M., Wood. G., Walling, D., Morgan, R., Zhang, Y., Anthony, S. and Hutchins, M. 2002. *Prediction of Sediment Delivery to Watercourses from Land Phase II*. Bristol: Environment Agency.

Meadows, T. 2014. *Forecasting long-term sediment yield from the upper North Fork Toutle River, Mount St. Helens, USA*. PhD thesis, University of Nottingham.

Metcalfe, P., Beven, K. and Freer, J. 2015. Dynamic TOPMODEL: A new implementation in R and its sensitivity to time and space steps. *Environmental Modelling & Software*. **72**, pp.155-172.

Metcalfe, P., Beven, K., Hankin, B. and Lamb, R. 2017. A modelling framework for evaluation of the hydrological impacts of nature-based approaches to flood risk management, with application to in-channel interventions across a 29-km^2 scale catchment in the UK. *Hydrological Processes.* **31**(9), pp. 1734-1748.

Metcalfe, P., Beven, K., Hankin, B. and Lamb, R. 2018. A new method, with application, for analysis of the impacts on flood risk of widely distributed

enhanced hillslope storage. *Hydrology and Earth System Sciences*. **22**(4), pp.2589-2605.

Minitab. 2019. *Kruskal Wallis multiple comparisons.* [Online]. [Accessed 28 August 2021]. Available from: https://support.minitab.com

Montgomery, D.R., Collins, B.D., Buffington, J.M. and Abbe, T.B. 2003. Geomorphic effects of wood in rivers. *American Fisheries Society Symposium*. 37, pp.21-47.

Mott Macdonald. 2020. *Mott MacDonald to develop UK guidance on the delivery of natural flood management measures*. [Online]. [Accessed 17 September 2020]. Available from: https://www.mottmac.com/releases/mott-macdonald-to-develop-uk-guidance-on-the-delivery-of-natural-flood-management-measures

Muchan, K., Matthews, B., Turner, S., Crane, E., Lewis, M. and Clemas, S. 2019. *Hydrological summary for the United Kingdom: November 2019.* Wallingford: Centre for Ecology and Hydrology.

Muhawenimana, V. 2019. *Ecohydraulics of instream flow alterations*. Ph.D. thesis, Cardiff University.

Nagayama, S. and Nakamura, F. 2010. Fish habitat rehabilitation using wood in the world. *Landscape and Ecological Engineering*. **6**(2), pp.289-305.

Nakamura, F. and Swanson, F.J. 1993. Effects of coarse woody debris on morphology and sediment storage of a mountain stream system in western Oregon. *Earth Surface Processes and Landforms.* **18**(1), pp.43-61.

National River Flow Archive. [no date]. *27084 – Eastburn Beck at Crosshills*. [Online]. [Accessed 1 June 2020]. Available from: https://nrfa.ceh.ac.uk/data/station/info/27084

National Trust, 2015. *From source to sea: natural flood management – the Holnicote experience*. Swindon: National Trust.

Neuhold, C., Stanzel, P. & Nachtnebel, H.P. 2009. Incorporating river morphological changes to flood risk assessment: uncertainties, methodology and application. *Natural Hazards and Earth System Sciences*. **9**(3), pp. 789-799.

Ngai, R., Wilkinson, M., Nisbet, T., Harvey, R., Addy, S., Burgess-Gamble, L., Rose, S., Maslen, S., Nicholson, A., Page, T., Jonczyk, J. and Quinn, P. 2017.

Working with Natural Processes–Evidence Directory, Appendix 2: Literature Review, Report No. SC150005. Bristol: Environment Agency.

Nicholas, A.P. 2013. Modelling the continuum of river channel patterns. *Earth Surface Processes and Landforms*. **38**(10), pp. 1187-1196.

Nichols, R.A. and Ketcheson, G.L. 2013. A Two-Decade Watershed Approach to Stream Restoration Log Jam Design and Stream Recovery Monitoring: Finney Creek, Washington. *Journal of the American Water Resources Association.* **49**(6), pp.1367-1384.

Nicholson, A.R. 2013. *Quantifying and simulating the impact of flood mitigation features in a small rural catchment*. PhD Thesis, Newcastle University.

Nicholson, A.R., O'Donnell, G.M., Wilkinson, M.E. and Quinn, P.F. 2020. The potential of runoff attenuation features as a Natural Flood Management approach. *Journal of Flood Risk Management*. **13**(S1), p.e12565.

Nicholson, A.R., Quinn, P. and Wilkinson, M. 2017. *Case study 16, Belford Natural Flood Management Scheme, Northumberland*. Bristol: Environment Agency.

Nicholson, A.R., Wilkinson, M.E., O'Donnell, G.M. and Quinn, P.F. 2012. Runoff attenuation features: a sustainable flood mitigation strategy in the Belford catchment, UK. *Area.* **44**(4), pp.463-469.

Nisbet, T. 2017. Slowing the flow at Pickering. In: Edwards, D., Morris, J. and O'Brien, L. eds. *Forest Research Impact Case Studies, Interim Report*. [no place]: Forest Research, pp.23-31

Nisbet, T., Roe, P., Marrington, S., Thomas, H., Broadmeadow, S. and Valatin, G. 2015. *Project RMP5455: Slowing the Flow at Pickering, Final Report Phase II*. London: DEFRA.

Nisbet, T., Thomas, H. and Roe, P. 2017. *Working with Natural Processes – Case study 12: Slowing the flow at Pickering, Report No. SC150005.* Bristol: Environment Agency.

North Yorkshire County Council (NYCC). [no date]. *Flood Investigation Report, South Craven.* [Online]. Northallerton: North Yorkshire County Council. [Accessed 29 August 2021]. Available from: https://www.northyorks.gov.uk/flood-and-water-management

O'Connell, P.E., Ewen, J., O'Donnell, G. and Quinn, P. 2007. Is there a link between agricultural land-use management and flooding? *Hydrological Earth System Sciences*. **11**(1), pp.96-107.

Office of Science and Technology (OST). 2004. *Foresight. Future Flooding. Executive Summary.* London: Office of Science and Technology.

Olsen, A.S., Zhou, Q., Linde, J.J. and Arnbjerg-Nielsen, K. 2015. Comparing methods of calculating expected annual damage in urban pluvial flood risk assessments. *Water*. **7**(1), pp.255-270.

Palmer, M.W. 2012. *Agricultural fine sediment: Sources, pathways and mitigation.* PhD Thesis, Newcastle University.

Pan, C. and Shangguan, Z. 2006. Runoff hydraulic characteristics and sediment generation in sloped grassplots under simulated rainfall conditions. *Journal of Hydrology*. **331**(1-2), pp.178-185.

Parry, L.E., Holden, J. and Chapman, P.J. 2014. Restoration of blanket peatlands. *Journal of Environmental Management. **133***, pp.193-205.

Parry, S., Marsh, T. and Kendon, M. 2013. 2012: from drought to floods in England and Wales. *Weather*. **68**(10), pp.268-274.

Penning-Rowsell, E.C. 2014. A realistic assessment of fluvial and coastal flood risk in England and Wales. *Transactions of the Institute of British Geographers.* **40**(1), pp.44-61.

Pinto, C., Ing, R., Browning, B., Delboni, V., Wilson, H., Martyn, D. and Harvey, G.L. 2019. Hydromorphological, hydraulic and ecological effects of restored wood: findings and reflections from an academic partnership approach. *Water and Environment Journal*. **33**(3), pp.353-365.

Pitt, M. 2008. *Learning lessons from the 2007 floods*. London: Cabinet Office.

Poeppl, R.E., Coulthard, T., Keesstra, S.D. and Keiler, M. 2019. Modelling the impact of dam removal on channel evolution and sediment delivery in a multiple dam setting. *International Journal of Sediment Research*. **34**(6), pp.537-549.

Quinn, P., O'Donnell, G., Nicholson, A., Wilkinson, M., Owen, G., Jonczyk, J., Barber, N., Hardwick, M., and Davies, G. 2013. *Potential use of Runoff Attenuation Features in small rural catchments for flood mitigation*. England: Newcastle University, Environment Agency, Royal Haskoning DHV.

Rajaratnam, N. and Berry, B. 1977. Erosion by circular turbulent wall jets. *Journal of Hydraulic Research*. **15**(3), pp.277-289.

Reaney, S.M., Lane, S.N., Heathwaite, A.L. and Dugdale, L.J. 2011. Risk-based modelling of diffuse land use impacts from rural landscapes upon salmonid fry abundance. *Ecological Modelling*, **222**(4), pp.1016-1029.

Reid, H.E., Williams, R.D., Brierley, G.J., Coleman, S.E., Lamb, R., Rennie, C.D. and Tancock, M.J. 2019. Geomorphological effectiveness of floods to rework gravel bars: insight from hyperscale topography and hydraulic modelling. *Earth Surface Processes and Landforms.* **44**(2), pp.595-613.

Renard, K.G. and Ferreira, V.A. 1993. RUSLE model description and database sensitivity. *Journal of Environmental Quality*. **22**(3), pp.458-466.

Reynard, N.S., Kay, A.L., Anderson, M., Donovan, B. and Duckworth, C. 2017. The evolution of climate change guidance for fluvial flood risk management in England. *Progress in Physical Geography.* **41**(2), pp.222-237.

Reynard, N.S., Prudhomme, C. and Crooks, S.M. 2001. The flood characteristics of large UK rivers: potential effects of changing climate and land use. Climatic Change. **48**(2-3), pp.343-359.

Robichaud, P.R., Pierson, F.B., Brown, R.E. and Wagenbrenner, J.W. 2008. Measuring effectiveness of three postfire hillslope erosion barrier treatments, western Montana, USA. *Hydrological Processes: An International Journal*. **22**(2), pp.159-170.

Robichaud, P.R., Wagenbrenner, J.W., Brown, R.E., Wohlgemuth, P.M. and Beyers, J.L. 2008. Evaluating the effectiveness of contour-felled log erosion barriers as a post-fire runoff and erosion mitigation treatment in the western United States. *International Journal of Wildland Fire*. **17**(2), pp.255-273.

Robison, E.G. and Beschta, R.L. 1990. Coarse woody debris and channel morphology interactions for undisturbed streams in southeast Alaska, USA. *Earth Surface Processes and Landforms*. **15**(2), pp.149-156.

Robson, A., Beven, K. and Neal, C. 1992. Towards identifying sources of subsurface flow: a comparison of components identified by a physically based runoff model and those determined by chemical mixing techniques. *Hydrological processes*. **6**(2), pp.199-214.

Rogers, S., Rose, S., Spence, J. and Hester, N. 2015. *Holnicote payments for ecosystem services (PES) pilot research project 2014-2015: Final Report to DEFRA on Project NR0156*. Buxton: Penny Anderson Associates Ltd.

Roni, P., Beechie, T., Pess, G. and Hanson, K. 2015. Wood placement in river restoration: fact, fiction, and future direction. *Canadian Journal of Fisheries and Aquatic Sciences*. **72**(3), pp.466-478.

Ruiz-Villanueva, V., Bladé, E., Sánchez-Juny, M., Marti-Cardona, B., Díez-Herrero, A. and Bodoque, J.M. 2014. Two-dimensional numerical modelling of wood transport. *Journal of Hydroinformatics*, **16**(5), pp.1077-1096.

Rural Payments Agency. 2020. *Countryside Stewardship: Higher Tier Manual*. Reading: Rural Payments Agency.

Rural Payments Agency. 2021. Countryside Stewardship: Higher Tier Manual. Annex 2c: Indicative designs for leaky woody dams. [Online]. Reading: Rural Payments Agency. [Accessed 11 July 2021]. Available from: https://www.gov.uk/guidance/countryside-stewardship-higher-tier-manual-for-agreements-starting-on-1-january-2022/annex-2c-indicative-designs-for-leaky-woody-dams

Sawyer, A.H., Bayani Cardenas, M. and Buttles, J. 2011. Hyporheic exchange due to channel-spanning logs. *Water Resources Research*. **47**(8), pp. 1-12.

Schalko, I., Lageder, C., Schmocker, L., Weitbrecht, V. and Boes, R.M. 2019. Laboratory Flume Experiments on the Formation of Spanwise Large Wood Accumulations: Part II—Effect on local scour. *Water Resources Research.* **55**(6), pp.4871-4885.

Schaller, N., Kay, A.L., Lamb, R., Massey, N.R., Van Oldenborgh, G.J., Otto, F.E., Sparrow, S.N., Vautard, R., Yiou, P., Ashpole, I. and Bowery, A. 2016. Human influence on climate in the 2014 southern England winter floods and their impacts. *Nature Climate Change.* **6**(6), pp.627-634.

Sear, D.A., Millington, C.E., Kitts, D.R. and Jeffries, R. 2010. Logjam controls on channel: floodplain interactions in wooded catchments and their role in the formation of multi-channel patterns. *Geomorphology*. **116**(3-4), pp.305-319.

Sefton, C., Matthews, B., Lewis, M. and Clemas, S. 2020. *Hydrological summary for the United Kingdom: February 2020.* Wallingford: Centre for Ecology and Hydrology.

SEPA. 2016. *Natural flood management handbook.* Stirling: SEPA

Shepherd, M., Labadz, J., Caporn, S., Crowle, A., Goodison, R., Rebane, M. and Waters, R. 2013. *Restoration of degraded blanket bog (NEER003).* York: Natural England.

Shields, A. 1936. Anwendung der Aehnlichkeitsmechanik und der Turbulenzforschung auf die Geschiebebewegung. PhD Thesis, *Technical University Berlin*.

Short, C., Clarke, L., Carnelli, F., Uttley, C. and Smith, B. 2019. Capturing the multiple benefits associated with nature-based solutions: Lessons from a natural flood management project in the Cotswolds, UK. *Land degradation & development*. **30**(3), pp.241-252.

Shuster, W.D., Bonta, J., Thurston, H., Warnemuende, E. and Smith, D.R. 2005. Impacts of impervious surface on watershed hydrology: a review. *Urban Water Journal*. **2**(4), pp.263-275

Shustikova, I., Domeneghetti, A., Neal, J.C., Bates, P. and & Attilio Castellarin. 2019. Comparing 2D capabilities of HEC-RAS and LISFLOOD-FP on complex topography. *Hydrological Sciences Journal*. **64**(14), pp.1769-1782.

Shuttleworth, E.L., Evans, M.G., Pilkington, M., Spencer, T., Walker, J., Milledge, D. and Allott, T.E. 2019. Restoration of blanket peat moorland delays stormflow from hillslopes and reduces peak discharge. *Journal of Hydrology X*. **2**, 100006.

Skinner, C.J., Coulthard, T.J., Schwanghart, W., Wiel, M.J. and Hancock, G. 2018. Global sensitivity analysis of parameter uncertainty in landscape evolution models. *Geoscientific Model Development*. **11**(12), pp.4873-4888.

Skinner, K.S. and Bruce-Burgess, L. 2005. Strategic and project level river restoration protocols—key components for meeting the requirements of the Water Framework Directive (WFD). *Water and Environment Journal*. **19**(2), pp.135-142.

Slowing the Flow Partnership. 2016. *Slowing the Flow Partnership Briefing: Boxing Day 2015 Flood Event*. Farnham: Forest Research.

Smock, L.A., Metzler, G.M. and Gladden, J.E. 1989. Role of debris dams in the structure and functioning of low-gradient headwater streams. *Ecology.* **70**(3), pp.764-775.

Stewardson, M. and Rutherfurd, I. 2008. Conceptual and mathematical modelling in river restoration: Do we have unreasonable confidence? In: Darby, S. and Sear, D. eds. *River Restoration: Managing uncertainty in restoring physical habitat*. Chichester: Wiley, pp.61-79.

Thomas, H. and Nisbet, T. 2012. Modelling the hydraulic impact of reintroducing large woody debris into watercourses. *Journal of Flood Risk Management*. **5**(2), pp.164-174.

Thorne, C. 2014. Geographies of UK flooding in 2013/4. *The Geographical Journal.* **180**(4), pp.297-309.

Trotter, S., Hodson, S., Lindop, S., Milner, S., McHale, S., Worman, C., Flitcroft, C. and Bonn, A. 2005. Gully blocking techniques. In: Evans, M., Allott, T., Holden, J., Flitcroft, C., and Bonn, A. eds. *Understanding Gully Blocking in Deep Peat.* Castleton: Moors for the Future, pp.11-26.

Valters, D. 2017. *Modelling catchment sensitivity to rainfall resolution and erosional parameterisation in simulations of flash floods in the UK.* Ph.D. thesis, University of Manchester.

Vaze, J., Teng, J. and Spencer, G. 2010. Impact of DEM accuracy and resolution on topographic indices. *Environmental Modelling & Software*. **25**(10), pp.1086-1098.

Verstraeten, G. and Poesen, J. 1999. The nature of small-scale flooding, muddy floods and retention pond sedimentation in central Belgium. *Geomorphology.* **29**(3-4), pp.275-292.

Wagenbrenner, J.W., MacDonald, L.H. and Rough, D. 2006. Effectiveness of three post-fire rehabilitation treatments in the Colorado Front Range. *Hydrological Processes: An International Journal*. **20**(14), pp.2989-3006.

Wallage, Z.E., Holden, J. and McDonald, A.T. 2006. Drain blocking: an effective treatment for reducing dissolved organic carbon loss and water discolouration in a drained peatland. *Science of the Total Environment*. **367**(2-3), pp.811-821.

Wallerstein, N. and Thorne, C.R. 1997. *Impacts of woody debris on fluvial processes and channel morphology in stable and unstable streams.* Nottingham: University of Nottingham.

Wallerstein, N.P. and Thorne, C.R. 2004. Influence of large woody debris on morphological evolution of incised, sand-bed channels. *Geomorphology.* **57**(1-2), pp.53-73.

Walsh, P., Jakeman, A. and Thompson, C. 2020. Modelling headwater channel response and suspended sediment yield to in-channel large wood using the Caesar-Lisflood landscape evolution model. *Geomorphology*, **363**. p.107209.

Waylen, K.A., Holstead, K.L., Colley, K. and Hopkins, J. 2018. Challenges to enabling and implementing Natural Flood Management in Scotland. *Journal of Flood Risk Management.* **11**, pp.S1078-S1089.

Wells, J. 2019. *Natural Flood Management: Assessing the barriers to wider implementation*. PhD Thesis, Nottingham Trent University.

Wells, J., Labadz, J.C., Smith, A. and Islam, M.M. 2020. Barriers to the uptake and implementation of natural flood management: A social-ecological analysis. Journal of flood risk management, **13**(S1), p.e12561.

Wentworth, C.K., 1922. A scale of grade and class terms for clastic sediments. *The Journal of Geology*. **30**(5), pp.377-392.

Wilby, R.L., Beven, K.J. and Reynard, N.S. 2007. Climate change and fluvial flood risk in the UK: More of the same? *Hydrological Processes.* **22**(14), pp.2511-2523.

Wilcock, P.R. & Crowe, J.C. 2003. Surface-based transport model for mixed-size sediment. *Journal of Hydraulic Engineering*. **129**(2), pp. 120-128.

Wildman, L.A. and MacBroom, J.G. 2005. The evolution of gravel bed channels after dam removal: Case study of the Anaconda and Union City Dam removals. *Geomorphology*. **71**(1-2), pp.245-262.

Wilkinson, M.E., Addy, S., Quinn, P.F. and Stutter, M. 2019. Natural flood management: small-scale progress and larger-scale challenges. *Scottish Geographical Journal*. **135**(1-2), pp.23-32.

Wilkinson, M.E., Holstead, K. and Hastings, E. 2013. *Natural Flood Management in the context of UK reservoir legislation*. Aberdeen: Centre of Expertise for Water.

Wilkinson, M.E., Quinn, P.F. and Welton, P. 2010. Runoff management during the September 2008 floods in the Belford catchment, Northumberland. *Journal of Flood Risk Management.* **3**(4), pp.285-295.

Wilkinson, M.E., Quinn, P.F., Barber, N.J. and Jonczyk, J. 2014. A framework for managing runoff and pollution in the rural landscape using a Catchment Systems Engineering approach. *Science of the Total Environment.* **468-469**, pp.1245-1254.

Wilkinson, M.E., Quinn, P.F., Benson, I. and Welton, P. 2010. Runoff management: mitigation measures for disconnecting flow pathways in the Belford Burn catchment to reduce flood risk. In: British Hydrological Society. ed. *British Hydrological Society International Symposium, 2010, Newcastle upon Tyne*. Newcastle upon Tyne: British Hydrological Society.

Wohl, E. 2011. Threshold-induced complex behavior of wood in mountain streams. *Geology.* **39**(6), pp.587-590.

Wohl, E. 2013. Floodplains and wood. *Earth-Science Reviews*. **123**, pp.194-212.

Wood-Smith, R.D. and Buffington, J.M. 1996. Multivariate geomorphic analysis of forest streams: implications for assessment of land use impacts on channel condition. *Earth Surface Processes and Landforms*. **21**(4), pp.377-393.

Yalin, M.S. & Karahan, E. 1979. Inception of sediment transport. *Journal of the Hydraulics Division*. **105**(11), pp. 1433-1443.

Yorkshire Dales National Park Authority (YDNPA). 2017. *Natural Flood Management- a practical guide for farmers*. Leyburn: YDNPA.

Yorkshire Dales Rivers Trust (YDRT). 2018a. *Naturally Resilient – Natural Flood Management techniques Level 2, Leaky Dams*. Pateley Bridge: YDRT.

Yorkshire Dales Rivers Trust (YDRT). 2018b. *Naturally Resilient – Natural Flood Management techniques Level 1, Low level earth bunds*. Pateley Bridge: YDRT.

Yorkshire Peat Partnership (YPP). 2017. *Gully and grip blocking or sediment trapping techniques.* Skipton: YPP.

Ziliani, L., Surian, N., Botter, G. and Mao, L. 2020. Assessment of the geomorphic effectiveness of controlled floods in a braided river using a reduced-complexity numerical model. *Hydrology and Earth System Sciences*. **24**(6), pp.3229-3250.

Appendix A
CAESAR-Lisflood model set up, sensitivity analysis and improvement

A.1 Methodology

A.1.1 Parameterisation and sensitivity analysis

A.1.1.1 Rainfall

- All rainfall rate values within the time series were either increased or decreased by 10% and 20%.

A.1.1.2 Manning's n

- A literature review was used to gather appropriate values from Chow (1959), McHugh et al., (2002), Kalyanapu et al., (2009), Grimaldi et al., (2010), Brunner (2016).
- Manning's n values per land cover from the literature review were then averaged and increased and decreased by 10% and 20% (Table A.1).

Table A.1: Values of Manning's n roughness co-efficient implemented for the 10 m resolution sensitivity analysis.

	Avg.	Min.	Max.	Avg. -20%	Avg. -10%	Avg. +10%	Avg. +20%	Min. -10%
Discontinuous urban fabric	0.068	0.050	0.080	0.055	0.061	0.075	0.082	0.045
Pastures	0.187	0.040	0.325	0.149	0.168	0.205	0.224	0.036
Broad leaved forest	0.247	0.100	0.600	0.197	0.222	0.271	0.296	0.090
Coniferous forest	0.252	0.100	0.600	0.202	0.227	0.277	0.302	0.090
Mixed Forest	0.250	0.080	0.600	0.200	0.225	0.275	0.300	0.072
Natural grassland	0.146	0.030	0.368	0.116	0.131	0.160	0.175	0.027
Moors and heathland	0.296	0.050	0.700	0.237	0.266	0.326	0.355	0.045
Peat Bogs	0.107	0.065	0.183	0.086	0.096	0.118	0.128	0.059

A.1.1.3 m Parameter

- The *m* parameter in CAESAR-Lisflood controls the storage and release of water from the lumped exponential store of water of hydrological model (Coulthard et al., 2002).

- Affects the rise and decay of the hydrograph, with typical values range from 0.005 for a higher, flashier flood hydrograph to 0.02, for lower, longer flood hydrograph (Welsh et al., 2009).
- Six lumped values were tested between 0.001 and 0.03 (Table A.2).

Table A.2: Values of the m parameter implemented for the 10 m resolution sensitivity analysis.

	Parameter value implemented					
***m* parameter**	0.001	0.002	0.005	0.01	0.02	0.03

A.1.1.4 In-out difference allowed

- The 'input-output difference allowed' parameter determines whether CAESAR-Lisflood runs in a steady or unsteady state, allowing to speed up model operation.
- The parameter value is the difference between input and output discharge (m^3s^{-1}) allowed to run CAESAR-Lisflood in steady state and should be set close to the low flow or the annual mean discharge value.
- Coulthard et al., (2013) showed that CAESAR-Lisflood running in non-steady state resulted in a lower cumulative sediment yield compared to running in a forced steady state.
- For the Eastburn Beck sensitivity analysis, a baseline value for the in-out difference was set to 1 m^3s^{-1}. Additional values included the annual mean flow at the catchment outlet (0.89 m^3s^{-1}), along with a lower value of 0.5 m^3s^{-1} and a higher value of 5 m^3s^{-1}.

A.1.1.5 Grain size distribution

- Grain size distribution is applied in CAESAR-Lisflood as a series of 9 grain size fractions and their associated proportions.
- Grain size distribution will influence the quantity of sediment being eroded, transported and deposited in CAESAR-Lisflood, and has been previously shown to alter erosion patterns and rates (Hancock and Coulthard, 2012).
- There was a lack of quantitative data available on grain size distribution in the Eastburn Beck catchment.
- Field visits were conducted and identified coarse sediment deposits and reports of a gravel trap at the catchment outlet that fills regularly.

- For the purpose of the sensitivity analysis, the default grain size distribution in CAESAR-Lisflood based off results from the River Swale was used.
- This was altered by increasing and decreasing the nine grain size fractions by 20%, 50% and 75% to result in the grain size distribution cumulative proportion curves in Figure A.1.

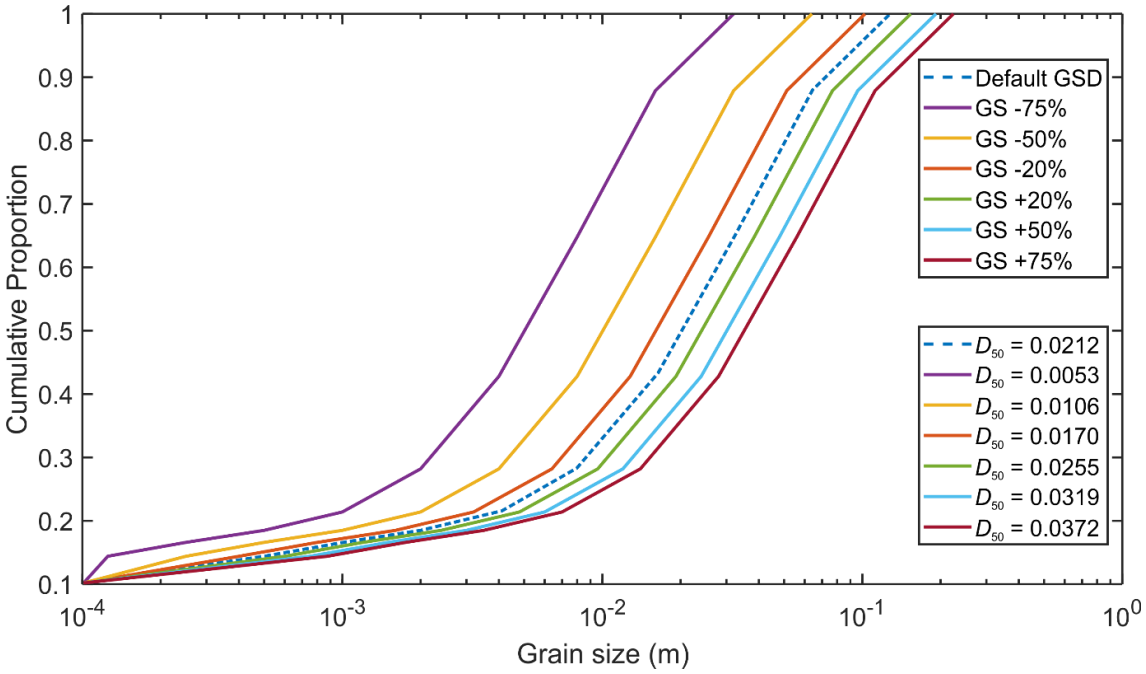

Figure A.1: Grain size distributions implemented for the 10 m sensitivity analysis.

A.1.1.6 Vegetation critical shear stress (VCS)

- VCS is the shear stress threshold of water flow that above which vegetation will be removed by fluvial erosion.
- A low value causes vegetation to be swept away easily and higher values result in more resistant vegetation (Meadows, 2014).
- The default value in CAESAR-Lisflood is 5 N m^{-2} and values between 2.5 N m^{-2} and 15 N m^{-2} were tested (Table A.3).

Table A.3: Values of vegetation critical shear stress implemented for the 10 m resolution sensitivity analysis.

	Parameter value implemented			
Vegetation critical shear stress	2.5	5	10	15

A.1.1.7 Evaporation rate

- The evaporation rate (m day^{-1}) selected in CAESAR-Lisflood will remove the selected depth in cells that have water present.

- Implications for erosional processes within CAESAR-Lisflood, as erosion is only active in wet cells.
- When evaporation rate is set to zero and rainfall causes water to settle in a depression, this will not be removed.
- For the purpose of the sensitivity analysis, a range of evaporation rate values of different magnitudes were tested (Table A.4).
- For context, the mean evapotranspiration rate over well-watered grass according to the CHESS-PE (Robinson et al., 2016) for the floodplain in the Eastburn Beck catchment was 0.00031 m day^{-1}.

Table A.4: Values of evaporation rate implemented for the 10 m resolution sensitivity analysis.

	Parameter value implemented			
Evaporation rate	0	0.0003	0.003	0.03

A.1.2 Assessing model performance

A.1.2.1 Water and sediment discharge

- Water and sediment discharge at the catchment outlet were exported every hour of the model simulation.
- Magnitude was analysed through percentage change occurring from changes made to parameter values to peak discharge for both water and sediment discharge.
- Duration was analysed through the percentage change to volume of water and sediment produced from the 25th to 29th December 2015.

A.1.2.2 Spatial water outputs

- For the purpose of flood extent evaluation, the water depths occurring on the equivalent modelled day to that of Boxing Day 2015 were exported (Day 56).
- Due to the space required to store such files, daily output was chosen, and it is acknowledged that the modelled maximum flood extent may have been before or after the start of Day 56 and thus missed in this analysis.
- To accommodate for model uncertainty, all values of 0.05 m or less were removed from the analysis following visual comparison with aerial imagery of the stream network, assuming more water would be visible in the flood event.

A.1.2.3 Spatial geomorphological outputs

- Elevations were exported from the model at the start of every simulated day.
- To gain an understanding of net elevation change, the final elevation output (equivalent of 29th December) was subtracted from the initial elevation output (equivalent of 24th December) using the Raster Calculator in ArcGIS.
- To accommodate for error in vertical heights of the DEM and a level of detection, all values of 0.05 m or less were removed from the analysis.
- Histograms of the percentage areal coverage of different magnitudes of net elevation change were created.

A.1.2.4 Assessment against observed catchment discharge

- Modelled water discharge was evaluated against the Environment Agency flow data for the Eastburn Beck gauge at Cross Hills (the catchment outlet).
- Fifteen minute interval observed data was averaged to get observed discharge at hourly intervals and thus the same time step as the modelled discharge.
- To assess model performance, Hydrotest (Dawson et al., 2007) was used.
- Hydrotest is an open access website that provides a simple to use way of assessing model performance through twenty-one evaluation metrics commonly used in the literature.
- Statistical metrics include mean absolute error (MAE), root mean squared error (RMSE), Nash-Sutcliffe efficiency (NSE) and persistence index (PI).
- Discharge from the beginning of the 25th December to the end of the 29th December was tested.
- For the purpose of the finding an optimum parameter set, modelled discharge for each of the parameter values tested were run through Hydrotest.
- Each model simulation within a parameter was ranked based on the 21 metrics, where a parameter value gets a score of one if it has the best performance, and the scores were summed.

- The best performing values for each parameter were combined to create the optimum parameter set.

A.1.3 CAESAR-Lisflood Improvements

A number of model improvements were made from the original sensitivity analysis model to improve computational efficiency and catchment representation within the model. Further details of model improvements made can be found in Chapter 2, but can be summarised as:

- Including a bedrock layer
- Spatially distributed m parameter
- Shortening the model simulation for new rainfall product
- Additon of spatially distributed and higher temporal resolution rainfall
- Shortening model simulation of computational efficiency
- Enabling suspended sediment transport

Assessment of changes occurring to the model's outputs from improvements made as a whole aligned with the assessments made as part of the sensitivity analysis. Differences were that once the NIMROD rainfall data was included, net elevation change and water and sediment volumes calculated at the catchment outlet were calculated between the 24th and 28th December as the modelling suggested the event was entirely within this timeframe.

A.1.4 Uncertainty analysis of most sensitive parameters for sediment outputs

- A lack of sediment validation data is an issue in the project, therefore the most sensitive parameters for sediment outputs needed to be tested to understand the uncertainty in the sediment yield results.
- Step wise changes of 5% were made to the Manning's n values up to ±50% of the minimum values found in the literature and the grain size distributions used as part of the initial sensitivity analysis were taken and the smallest of the two (GSD -75% and GSD -50%) were removed after a more thorough investigation into the sediment sizes occurring within the catchment, leaving five possible grain size distributions.
- All possible grain size distributions were modelled in combination with all possible Manning's n values, resulting in 105 model simulations.

- Sediment yield occurring between the 24th and 28th December was calculated for each simulation.
- The minimum, median and maximum sediment yields were calculated from the 105 model runs and the associated Manning's n values and GSD were used in future scenario testing as possible "sediment response catchments" or SRCs.
- A second set of models were created with the inclusion of a separate Manning's n value for the channels.

A.1.5 Increasing model resolution

- For the purpose of including natural flood management measures into CAESAR-Lisflood in future work, it was necessary to reduce the model resolution from 10m to 4m
- Increasing the model resolution also allowed lateral erosion to be enabled as the channel would be represented by more than 1 cell in width.
- Lateral erosion rate is calculated based on the radius of curvature according to the edge counting method in Coulthard and Van de Wiel (2006).
- A value of 0.0001 is stated within the literature as a suitable value for a meandering river and a value of 0.00001 was also tested, with the later resulting in a better representation of the channel in reference to aerial imagery.
- The bedrock layer was also edited so that channel walls within the settlements near the catchment outlet were represented as unerodible as it was thought that channel walls would inhibit lateral channel movement.

A.1.5.1 Model spin up

- Model spin up allows for model self-adjustment, including smoothing of sharp edges and steps in the DEM and the creation of a spatially heterogeneous grain size distribution throughout the catchment.
- Spin up is often represented by elevated levels of sediment production.
- Spin up was achieved by taking a five month long rainfall time series from a tipping bucket rain gauge within the catchment and applying this to the catchment four times.

- The spin up period was limited by computational run times, with run times of over 100 hours.
- Previous studies have chosen much longer spin-up periods, although their model runs have been much longer also (e.g. 10 years spin up in a 30 year simulation, Skinner et al., 2018).
- The resulting DEMs and grain size distributions were used as the initial conditions in the NFM implementation model scenarios.

A.1.6 Sub-catchment modelling

To allow for a detailed 2 m resolution comparison with a hydraulic model, a sub-catchment model was needed to be set up to due to the limitations in the model extent capacity of CAESAR-Lisflood.

Due to the sub-catchment's smaller size, the in-out difference should be expected to change and therefore values of 1, 0.5, 0.1 and 0 m^3s^{-1} were tested to assess their impact on model run times and outputs.

As with the larger models, spin up was required to allow for self-adjustment of the model. The same tipping bucket rainfall series was used for model spin up, which took 23 days to run, limiting the potential for a number of scenarios as with the lower resolution models. The resulting DEM and spatial grain size distribution was taken forward for model runs for the comparison with the hydraulic model.

A.2 Results

A.2.1 Initial sensitivity analysis

Only parameters that caused over 30% change from the baseline in regard to water or sediment peak discharge or volume are detailed in subsequent sections. Percentage change for all parameters can be found in Table A.5.

Table A.5: Percentage change of water discharge and sediment discharge away from the baseline for the 10 m resolution sensitivity analysis.

	Alteration	% Change in peak Qw	% Change in Qw volume	% Change in peak Qs	% Change in Qs volume
Rainfall	**-20%**	-19.8	-19.7	-1.42	0.95
	-10%	-10.1	-9.91	-0.49	2.42
	+10%	10.2	10.2	42.8	55.4
	+20%	32.7	31.5	59.4	69.9
m	**0.001**	0.42	0.4	-20.1	-24.0
	0.005	0.1	-2.3	0.73	-0.83
	0.01	-2.23	-9.8	-1.1	3.46
	0.02	-27.6	-23.2	-29.6	-7.34
	0.03	-55.1	-35.4	-54.4	-29.5
GSD	**-75%**	1.04	0.3	160.4	213.5
	-50%	1.25	0.27	95.3	117.6
	-20%	0.38	0.21	47.5	63.6
	+20%	0.05	0.06	-5.3	-2.12
	+50%	1.56	0.08	-13.7	-17.4
	+75%	-0.02	0.14	-37.3	-36.2
Manning's n	**Min.**	0.13	0.24	-99.1	-99.5
	Max.	0.33	-0.45	-14.5	18.8
	Avg.-20%	1.66	0.14	0.53	-2.61
	Avg.-10%	-0.06	0.07	20.6	13
	Avg.+10%	0.02	-0.03	9.6	12.9
	Avg.+20%	0.32	-0.01	23.2	24.7
	Min.-10%	5.96	0.79	-99.4	-99.7
IOD	**0.5**	-0.22	-1.03	3.36	11.27
	0.89	-0.06	-0.15	-3.33	4.23
	5	0.52	2.33	-8.52	-7.73
	10	0	7.21	-4.99	-4.83
Vegetation critical shear stress	**2.5**	0.29	0.15	-19.5	-22.8
	10	0.12	0.09	-25.1	-26.4
	15	0.21	0.16	-25.4	-27.2
Evap.	**0.0003**	1.43	0.01	23.2	30.4
	0.003	0.75	-0.61	3.24	5.77
	0.03	0.36	-4.89	-0.72	7.88

A.2.1.1 Sensitivity of water outputs

- Rainfall affected the magnitude of the peak discharge (Figure A.2a).
- Peak water discharge increased by 32.7 % when increasing rainfall intensity by 20 % and decreased by 19.8 % when decreasing rainfall intensity by 20 %.
- Total flood volume increased by 31.5 % when increasing rainfall intensity by 20 % and decreased by 19.7 % when decreasing rainfall intensity by 20 %.
- Whole catchment water volume increased by up to 20.4 % when increasing rainfall intensity by 20 % and decreased by up to 15.3 % when decreasing rainfall intensity by 20 % (Figure A.2b).

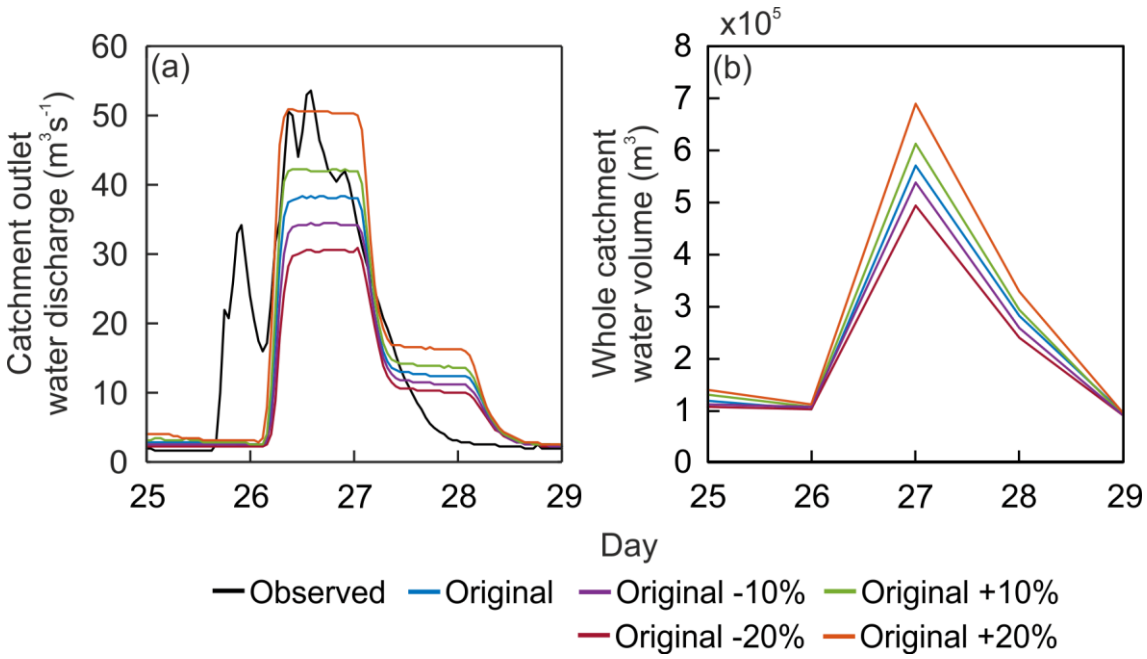

Figure A.2: (a) Catchment outlet water discharge and (b) whole catchment water volume produced with altered rainfall intensity (up to ±20%) for the 10 m resolution sensitivity analysis.

- The most sensitive parameter for water outputs, affecting both peak discharge magnitude and time of peak.
- The smallest value (0.001) caused a steeper rising limb gradient compared to the largest value (0.03) (Figure A.3a).
- The largest value tested (0.03) resulted in a 55.1 % decrease in peak discharge, 35.4 % decrease in flood volume and difference in peak timing of 22 hours compared to smallest value tested (0.001).

- Greatest differences in whole catchment water volume were observed on Day 27 and Day 29 (Figure A.3b).
- On Day 27, there was little difference when m was between 0.001 and 0.01, however values greater than 0.01 saw reduced water volumes.
- On Day 29, as the m value increased, the water volume increased (Figure A.3b).

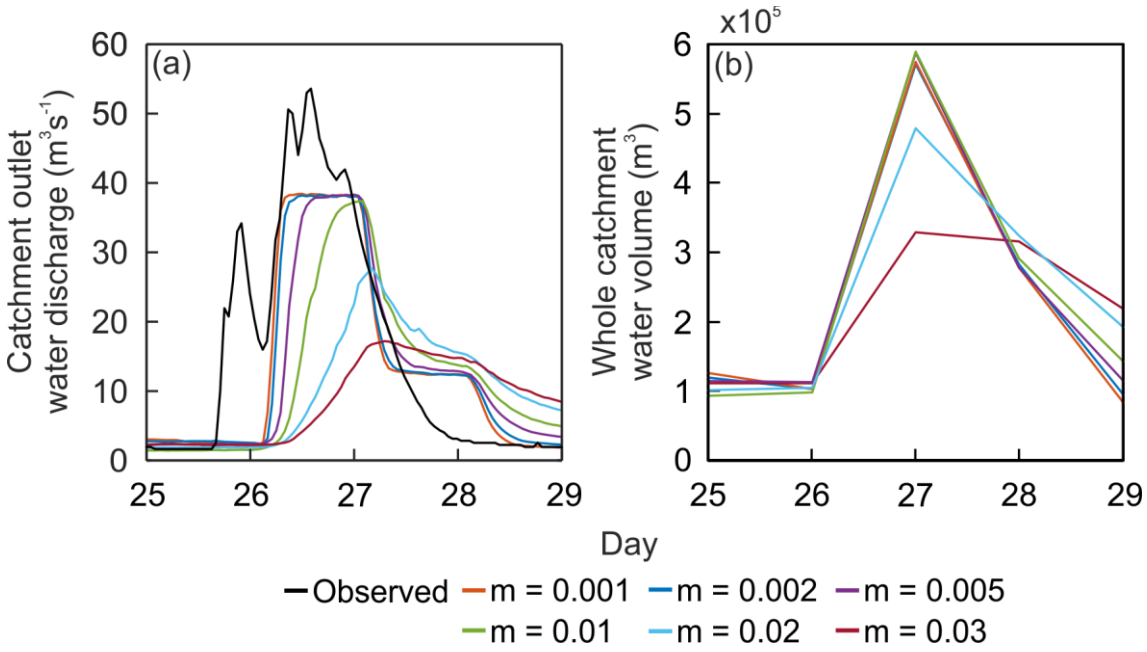

Figure A.3: (a) Catchment outlet water discharge and (b) whole catchment water volume produced with altered m parameter values for the 10 m resolution sensitivity analysis.

A.2.1.2 Sensitivity of sediment outputs

- Little effect on sediment discharge when decreasing rainfall intensity, however, magnitude of sediment discharge was noticeably higher for increased rainfall intensities (Figure A.4).
- Increasing rainfall intensity by 20 % resulted in peak sediment discharge increasing by 59.4 % compared to decreasing rainfall intensity by 20 % resulting in peak discharge decreasing by 1.42 %.
- Regardless of rainfall intensity, the catchment was deposition dominant.
- Increasing rainfall intensity increased the total area experiencing geomorphic change (Figure A.5).
- Within the channels, decreasing rainfall intensity by 20 % resulted in more deposition overall (61.2 %) and a greater percentage of deposition over 1

m compared to increasing rainfall intensity by 20 % (57.3 % deposition overall) (Figure A.5a).

- On the hillslopes and floodplain, there was less of a difference between increasing and decreasing rainfall intensity.
- Increasing rainfall intensity caused a general increase in deposition throughout the catchment (Figure A.5b).

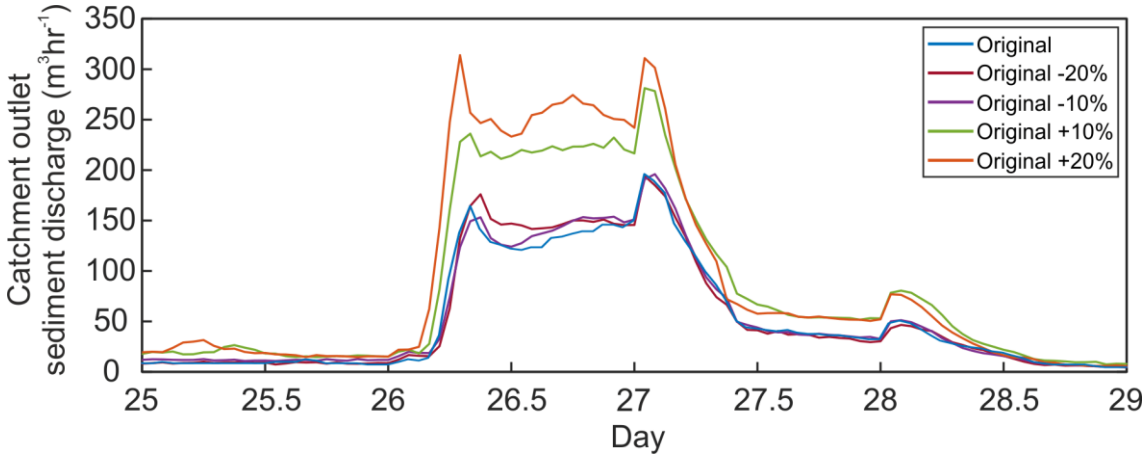

Figure A.4: Catchment outlet sediment discharge produced with altered rainfall intensity (up to ±20%) for the 10 m resolution sensitivity analysis.

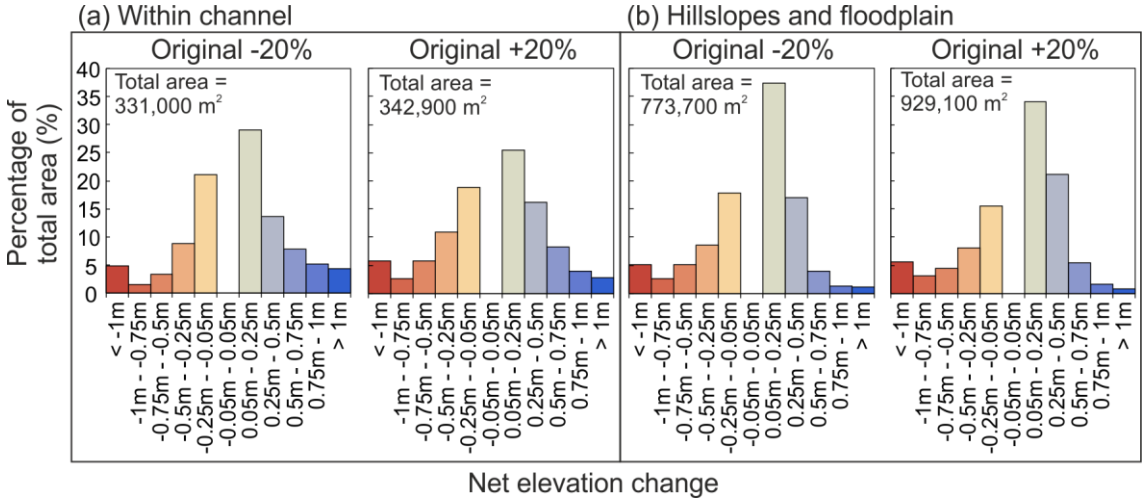

Figure A.5: Histograms of net elevation change produced with altered rainfall intensity (±20%) for the 10 m resolution sensitivity analysis for (a) in-channel change and (b) hillslopes and floodplain change. The smallest fraction (-0.05 to 0.05 m) omitted for clarity.

- Decreasing GSD by 75 % had a larger effect on peak discharge (+ 160.4 %) compared to increasing GSD by 75 % (- 37.3%) (Figure A.6).
- Decreasing GSD by 75 % had a larger effect on sediment volume (+ 213.5 %) compared to increasing GSD by 75 % (- 36.2 %).

- Both increases and decreases in GSD resulted in deposition dominant channels, hillslopes and floodplains (Figure A.7).
- Increasing GSD increased the area experiencing geomorphic change within channels but decreased the geomorphologically active area on hillslopes and the floodplain (Figure A.7).
- Increasing GSD resulted in channels exhibiting more deposition of the lowest magnitude and less erosion of the highest magnitude (Figure A.7a).
- Increasing GSD resulted in hillslopes and floodplains exhibiting more low magnitude deposition and decreasing GSD resulted in more high magnitude erosion (Figure A.7b).

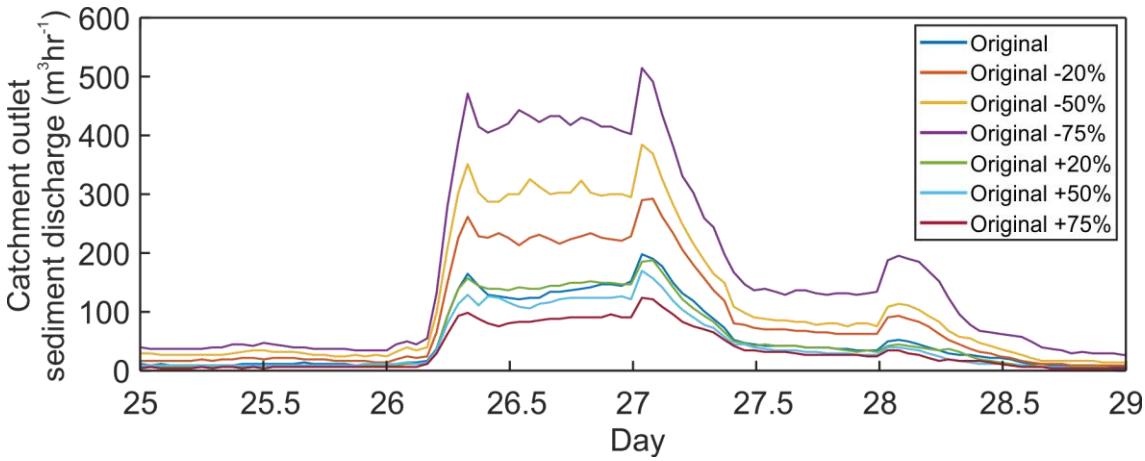

Figure A.6: Catchment outlet sediment discharge produced with altered grain size distribution (up to ±75%) for the 10 m resolution sensitivity analysis.

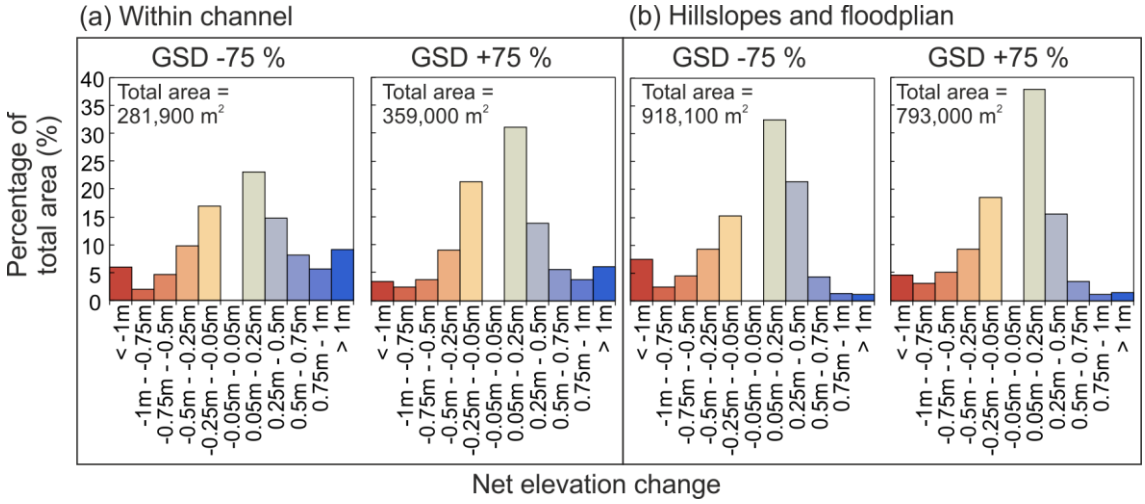

Figure A.7: Histograms of net elevation change produced with altered grain size distribution (±75%) for the 10 m resolution sensitivity analysis for (a) in-channel change and (b) hillslopes and floodplain change.

- Decreasing Manning's n to the minimum values cited in the literature resulted in a 99.1 % decrease in peak discharge and a 99.5 % decrease in sediment volume (Figure A.8).
- Increasing Manning's n to the average values +20 % resulted in an increase of 23.2 % to peak discharge and 24.7 % to sediment volume.
- Maximum Manning's n values resulted in a decrease to peak discharge (14.5 %) but increase in sediment volume (18.8 %).
- A large increase in the total area experiencing geomorphic change was observed when increasing the values of Manning's n (Figure A.9).
- Within the channels, the smallest values of Manning's n resulted in similarly active erosion (49.8%) and deposition (50.2%) with the majority being of the lowest magnitude (Figure A.9a).
- The highest values of Manning's n resulted in deposition dominant channels (70.6%), with larger areas of high magnitude erosion and deposition.
- A similar pattern was seen on the hillslopes and floodplain, the lowest values of Manning's n were similarly erosional and depositional and the highest values of Manning's n were deposition dominant (Figure A.9b).

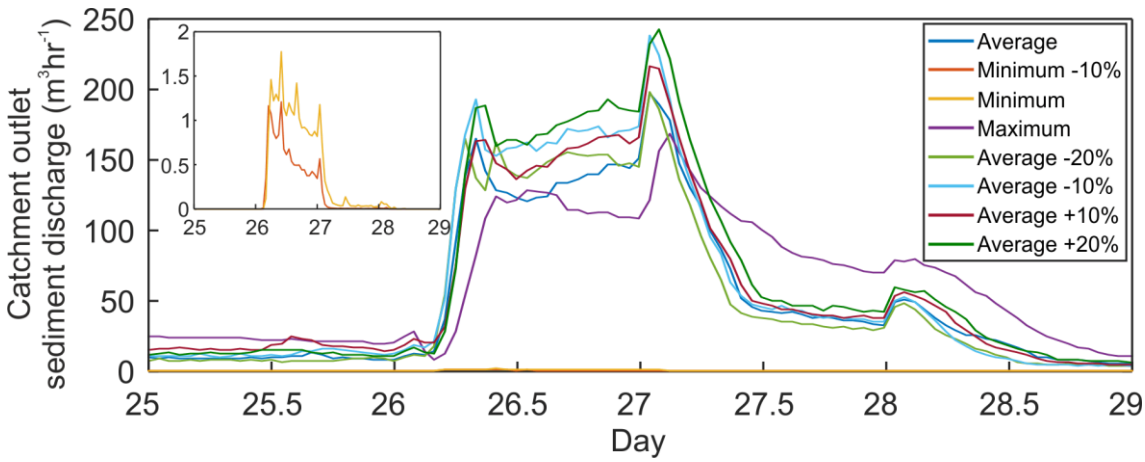

Figure A.8: Catchment outlet sediment discharge produced with altered Manning's n values for the 10 m resolution sensitivity analysis. Note the change in y-axis scale on subset graph to show the discharge of Minimum and Minimum-10% values.

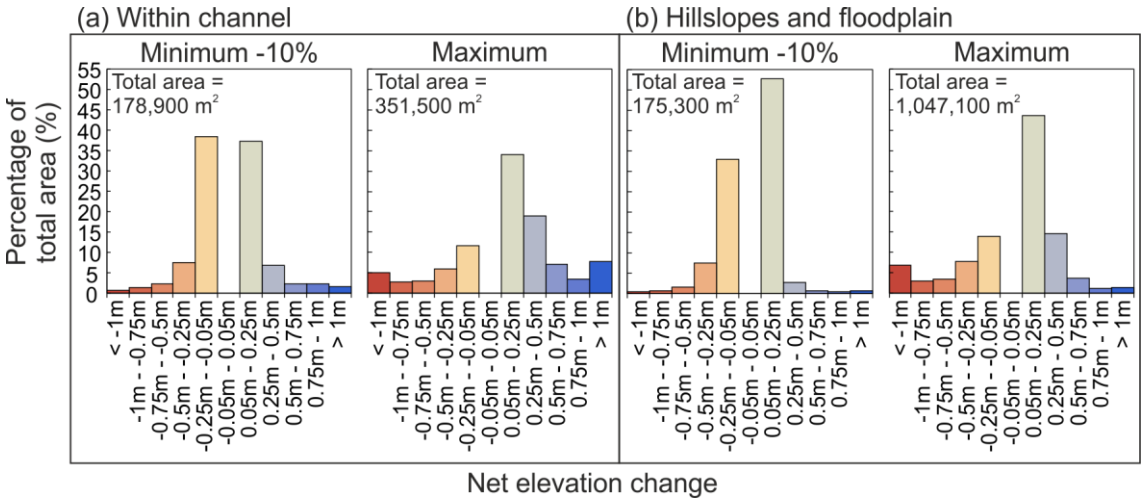

Figure A.9: Histograms of net elevation change produced with altered Manning's n values for the 10 m resolution sensitivity analysis for (a) in-channel change and (b) hillslopes and floodplain change.

A.2.1.3 Finding an optimum parameter set

- The results of the efficiency analysis reflect the results of the CAESAR-Lisflood sensitivity analysis, whereby the *m* parameter was the most sensitive.
- RMSE decreased by 6.598 when going from the worst (m = 0.03) to best (m = 0.001) fitting hydrograph.
- NSE increased from 0.021 to 0.799 between the worst (m = 0.03) and best (m=0.001) fitting hydrographs.
- The other parameters showed much smaller differences in efficiency between the worst and best fitting hydrographs (Table A.6).

Table A.6: A summary of model efficiency metrics for the 10 m resolution sensitivity analysis.

			RMSE	MRE	R^2	IoA	NSE
		Baseline	5.588	0.167	0.804	0.935	0.79
GSD	**Best**	**GSD +50%**	5.549	0.164	0.806	0.936	0.793
	Worst	**GSD -20%**	5.601	0.159	0.802	0.935	0.789
Manning's n	**Best**	**Minimum -10%**	5.509	0.134	0.806	0.938	0.796
	Worst	**Maximum**	6.311	0.201	0.743	0.915	0.732
m	**Best**	**0.001**	5.462	0.235	0.81	0.939	0.799
	Worst	**0.03**	12.06	1.132	0.055	0.392	0.021
Evap.	**Best**	**0.003**	5.591	0.174	0.804	0.935	0.79
	Worst	**0.03**	5.776	-0.021	0.796	0.931	0.776
IOD	**Best**	**1**	5.588	0.167	0.804	0.935	0.79
	Worst	**10**	5.955	0.317	0.767	0.927	0.761
VCS	**Best**	**15**	5.575	0.168	0.805	0.935	0.791
	Worst	**2.5**	5.594	0.161	0.802	0.935	0.789

- Figure A.10a shows that the maximum discharge was the same for both the baseline and optimum parameter set.
- Timing of the flood wave was affected where the optimum parameter set caused discharge to increase two hours earlier than the baseline.
- There was a lack of complexity to the modelled hydrograph that was present in the observed hydrograph.
- A noticeable decrease in whole catchment water volume was observed with up to 47 % less water volume occurring throughout the catchment for the optimum parameter set (Figure A.10b).

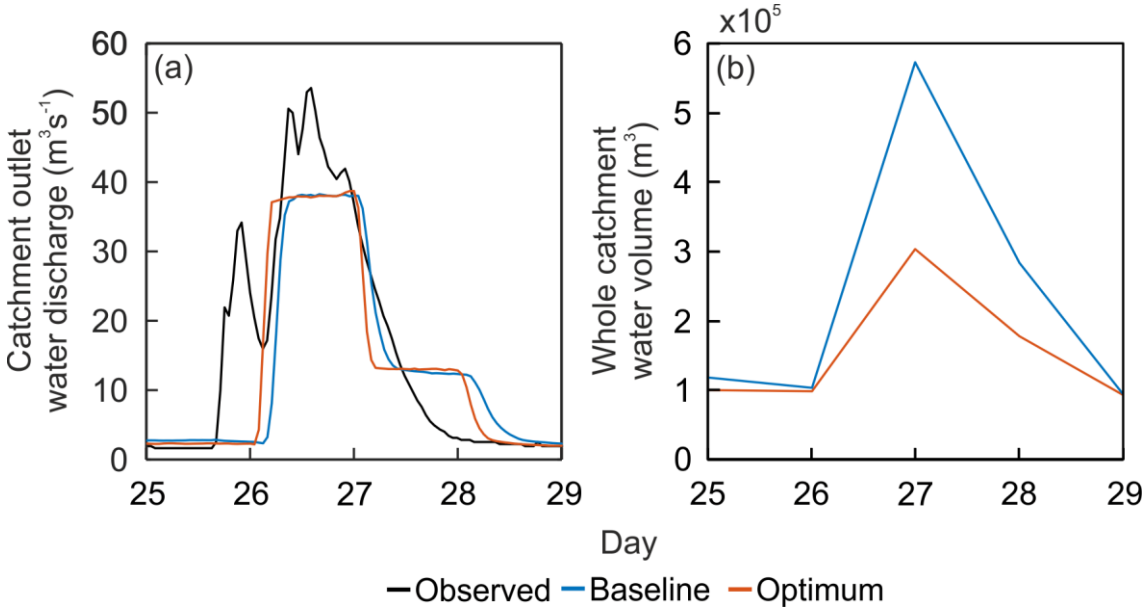

Figure A.10: (a) Catchment outlet water discharge and (b) whole catchment water volume produced with the baseline and optimum parameter sets at 10 m model resolution.

- The largest difference between the baseline and optimum parameter sets related to the sediment discharge (Figure A.11).
- Using the optimum parameter set resulted in a 99.7 % decrease in peak discharge, and 99.8 % decrease in sediment volume.
- Using the optimum parameter set resulted in a large decrease in the geomorphologically active area (Figure A.12).
- Within the channels, the optimum resulted in 94.2% of the active area being in the lowest magnitude of erosion and deposition (Figure A.12a).
- Using the optimum parameter set, the channels were similarly erosional (51.1%) and depositional (48.9%), whereas the baseline channels were deposition dominant (59.3%).

- On the hillslopes and floodplains, the optimum resulted in 96.7% of the active area being of the lowest magnitude erosion and deposition (Figure A.12b).
- For the optimum parameter set, the hillslopes and floodplains were erosion dominant (54%) compared to the baseline parameter set where they were deposition dominant (59.9%) (Figure A.12b).

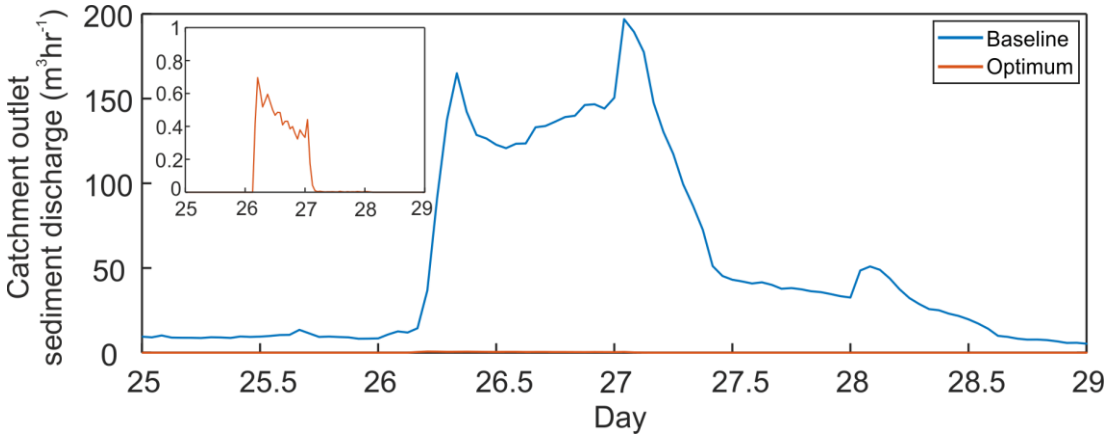

Figure A.11: Catchment outlet sediment discharge produced with the baseline and optimum parameter sets at 10 m model resolution. Note the change in y-axis scale on subset graph to show the discharge of the optimum parameter set.

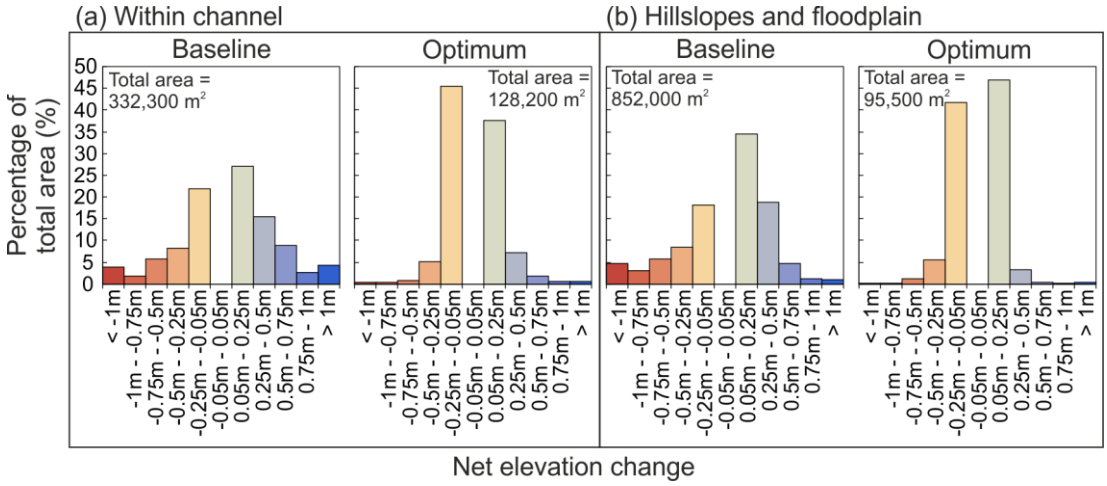

Figure A.12: Histograms of net elevation change for the baseline and optimum parameter sets at 10 m model resolution for (a) in-channel change and (b) hillslopes and floodplain change.

A.2.2 Model improvements

A number of changes were made to CAESAR-Lisflood to improve hydrograph fit to the observed data, how realistic CAESAR-Lisflood was and model computing efficiency. Of the changes made, the majority had a larger impact on the sediment discharge compared to water discharge (Table A.7).

Table A.7: Percentage change of water discharge and sediment discharge as a result of 10 m resolution CAESAR-Lisflood model improvements.

Change from	Alteration made	% Change in Peak Qw	% Change in Qw volume	% Change in Peak Qs	% Change in Qs volume
Optimum	**Bedrock inclusion**	0.47	-0.03	1050	1880
Bedrock inclusion	**Spatial m inclusion**	-0.33	-1.49	1.18	13.67
Spatial m inclusion	**December only**	0.57	-0.06	125.3	125.1
December only	**High res. rain inclusion**	40.3	-10.2	-1.06	-32.4
Spatial rain inclusion	**> 1 month Simulation Length**	-0.309	-0.022	12.4	-7.44
20th December onwards (CL1.9b)	**New version of CAESAR-Lisflood (1.9h)**	1.36	-1.36	22.8	8.51
New version of CAESAR-Lisflood (1.9h)	**Suspended sediment enabled**	0.23	-0.25	46.6	-1.33

A.2.2.1 Inclusion of bedrock layer

- When including bedrock within CAESAR-Lisflood, the maximum sediment discharge increased from 0.69 m^3hr^{-1} to 8.01 m^3hr^{-1}.
- There was an 1880 % increase in sediment volume (Figure A.13).
- Including bedrock resulted in sediment discharge occurring throughout the simulation compared to a baseline discharge of zero when not using a bedrock layer.
- Including bedrock resulted in a larger geomorphologically active area (Figure A.14).
- When including bedrock in CAESAR-Lisflood, the channels were similarly erosional (50.3 %) and depositional (49.7 %) (Figure A.14b).
- Channels had higher magnitude erosion when including bedrock (Figure A.14a).
- The hillslopes and floodplain were erosion dominant when including bedrock where there was an increase in higher magnitude erosion (Figure A.14b).

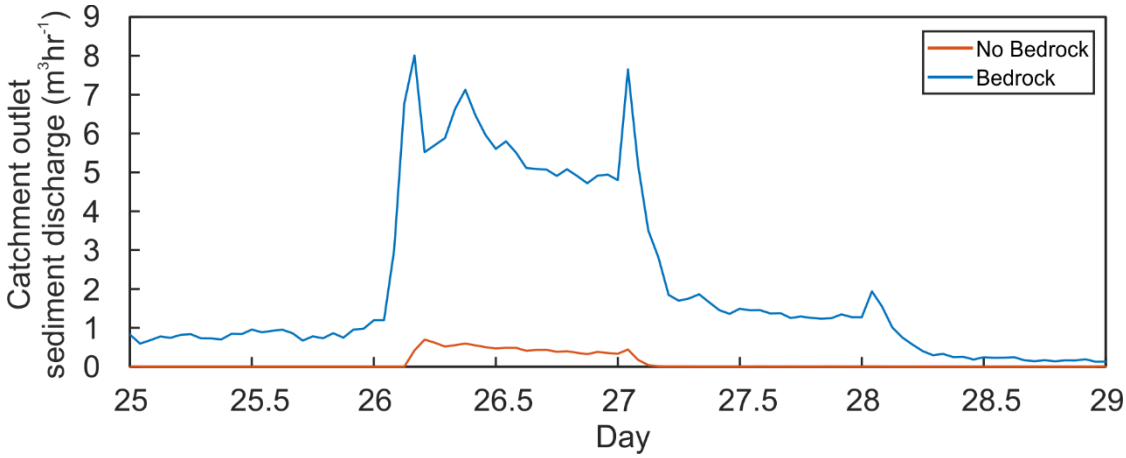

Figure A.13: Catchment outlet sediment discharge produced with and without the inclusion of a bedrock layer for the optimum parameter set at 10 m model resolution.

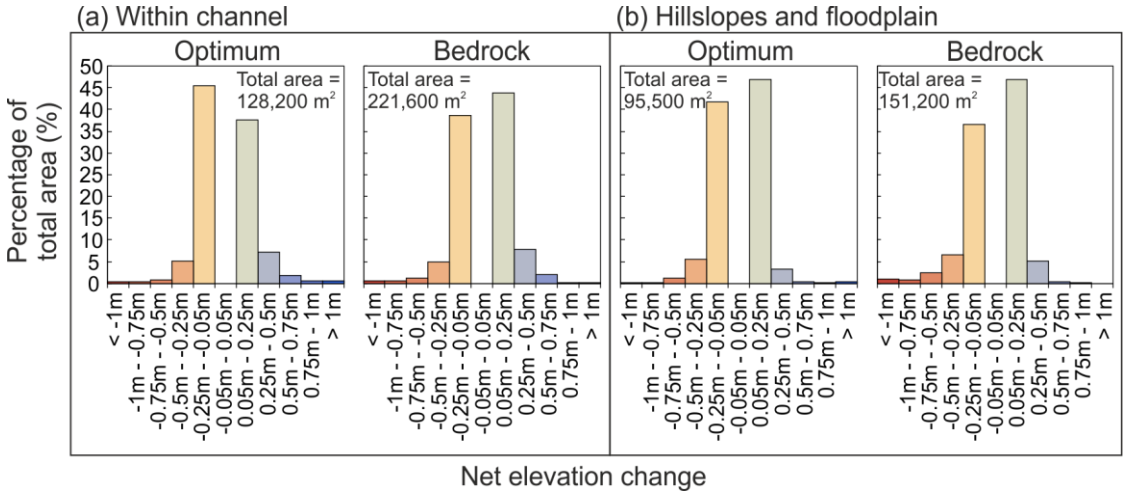

Figure A.14: Histograms of net elevation change produced with and without the inclusion of a bedrock layer for the optimum parameter set at 10 m model resolution for (a) in-channel change and (b) hillslopes and floodplain change.

A.2.2.2 Decreasing the simulation period

- There was a noticeable difference in sediment discharge when reducing the simulation time with a 125.3% increase in peak discharge, and a 125.1% increase in sediment volume (Figure A.15).
- Shortening the simulation time increased the geomorphologically active area (Figure A.16).
- Reducing the simulation length resulted in increases to the higher magnitude erosion and deposition both within the channels and on the hillslopes and floodplain (Figure A.16).
- Overall, the model remained deposition dominant within the channels and the hillslopes and floodplain remain erosion dominant when reducing the simulation length.

- Reducing the simulation length had less of an impact on the time CAESAR-Lisflood took to run than expected.
- On an OEGStone CS-B x64-based PC, with an Intel® Core™ i7-4790 @ 3.60Ghz processor, with 16GB RAM and 250GB SSD Hard drive, running the model for November and December took 1 hour and 40 minutes, whereas running the model for December only took 1 hour and 20 minutes.

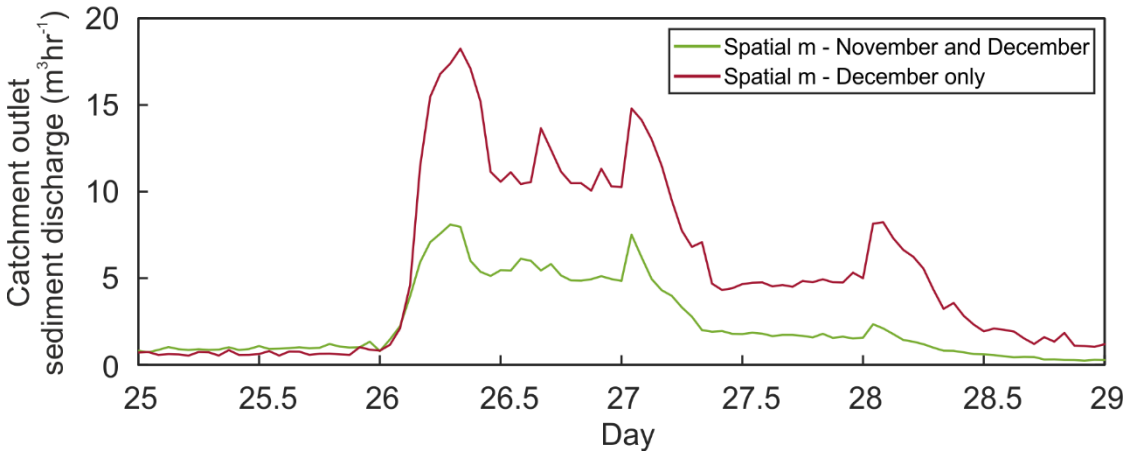

Figure A.15: Catchment outlet sediment discharge produced with shortened simulation lengths at 10 m model resolution.

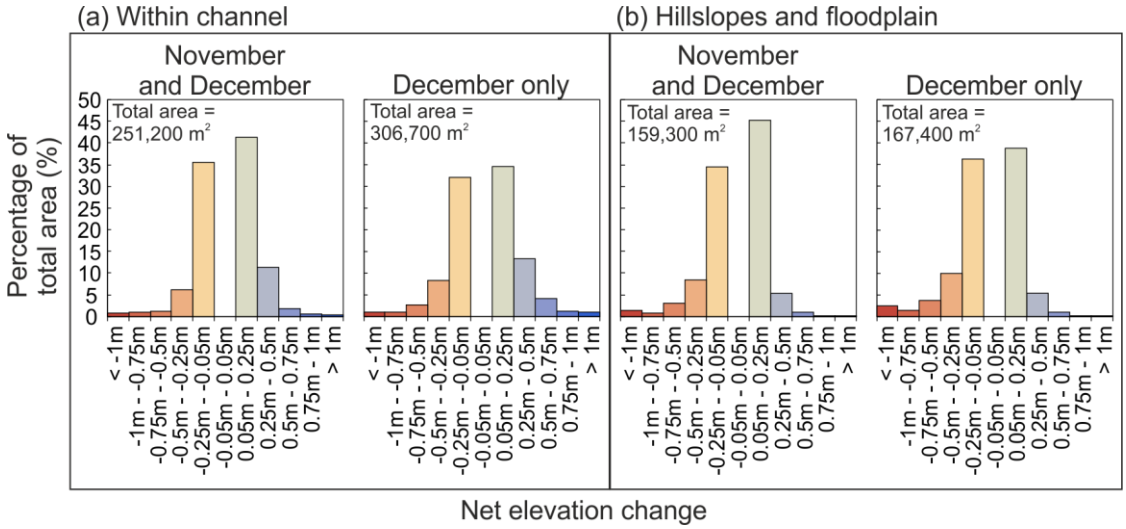

Figure A.16: Histograms of net elevation change produced with shortened simulation lengths at 10 m model resolution for (a) in-channel change and (b) hillslopes and floodplain change.

A.2.2.3 Inclusion of a higher temporal and spatial resolution rainfall product

- There were noticeable differences to the hydrograph when changing the rainfall from the low resolution, GEAR dataset (1 day, spatially lumped) to the high resolution, NIMROD radar dataset (1 hour, 1 km spatial resolution) (Figure A.17a).

- Overall, the hydrograph shape was much different, with NIMROD rainfall causing more complexity and multiple peaks in discharge.
- This resulted in a hydrograph that fit the observed data much more closely, particularly on the rising limb (Figure A.17a).
- When using the NIMROD rainfall, maximum discharge increased by 40.3 %, however flood volume decreased by 10.2 %.
- A greater whole catchment water volume occurred for the high resolution rainfall product, which also occurred earlier in the simulation (Figure A.17b).

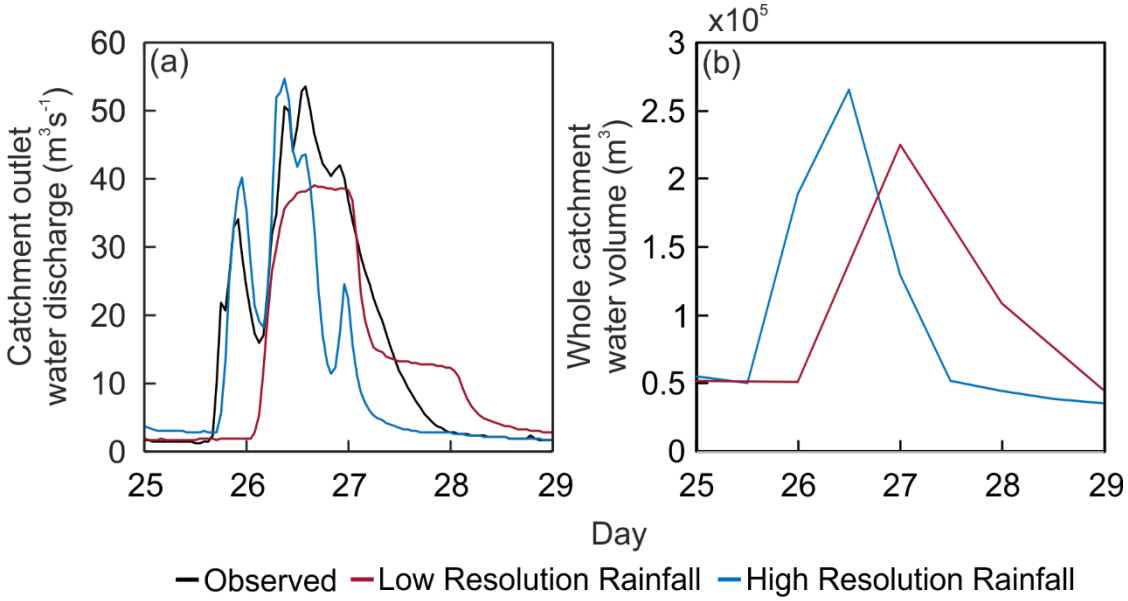

Figure A.17: (a) Catchment outlet water discharge and (b) whole catchment water volume produced with low and high resolution rainfall products at 10 m model resolution.

- Little difference in peak sediment discharge between the two rainfall products (Figure A.18).
- The peak sediment discharge of the high resolution rainfall simulation occurred 12 hours before the low resolution rainfall simulation.
- When including the high resolution rainfall a volumetric decrease in sediment yield of 32.4 % occurred.
- Including the high resolution rainfall product increased the geomorphologically active area (Figure A.19).
- Within the channels, there was little difference between the two rainfall products (Figure A.19a).

- On the floodplains, the high resolution rainfall caused a decrease in magnitude of erosion and a small increase in the magnitude of deposition (Figure A.19b).

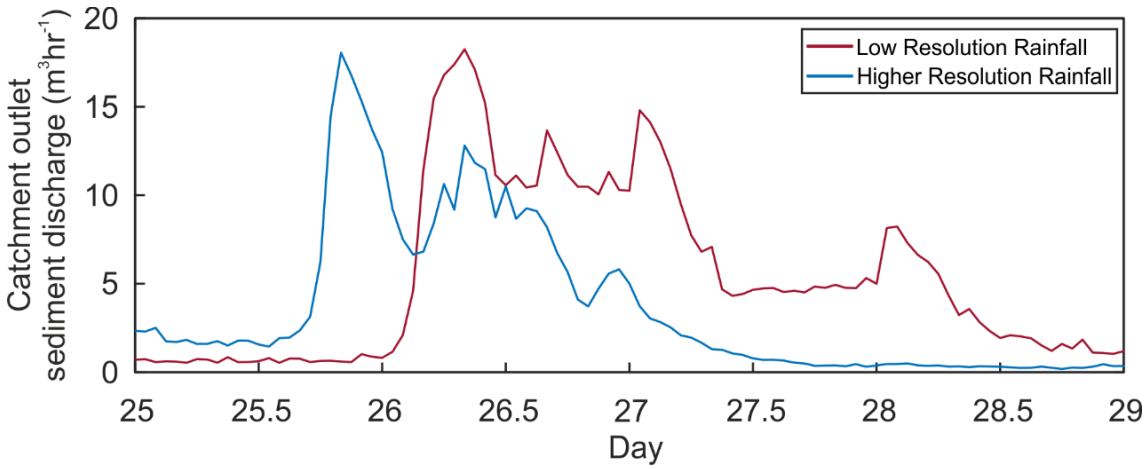

Figure A.18: Catchment outlet sediment discharge produced with low and high resolution rainfall products at 10 m model resolution.

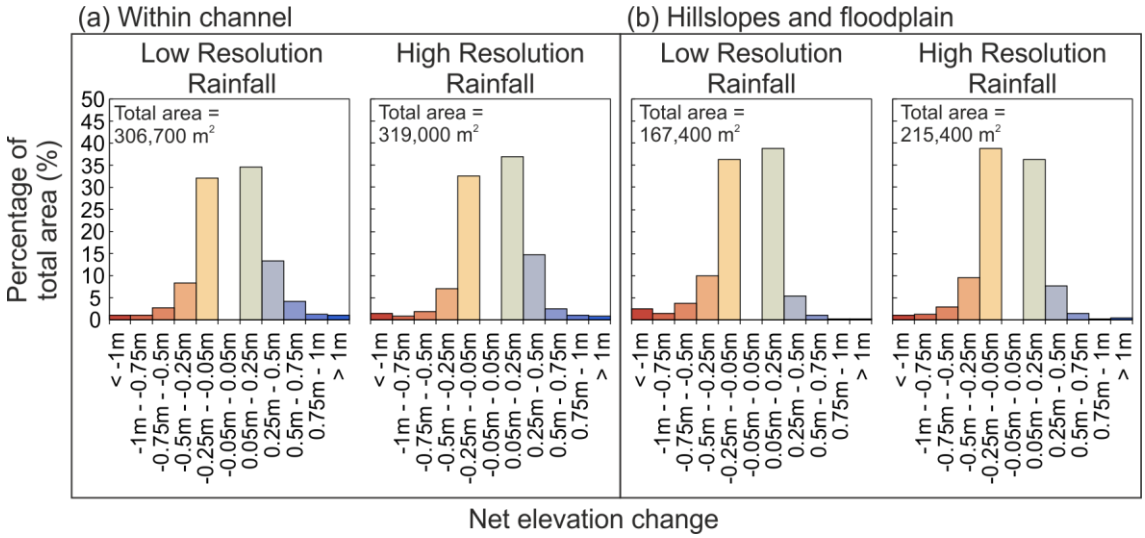

Figure A.19: Histograms of net elevation change produced with low and high resolution rainfall products at 10 m model resolution for (a) in-channel change and (b) hillslopes and floodplain change.

A.2.2.4 Inclusion of suspended sediment and use of new version of CAESAR-Lisflood

- An increase in peak sediment discharge was observed when using the newer version of CAESAR-Lisflood (22.8 %) and when enabling suspended sediment transport in the newer version of CAESAR-Lisflood (46.6 %) (Figure A.20).
- An increase in sediment yield of 8.1 % was observed between the two versions of CAESAR-Lisflood but a small decrease of 1.5 % was observed

when enabling suspended sediment in the newer version of the model (Figure A.20).

- Changing the version of the model led to a reduction in the geomorphologically active area (Figure A.21).
- Enabling suspended sediment increased the area experiencing net elevation change within the channel but decreased the area experiencing net elevation change on the hillslopes and floodplain (Figure A.21).
- A decrease in the magnitude of net elevation change was observed both within channels and on hillslopes and floodplains between the two versions of CAESAR-Lisflood tested (Figure A.21).
- The inclusion of suspended sediment resulted in an increase in the percentage of the total area experiencing deposition and a decrease to erosion within channels (Figure A.21a). Little difference was observed on the hillslopes and floodplain (Figure A.21b).

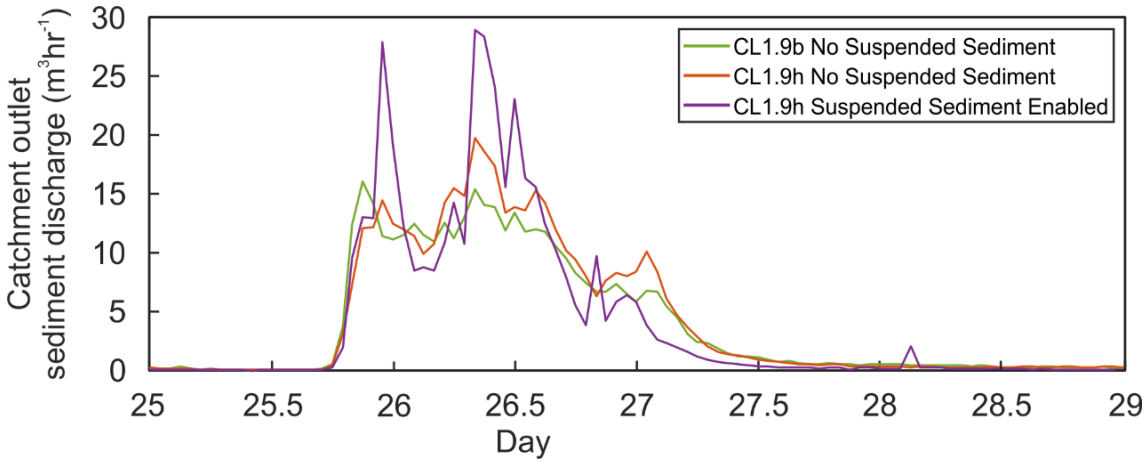

Figure A.20: Catchment outlet sediment discharge for the two versions of CAESAR-Lisflood used within the study and for the inclusion of suspended sediment at 10 m model resolution.

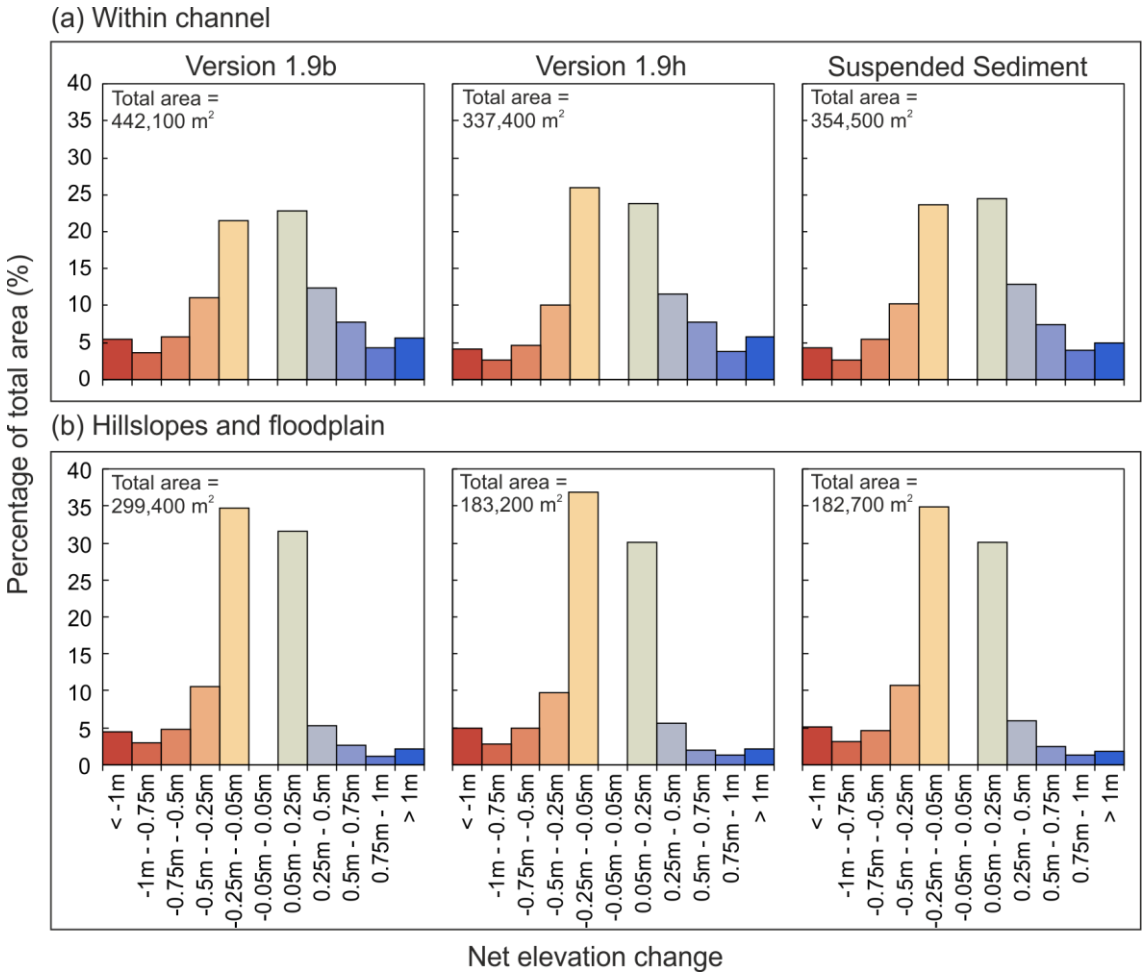

Figure A.21: Histograms of net elevation change for the two versions of CAESAR-Lisflood used within the study and for the inclusion of suspended sediment at 10 m model resolution for (a) within channels and (b) on the hillslopes and floodplain.

A.2.3 Parameter uncertainty

- A lack of sediment validation data and the model's high sensitivity to Manning's n and GSD highlighted a need to have a range of possible sediment response scenarios, called "sediment response catchments" or SRCs.
- The lower sediment yields resulted from a combination of low Manning's n and large grain sizes.
- The greater sediment yields resulted from a combination of high Manning's n and small grain sizes (Figure A.22).
- There was little difference in catchment outlet water discharge with increasing SRC (Figure A.23a).
- Increasing the SRC resulted in a decrease in whole catchment water volume (Figure A.23b).
- Greater differences seen in sediment discharge (Figure A.24).

- Flood volume increased by 3.2 % between minimum and median SRCs and 4.4 % between median and maximum SRCs (Table A.8).
- Sediment yield increased by 709 % between the minimum and median SRCs and by 186 % between the median and maximum SRCs (Table A.8).
- The total area which was geomorphologically active increased greatly with increasing SRCs (Figure A.25).
- Channels were deposition dominant for the three SRCs, hillslopes were erosion dominant (Figure A.25).
- Magnitude of net elevation change increased between the minimum and median and median and maximum SRCs (Figure A.25).

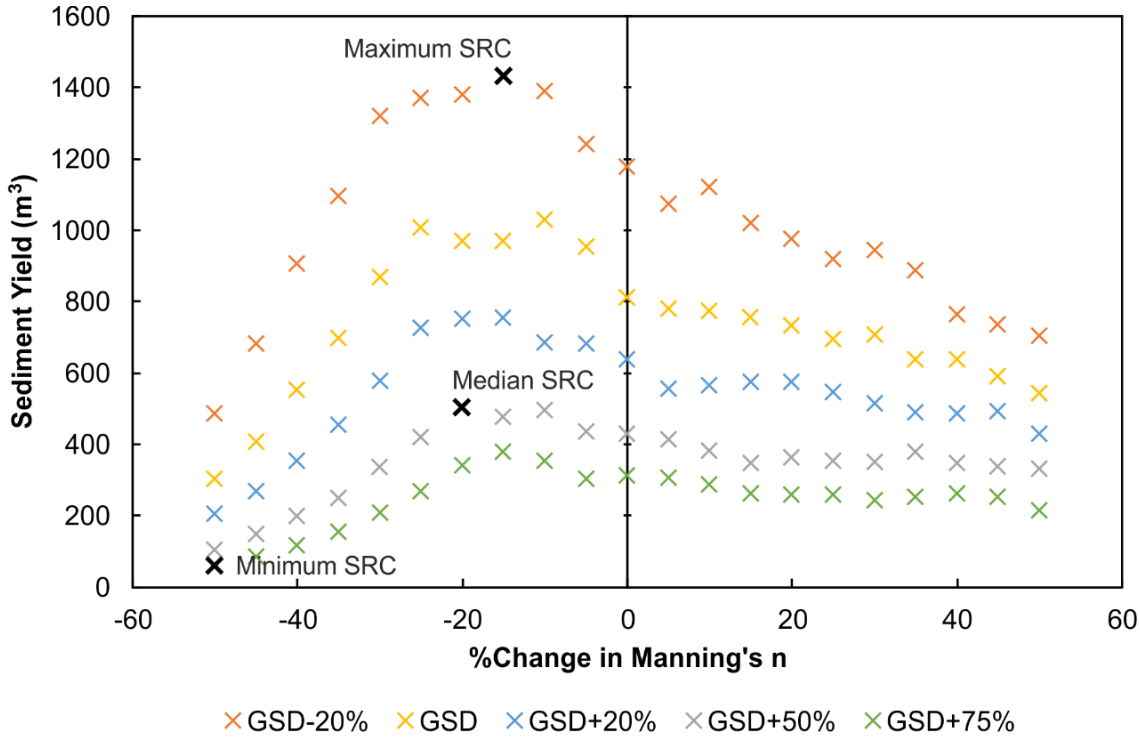

Figure A.22: Catchment outlet sediment yield occurring from possible combinations of the GSD and Manning's n at 10 m model resolution. Highlighted points are the three statistically chosen parameter value combinations.

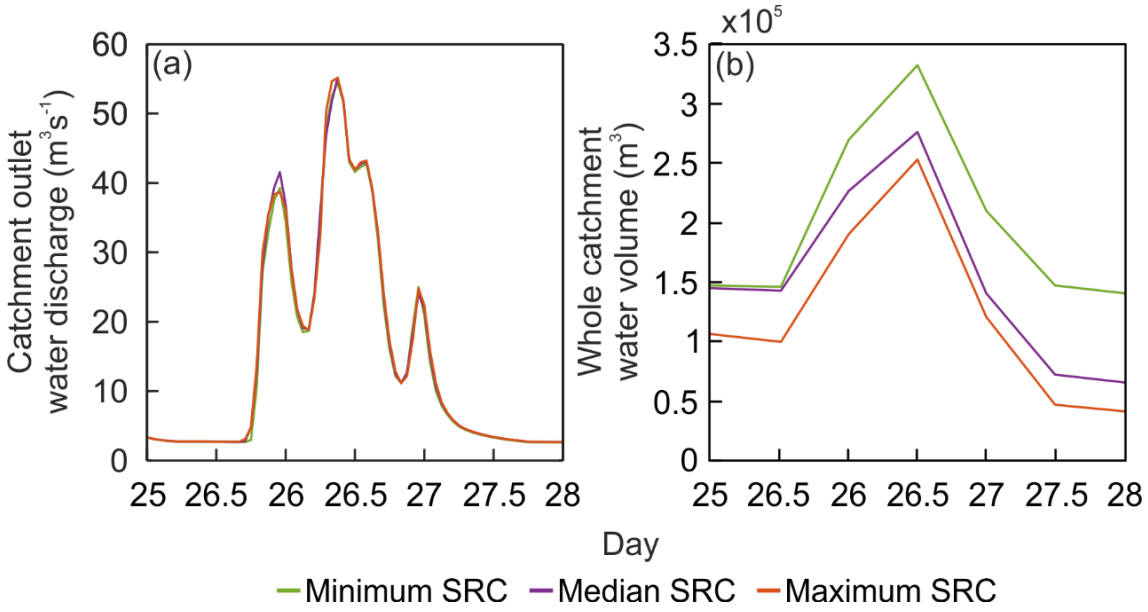

Figure A.23: (a) Catchment outlet water discharge and (b) whole catchment water volume produced for the three selected SRCs at 10 m model resolution.

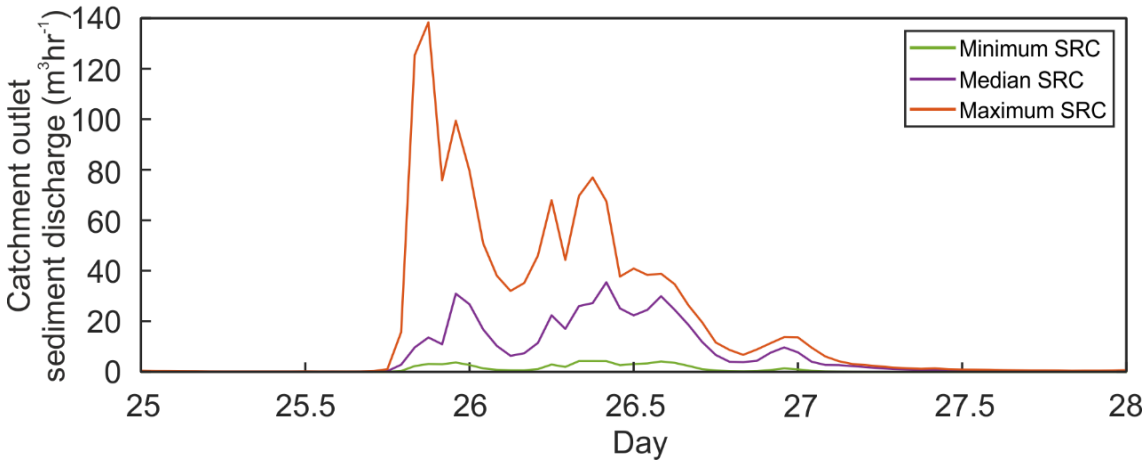

Figure A.24: Catchment outlet sediment discharge for the three selected SRCs at 10 m model resolution.

Table A.8: Summary metrics for catchment outlet water and sediment discharges for the three selected SRCs at 10 m model resolution.

SRC	Peak water discharge (m^3s^{-1})	Flood volume (m^3)	Peak sediment discharge (m^3hr^{-1})	Sediment yield (m^3)
Minimum	54.5	4.04 x10^6	4.2	61.9
Median	55.1	4.17 x10^6	35.4	500.9
Maximum	55.1	4.22 x10^6	138.4	1431.7

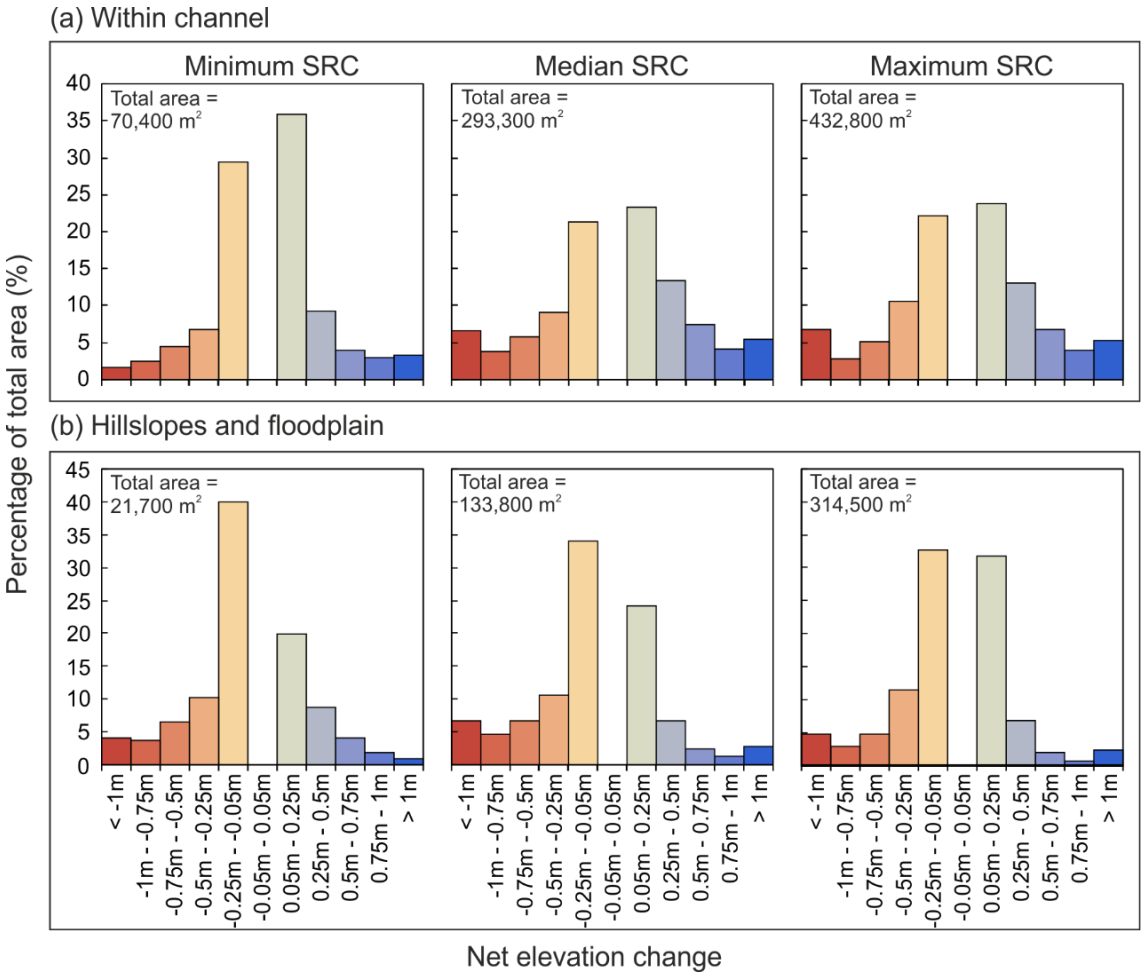

Figure A.25: Histograms of net elevation change for the three selected SRCs at 10 m model resolution for (a) within channels and (b) on the hillslopes and floodplain.

A.2.3.1 Inclusion of a separate Manning's n value for main channels

- Less than 2 % change in peak water discharge and flood volume when adding a separate channel Manning's n value.
- Adding a channel Manning's n value decreased the peak sediment discharge and sediment yield (Figure A.26).
- Greater change for minimum and maximum SRCs, with sediment yields decreasing by 45.4 % and 22.3 % respectively.
- The median SRC saw a decrease of 16.2 % in sediment yield.
- The addition of a Manning's n value for the channel resulted in an increase to the area experiencing geomorphic change within the channels for the Median SRC however a decrease for the Minimum SRC and Maximum SRC (Figure A.27a).
- Within channels, an increase in magnitude of erosion and deposition for minimum SRC occurred when including a separate channel Manning's n.

Little difference in magnitudes of net elevation change for median and maximum SRCs (Figure A.27a).

- The inclusion of a separate Manning's n value for the channel resulted in a decrease in the area experiencing geomorphic change on the hillslopes and floodplain for the three SRCs (Figure A.27b).
- On the hillslopes and floodplain, an increase in the magnitude of erosion and deposition occurred for the minimum SRC, but little change was observed for the median and maximum SRC when including a separate Manning's n value for the channel (Figure A.27b).

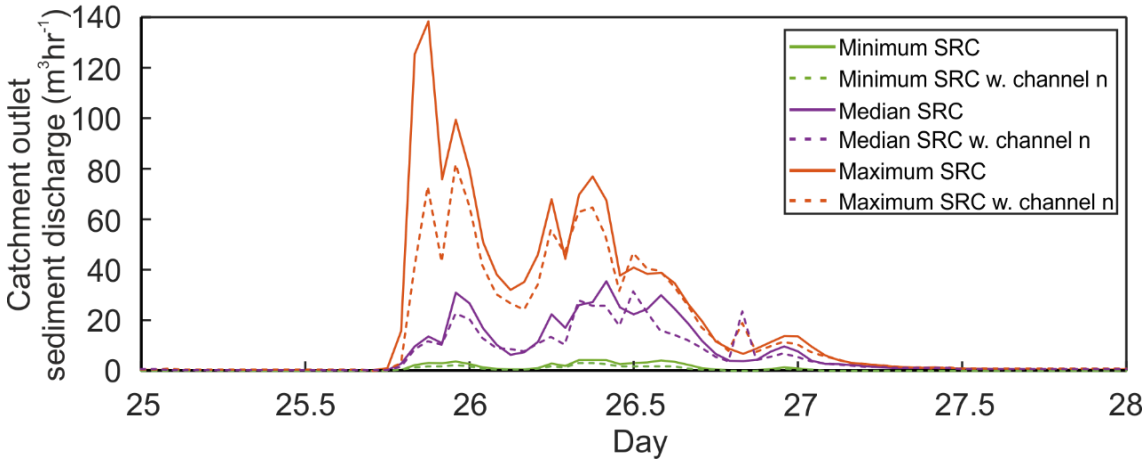

Figure A.26: Catchment outlet sediment discharge for the inclusion of a separate Manning's n value for the channel at 10 m model resolution.

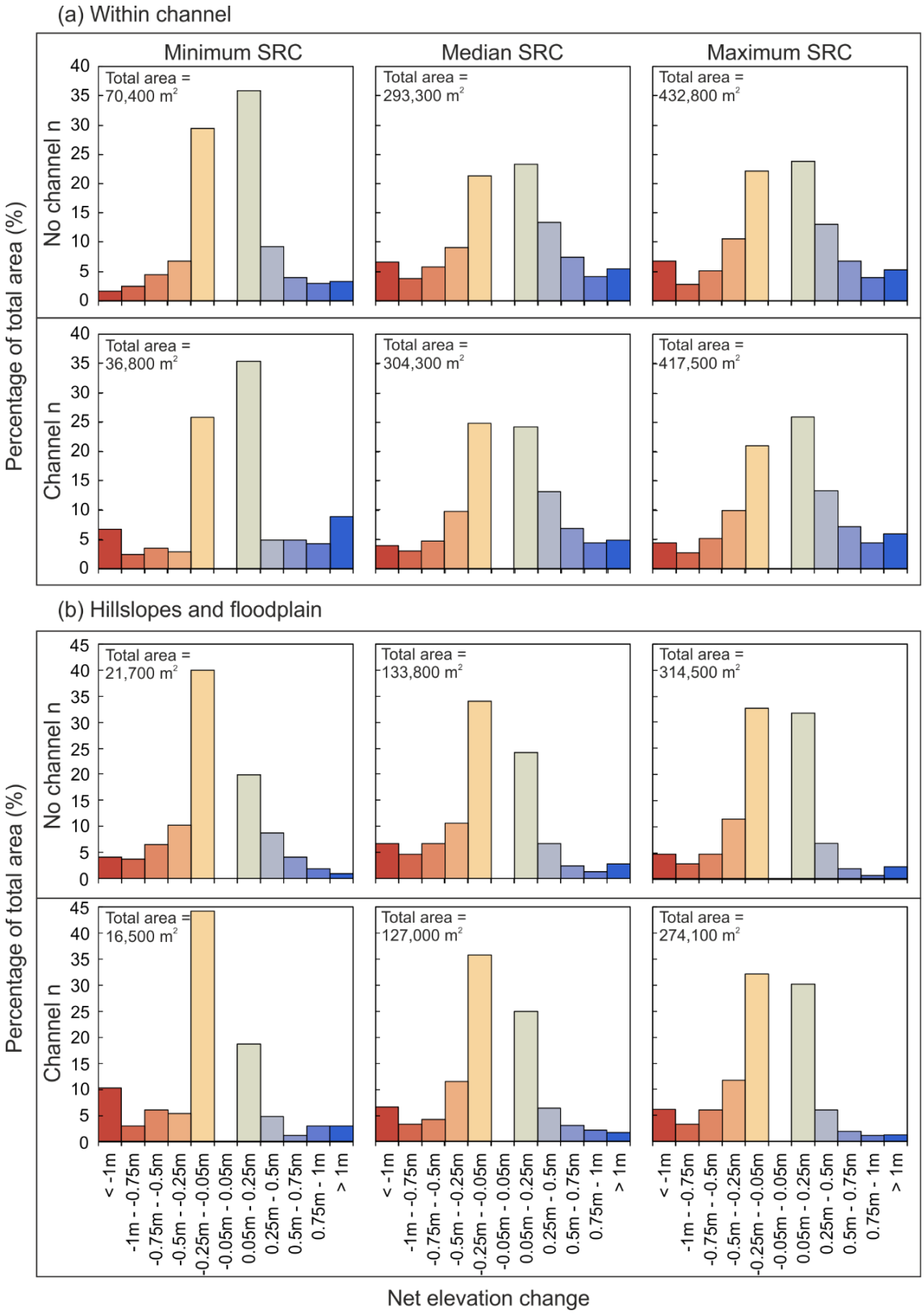

Figure A.27: Histograms of net elevation change to test the inclusion of a separate value of Manning's n for the channel at 10 m model resolution for (a) within channels and (b) on hillslopes and floodplain.

A.2.4 Altering model resolution

- Small increases in peak water discharge and flood volume were observed when increasing the model resolution (Table A.9) which were less observable in the hydrographs (Figure A.28a).
- Whole catchment water volume was noticeably greater for the 10 m resolution Minimum SRC compared to the other scenarios (Figure A.28b).
- Large decreases in peak sediment discharge and sediment yield were observed for the minimum and maximum SRC when increasing model resolution. There was little change to the median SRC (Table A.9).
- At the peak of the event, whole catchment water volume was smaller for the Median and Maximum SRC (Figure A.28b).
- Sediment discharge remained higher for the majority of the simulation for the 10 m resolution models compared to the 4 m resolution models for the Minimum and Maximum SRCs (Figure A.29).
- For the median SRC, prior to the event peak, the 4 m resolution model resulted in higher sediment discharge, after the event peak, the 10 m resolution model resulted in higher sediment discharge (Figure A.29).
- In channels, an increase in model resolution increased the geomorphologically active area and increased the area experiencing erosion (Figure A.30a).
- On the hillslopes and floodplain, an increase in model resolution increased the geomorphologically active area and increased the area experiencing deposition (Figure A.30b).

Table A.9: Catchment outlet summary metrics for the increase in model resolution from 10 m to 4 m.

SRC		Peak Qw (m^3s^{-1})	Flood Volume (m^3)	Peak Qs (m^3hr^{-1})	Sediment Yield (m^3)
Minimum	10m	54.3	4,020,305	2.79	33.8
	4m	60.7	4,231,164	1.39	8.62
	%Change	**11.8**	**5.24**	**-50.1**	**-74.5**
Median	10m	55.4	4,081,226	31.4	419.4
	4m	59.0	4,249,581	31.6	431.4
	%Change	**6.39**	**4.13**	**0.791**	**2.87**
Maximum	10m	55.8	4,133,967	81.8	1112.3
	4m	59.1	4,283,041	73.0	766.7
	%Change	**5.92**	**3.61**	**-10.8**	**-31.1**

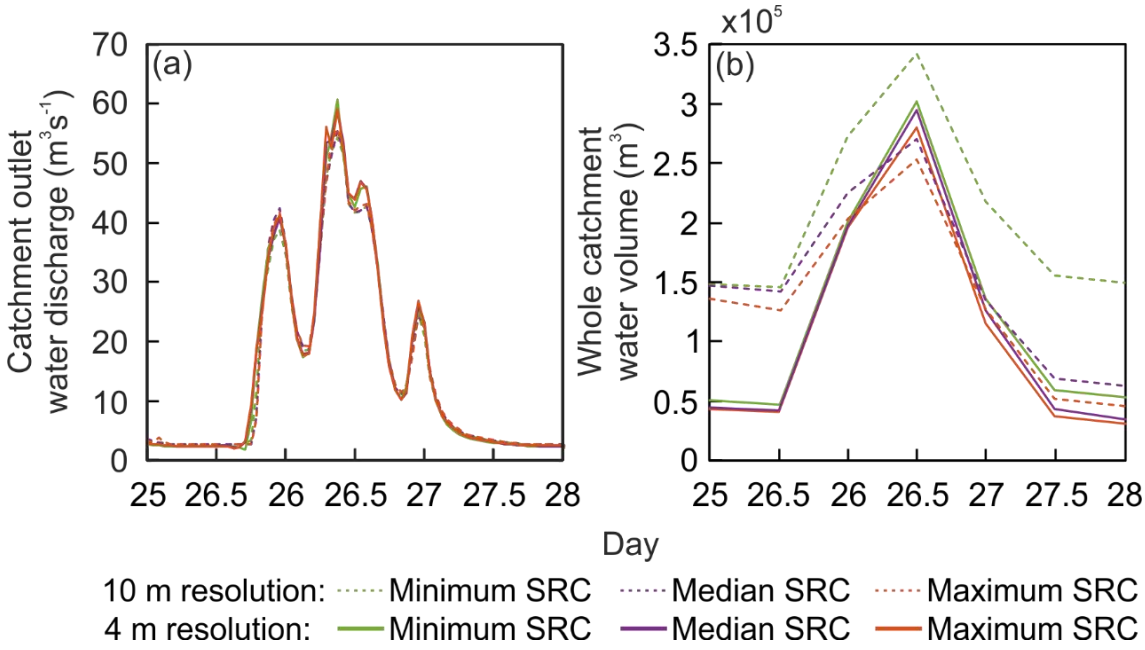

Figure A.28: (a) Catchment outlet water discharge and (b) whole catchment water volume produced with 10 m and 4 m model resolutions.

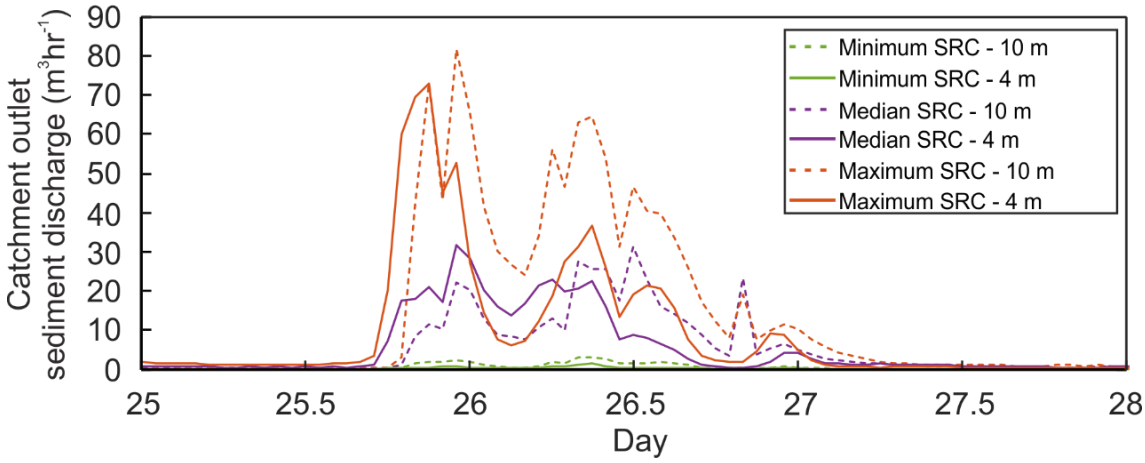

Figure A.29: Catchment outlet sediment discharge for the 10 m and 4 m model resolutions.

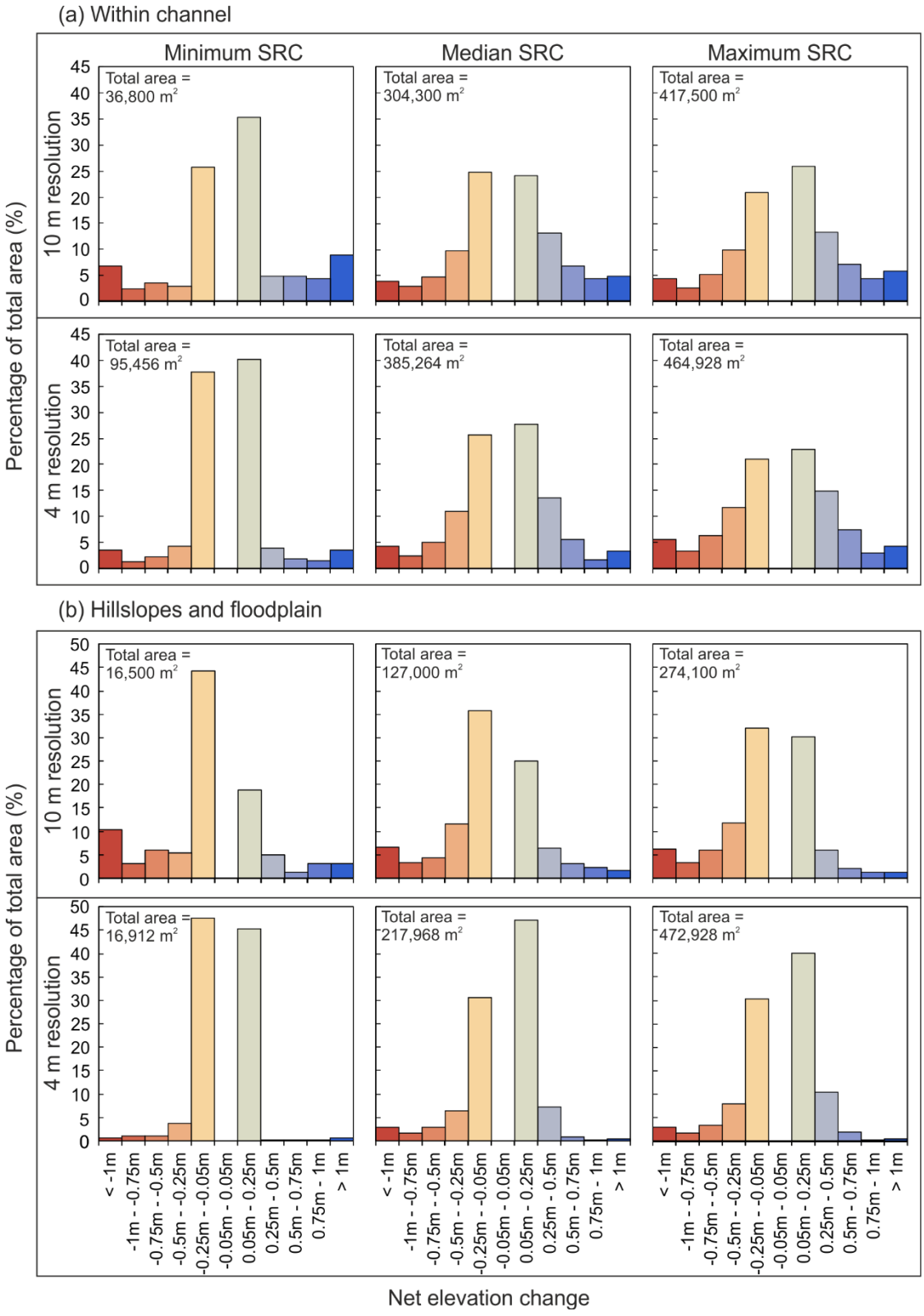

Figure A.30: Histograms of net elevation change to test the change in model resolution from 10 m to 4 m for (a) within channels and (b) on hillslopes and floodplain.

A.2.4.1 Lateral Erosion

- Less than 3 % decrease to catchment outlet peak water discharge and less than 1 % decrease to catchment outlet sediment yield when switching on lateral erosion.
- Adding lateral erosion to the Minimum SRC resulted in a 13 % increase in peak sediment discharge and 20 % increase in sediment yield (Figure A.31).
- A greater increase in peak sediment discharge and sediment yield occurred in the Median SRC (150 % and 173 % respectively) and Maximum SRC (99.5 % and 195 % respectively).
- The inclusion of lateral erosion increased the geomorphologically active area both within channels and on the hillslopes and floodplains (Figure A.32).
- Within channels, the inclusion of lateral erosion resulted in a slight increase in the percentage of deposition occurring for the Minimum SRC, but a slight increase in erosion for the Median SRC and Maximum SRC (Figure A.32a).
- Within channels, all three SRCs saw a decrease in the magnitude of erosion when including lateral erosion.
- On the hillslopes and floodplain a decrease in the percentage of erosion occurred for the Minimum and Maximum SRCs, there was little difference in the Median SRC when including lateral erosion (Figure A.32b).
- On the hillslopes and floodplains all three SRCs saw a decrease in the magnitude of net elevation change when lateral erosion was included.

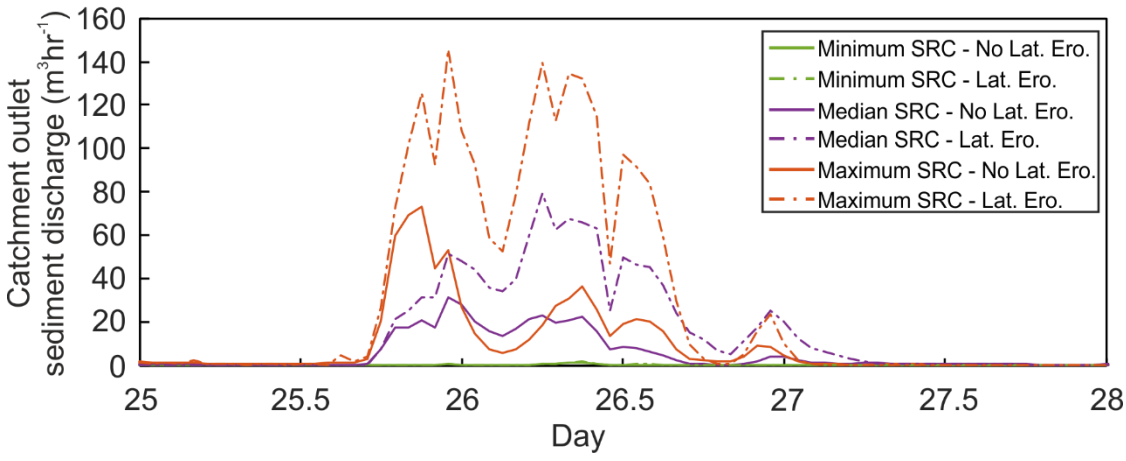

Figure A.31: Catchment outlet sediment discharge for the inclusion of lateral erosion and unerodible walls in settlements at 4 m model resolution.

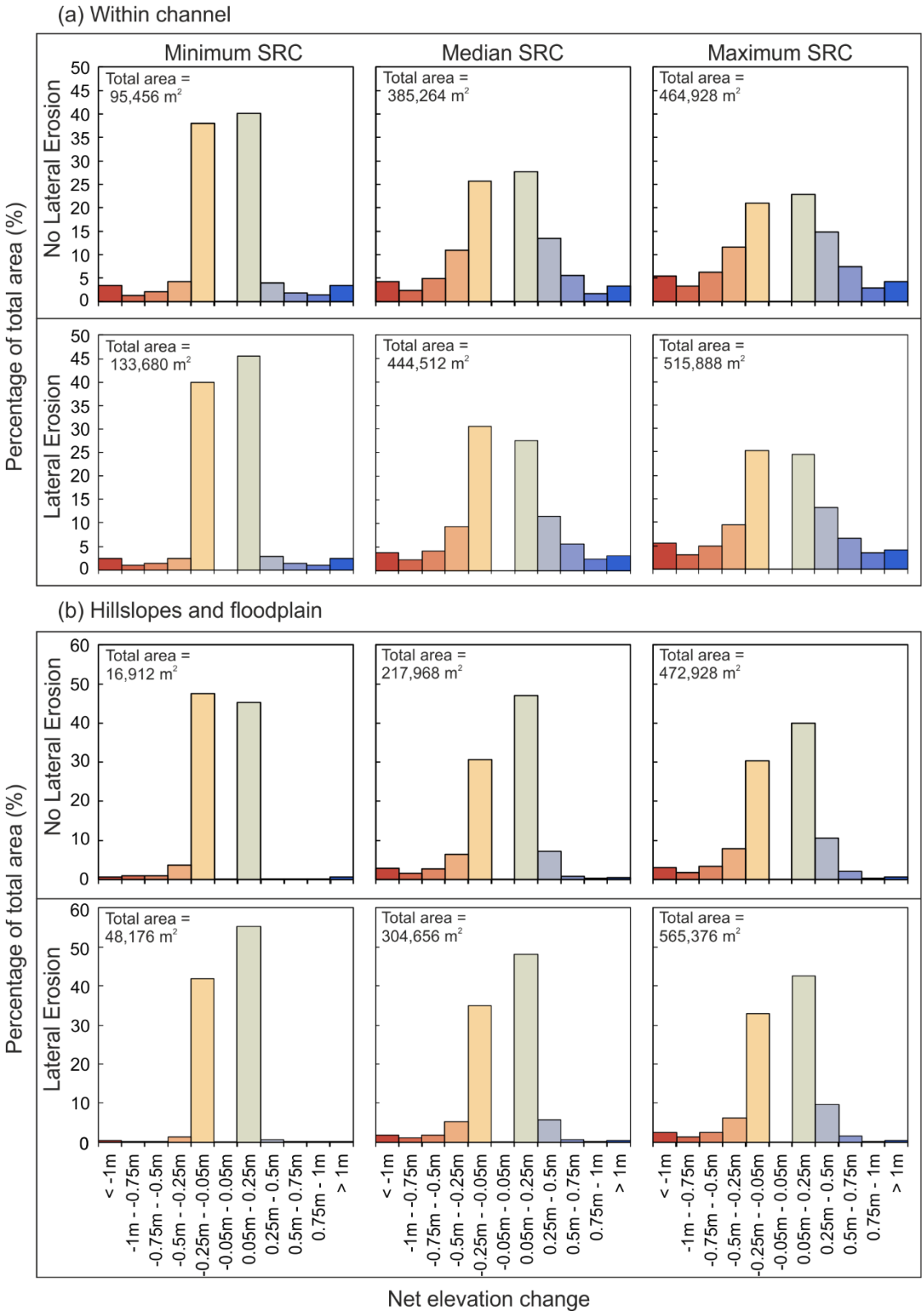

Figure A.32: Histograms of net elevation change to test the inclusion of lateral erosion and unerodible walls in settlements at 4 m model resolution for (a) within channels and (b) on hillslopes and floodplain.

A.2.4.2 Effect of spin-up

- Less than 2 % change to both peak water discharge and flood volume after the spin-up period was completed and the Boxing Day event was run again.
- For the Minimum SRC, an increase in peak sediment discharge (21 %) and sediment yield was seen post spin-up (36 %) (Figure A.33).
- For the Median and Maximum SRCs, decreases to peak sediment discharge (69.8 % and 69.7 % respectively) and sediment yield (74.7 % and 71.4 % respectively) were observed post spin-up (Figure A.33).
- After the spin-up period, the geomorphologically active area within channels was lower and the magnitude of net elevation change decreased for all three SRCs. The Median and Maximum SRCs also saw an increase in the ratio of deposition to erosion (Figure A.34a).
- On the hillslopes and floodplain, the Minimum SRC saw a decrease in geomorphologically active area whereas the Median SRC and Maximum SRC saw an increase in geomorphologically active area (Figure A.34b). There was little difference in the magnitudes of net elevation change.
- Mean D_{50} remained the same before and after the spin up period, however, variation increased with standard deviation increasing for all three SRCs and range increasing for the Minimum and Median SRCs. A small decrease in the range of D_{50} was observed for the Maximum SRC (Table A.10).

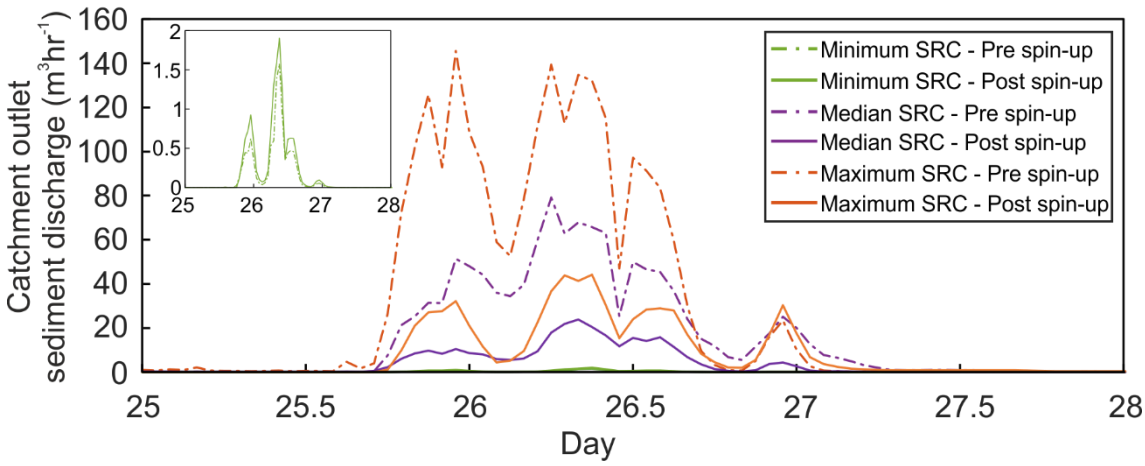

Figure A.33: Catchment outlet sediment discharge for the Boxing Day event ran before a spin-up period and after a spin-up period at 4 m model resolution.

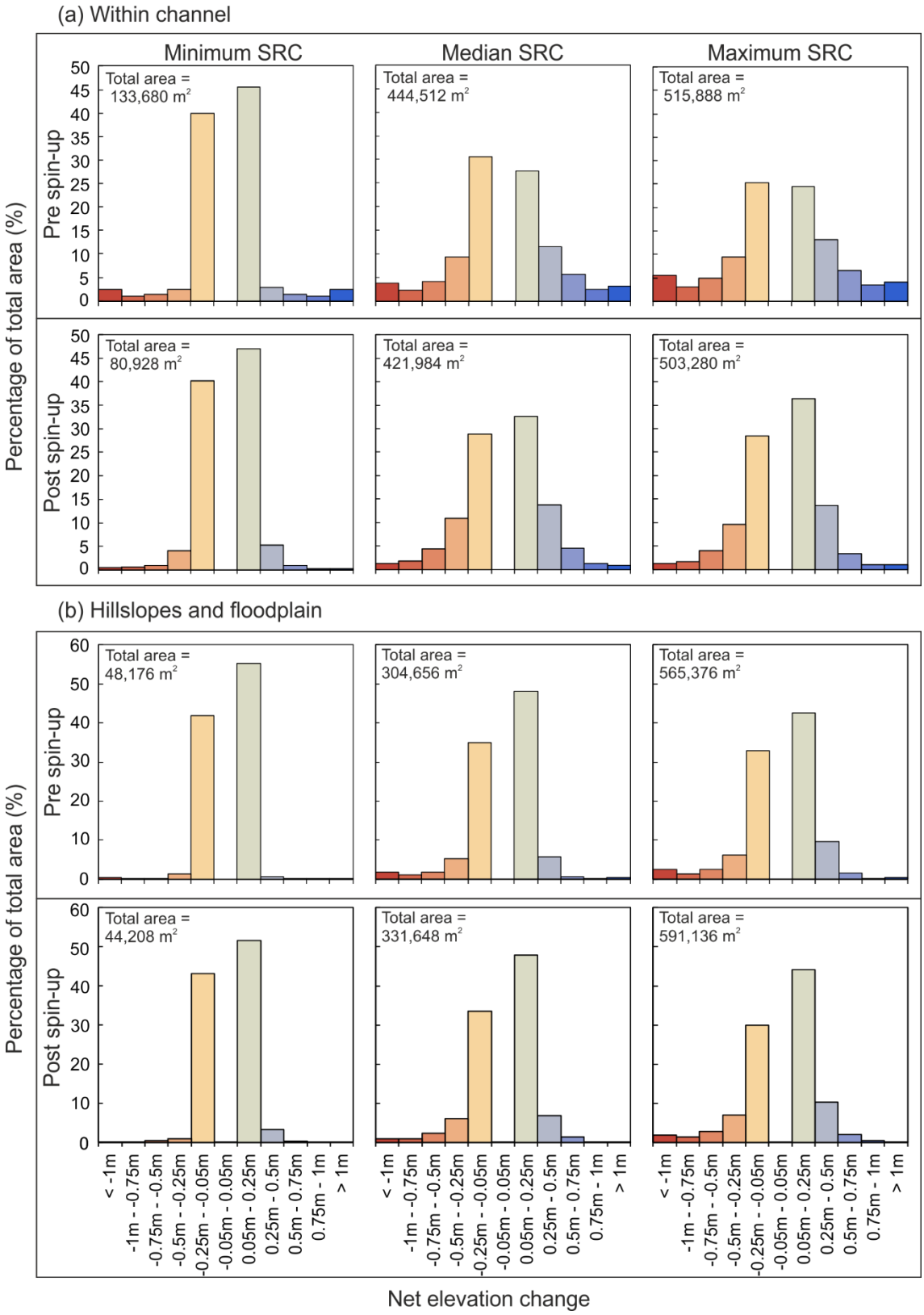

Figure A.34: Histograms of net elevation change to test the effect of a spin-up period at 4 m model resolution for (a) within channels and (b) on hillslopes and floodplain.

Table A.10: Whole catchment summary statistics for the spatially distributed D_{50} at the beginning of the pre and post spin-up events at 4 m model resolution.

SRC	**Mean (m)**		**Standard Deviation (m)**		**Range (m)**	
	Pre	Post	Pre	Post	Pre	Post
Minimum	0.035	0.035	0.001	0.004	0.052	0.133
Median	0.031	0.031	0.004	0.006	0.100	0.111
Maximum	0.016	0.016	0.003	0.004	0.057	0.054

A.2.5 Sub-catchment modelling at 2 m resolution

- To be able to increase the resolution of the CAESAR-Lisflood further to 2 m, the extent of the model needed to be decreased.
- In the following sections are the results of changes made to the 2 m resolution model.

A.2.5.1 Changing the In-Out Difference

- In-Out Difference (IOD) should be related to the low flow discharge, where below the set value, time steps for the flow and erosion/deposition models are detached, speeding up model processing.
- Table A.11 identifies key differences when altering the IOD, of particular note is the increase in model run times between when IOD was set at 0 compared to 0.1.
- A small decrease in peak sediment discharge and sediment yield was observed when IOD = 0.1. Larger decreases resulted from greater IOD values (Figure A.35).
- Geomorphically active area decreased when increasing the IOD for both within channels and on the hillslopes and floodplain (Table A.12).
- There was little difference in the ratios of magnitudes of net elevation change when changing the value of the IOD (Figure A.36).

Table A.11: Summary metrics for changing the value of the in-out difference in the 2 m resolution sub-catchment model.

Value of In-Out Difference (IOD)	**0**	**0.1**	**0.5**	**1**
Peak Water Discharge (m^3s^{-1})	18.1	18.2	18.2	19.0
%Change from IOD=0		**0.79**	**1.05**	**5.47**
Flood Volume (m^3)	1,378,476	1,389,605	1,461,231	1,563,135
%Change from IOD=0		**0.81**	**6.00**	**13.4**
Peak Sediment Discharge (m^3hr^{-1})	120.7	116.4	83.8	97.7
%Change from IOD=0		**-3.59**	**-30.6**	**-19.1**
Sediment Yield (m^3)	1344.0	1329.5	1168.7	1154.0
%Change from IOD=0		**-1.07**	**-13.0**	**-14.1**
Time Taken	4 days, 2 hours, 19 mins	1 day, 21 hours, 58 mins	1 day, 8 hours, 54 mins	23 hours, 5 mins

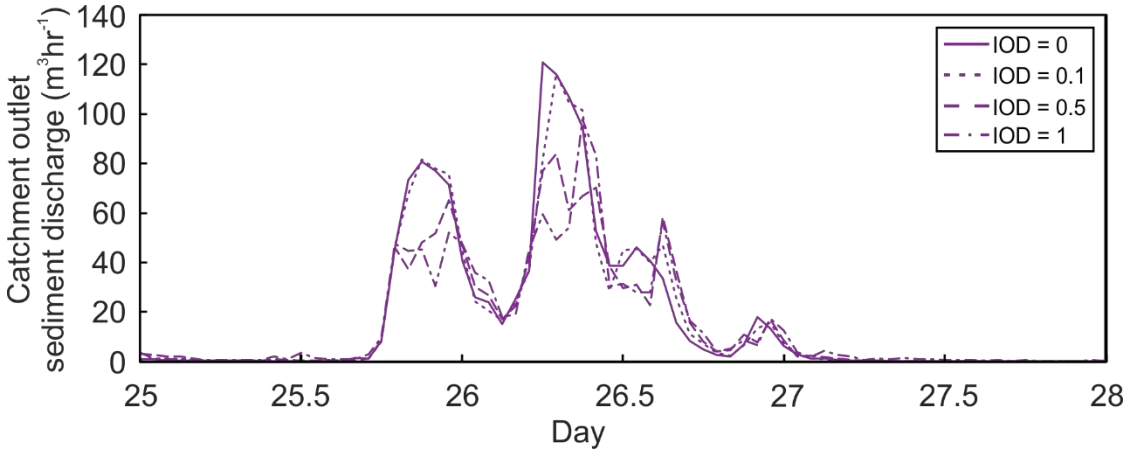

Figure A.35: Sub-catchment outlet sediment discharge for the Boxing Day event to evaluate the effect of changing the IOD value at 2 m model resolution.

Table A.12: Total area in the sub-catchment experiencing net elevation change with altered IOD values at 2 m model resolution.

Value of In-Out Difference (IOD)	**0**	**0.1**	**0.5**	**1**
Geomorphically active area within channels (m^2)	125,188	122,740	117,680	117,624
%Change from IOD=0		**-1.96**	**-6.00**	**-6.04**
Geomorphically active area on hillslopes and floodplain (m^2)	76,156	73,940	65,080	64,744
%Change from IOD=0		**-2.91**	**-14.5**	**-15.0**

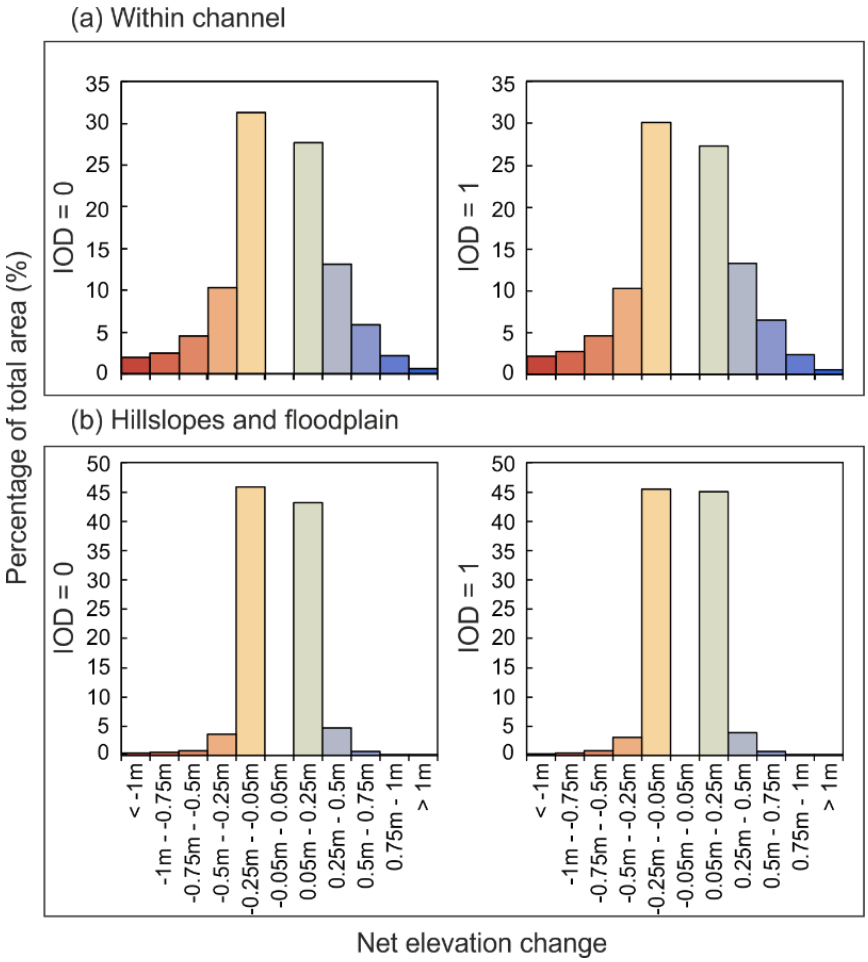

Figure A.36: Histograms of net elevation change to test the effect of values of IOD on the sub-catchment model at 2 m model resolution for (a) within channels and (b) on hillslopes and floodplain.

A.2.5.2 Effect of spin-up

- Less than 1 % difference in the peak water discharge and flood volume before and after the spin up period was applied.
- A 38 % decrease occurred to the peak sediment discharge and a 36 % decrease occurred to the sediment yield after the spin-up (Figure A.37).
- A 1.1 % increase in the geomorphologically active area within the channels occurred after the spin-up period. An increase in the ratio of deposition compared to erosion occurred alongside a decrease in magnitude of both erosion and deposition (Figure A.38a).
- A 1.5 % decrease in geomorphologically active area on the hillslopes and floodplain occurred after the spin up period. A small increase in magnitude of erosion was observed (Figure A.38b).

- Little difference in mean D_{50} was observed after the spin-up period, however the range of D_{50} values throughout the catchment increased by 0.079 m and the standard deviation increased by 0.005 m.

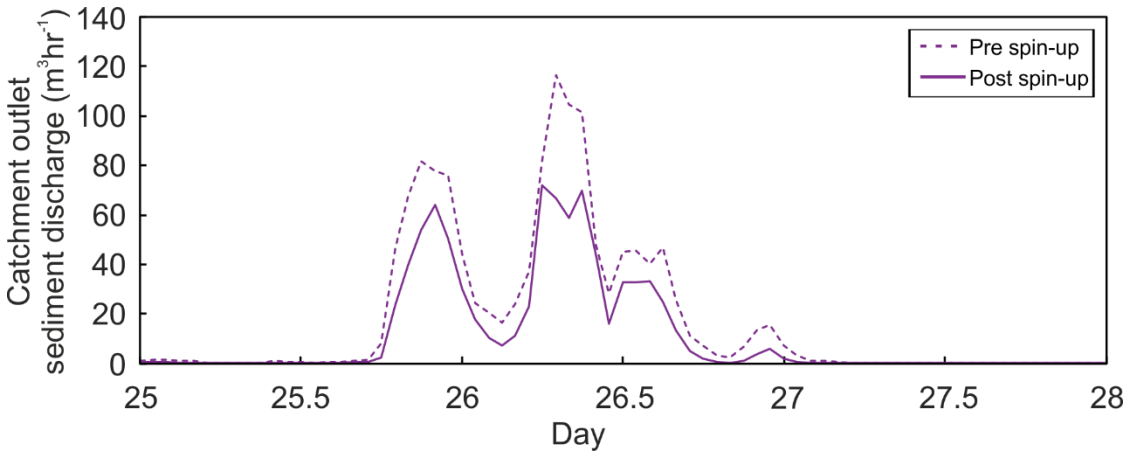

Figure A.37: Sub-catchment outlet sediment discharge for the Boxing Day event to evaluate the effect of the spin-up period at 2 m model resolution.

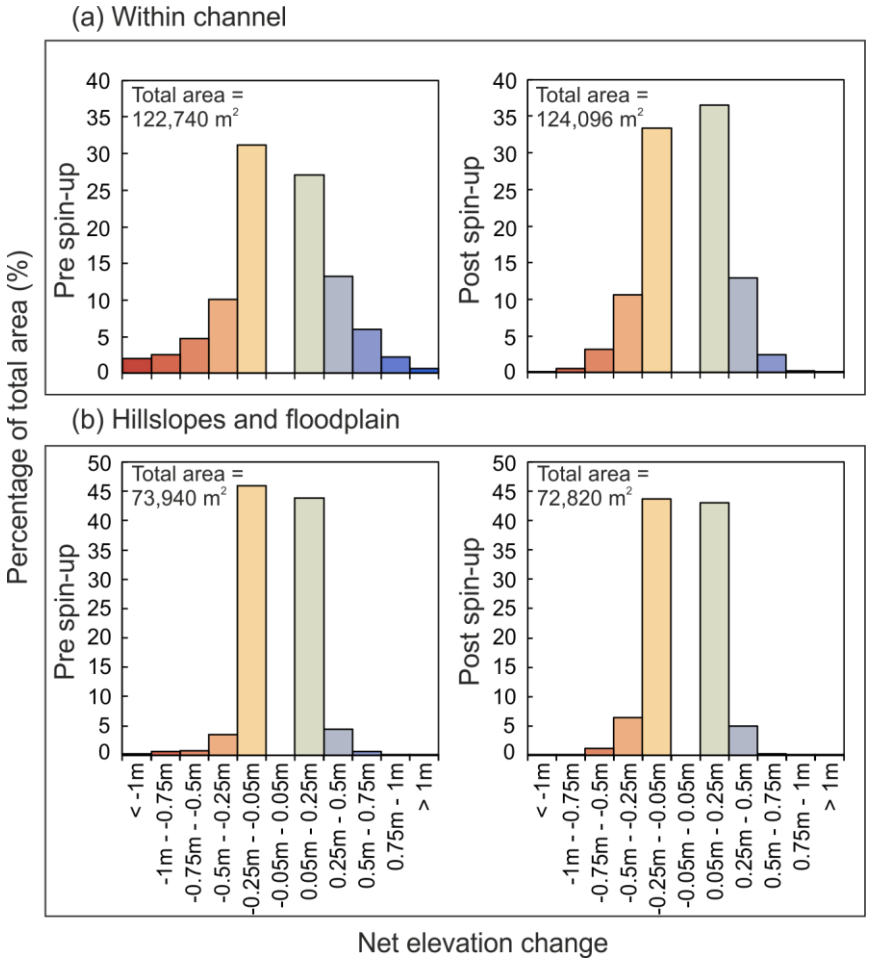

Figure A.38 Histograms of net elevation change to test the effect of the spin-up period on the sub-catchment model at 2 m model resolution for (a) within channels and (b) on hillslopes and floodplain.

A.3 Parameter values used in CAESAR-Lisflood not assessed in model set up

The majority of parameters found in Table A.13 were left unchanged from the values suggested in the CAESAR-Lisflood manual, those in bold were tested as part of the sensitivity analysis.

Table A.13: CAESAR-Lisflood parameter values

Numerical				
Min time step (s)				1
Max time step (s)				3600
Sediment				
Sediment response catchment		Min	Med	Max
GS (1)	Grain size (m)	**0.000875**	**0.00075**	**0.0004**
	Proportion	**0.144**	**0.144**	**0.144**
	Fall Velocity (m/s)	**0.13**	**0.11**	**0.055**
GS (2)	Grain size (m)	**0.00175**	**0.0015**	**0.0008**
	Proportion	**0.022**	**0.022**	**0.022**
GS (3)	Grain size (m)	**0.0035**	**0.003**	**0.0016**
	Proportion	**0.019**	**0.019**	**0.019**
GS (4)	Grain size (m)	**0.007**	**0.006**	**0.0032**
	Proportion	**0.029**	**0.029**	**0.029**
GS (5)	Grain size (m)	**0.014**	**0.012**	**0.0064**
	Proportion	**0.068**	**0.068**	**0.068**
GS (6)	Grain size (m)	**0.028**	**0.024**	**0.0128**
	Proportion	**0.146**	**0.146**	**0.146**
GS (7)	Grain size (m)	**0.056**	**0.048**	**0.0256**
	Proportion	**0.22**	**0.22**	**0.22**
GS (8)	Grain size (m)	**0.112**	**0.096**	**0.0512**
	Proportion	**0.231**	**0.231**	**0.231**
GS (9)	Grain size (m)	**0.224**	**0.192**	**0.01024**
	Proportion	**0.121**	**0.121**	**0.121**
Bedrock erosion threshold (Pa)				0
Bedrock erosion rate (m/Pa/Yr)				0
Max velocity used to calcluated Tau from vel.				5
Max erode limit				0.01
Active layer thickness (m)				0.1
In channel lateral erosion rate				10
Lateral erosion rate				**0.00001**
Number of passes for edge smoothing				200
Number of cells to shift lateral erosion downstream				2
Max difference allowed in cross channel smoothing				0.0001
Hydrology				
Rainfall				**CEH-GEAR / NIMROD**

Continued onto the next page

Vegetation	
Vegetation critical shear	**15**
Grass maturity (yrs)	0
Proportion of erosion that can occur when vegetation is fully grown	0.1
Slope processes	
Creep rate	0.0025
Slope failure threshold	45
Soil erosion rate	0
Flow model	
Input/output difference allowed	**10m/4m = 1 2m= 0.1**
Min Q for depth calc (dependent on cell size)	0.04
Max Q for depth calc	1000
Water depth threshold above which erosion will happen (m)	0.01
Slope for edge cells	0.002
Evaporation rate (m/day)	**0.003**
Courant number	0.3
hflow threshold	0.0001
Froude # flow limit	0.8
Manning's n	**Chapter 3, see: Figure 2.9 and Table 3.1** **Chapter 4, see: Table 4.1**

A.4 References

Brunner, G.W. 2016. HEC-RAS River Analysis System 2D Modeling User's Manual. California: U.S. Army Corps of Engineers.

Chow, V.T. 1959. *Open-channel Hydraulics* (Vol. 1). New York: McGraw-Hill.

Coulthard, T.J. and Van De Wiel, M.J. 2006. A cellular model of river meandering. *Earth Surface Processes and Landforms.* **31**(1), pp.123-132.

Coulthard, T.J., Macklin, M.G. and Kirkby, M.J. 2002. A cellular model of Holocene upland river basin and alluvial fan evolution. *Earth Surface Processes and Landforms.* **27**, pp.269-288.

Coulthard, T.J., Neal, J.C., Bates, P.D., Ramirez, J., de Almeida, G.A. and Hancock, G.R. 2013. Integrating the LISFLOOD-FP 2D hydrodynamic model with the CAESAR model: implications for modelling landscape evolution. *Earth Surface Processes and Landforms*. **38**(15), pp.1897-1906.

Dawson, C.W., Abrahart, R.J. and See, L.M. 2007. HydroTest: a web-based toolbox of evaluation metrics for the standardised assessment of hydrological forecasts. *Environmental Modelling & Software*. **22**(7), pp.1034-1052.

Grimaldi, S., Petroselli, A., Alonso, G. and Nardi, F. 2010. Flow time estimation with spatially variable hillslope velocity in ungauged basins. *Advances in Water Resources*. **33**(10), pp.1216-1223.

Hancock, G.R. and Coulthard, T.J. 2012. Channel movement and erosion response to rainfall variability in southeast Australia. *Hydrological Processes*. **26**(5), pp.663-673.

Kalyanapu, A.J., Burian, S.J. and McPherson, T.N., 2009. Effect of land use-based surface roughness on hydrologic model output. *Journal of Spatial Hydrology*, **9**(2).

McHugh, M., Wood. G., Walling, D., Morgan, R., Zhang, Y., Anthony, S. and Hutchins, M. 2002. *Prediction of Sediment Delivery to Watercourses from Land Phase II*. Bristol: Environment Agency.

Meadows, T. 2014. *Forecasting long-term sediment yield from the upper North Fork Toutle River, Mount St. Helens, USA.* Ph.D. thesis, University of Nottingham.

Robinson, E., Blyth, E., Clark, D., Comyn-Platt, E., Finch, J. and Rudd, A. 2016. *Climate hydrology and ecology research support system potential evapotranspiration dataset for Great Britain (1961-2015) [CHESS-PE]. NERC Environmental Information Data Centre*. [Online]. [Accessed 9 May 2018]. Available from: https://doi.org/10.5285/8baf805d-39ce-4dac-b224-c926ada353b7

Skinner, C.J., Coulthard, T.J., Schwanghart, W., Wiel, M.J. and Hancock, G. 2018. Global sensitivity analysis of parameter uncertainty in landscape evolution models. *Geoscientific Model Development*. **11**(12), pp.4873-4888.

Welsh, K.E., Dearing, J.A., Chiverrell, R.C. and Coulthard, T.J. 2009. Testing a cellular modelling approach to simulating late-Holocene sediment and water transfer from catchment to lake in the French Alps since 1826. *The Holocene.* **19**(5), pp.785-798.

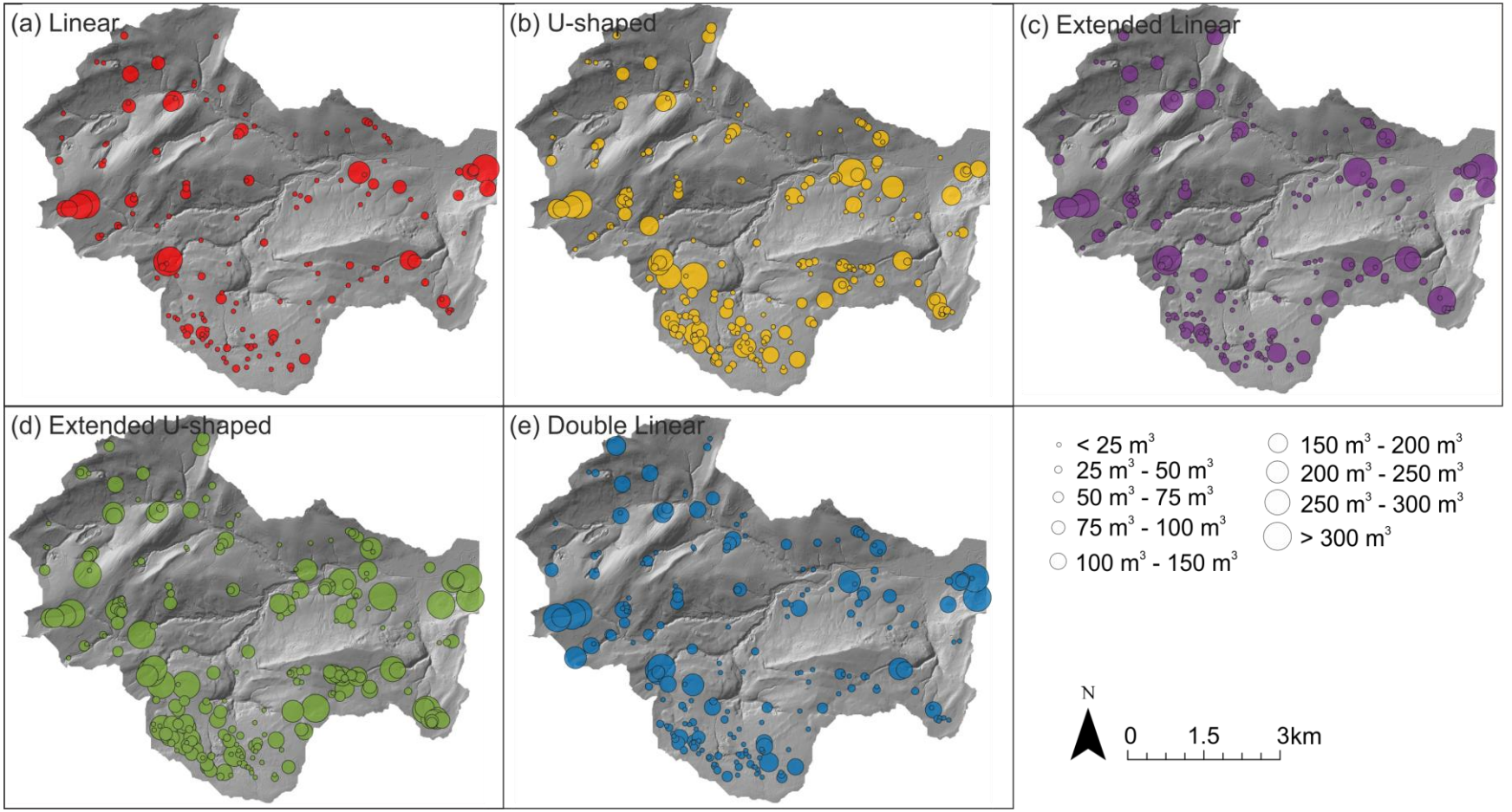

Figure B.1: Graduated symbols of the water volume held behind RAFs for the median SRC.

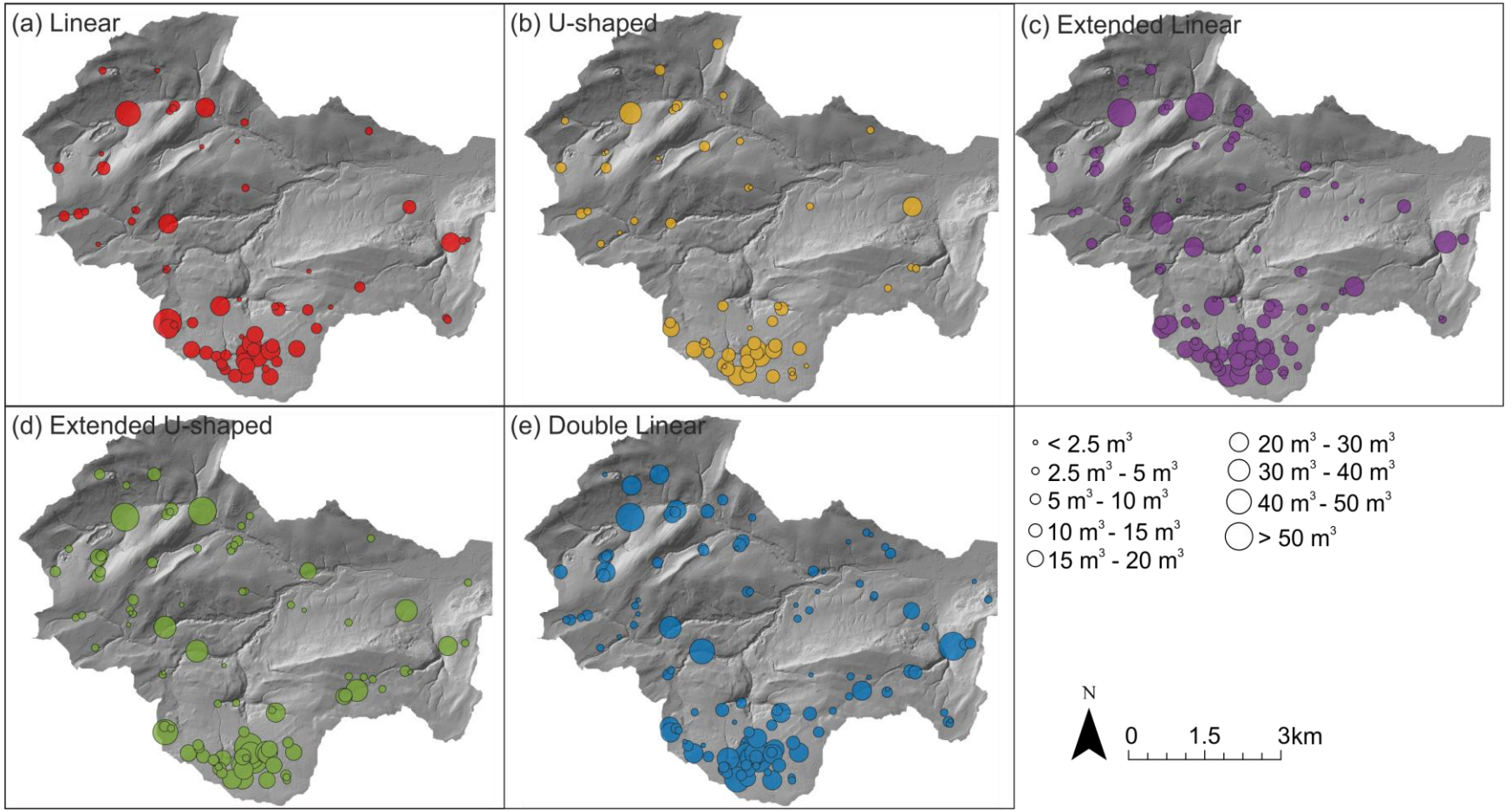

Figure B.2: Graduated symbols of positive geomorphological volumetric change for the median SRC.

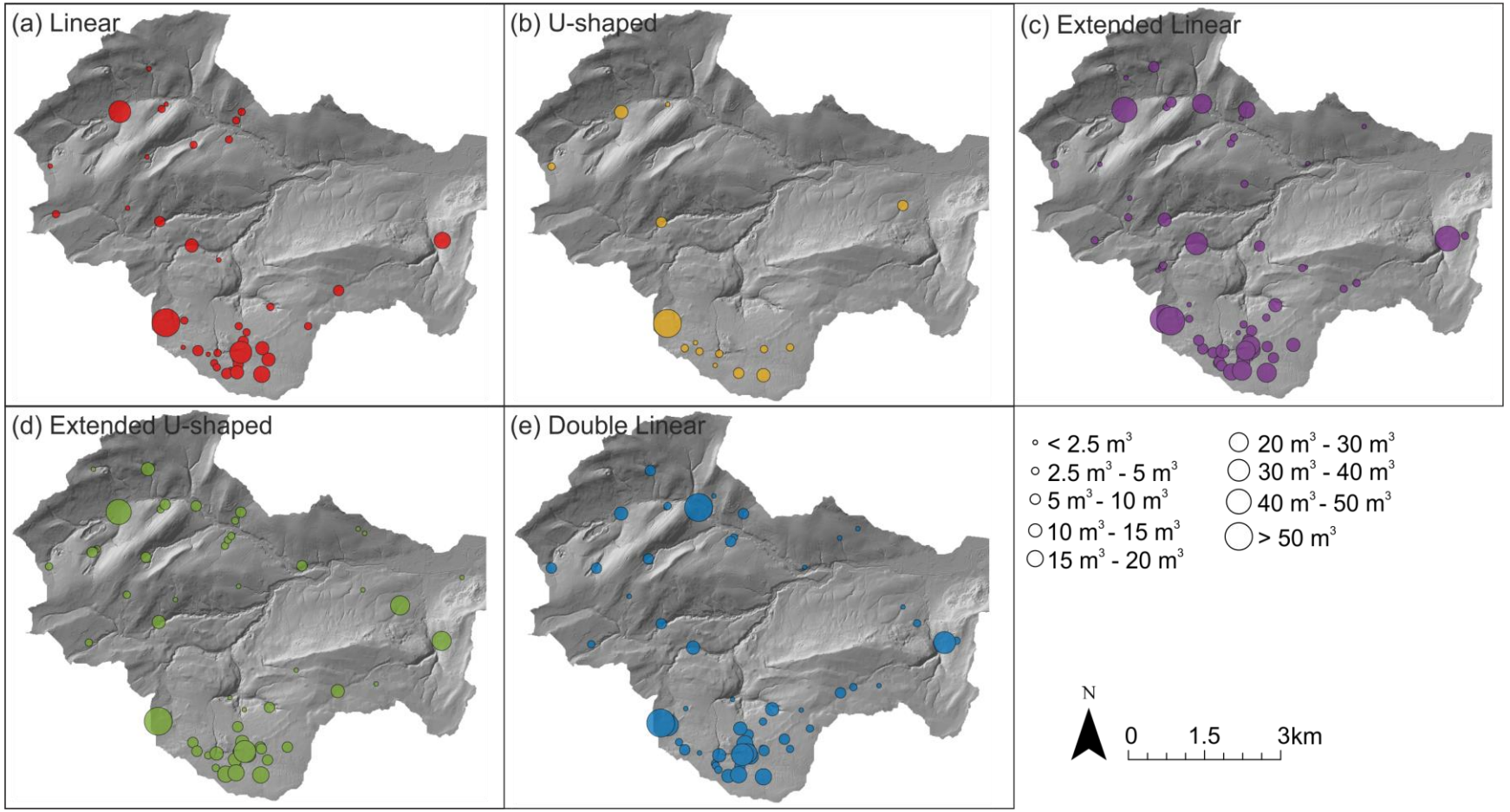

Figure B.3: Graduated symbols of negative geomorphological volumetric change for the median SRC.